

SIMULATION OF THE DIFFUSION OF ENDOCRINE DISRUPTING COMPOUNDS IN SILICALITE BY MOLECULAR DYNAMICS

By

Thomas GABRY

A thesis submitted to the Faculty of the

WORCESTER POLYTECHNIC INSTITUTE

In partial fulfillment of the requirements for the Degree of

Master of Science

In

Chemical engineering

May 2012

Acknowledgements

I would like to thank my advisor Professor Deskins for his time, help and support throughout my master program. I would also like to thank my co-advisor Professor Thompson for his insight on the direction that this thesis should take.

I would like to thank my friends and coworkers at WPI, especially Jean-Francois Roux, Florent Allain, Julien Courtois, Gaetan Lemoine and Matt Perrone.

I would also like to thank the faculty, staff and students of the Chemical Engineering department.

Finally, I would like to thank my family and friends overseas for their support and trust during the past 2 years.

Contents

List of Tables	6
List of Figures	7
Abstract.....	11
Introduction:.....	13
Background information:.....	14
I- Endocrine Disrupting Chemicals:	14
1- Bisphenol-A.....	14
2- Nonylphenol.....	17
II- Zeolites for separation:.....	18
Silicalite	20
III- Molecular modeling	20
1- Molecular Dynamics:.....	21
A. Algorithm	21
B. The velocity Verlet Algorithm (VV):	22
C. NVT Thermostat:.....	23
D. Periodic Boundary Conditions.....	23
E. Force Field:.....	24
Methodology:.....	33
I- Parameters for our system:	33
1- Silicalite:	33
2- Water:	36
3- Benzene:.....	37
4- Toluene:	39
5- Phenol:	41
6- Neopentane:	43
7- Nonylphenol:.....	44
8- Bisphenol-A.....	48
9- Simulation Controls:.....	51
II- Simulations of interest.....	52
1- Self diffusivity versus transport diffusivity:.....	52
2- Mean Square displacement, Self-diffusion coefficient and Energy of activation:.....	52

3- Diffusional Anisotropy	54
4- Mean-square displacement calculation:.....	55
5- Radial distribution functions (rdfs)	56
Results and Discussion	58
I- Water	58
1- Diffusion	58
A- TIP3P water model.....	58
B- SPC water model.....	65
2- Radial distribution functions.....	71
A- TIP3P water molecule:	71
B- SPC water model.....	75
3- Discussion.....	79
II- Benzene:.....	84
1- OPLS-AA and OPLS-UA results	84
2- Comparison with literature:.....	89
III- Phenol:	92
IV- Toluene:	99
V- Neopentane:	107
VI- Nonylphenol:.....	110
VII- Bisphenol A:	117
Conclusions	123
References	126
Appendices.....	130
Appendix 1: Examples of input files for DL_POLY.....	130
CONTROL:.....	130
CONFIG:.....	131
TIP3P water/silicalite	131
SPC water / silicalite.....	167
Benzene / silicalite	170
Phenol / silicalite.....	171
Toluene / silicalite.....	172
Neopentane / silicalite	173

Nonylphenol / silicalite	174
Bisphenol-a / silicalite	177
FIELD:	179
TIP3P water / silicalite.....	179
SPC water / silicalite.....	180
OPLS-AA benzene / silicalite	180
OPLS-AA phenol / silicalite.....	182
OPLS-AA toluene / silicalite.....	185
OPLS-AA neopentane / silicalite	187
OPLS-AA nonylphenol / silicalite	190
OPLS-AA bisphenol-A / silicalite.....	197
Appendix 2: DL_FIELD CHARMM.sf examples	201
Toluene	201
Nonylphenol:.....	202
Bisphenol-A:.....	204
Appendix 3: Programs used to calculated averaged mean square displacement in the x, y and z direction.	
.....	206
Coordinates from HISTORY file:	206
Calculate MSD _{x,y,z} for each atom of one type:.....	208
Calculate averaged MSD _{x,y,z} for one atom type.....	210

List of Tables

Table 1: Lattice parameters of Pnma Silicalite structure	33
Table 2: Parameters for Silicalite simulations.....	34
Table 3: Electrostatic and Van der Waals parameters for silicalite	34
Table 4: Three-Body potential for silicalite simulations	34
Table 5: SPC and TIP3P parameters used for our simulations.....	37
Table 6: Parameters used for Benzene simulations.....	38
Table 7: Parameters used for Toluene simulations	41
Table 8: Parameters used for Phenol simulations	42
Table 9: Parameters used for Neopentane simulations	44
Table 10: Parameters used for Nonylphenol simulations.....	47
Table 11: Parameters used for Bispehnol-A simulations.....	51
Table 12: Diffusion coefficients of TIP3P water in silicalite [$10^{-9} \text{ m}^2.\text{s}^{-1}$], β and δ parameters as function of T	65
Table 13: Diffusion coefficients of SPC water in silicalite [$10^{-9} \text{ m}^2.\text{s}^{-1}$], β and δ parameters as function of T	71
Table 14: Summary of results for self-diffusion coefficient of water in silicalite found in literature.....	79
Table 15: Different results for the diffusion coefficient of benzene in silicalite found in literature. <i>a</i> Rungsirisakun et al. ran simulations with 2 benzene molecule per cell.....	89
Table 16: Diffusion coefficients of neopentane in silicalite [$10^{-9} \text{ m}^2.\text{s}^{-1}$], β and δ parameters as function of T	109
Table 17: Diffusion coefficients of bisphenol-A in silicalite [$10^{-9} \text{ m}^2.\text{s}^{-1}$], β and δ parameters as function of T	122
Table 18: Summary of the most important self-diffusion coefficients obtained throughout this report	125

List of Figures

Figure 1: Molecular formula of Bisphenol-A.....	15	
Figure 2: Three-dimensional molecular structure of Bisphenol-A.....	15	
Figure 3: Different isomers of nonylphenol	17	
Figure 4: Nonyphenol ethoxylates structure	17	
Figure 5:Lennard-Jones potential for Oxygen in water with $\sigma_{OO}=3.1506 \text{ \AA}$ and $\varepsilon_{OO} = 0.6357 \text{ kJ}\cdot\text{mol}^{-1}=76.46\text{K}$	28	
Figure 6: Bond stretching.....	30	
Figure 7: Angle bending	30	
Figure 8: Torsional potential	31	
Figure 9: Silicalite x-axis, zigzag channel.....	35	
Figure 10: Silicalite y-axis, straight channel (into the plane of the page).....	35	
Figure 11: Silicalite z-axis, mixed channel.....	36	
Figure 12: SPC water molecule	Figure 13: TIP3P water molecule	37
Figure 14: OPLS-AA Benzene(left) and OPLS-UA Benzene (right).....	38	
Figure 15: OPLS-AA Toluene molecule alone (left) and after 1ps in the silicalite structure(right, the zeolite is not shown for better readability)	39	
Figure 16: OPLS-AA rigid toluene molecule (left) and OPLS-UA toluene molecule (right)	40	
Figure 17: OPLS-AA Phenol molecule (left) and OPLS-UA molecule(right).....	41	
Figure 18: OPLS-AA neopentane	43	
Figure 19: OPLS-AA linear Nonylphenol molecule	44	
Figure 20: BPA molecule simulated using OPLS-AA Force field at various timesteps	48	
Figure 21: OPLS-AA BPA molecule (left) and OPLS-AA BPA molecule(right) with rigid rings	49	
Figure 22: Distances rOO and rOH between two water molecules	56	
Figure 23: Average mean square displacement of water molecules in silicalite at 300K. MSDx is along the x-direction, MSDy is along the y-direction, and MSDz is along the z-direction. MSDs were calculated using the program described in the methodology section.....	59	
Figure 24: Mean square displacement calculated by DL_POLY for 16 water molecules in silicalite at 300K with trend line shown.....	60	
Figure 25: Average mean square displacement of water molecules in silicalite at 350K. MSDx is along the x-direction, MSDy is along the y-direction, and MSDz is along the z-direction. MSDs were calculated using the program described in the methodology section.....	61	
Figure 26: Average mean square displacement of water molecules in silicalite at 400K. MSDx is along the x-direction, MSDy is along the y-direction, and MSDz is along the z-direction.....	61	
Figure 27: Average mean square displacement of water molecules in silicalite at 440K. MSDx is along the x-direction, MSDy is along the y-direction, and MSDz is along the z-direction.....	62	
Figure 28: Average mean square displacement of water molecules in silicalite at 490K. MSDx is along the x-direction, MSDy is along the y-direction, and MSDz is along the z-direction.....	62	
Figure 29: Average mean square displacement of water molecules in silicalite at 600K. MSDx is along the x-direction, MSDy is along the y-direction, and MSDz is along the z-direction.....	63	
Figure 30: Fitting of α coefficient at 300K for MSDy	64	

Figure 31: Average mean square displacement of rigid water molecules in silicalite at 300K. MSDx is along the x-direction, MSDy is along the y-direction, and MSDz is along the z-direction.....	66
Figure 32: Mean square displacement calculated by DL_POLY of rigid water molecules in silicalite at 300K with trend line shown	66
Figure 33: Average mean square displacement of rigid water molecules in silicalite at 350K. MSDx is along the x-direction, MSDy is along the y-direction, and MSDz is along the z-direction.....	67
Figure 34: Mean square displacement calculated by DL_POLY of rigid water molecules in silicalite at 350K with trend line shown	67
Figure 35: Average mean square displacement of rigid water molecules in silicalite at 400K. MSDx is along the x-direction, MSDy is along the y-direction, and MSDz is along the z-direction.....	68
Figure 36: Average mean square displacement of rigid water molecules in silicalite at 440K. MSDx is along the x-direction, MSDy is along the y-direction, and MSDz is along the z-direction.....	68
Figure 37: Mean square displacement calculated by DL_POLY of rigid water molecules in silicalite at 440K with trend line shown	69
Figure 38: Average mean square displacement of rigid water molecules in silicalite at 490K. MSDx is along the x-direction, MSDy is along the y-direction, and MSDz is along the z-direction.....	69
Figure 39: Average mean square displacement of rigid water molecules in silicalite at 600K. MSDx is along the x-direction, MSDy is along the y-direction, and MSDz is along the z-direction.....	70
Figure 40: Radial distribution function gOO versus rOO at 300K, 350K and 400K for water	72
Figure 41: Radial distribution function gOO versus rOO at 440K, 490K and 600K for water	72
Figure 42: Radial distribution function gOH versus rOH at 300K, 350K and 400K for water.....	73
Figure 43: Radial distribution function gOH versus rOH at 440K, 490K and 600K for water.....	73
Figure 44: Radial distribution function gOZ-H versus rOZ-H at 300K, 350K and 400K for water	74
Figure 45: Radial distribution function gOZ-H versus rOZ-H at 440K, 490K and 600K for water	75
Figure 46: Radial distribution function gOO versus rOO at 300K, 350K and 400K for rigid water	75
Figure 47: Radial distribution function gOO versus rOO at 440K, 490K and 600K for water	76
Figure 48: Radial distribution function gOH versus rOH at 300K, 350K and 400K for rigid water	77
Figure 49: Radial distribution function gOH versus rOH at 440K, 490K and 600K for rigid water	77
Figure 50: Radial distribution function gOZ-H versus rOZ-H at 300K, 350K and 400K for rigid water	78
Figure 51: Radial distribution function gOZ-H versus rOZ-H at 440K, 490K and 600K for rigid water	78
Figure 52: Number of Hbonds as a function of temperature for SPC and TIP3P models and Fleys results	81
Figure 53: Activation energy of water molecule in silicalite versus temperature	82
Figure 54: MSD of OPLS-AA benzene molecule at 300K, coordinates written every 500steps. MSDx is along the x-direction, MSDy is along the y-direction, and MSDz is along the z-direction.....	84
Figure 55: MSD of OPLS-AA benzene molecule at 300K, coordinates written every 200steps. MSDx is along the x-direction, MSDy is along the y-direction, and MSDz is along the z-direction.....	85
Figure 56: MSD of OPLS-AA benzene molecule at 400K, coordinates written every 500steps. MSDx is along the x-direction, MSDy is along the y-direction, and MSDz is along the z-direction.....	85
Figure 57: MSD of OPLS-AA benzene molecule at 400K, coordinates written every 200steps. MSDx is along the x-direction, MSDy is along the y-direction, and MSDz is along the z-direction.....	86
Figure 58: MSD of OPLS-UA benzene molecule at 300K, coordinates written every 500steps. MSDx is along the x-direction, MSDy is along the y-direction, and MSDz is along the z-direction.....	86

Figure 59: MSD of OPLS-UA benzene molecule at 300K, coordinates written every 200steps. MSDx is along the x-direction, MSDy is along the y-direction, and MSDz is along the z-direction.....	87
Figure 60: MSD of OPLS-UA benzene molecule at 400K, coordinates written every 500steps. MSDx is along the x-direction, MSDy is along the y-direction, and MSDz is along the z-direction.....	87
Figure 61: MSD of OPLS-UA benzene molecule at 400K, coordinates written every 200steps. MSDx is along the x-direction, MSDy is along the y-direction, and MSDz is along the z-direction.....	88
Figure 62: MSD of OPLS-AA phenol molecule at 300K, coordinates written every 500steps. MSDx is along the x-direction, MSDy is along the y-direction, and MSDz is along the z-direction.	92
Figure 63: MSD of OPLS-AA phenol molecule at 300K, coordinates written every 200steps. MSDx is along the x-direction, MSDy is along the y-direction, and MSDz is along the z-direction.	93
Figure 64: MSD of OPLS-AA phenol molecule at 400K, coordinates written every 500steps. MSDx is along the x-direction, MSDy is along the y-direction, and MSDz is along the z-direction.	93
Figure 65: MSD of OPLS-AA phenol molecule at 400K, coordinates written every 200steps. MSDx is along the x-direction, MSDy is along the y-direction, and MSDz is along the z-direction.	94
Figure 66: MSD of OPLS-UA phenol molecule at 300K, coordinates written every 500steps. MSDx is along the x-direction, MSDy is along the y-direction, and MSDz is along the z-direction.	94
Figure 67: MSD of OPLS-UA phenol molecule at 400K, coordinates written every 500steps. MSDx is along the x-direction, MSDy is along the y-direction, and MSDz is along the z-direction.	95
Figure 68: Radial distribution function between the hydrogen of the phenol alcohol group and the oxygen atom of the silicalite framework at 300K.	96
Figure 69: Example of hydrogen bond between hydrogen of the alcohol group of the phenol molecule and the oxygen of silicalite	97
Figure 70: MSD of OPLS-AA toluene molecule at 300K, coordinates written every 500steps. MSDx is along the x-direction, MSDy is along the y-direction, and MSDz is along the z-direction.....	99
Figure 71: MSD of OPLS-AA toluene molecule at 300K, coordinates written every 200steps. MSDx is along the x-direction, MSDy is along the y-direction, and MSDz is along the z-direction.....	100
Figure 72: MSD of OPLS-AA toluene molecule at 400K, coordinates written every 500steps. MSDx is along the x-direction, MSDy is along the y-direction, and MSDz is along the z-direction.....	100
Figure 73: MSD of OPLS-AA toluene molecule at 400K, coordinates written every 200steps. MSDx is along the x-direction, MSDy is along the y-direction, and MSDz is along the z-direction.....	101
Figure 74: MSD of OPLS-AA rigid toluene molecule at 300K, coordinates written every 500steps. MSDx is along the x-direction, MSDy is along the y-direction, and MSDz is along the z-direction.....	102
Figure 75: MSD of OPLS-AA rigid toluene molecule at 300K, coordinates written every 200steps. MSDx is along the x-direction, MSDy is along the y-direction, and MSDz is along the z-direction.....	102
Figure 76: MSD of OPLS-AA rigid toluene molecule at 400K, coordinates written every 500steps. MSDx is along the x-direction, MSDy is along the y-direction, and MSDz is along the z-direction.....	103
Figure 77: MSD of OPLS-AA rigid toluene molecule at 400K, coordinates written every 200steps. MSDx is along the x-direction, MSDy is along the y-direction, and MSDz is along the z-direction.....	103
Figure 78: MSD of OPLS-UA toluene molecule at 300K, coordinates written every 500steps. MSDx is along the x-direction, MSDy is along the y-direction, and MSDz is along the z-direction.....	104
Figure 79: MSD of OPLS-UA toluene molecule at 300K, coordinates written every 200steps. MSDx is along the x-direction, MSDy is along the y-direction, and MSDz is along the z-direction.....	105

Figure 80: MSD of OPLS-UA toluene molecule at 400K, coordinates written every 500steps. MSDx is along the x-direction, MSDy is along the y-direction, and MSDz is along the z-direction.....	105
Figure 81: MSD of OPLS-UA toluene molecule at 400K, coordinates written every 500steps. MSDx is along the x-direction, MSDy is along the y-direction, and MSDz is along the z-direction.....	106
Figure 82: Mean square displacement of neopentane at 300K in silicalite. MSDx is along the x-direction, MSDy is along the y-direction, and MSDz is along the z-direction. These results were obtained using the program described in the methodology section.	107
Figure 83: Mean square displacement of neopentane at 400K in silicalite. MSDx is along the x-direction, MSDy is along the y-direction, and MSDz is along the z-direction.	108
Figure 84: Mean square displacement of nonylphenol at 300K in silicalite. MSDx is along the x-direction, MSDy is along the y-direction, and MSDz is along the z-direction.	110
Figure 85: Mean square displacement of nonylphenol linear carbon chain at 300K in silicalite. MSDx is along the x-direction, MSDy is along the y-direction, and MSDz is along the z-direction.....	111
Figure 86: Mean square displacement of nonylphenol at 400K in silicalite. MSDx is along the x-direction, MSDy is along the y-direction, and MSDz is along the z-direction.	111
Figure 87: Mean square displacement of nonylphenol linear carbon chain at 400K in silicalite. MSDx is along the x-direction, MSDy is along the y-direction, and MSDz is along the z-direction.....	112
Figure 88: Movement of NP linear molecule in silicalite at 300K at t=0 (left, where the arrow shows the sinusoidal channel) and at t=1500ps (right, where the arrow shows the straight channel)	113
Figure 89: Radial distribution function between the hydrogen of the alcohol group of nonylphenol and the oxygen of the framework at 300K	114
Figure 90: Radial distribution function between the hydrogen of the alcohol group of nonylphenol and the oxygen of the framework at 400K	115
Figure 91: Movement of NP linear molecule in silicalite at 400K at t=0 (top left) and at different times. The molecule diffuses along the x axis in these pictures.....	116
Figure 92: Mean square displacement of OPLS-AA BPA molecule at 300K in silicalite. MSDx is along the x-direction, MSDy is along the y-direction, and MSDz is along the z-direction.....	117
Figure 93: Mean square displacement of OPLS-AA BPA molecule at 400K in silicalite. MSDx is along the x-direction, MSDy is along the y-direction, and MSDz is along the z-direction.....	118
Figure 94: Mean square displacement of OPLS-UA BPA molecule at 300K in silicalite. MSDx is along the x-direction, MSDy is along the y-direction, and MSDz is along the z-direction.....	118
Figure 95: Mean square displacement of OPLS-UA BPA molecule at 400K in silicalite. MSDx is along the x-direction, MSDy is along the y-direction, and MSDz is along the z-direction.....	119
Figure 96: Radial distribution function between the hydrogen of the alcohol group of bisphenol-A and the oxygen of the framework at 300K	120
Figure 97: Radial distribution function between the hydrogen of the alcohol group of bisphenol-A and the oxygen of the framework at 300K	121

Abstract

In this thesis we investigated the separation of two endocrine disrupting chemicals (EDC), bisphenol-A (BPA) and nonylphenol (NP) from water over the defect free silicalite zeolite. Two force-fields were investigated, the OPLS-AA force-field which is an all-atom one, and the OPLS-UA force-field which is a united atom one. In order to be able to simulate BPA, we simulated and studied the diffusion of different molecules in silicalite.

We compared two famous bulk water models, the non-rigid TIP3P modified for CHARMM model and the rigid SPC model, to literature and simulated the diffusion of these water molecules at temperatures from 300K to 600K. We found that these models coupled with our parameters for silicalite compared poorly with literature except for values calculated by Yazaydin et al. The mean-square displacements (MSDs) were more important in the x-direction (sinusoidal channel) than in the expected y-direction (straight channels) for both models resulting in small self-diffusion coefficient values. Results tended to improve as temperature increased. We believe that the high number of hydrogen bonds, implying the presence of clusters of water molecules, is responsible for the poor self-diffusion coefficient. The charges chosen to describe our silicalite zeolite, +2.05, may also be a reason of our small self-diffusion coefficient.

We then investigated the self-diffusion of aromatic molecules at 300 and 400K. Benzene, phenol and toluene were studied. We found self-diffusion coefficients for benzene that did not compare well to experiments but that was close to simulation work done by Rungsirisakun et al. Our diffusion coefficients for benzene were several orders of magnitude bigger than the experimental values found in literature for both force-fields. The diffusion patterns for both phenol and toluene did not allow us to calculate self-diffusion coefficients for both investigated force-fields. We believe that the jumps in the MSDs of these molecules are due to the rotation that they undergo in the nanopores. Phenol anchors to the framework by hydrogen-bonds between the hydrogen of its alcohol group and the oxygen of the framework. The diffusion seems to happen when the alcohol group is in a line with one channel. The same diffusion phenomenon was seen for toluene molecule but was related to the methyl group attached to its benzene ring. When this group is in front of a channel, the energetic barrier is reduced and the molecule can diffuse through it.

Finally bigger molecules were simulated and studied. Neopentane seemed to have a very low self-diffusion coefficient in silicalite if it could move at all. We report values of self-diffusion of $1.3 \cdot 10^{-14} \text{ m}^2.\text{s}^{-1}$ at both 300K and 400K. This value seems a little high compared to benzene experimental self-diffusion coefficient values that are in the same order of magnitude at both temperatures. The linear nonylphenol molecule that we simulated seemed to diffuse through silicalite with patterns that were close to the one seen for phenol. The hydrogen bonding between its alcohol group and the framework slows down its diffusion in silicalite. With the same reasoning as for phenol we decided not to calculate diffusion coefficient for NP. The last molecule investigated was bisphenol-A (BPA). We found that BPA almost did not diffuse through silicalite. The size of the molecule can explain why it did not diffuse, but we believe that the angle between the two phenol groups should be able to bend enough for it to diffuse, slowly, through silicalite. Our conclusion is that the two phenol groups at both ends of the molecules are the most important factor in its very slow diffusion. Hydrogen bonding is taking place at both ends making it very hard for the molecule to move in the framework. We decided to generate self-diffusion coefficients for this molecule because the diffusion process did not have jumps. We found self-diffusion coefficient that are $3 \cdot 10^{-15} \text{ m}^2.\text{s}^{-1}$ and $15 \cdot 10^{-15} \text{ m}^2.\text{s}^{-1}$ at 300 and 400K respectively for the OPLS-AA force-field, and $11.6 \cdot 10^{-15} \text{ m}^2.\text{s}^{-1}$ and $6.68 \cdot 10^{-15} \text{ m}^2.\text{s}^{-1}$ at 300 and 400K respectively for the OPLS-UA force-field. The last result was unexpected as we thought that the self-diffusion coefficient was going to increase with temperature. We believe that running much longer simulations for every molecule that we studied should give more reasonable and reliable results as the self-diffusion coefficients values are very small.

Introduction:

Endocrine disrupting compounds are a family of molecules that can interfere with human or animal endocrine systems. Their effects are negative and can lead to various problems. Contacts with these molecules are usually through food or water. Their increasing production and usage are drawing more attention. In this report we decided to focus on two endocrine disrupting molecules in particular, bisphenol-A and nonylphenol.

Different techniques exist to separate them but none of them achieves a total removal or a harmless deterioration. Therefore new techniques need to be investigated. In this report we study the diffusion of bisphenol-A and nonylphenol, as well as other smaller molecules (water, benzene, phenol, toluene, neopentane) in an all-silica zeolite structure, silicalite, by molecular dynamics simulations based on OPLS force-fields.

This thesis starts with an introductory section on where background information on endocrine disruptive compounds, zeolites and molecular dynamics will be given. The following part covers the methodology, i.e. the parameters used for each simulation, as well as an explanation on the results we chose to study. The last part is the investigation of the different diffusion patterns of our molecules of interest.

Background information:

In this part of the report we first take an in-depth look at our molecules of interest bisphenol-A and nonylphenol. We then explain why we decided to work with silicalite to separate them from water. Finally we give more details on the simulations we ran.

I- Endocrine Disrupting Chemicals:

Endocrine Disrupting Compounds (EDCs) are chemical compounds that have variable effects on our health and environment. They interact with the endocrine system by leading to the releasing of more or less hormones which can have different negative effects such as infertility, sexual underdevelopment, attention deficit or hyper activity¹. The increasing usage of pharmaceuticals, industrial and/or household chemicals release more EDCs in our environment is therefore a growing concern. This group of molecules has not drawn much attention in the past because they are usually in solution at very low concentrations and are hard to be detected. The development of new techniques and the improvement of existing ones now allow us to trace low levels of EDCs in different systems.² Several groups are now trying to generate databases to evaluate how important this exposure actually is in different places around the world¹.

1- Bisphenol-A

The EDC family is composed of a wide range of chemicals with varying properties and fates in a variety of environments. One molecule in particular, Bisphenol-A (BPA), has been of interest. BPA is a colorless solid soluble in organic solvents but only slightly in water. Figure 1 shows the BPA structure.

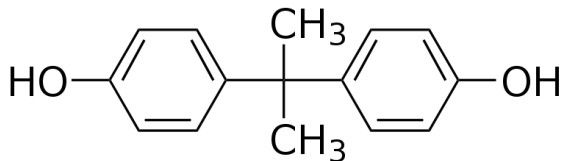


Figure 1: Molecular formula of Bisphenol-A

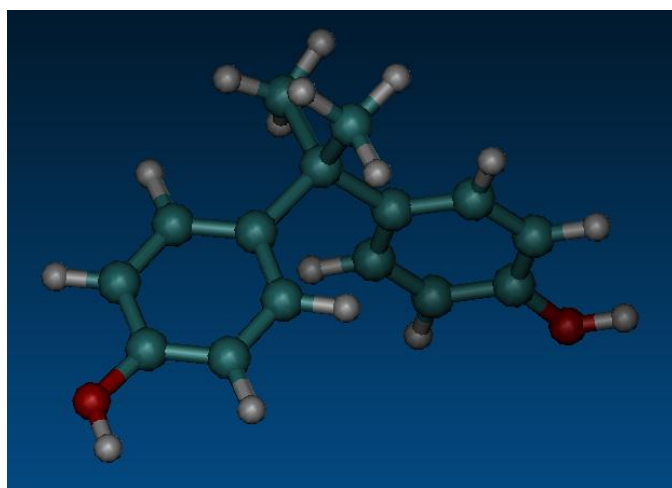


Figure 2: Three-dimensional molecular structure of Bisphenol-A

This molecule has received attention because of its widespread usage in our everyday life. BPA is considered a high volume industrial chemical³ and different sources evaluate its production to be between 2.2 and 3.2 million tons a year worldwide. These numbers are predicted to increase by 7% in the next few years⁴. 72% of the production is polymerized to form polycarbonate plastics and 21% to form epoxy resins. These polymers and resins are then used as drink containers, in metal food cans, as inner coating for reservoirs and pipes but also as digital media (CDs, DVDs), for sports safety equipment or automobiles^{1,55}. The ester bonds creating these polymers can be broken under high temperature freeing BPA molecules in liquid solutions. A paper from 1993 by Krishnan et al.⁵ showed that BPA was found in solution after clean water was autoclaved in a polycarbonate flask. More than 1.8 million pounds are released to the environment in the US, often where commercial or waste plastics are processed or recycled. A paper from the US Geological Survey⁶ points out that BPA is found in wastewater treatment plants (WWTPs) effluents at a concentration of around 1 µg.L⁻¹. Bisphenol-A can also be found in indoor or outdoor air and in floor dusts.

The number of papers on BPA is increasing because there is still debate on how toxic BPA is for human health^{7,3, 4, 8}. Some sources argue that Bisphenol-A is not toxic at low doses. Various other papers argue that BPA has significant effects on animals and humans. BPA exposure seems to increase the incidence of cancer, the development of antibiotic resistance bacteria², to have effect on obesity⁹ or could create neurological health issues. Howdeshell et al.¹⁰ argue that effects of high dose exposure to BPA became apparent over the past 50 years and are consistent with the ones seen in animals. Some other sources agree that if BPA has an effect it would most likely be on fetuses, young children and women^{3, 10}. Research suggests that BPA does not persist in the human body except in body fat⁴. The Center for Disease Control discovered that in a pool of 2,517 people almost 93% of them were exposed to BPA, and that females had a higher concentration than males. Typical human exposure to BPA seems to be continuous⁶ but no study to our knowledge looked into the effects of a continuous exposure on animals or humans. Nevertheless, the potential negative effects of BPA exposure warrant the need to control our exposure to this compound.

The main source of Bisphenol-A(BPA) exposure for humans seems to be through food and water.^{3, 4} There is therefore a need to separate BPA from liquid solutions, more specifically, from water. Unfortunately, no basic wastewater or drinking water treatment eliminates EDCs¹: EDCs are usually very stable and the residence time though the bacterial sludge used in most WWTPs is too small to destroy BPA. Different techniques are used to try to get rid of BPA⁶. Chemical degradation by micro-organisms or UV light has a major drawback as it could produce smaller and still hazardous molecules present at low concentrations. Membrane bioreactors seem to give promising results if the effluents are disinfected with chlorine compounds⁶. Granular activated carbon is a well-known adsorbent of BPA but has a great affinity for dissolved humic acids that may reduce the sorption of EDCs and does not seem to be very selective. Nevertheless, an anionic adsorbent based on granular Mg-Al layered double hydroxide gave promising results for relatively low cost¹. Kim et al.¹¹ created an organic-inorganic hybrid mesoporous material that was highly selectivity for BPA against phenol compared to powder activated carbon. Nevertheless, new adsorbents with a high selectivity towards BPA need to be discovered or manufactured.

2- Nonylphenol

Nonylphenol (NP) and nonylphenol ethoxylates (NPE) are members of the alkylphenol and alkylphenol ethoxylate family of non-ionic surfactant. They also both belong to the Endocrine Disruptive Compound group according to the Pesticide Action Network North America⁵⁶. While NP and NPEs seem to be less publically known than BPA, a number of studies has been led on ways to separate them^{12, 13, 14, 15, 16}. Most of these studies deal with the separation of different NP isomers or the separation of NP from NPEs. NP is a pale, yellow viscous liquid at room temperature even if the pure product is colorless. NP is produced by the alkylation of phenol with nonenes. Nonylphenol compounds are usually highly branched and the nonyl group attaches at the 4- and sometimes 2-position of the phenol ring. This gives rise to a number of possible configurations for NP. Figure 3 gives a few examples.

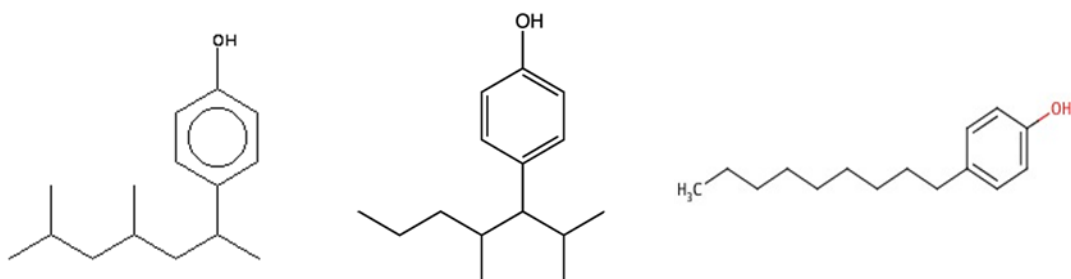


Figure 3: Different isomers of nonylphenol

NPEs are oily orange liquid and waxy solids. They are manufactured by reacting nonylphenol and ethylene oxide. NPEs are hydrophobic at one end and hydrophilic at the other. That is why they are mostly used as surfactants.

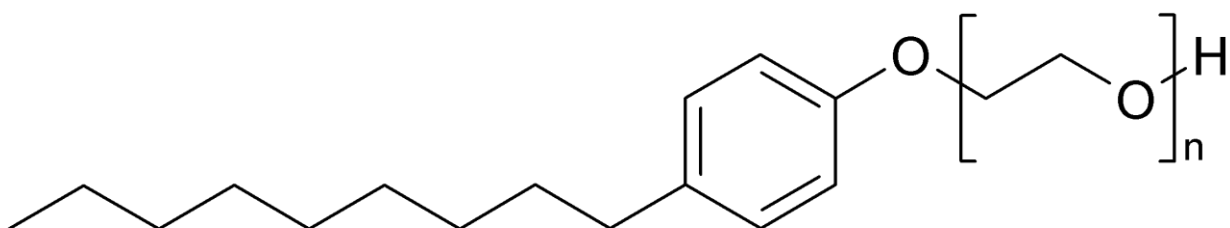


Figure 4: Nonyphenol ethoxylates structure

Both molecules are produced in large quantities and have a various number of applications. The production of NP in 1997 was around 77,000 tons in Europe. NP is used as a building block for monomers that are further manufactured to give resins and polymers¹⁷. Nonylphenol (NP) is mostly used as an intermediate for the reaction of NPE (60% of the production in Europe). The length of NPEs can be varied by the ratio of phenol and ethylene oxide that is used during the reaction. NPEs are used as cleaning and washing agents, surface active or foaming agents. We can find NPE containing products in a variety of industry like institutional cleaning, textile and leather auxiliaries, emulsion polymerization or paint production¹⁷. The large production of NP and NPE leads to an increase of their release in our environment. NPEs can be degraded in the environment, but that degradation leads to a production of smaller and more resistant NP. It has been shown that NP has negative effects on aquatic species. NP takes a long time to degrade and therefore its accumulation is steadily increasing. Similar to BPA, the exposure to NPs and NPEs is mostly through inhalation of particles in the air or ingestion of contaminated food products. The main problem with NP is that waste water treatment plants do not degrade or separate it efficiently from water. Therefore a need to find an efficient way to separate it from water is needed.

II- Zeolites for separation:

One of the main features of EDCs is that they are very stable and have multiple functional groups that make transport and degradation in mesoporous structures complex. Motivated by the need to remove BPA and other EDCs from water streams, we investigated how zeolites could be used for EDC separations.

Zeolites are microporous, aluminosilicate minerals with well-defined structures. Channels of different sizes and cages are interconnected to create a multidimensional porous system. Zeolites are also called “molecular sieves” because of their ability to selectively sort molecules based on their size and moieties. Only certain molecules are allowed to adsorb or go through their microporous structure. This can impact their diffusion, leading to selectivity between guest molecules as some of them will diffuse along the pores much faster than others. These selectivity characteristics motivated this work to study how zeolites could be used to separate BPA from

water; some zeolites are known to be very hydrophobic and the difference in size and groups between water and BPA is very important.

The framework of zeolites is based on TO_4 tetrahedra, where T is a site that can either be a silicon or an aluminum atom. These tetrahedral primary building units (BUs) can then form secondary building units of various types such as 6-rings, 8-rings or 12-rings^{18, 19, 20, 21}. These different BUs create the complex but precisely repetitive zeolite structure. An all silica zeolite has a Si/O ratio of $\frac{1}{2}$, giving it a neutral structure since Si atoms are formally 4+ and O atoms are 2-. When the Si atoms (4+) are replaced by Al atoms (3+), the total charge of the zeolite becomes negative and cations like H^+ , Na^+ , K^+ , Ca^{2+} or Mg^{2+} must be added to the framework to remain neutral. These non-framework cations play an important role as some molecules might interact with them more strongly than others leading to an even lower diffusivity^{22, 23, 24, 25, 26, 27, 18, 19, 20}. Zeolite catalytic activity is mostly linked to these cations, most importantly H^+ . Silanol nests or Brønsted acid sites for instance can be formed. The acid sites concentration is linked to the Si/Al ratio of the T sites and activity usually increases with a higher number of aluminum atoms.

Because of these very interesting characteristics zeolites are used in a wide range of industries. Natural zeolites are good ion-exchangers and are used in wastewater and drinking water treatment as heavy metal removers^{28, 59}. The petrochemical industry uses their catalytic properties for organic reactions like fluid catalytic or deep catalytic cracking, isomerization of olefins or xylenes and hydrocarbon synthesis^{29, 30, 28, 31, 27}. They are also used to treat nuclear waste products^{28, 59}. They can remove fission products since their alumino-silica structure has a great resistance to radiation. Once they are loaded with waste products they can be hot-pressed to form a very durable ceramic form, trapping the waste product. To date, over 190 natural and synthetic zeolites are known with different structures, pore sizes and properties. We chose to work with silicalite, a common synthetic zeolite, for our project because of its pore size, structure and great hydrophobicity.

Silicalite

Zeolites having the MFI structure are among the most studied zeolite for their very special characteristics and widespread usage. MFI stands for Mobil 5(ring) and is part of the pentasil zeolites. It also is known as ZSM-5, and can have a Si/Al ratio in the range of about 35 to infinity. The all silica end member is called Silicalite. MFI zeolites are used for instance during the alkylation of benzene³⁰, for xylene isomerization or shape selective cracking^{28,57}. The lattice structure of MFI consists of straight (y axis) and zigzag (x axis) channels. The z-axis channel is a mix of straight and sinusoidal channels.

The straight channel cross section, around $5.7 \times 5.2 \text{ \AA}$, is big enough to fit a benzene ring and let it diffuse through³². As said earlier, silicalite is an all-silicate zeolite (no Al atoms). This characteristic makes it very hydrophobic since theoretically no aluminum is present in the lattice and so, no non-framework atom is present to compensate the charge difference. This has a great impact of the diffusion of water since the interactions between water molecules are more important than the water-zeolite ones in silicalite. A unit cell of silicalite consists of 96 (SiO_2) tetrahedral units generating 2 straight channels and four sinusoidal channels. The framework density of silicalite is 1.8 g.cm^{-3} and the specific micropore volume is $0.19 \text{ cm}^3.\text{g}^{-1}$. More details about the simulation of silicalite will be given in the Methodology section of this report.

III- Molecular modeling

Molecular modeling (MM) aims at representing different system and physical properties at an atomic scale. This type of simulation can be used in a wide range of fields such as drug design, protein engineering or materials science⁵⁸. Computer simulations are useful when experiments are not possible for reasons like cost, time or experimental limitations. One advantage is that various thermophysical data can be determined from simulations. The heat of vaporization, activation energy^{33,57} density or free energy can be calculated using computer simulations. One should be able to simulate almost any system using molecular modeling and while computer power has tremendously increased over the past decades, atomic systems usually do not exceed several hundred atoms due to computer limitations.

1- Molecular Dynamics:

One method of molecular modeling is molecular dynamics (MD). In this method molecular motion is simulated at finite temperature over a time length. The two crucial features of a MD simulation are the algorithm and the force-field (FF). The algorithm is the mathematical and computational procedure that will be followed during the simulation. Efforts have always been put in finding faster and more reliable algorithms. A force field is a set of equations and parameters used to describe the interactions between the different atoms or molecules of system. These interactions can be divided into two categories: intramolecular and intermolecular interactions. Intermolecular potentials describe the interactions between atoms that are not in the same molecule or separated by more than 3 bonds. They can be described either as electrostatic or van der Waals interactions. Intramolecular interactions describe the behavior of bonded atoms, or atoms within a molecule. They are divided in 3 categories: bonds, angles and dihedrals. A more in depth description of the algorithm and all these interactions are given below.

A. Algorithm

One very important hypothesis made by MD is the Born-Oppenheimer approximation. This approximation de-couples the nuclei and the electron motion based on the assumption that electrons velocities are far greater than those of nuclei. This approximation is very important because most of the time systems studied by MD are too large to be explored by quantum mechanics and we are interested in the motion of individual atoms⁵⁸. MD computes a series of states and transport properties by integrating the Newton's law of motion⁵⁹. The second law of Newton says that the force applied on a particle is equal to its change of momentum:

$$\vec{F} = m\vec{a} = m \frac{d^2\vec{r}}{dt^2} \quad (1)$$

where m is the mass of the particle, a its acceleration and r its (x,y,z) coordinates.

With this equation and a knowledge of the particles position and velocity, we can estimate the trajectory of our system as a function of time.

For a MD simulation a series of calculations is repeated for each step to determine the system's evolution with respect to time. Five steps are needed in order to start the simulation⁵⁸:

- Step1: The initial coordinates are read by the program.
- Step2: The velocity of each atom is determined. The initial velocities may be calculated based on the Maxwell-Boltzmann distribution, at the temperature chosen for the simulation:

$$\sum_{i=1}^N \frac{1}{2} m_i v_i^2 = \frac{3}{2} N_f k_b T \quad (2)$$

where m_i is the mass of atom i , v_i the initial velocity of atom i , N the total number of atoms in the system, k_b the Boltzmann constant, N_f the number of degrees of freedom and T the temperature of the system.

- Step3: The force applied to each atom is calculated using the equations of the force-field.

$$F = -\frac{dU}{dr} \quad (3)$$

U is the total energy of the system as defined in the following part dealing with force-field equations, and r is the coordinate of the atom.

- Step 4: Newton's law of motion is integrated using the known forces in order to find the coordinates and velocity of our atoms at a new time $t+\Delta t$.
- Step 5: The force applied on each atom is calculated using the new velocities and coordinates found at step 4 for the new time.

Steps 4 and 5 are repeated until the simulation ends.

Step 4 needs an algorithm in order to numerically integrate the equations of motion. There are different algorithms available, one of the most popular is the Velocity Verlet (VV) algorithm and is the one we used for our simulations.

B. The velocity Verlet Algorithm (VV):

The VV algorithm assumes that velocities and positions of all atoms are known. It proceeds in 2 steps:

- Step1: a half-step velocity is calculated:

$$\underline{v}\left(t + \frac{1}{2}\Delta t\right) = \underline{v}(t) + \frac{1}{2}\Delta t \underline{\underline{f}}(t) \quad (4)$$

Then using this result the full timestep coordinates are obtained:

$$\underline{r}(t + \Delta t) = \underline{r}(t) + \Delta t \underline{v}\left(t + \frac{1}{2}\Delta t\right) \quad (5)$$

- Step 2: Using the new positions obtained in step 1, the forces are calculated at the new time $\underline{\underline{f}}(t + \Delta t)$ and finally the velocity at the full timestep is calculated:

$$\underline{v}(t + \Delta t) = \underline{v}\left(t + \frac{1}{2}\Delta t\right) + \frac{1}{2}\Delta t \underline{\underline{f}}(t + \Delta t) \quad (6)$$

In the end the coordinates, velocities and forces at the new time step for each atom are calculated.

One of the reasons why VV is one of the most popular algorithms is because of its relative simplicity. It is also reversible (similar to real equations of motion) and has a small energy drift over long simulation times.

C. NVT Thermostat:

We used the NVT-Nosé-Hoover ensemble for our simulations³⁴. This means that the number of particles N, the volume of the system V and the temperature T are kept constant during the simulations. The temperature fluctuation with the NVT-Hoover thermostat was between 5 and 10% around the set temperature and the average temperature on a run was very near the set temperature.

D. Periodic Boundary Conditions

A common approach during MD simulations is to use periodic boundary conditions. This implies that the “original” simulation box is reproduced through space. Atoms in the reproduced boxes move the same way as in the central box. Therefore when an atom leaves the box from one side, it will reappear on the opposite side.

E. Force Field:

A force field (FF) refers to a set of parameters and equations that describe the potential energy (U) of an atomic or molecular system. The geometry of the atoms determines the energy of the system based on the FF equations and parameters. The parameterization of FFs is typically done by comparing results obtained in force field simulations and the results obtained by quantum mechanics and/or experiments. The potential energy is divided into 2 parts, the intermolecular and intramolecular interactions. Intermolecular interactions are further divided into two groups, electrostatic and van der Waals interactions. Intramolecular are usually described by three main components: bond stretching, angle bending and torsional potentials.

$$\left\{ \begin{array}{l} U_{tot} = U_{inter} + U_{intra} \\ U_{inter} = U_{elec} + U_{VdW} \\ U_{intra} = U_{bond} + U_{angle} + U_{tors} \end{array} \right. \quad (7)$$

1- Force field choice

For this work, we chose to work with the OPLS (Optimized potentials for Liquid Simulations) force field^{35, 36, 37}. Two different OPLS force fields are available, the OPLS-UA which is a united atom force field and the OPLS-AA which is an all atom force field. United atom force fields do not model the hydrogen atoms adjacent to carbon atoms, but hydrogen atoms are implicitly modeled in the carbon force field parameters. In contrast all-atom force fields include every atom explicitly. Each force-field has proven to have excellent results compared to liquid phase experiments for molecular volumes, heats of vaporization or interaction energies. Our molecules of interest in this work have benzene rings and OPLS-UA treats these molecules as rigid while the OPLS-AA has parameters for bonds, angles and dihedrals potentials, or allows the aromatic rings to move during simulation and have some flexibility. We compared the performance of these two force-fields and assessed the importance of keeping a molecule rigid or not.

We decided to use two very well-known force-fields to describe our water molecules: The SPC model and the TIP3P modified for CHARMM^{36, 38}. Both of these models are 3-site models, meaning that each atom of H₂O is modeled individually. SPC treats water as a rigid molecule while the TIP3P modified can either be rigid or non-rigid. We used the non-rigid TIP3P model in order to determine what impact vibrational motion would have on the diffusivity of water in nanoporous materials.

2- Intermolecular interactions:

a- Electrostatic potential:

The electrostatic potential arises from the unequal repartition of electron over the atoms of a molecule. This repartition is due to the electronegativity of individual atoms and leads to charge accumulation on different atoms in the molecule. Usually in order to account for these charges, force fields put partial charges on atoms and since polarization effects are often neglected, these charges are constant. The electrostatic potential is given by Coulomb's equation:

$$U_{elec} = \frac{1}{4\pi\epsilon_0\epsilon_r} \frac{q_i q_j}{r_{ij}} \quad (8)$$

Where ϵ_0 is the permittivity of vacuum, ϵ_r the relative dielectric constant of the system, q_i and q_j the partial charges of atom i and j respectively and r_{ij} the distance between atoms i and j.

Electrostatic interactions account for both short and long range interactions, but are repetitive in nature due to periodic boundary conditions. The Ewald sum is used in order to calculate these interactions in a periodic system and is expressed as the sum of three terms, the real space term, the reciprocal space term and the self-energy correction^{59,60}.

- Real space term:

Each ion is effectively neutralized at long range by a Gaussian charge distribution of opposite sign centered on the ion. This sum gives the real space part defined mathematically as:

$$U_{real} = \frac{1}{4\pi\epsilon_0} \sum_{i < j}^{N^*} \frac{q_i q_j}{r_{ij}} \operatorname{erfc}(\alpha r_{ij}) \quad (9)$$

where ϵ_0 is the permittivity of vacuum, $\operatorname{erfc}(x)$ the complementary error function, q_i and q_j the partial charge of atom i and j respectively, r_{ij} the distance between atom i and j and α is a number high enough to take into account only the closest images.

- Reciprocal space term:

For this term the Gaussian charges are superimposed with the same sign as ion charges thereby nullifying the effects of the first set of Gaussians. The potential is obtained by the Poisson's equation and is solved using Fourier series. It is expressed as:

$$U_{recip} = \frac{1}{2V_0\epsilon_0} \sum_{k \neq 0}^{\infty} \frac{\exp\left(-\frac{k^2}{4\alpha^2}\right)}{k^2} \left| \sum_{j=1}^N q_j \exp(-i\vec{k} \cdot \vec{r}_j) \right|^2 \quad (10)$$

where N is the number of ions in the system, V_0 the simulation cell volume and \vec{k} is a reciprocal lattice vector defined by:

$$\vec{k} = l\vec{u} + m\vec{v} + n\vec{w} \quad (11)$$

in this equation l, m, n are integers and $\vec{u}, \vec{v}, \vec{w}$ are the reciprocal basis vector.

- Self-energy correction term:

This third term is needed to correct the Gaussian acting on its own site and is a constant.

It is written as:

$$U_{self} = -\frac{1}{4\pi\epsilon_0} \sum_{molecules} \sum_{l < m}^{M^*} q_l q_m \left[\delta_{lm} \frac{\alpha}{\sqrt{\pi}} + \frac{erf(\alpha r_{lm})}{r_{lm}^{1-\delta_{lm}}} \right] \quad (12)$$

In this equation q^l and q^m are the partial charges of atom l and m respectively, and r^{lm} is the distance between atom l and m. In the end the total energy calculated by the Ewald sum is the following:

$$\begin{aligned}
U_{ewald} &= U_{real} + U_{recip} + U_{self} \\
&= \frac{1}{4\pi\epsilon_0} \sum_{i<j}^{N^*} \frac{q_i q_j}{r_{ij}} \operatorname{erfc}(\alpha r_{ij}) \\
&\quad + \frac{1}{2V_0\epsilon_0} \sum_{k \neq 0}^{\infty} \frac{\exp\left(-\frac{k^2}{4\alpha^2}\right)}{k^2} \left| \sum_{j=1}^N q_j \exp(-i\vec{k} \cdot \vec{r}_j) \right|^2 \\
&\quad - \frac{1}{4\pi\epsilon_0} \sum_{molecules} \sum_{l < m}^{M^*} q_l q_m \left[\delta_{lm} \frac{\alpha}{\sqrt{\pi}} + \frac{\operatorname{erf}(\alpha r_{lm})}{r_{lm}^{1-\delta_{lm}}} \right]^2
\end{aligned} \tag{13}$$

b- Van der Waals potential:

Van der Waals potentials describe short-range interactions between atoms that are from different molecules as well as two atoms that are in the same molecule. They usually are divided into two categories the repulsive forces and the dispersion forces. Repulsive forces can be explained by the Pauli principle; electrons with the same spin cannot occupy the same region in space. Dispersion forces are temporary attraction forces that are induced by the temporary dipoles formed by atoms even if the molecule is non-polar. The Lennard-Jones model is a very famous model used to describe these interactions. It is a pair potential function of distance between atoms of different molecules or atoms of the same molecule separated by at least 3 bonds. The Lennard-Jones 12-6 potential is one of the most used LJ potentials and is the following:

$$U_{LJ} = U_{rep} + U_{attrac} = 4\epsilon \left[\left(\frac{\sigma}{r_{ij}} \right)^{12} - \left(\frac{\sigma}{r_{ij}} \right)^6 \right] \tag{14}$$

In this equation σ is the Lennard-Jones size parameter, or collision diameter, and ϵ the potential well depth. At the separation distance $r_{min} = 2^{\frac{1}{6}} * \sigma$ we have $U_{LJ} = -\epsilon$. This can be seen in Figure5. The attractive part in r_{ij}^{-6} is the dispersive VdW interactions while the r_{ij}^{-12} term represents the repulsion of two atoms close together.

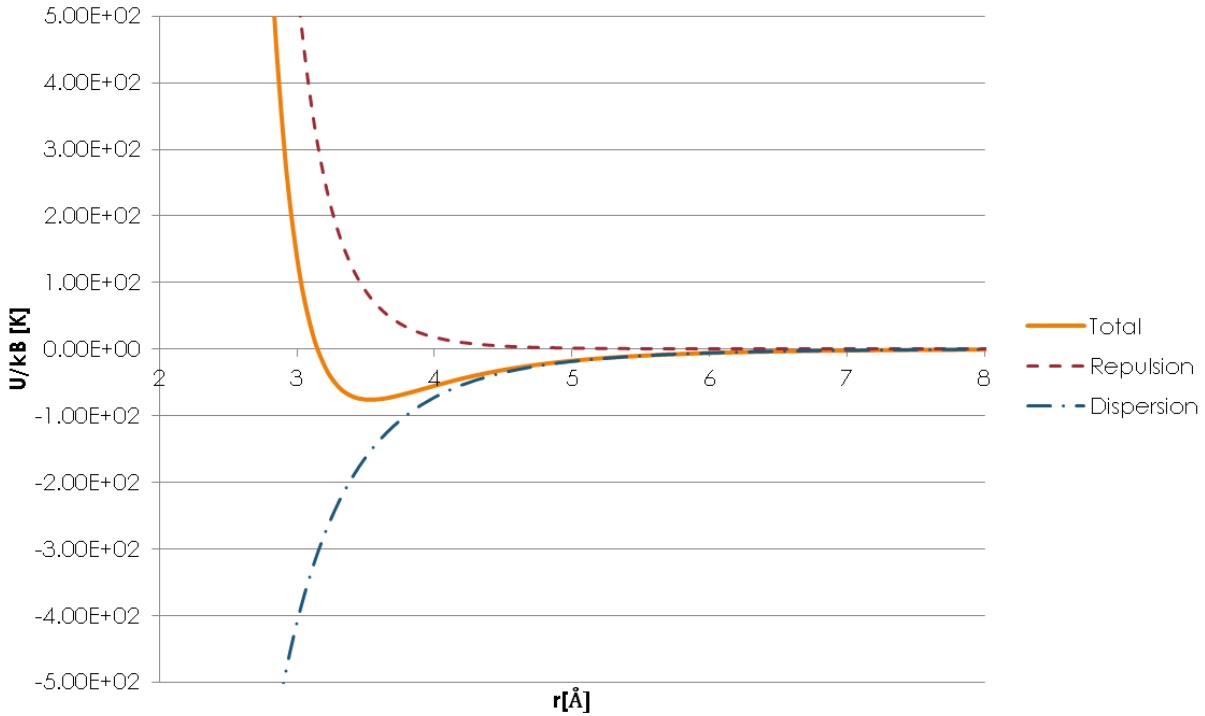


Figure 5:Lennard-Jones potential for Oxygen in water with $\sigma_{OO}=3.1506 \text{ \AA}$ and $\varepsilon_{OO} = 0.6357 \text{ kJ.mol}^{-1}= 76.46\text{K}$

LJ potential is a short range interaction and therefore it is common to truncate it, i.e. stop taking it into account, at a certain distance called the cut-off distance, or r_c .

The van der Waals potential is written as follows:

$$\begin{cases} U_{LJ} = U_{LJ}(r_{ij}), & r_{ij} \leq r_c \\ U_{LJ} = 0, & r_{ij} > r_c \end{cases} \quad (15)$$

It is important to note that the smallest length of the simulation box has to be at least two times bigger than the cut-off distance. This is implied by the use of periodic boundary conditions and the minimum-image convention. This convention states that atom i can only interact with the nearest image of atom j.

Usually the mixed parameters σ_{ij} and ε_{ij} are estimated using the parameters σ_{ii} and ε_{ii} describing interactions between the same atoms. Different rules, such as the Lorentz-Berthelot mixing rules, are used to estimate these mixed parameters. OPLS-AA force field uses the geometric mixing rules:

$$\begin{cases} \sigma_{ij} = \sqrt{\sigma_{ii}\sigma_{jj}} \\ \varepsilon_{ij} = \sqrt{\varepsilon_{ii}\varepsilon_{jj}} \end{cases} \quad (16)$$

c- Buckingham potential

Another way to describe the short range interactions is the Buckingham potential, which is an alternative to the Lennard-Jones potential. It is used for the zeolite structure, and is expressed as follows:

$$U(r_{ij}) = A \exp\left(-\frac{r_{ij}}{\rho}\right) - \frac{C}{r_{ij}^6} \quad (17)$$

where A, ρ and C are constants, and r^{ij} is the distance between atom i and j.

d- Three-body potential

A three body potential is often used to describe zeolite interactions. We used the screened Vessal potential to describe the zeolite silicalite based on the work of Auerbach et al.³⁹. The three-body expression is as following:

$$U(\theta_{jik}) = \frac{k}{8(\theta_{jik} - \pi)^2} \left\{ [(\theta_0 - \pi)^2 - (\theta_{jik} - \pi)^2]^2 \right\} \exp\left[-\left(\frac{r_{ij}}{\rho_1} + \frac{r_{ik}}{\rho_2}\right)\right] \quad (18)$$

In this equation θ_{jik} is the angle between atom j, i and k, θ_0 is the equilibrium angle, k, ρ_1 and ρ_2 are constants, r_{ij} and r_{ik} are the distances between atoms i and j and atoms i and k respectively.

3- Intramolecular interactions:

a- Bond stretching

The bond stretching potential describes the bonding between two neighboring atoms. The Morse potential, the Quartic, or the 12-6 potential could be used to calculate the bond stretching but OPLS uses a harmonic potential. In this potential the two atoms are bonded by a spring force.

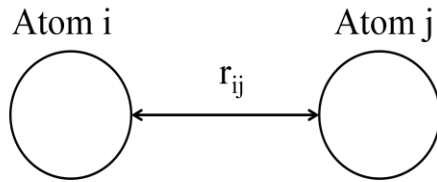


Figure 6: Bond stretching

$$U_{bond}(r_{ij}) = \frac{1}{2} K_r (r_{ij} - r_0)^2 \quad (19)$$

In this equation K_r is the force constant, or stiffness of the bond, r_{ij} is the distance between atom i and j, and r_0 is the equilibrium bond length. When we use a rigid molecule we assume that the bond lengths are constant and this potential is not needed.

b- Angle bending:

Two atoms that are bonded to the same atom make an angle θ_{ijk} . There are many potentials that could be used to describe the behavior of an angle such as the Quartic potential, the truncated harmonic, the cosine or the MM3 stretch-bend potential.

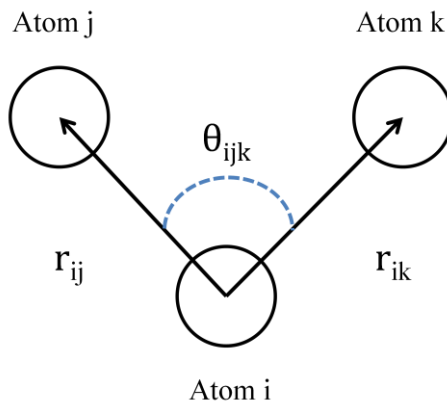


Figure 7: Angle bending

OPLS uses the harmonic potential that once again describes the angle as a spring.

$$U_{angle}(\theta_{ijk}) = \frac{1}{2} K_\theta (\theta_{ijk} - \theta_0)^2 \quad (21)$$

K_θ is the bond-bending constant, θ_{ijk} is the angle between atom j and k linked by atom i and θ_0 is the equilibrium angle.

c- Torsional potential

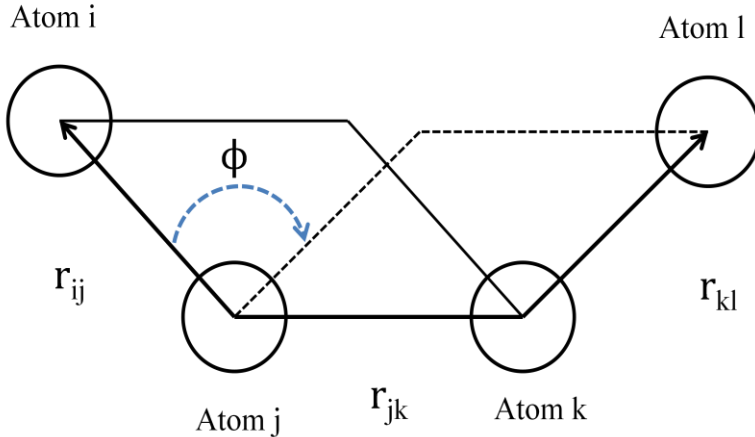


Figure 8: Torsional potential

The torsional potential describes the dihedral angle between four consecutive atoms of a molecule. It describes the way a molecule rotates (see Figure 9 for schematic of the dihedral angle ϕ) around a chemical bond and plays an important role in the conformation of a molecule. There are various torsional potentials such as the cosine potential, the triple cosine or Ryckaert-Bellemans potentials. The OPLS potential is defined as follows:

$$U_{dihedral}(\phi) = a_0 + 0.5 * [a_1(1 + \cos(\phi)) + a_2(1 - \cos(2\phi)) + a_3(1 + \cos(3\phi))] \quad (22)$$

In this equation a_0 , a_1 , a_2 and a_3 are constants and ϕ is the dihedral angle.

4- DL_POLY and DL_FIELD:

DL_POLY⁴⁰ is a molecular dynamics software that was developed at the Daresbury Laboratory starting in 1994. We used DL_POLY_2 version that is based on the replicated data parallelism method⁴⁰. DL_POLY is widely used in a great variety of fields such as interfaces and films, radiation damage studies or dissipative dynamic studies. We decided to use this software to study the diffusion of several different molecules in silicalite. In order to run a DL_POLY simulation at least 3 input files are needed: the FIELD, CONFIG

and CONTROL file. An in-depth description of these is given in the DL_POLY User Manual⁶⁰ and a few examples of these files used during our simulation are given in Appendix 1. After a simulation several output files are generated. Once again, a description of these and the other possible output files is given in the DL_POLY User manual.

We used DL_FIELD⁶², a software specifically designed to generate input files for DL_POLY. This software saves time and work for a wide range of molecules. Sample input files for DL_FIELD are available in Appendix 2.

One should note that DL_FIELD supports CHARMM and AMBER force fields but not the OPLS-AA or OPLS-UA force fields. Therefore, once the FIELD file (the file containing a description of the force field) was generated with DL_FIELD, we had to change our parameters in order to use the OPLS ones.

Methodology:

Depending on the force field one decides to use, the parameters describing the system will change. We simulated our molecules using the OPLS-AA force field and then ran the OPLS-UA force field in order to compare the results. In this section we give a description of the molecules we simulated and list the parameters used during our simulations. Then we explain which results we decided to look at and how we obtained them. Appendix 1 shows several examples of input files for our different systems.

I- Parameters for our system:

1- Silicalite:

As we stated earlier, the zeolite of interest for this thesis was silicalite. We used the coordinates of the orthorhombic (*Pnma*) structure given on the International Zeolite Association (IZA) structure database website⁶¹. We worked with two unit cells in the z-direction for our simulations (1 X 1 X 2 cell) as it is what is most common in literature^{33, 41, 22}. The parameters of a single unit cell are given in Table 1.

	a(Å)	b(Å)	c(Å)	α(deg)	β(deg)	γ(deg)
<i>Pnma</i>	20.090	19.738	13.142	90.00	90.00	90.00

Table 1: Lattice parameters of Pnma Silicalite structure

There are 96 Si atoms and 192 oxygen atoms in a unit cell, so our model had a total of 576 atoms in the zeolite framework. Bisphenol-A is a large molecule and may have difficulty fitting in the silicalite pores so we decided to work with a vibrating framework. Vibrations can have a great impact on the diffusion of molecules that barely fit in the zeolite framework. We used periodic boundary conditions in order to simulate a more realistic system. The bonds between O and Si atoms were held together by electrostatic interactions. We used the parameters from Auerbach et al.³⁹ to describe the short-range Buckingham interactions and a three-body potential used to keep the SiO₄ tetrahedral together. For partial charges, we decided to follow the same reasoning as Desbiens et al.⁴², wherein they argue that the formal charge of a silicon atom is around +4.0 and the bond between a silicon atom and an oxygen one in silicalite is roughly 50% ionic. Therefore, the partial charge should be close to +2.0 for Si and -1.0 for the oxygen atom of silicalite

(designated OZ in our work). Auerbach et al.³⁹ used a value of +2.4 which is relatively close to the one we used. These parameters are summarized in Table2, Table3 and Table4.

	Molecular weight[g.mol ⁻¹]	Partial charge
Si	28.0855	+2.050
OZ	15.9940	-1.025

Table 2: Parameters for Silicalite simulations

Type of VdW inter.	A[kJ]/ε[kJ]	ρ[Å]/σ[Å]	C[kJ.Å ⁶]
OZ-OZ	Buckingham	125997.200	0.3594
OZ-Si	Buckingham	1717021.83	0.50490
OZ-OZ ⁵⁸	Lennard-Jones	0.74497	2.8060
Si-Si	Lennard-Jones	0.00000	0.00000

Table 3: Electrostatic and Van der Waals parameters for silicalite

	K[kJ.rad ²]	ρ1[Å]	ρ2[Å]	θ ₀ [deg]
OZ-Si-OZ	70337.9600	0.3277	0.3277	109.47

Table 4: Three-Body potential for silicalite simulations

Note that examples of input files (CONTROL, CONFIG, and FIELD) are given in Appendix 1 at the end of this thesis.

Figure 10 to 12 are snapshots of the zeolite structure along the y-axis(straight channel), x-axis (zig-zag channel) and the z-axis (mix of Straight and zig-zag channels) that we generated with the parameters listed above.

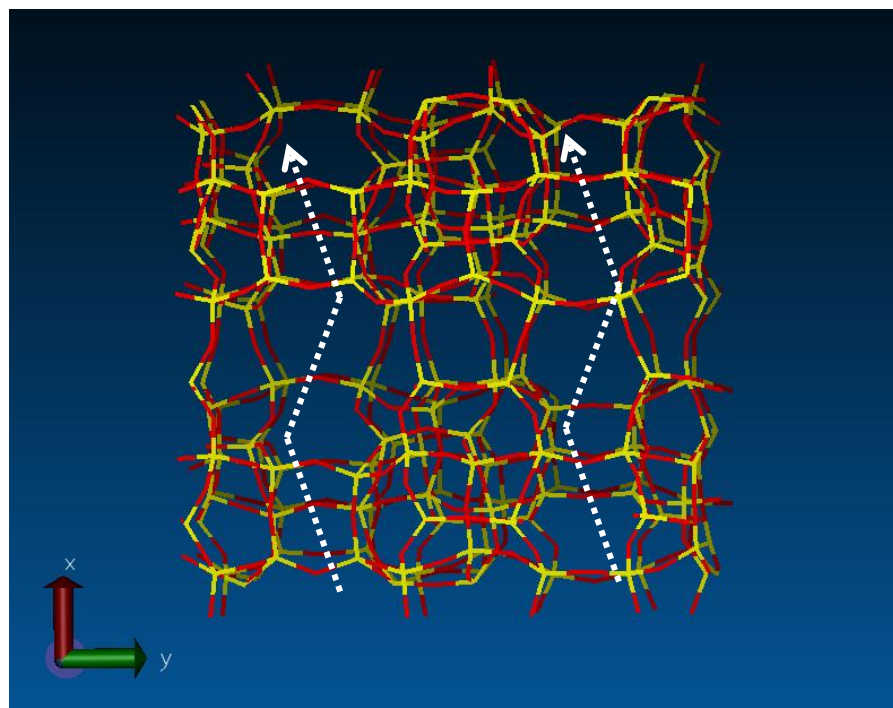


Figure 9: Silicalite x-axis, zigzag channel

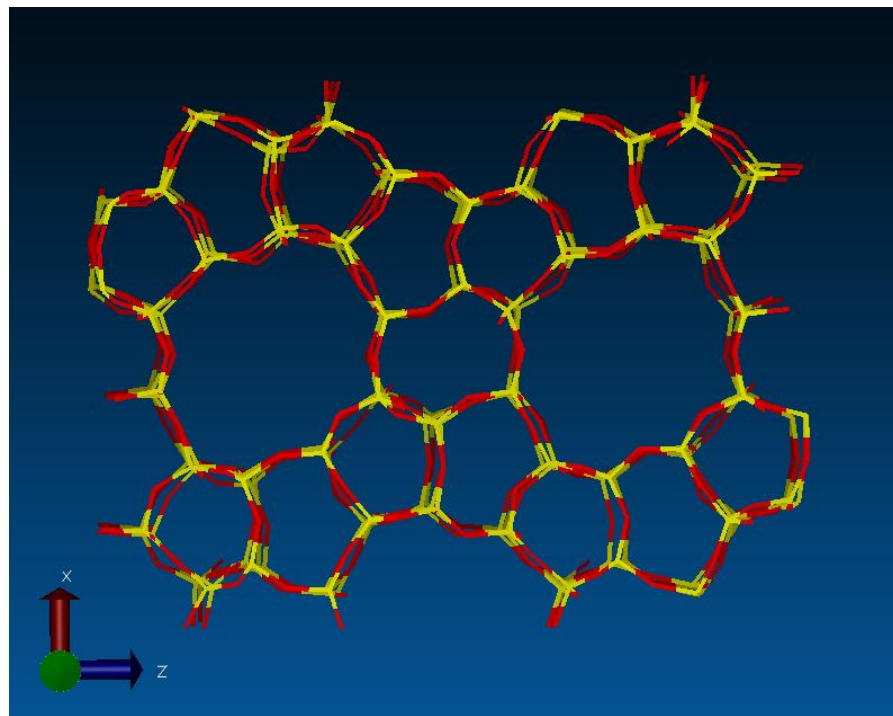


Figure 10: Silicalite y-axis, straight channel (into the plane of the page)

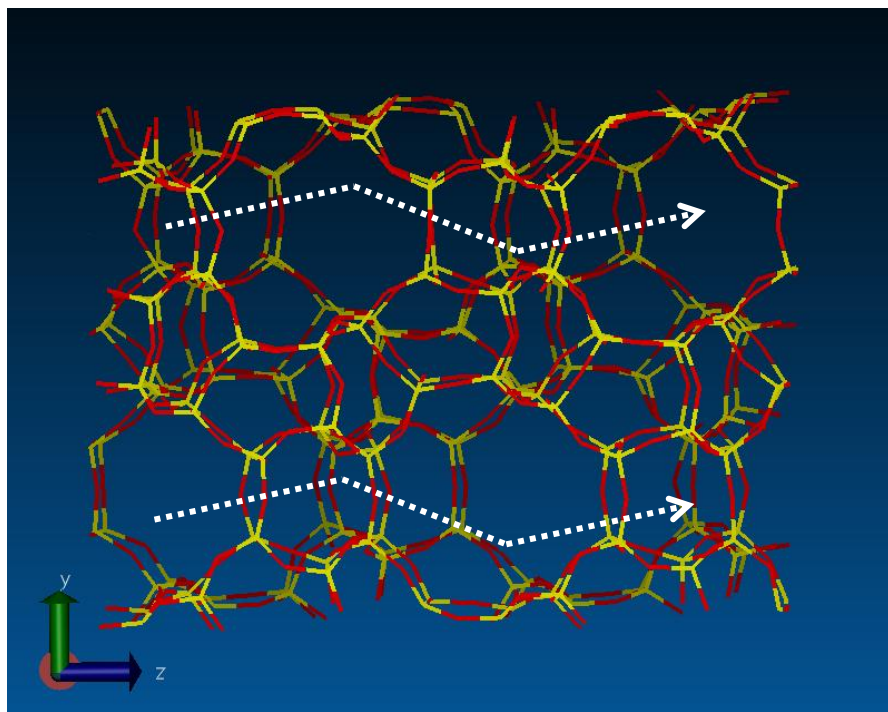


Figure 11: Silicalite z-axis, mixed channel

2- Water:

Water is a common and relatively simple molecule that has complex behavior. Its bulk liquid behavior is hard to reproduce during computational simulations and an important number of models have been developed to achieve this goal^{38, 36}. This behavior is due to the specificities of the water molecule itself; its attractive forces are linked to the so-called hydrogen bonds. In liquid phase, a water molecule can make up to 4 hydrogen bonds with 4 different neighboring molecules. As the temperature decreases, the number of H bonds increases until it reaches its maximum of 4.

As said earlier, we decided to work with two different models: The SPC model and the TIP3P modified for CHARMM model. We worked with 4 water molecules per intersection, i.e. 8 water molecules per unit cell or 16 water molecules for our simulations.

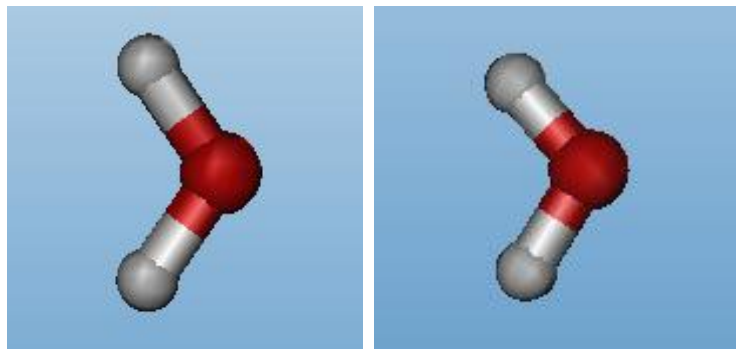


Figure 12: SPC water molecule

Figure 13: TIP3P water molecule

Obviously these two models have different parameters. Table 5 summarizes these parameters. Figures 12 and 13 show the structures for water molecules from the two force fields, with slight differences between the two.

		SPC	TIP3P modif. CHARMM
Charge	OH	-0.820	-0.834
	HO	0.410	0.417
Bond	r_{OH-HO} [Å]	1.0	0.9450
	K_r [kJ·Å ⁻²]	-	4623.08
Angle	θ_0 [deg]	109.47	104.52
	K_θ [kJ·mol ⁻¹ ·rad ⁻¹]	-	459.800
LJ parameters	$\sigma(OH)$ [Å]	3.1657	3.1506
	$\epsilon(OH)$ [kJ·mol ⁻¹]	0.6318	0.6357
	$\sigma(HO)$ [Å]	0.0000	0.4000
	$\epsilon(HO)$ [kJ·mol ⁻¹]	0.0000	0.1923

Table 5: SPC and TIP3P parameters used for our simulations

3- Benzene:

Benzene is common molecule. It is an aromatic ring composed of 6 carbon atoms and 6 hydrogen atoms. In this project, we worked with the OPLS-AA force field as well as the OPLS-UA force field. All the parameters were taken from Sources ³⁵, ³⁶. It is important to recall that the OPLS-AA allows the ring to vibrate and models the hydrogen atom explicitly into account while OPLS-UA keeps the ring rigid and hydrogen atoms are taken into account implicitly in the C parameters. These structures are shown in Figure 14. We ran simulations using both force-fields with one molecule of benzene per cell.

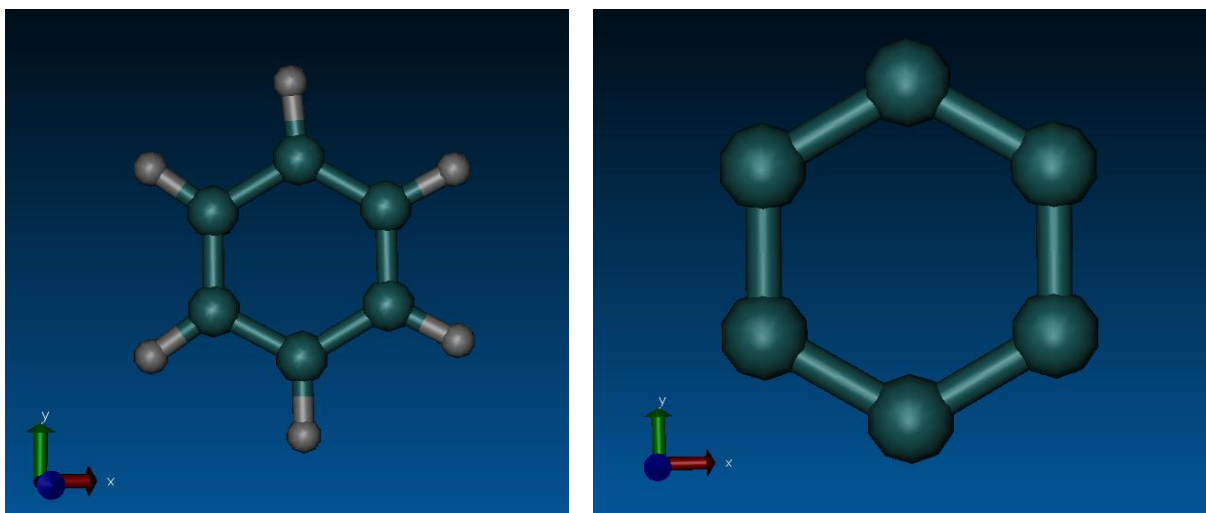


Figure 14: OPLS-AA Benzene(left) and OPLS-UA Benzene (right)

As noted earlier in this report, we used DL_FIELD to generate the different files and changed the parameters to fit the OPLS force field. These parameters are given in Table6. We used the Computational Chemistry Database website⁶¹ in order to obtain the coordinates of benzene.

		OPLS-AA	OPLS-UA
Charge	CA	-0.11500	0.00000
	HP	0.11500	-
Bond	CA-CA	$r_0 [\text{\AA}]$	1.4000
		$K_r [\text{kJ}\cdot\text{\AA}^{-2}]$	3924.59
	CA-HP	$r_0 [\text{\AA}]$	1.0800
		$K_r [\text{kJ}\cdot\text{\AA}^{-2}]$	3071.05
Angle	CA-CA-CA	$\theta_0 [\text{deg}]$	120.000
		$K_\theta [\text{kJ}\cdot\text{mol}^{-1}\cdot\text{rad}^{-1}]$	527.1840
	CA-CA-HP	$\theta_0 [\text{deg}]$	120.000
		$K_\theta [\text{kJ}\cdot\text{mol}^{-1}\cdot\text{rad}^{-1}]$	527.1840
Dihedral	X-CA-CA-X	$V0 [\text{kJ}\cdot\text{mol}^{-1}]$	0.0000
		$V1 [\text{kJ}\cdot\text{mol}^{-1}]$	0.0000
		$V2 [\text{kJ}\cdot\text{mol}^{-1}]$	30.30500
		$V3 [\text{kJ}\cdot\text{mol}^{-1}]$	0.0000
		Angle [deg]	180.0000
LJ parameters		$\sigma(\text{CA}) [\text{\AA}]$	3.5501
		$\epsilon(\text{CA}) [\text{kJ}\cdot\text{mol}^{-1}]$	0.2930
		$\sigma(\text{HP}) [\text{\AA}]$	2.4200
		$\epsilon(\text{HP}) [\text{kJ}\cdot\text{mol}^{-1}]$	0.1260

Table 6: Parameters used for Benzene simulations

4- Toluene:

Toluene is a fairly common molecule. It is composed of a benzene ring and a methyl group. We worked with 3 different toluene molecules in this project. The first one was simulated using the OPLS-AA parameters to describe the entire molecule. The second one had a rigid benzene ring, but the methyl group was allowed to move; this model still used the OPLS-AA force field. The last benzene model was simulated using the OPLS-UA force field. We simulated the second benzene model because of an interesting phenomenon which occurred when we simulated the molecule only using OPLS-AA parameters. Toluene should be a planar molecule and when it is simulated with the OPLS-AA parameters large vibrations due to the methyl group were present. This led to distortions in the structure, as shown in Figure 15 which illustrates a toluene molecule after 1ps in silicalite. Our simulations were done with one molecule of toluene per cell.

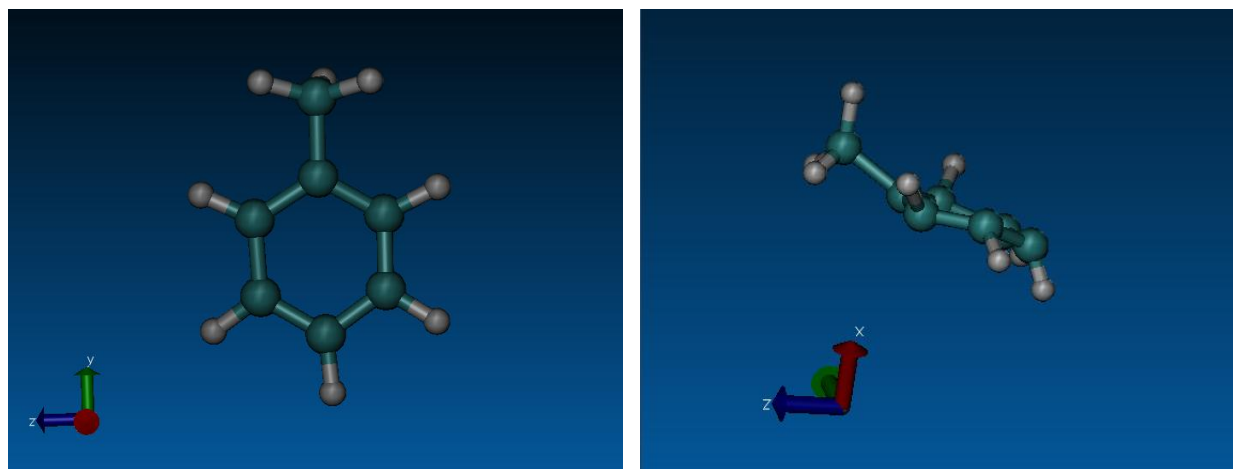


Figure 15: OPLS-AA Toluene molecule alone (left) and after 1ps in the silicalite structure(right, the zeolite is not shown for better readability)

We can see that the molecule lost its planar shape: the methyl group and the hydrogen atoms are moving out of the plane, and some of them are having a 90 degree-angle with the ring. This phenomenon is due to the OPLS-AA parameters. The OPLS-UA keeps the molecule completely rigid so we did not have this issue. We decided to test the OPLS-AA force field using a rigid ring, which was our second model.

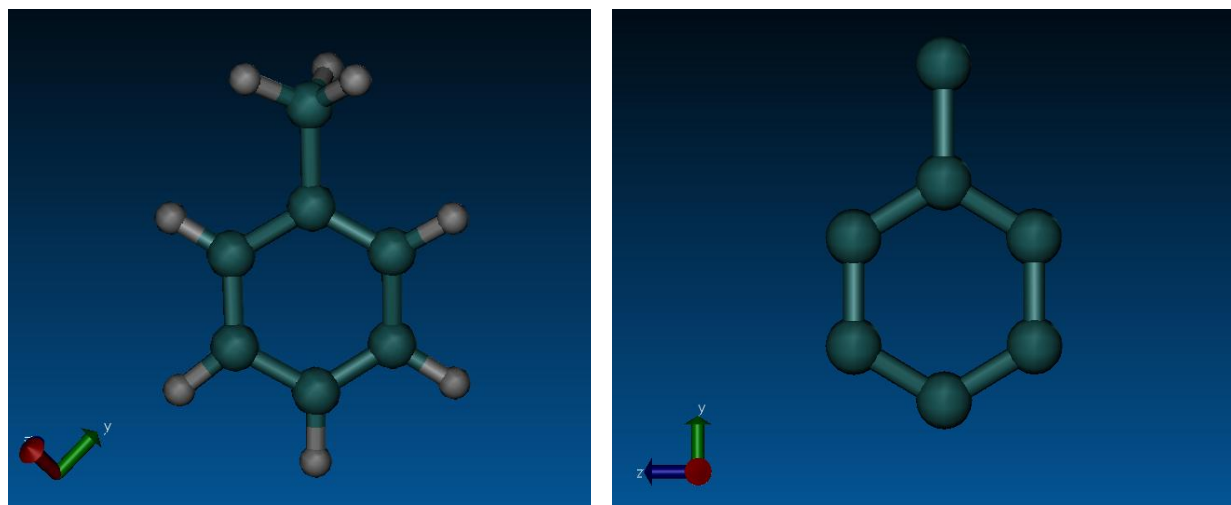


Figure 16: OPLS-AA rigid toluene molecule (left) and OPLS-UA toluene molecule (right)

All the parameters used for our simulations are given in the following table.

			OPLS-AA	OPLS-UA
Charge	CA		-0.11500	0.00000
	HP		0.11500	-
	CT3		-0.06500	0.00000
	HA		0.06000	-
Bond	CA-CA	$r_0 [\text{\AA}]$	1.4000	1.3350
		$K_r [\text{kJ} \cdot \text{\AA}^{-2}]$	3924.59	-
	CA-HP	$r_0 [\text{\AA}]$	1.0800	-
		$K_r [\text{kJ} \cdot \text{\AA}^{-2}]$	3071.05	-
Angle	CA-CT3	$r_0 [\text{\AA}]$	1.51000	1.5118
		$K_r [\text{kJ} \cdot \text{\AA}^{-2}]$	2652.65	-
	CT3-HA	$r_0 [\text{\AA}]$	1.0900	-
		$K_r [\text{kJ} \cdot \text{\AA}^{-2}]$	2845.12	-
Dihedral	CA-CA-CA	$\theta_0 [\text{deg}]$	120.000	120.000
		$K_\theta [\text{kJ} \cdot \text{mol}^{-1} \cdot \text{rad}^{-1}]$	527.1840	-
	CA-CA-HP	$\theta_0 [\text{deg}]$	120.000	-
		$K_\theta [\text{kJ} \cdot \text{mol}^{-1} \cdot \text{rad}^{-1}]$	527.1840	-
Angle	CA-CA-CT3	$\theta_0 [\text{deg}]$	120.000	-
		$K_\theta [\text{kJ} \cdot \text{mol}^{-1} \cdot \text{rad}^{-1}]$	585.7600	-
	CA-CT3-HA	$\theta_0 [\text{deg}]$	109.5000	-
		$K_\theta [\text{kJ} \cdot \text{mol}^{-1} \cdot \text{rad}^{-1}]$	292.8800	-
Dihedral	HA-CT3-HA	$\theta_0 [\text{deg}]$	107.8000	-
		$K_\theta [\text{kJ} \cdot \text{mol}^{-1} \cdot \text{rad}^{-1}]$	276.1440	-
	X-CA-CA-X	$V0 [\text{kJ} \cdot \text{mol}^{-1}]$	0.0000	-
		$V1 [\text{kJ} \cdot \text{mol}^{-1}]$	0.0000	-
Angle		$V2 [\text{kJ} \cdot \text{mol}^{-1}]$	30.30500	-
		$V3 [\text{kJ} \cdot \text{mol}^{-1}]$	0.0000	-
		Angle [deg]	180.0000	-

HA-CT3-CA-CA	V0 [kJ.mol-1]	0.0000	-
	V1 [kJ.mol-1]	0.0000	-
	V2 [kJ.mol-1]	0.0000	-
	V3 [kJ.mol-1]	0.0000	-
	Angle [deg]	180.0000	-
LJ parameters			
	$\sigma(\text{CA}) [\text{\AA}]$	3.5501	3.7500
	$\epsilon(\text{CA}) [\text{kJ.mol-1}]$	0.2930	0.4600
	$\sigma(\text{HP}) [\text{\AA}]$	2.4200	-
	$\epsilon(\text{HP}) [\text{kJ.mol-1}]$	0.1260	-
	$\sigma(\text{CT3}) [\text{\AA}]$	3.5000	3.9100
	$\epsilon(\text{CT3}) [\text{kJ.mol-1}]$	0.2760	0.6690
	$\sigma(\text{HA}) [\text{\AA}]$	2.5000	-
	$\epsilon(\text{HA}) [\text{kJ.mol-1}]$	0.1260	-

Table 7: Parameters used for Toluene simulations

5- Phenol:

Phenol is composed of a benzene ring and an alcohol group attached to the 4-site. Phenol was simulated using both OPLS force fields and did not have the issue of large vibrations that we observed with toluene. We ran simulations with one molecule of phenol per cell. The hydrogen of the OH group moved out of plane but this phenomenon is reasonable.

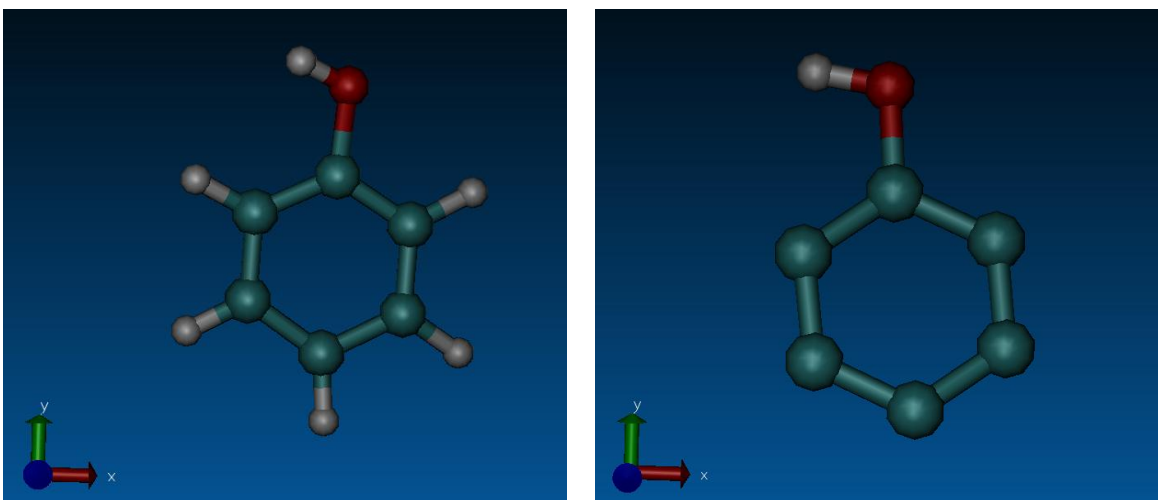


Figure 17: OPLS-AA Phenol molecule (left) and OPLS-UA molecule(right)

The parameters used for our simulations are summarized in Table 8.

			OPLS-AA	OPLS-UA
Charge	CA		-0.11500	0.00000
	CA(OH)		0.15000	0.26500
	HP		0.11500	-
	OH1		-0.58500	-0.70000
	H		0.43500	0.4350
Bond	CA-CA	r_0 [Å]	1.4000	1.3350
		K_r [kJ·Å ⁻²]	3924.59	-
	CA-HP	r_0 [Å]	1.0800	-
		K_r [kJ·Å ⁻²]	3071.05	-
	CA-OH1	r_0 [Å]	1.3800	1.3700
		K_r [kJ·Å ⁻²]	2677.76	-
	OH1-H	r_0 [Å]	0.9450	0.9697
		K_r [kJ·Å ⁻²]	4627.50	-
Angle	CA-CA-CA	θ_0 [deg]	120.000	-
		K_θ [kJ·mol ⁻¹ ·rad ⁻¹]	527.1840	-
	CA-CA-HP	θ_0 [deg]	120.000	-
		K_θ [kJ·mol ⁻¹ ·rad ⁻¹]	527.1840	-
	CA-CA-OH1	θ_0 [deg]	120.000	-
		K_θ [kJ·mol ⁻¹ ·rad ⁻¹]	585.2000	-
	CA-OH1-H	θ_0 [deg]	113.0000	-
		K_θ [kJ·mol ⁻¹ ·rad ⁻¹]	292.8800	-
Dihedral	X-CA-CA-X	V_0 [kJ·mol ⁻¹]	0.0000	-
		V_1 [kJ·mol ⁻¹]	0.0000	-
		V_2 [kJ·mol ⁻¹]	30.30500	-
		V_3 [kJ·mol ⁻¹]	0.0000	-
		Angle [deg]	180.0000	-
	CA-CA-OH1-H	V_0 [kJ·mol ⁻¹]	0.0000	-
		V_1 [kJ·mol ⁻¹]	0.0000	-
		V_2 [kJ·mol ⁻¹]	7.03076	-
		V_3 [kJ·mol ⁻¹]	0.0000	-
		Angle [deg]	180.0000	-
LJ parameters		σ (CA) [Å]	3.5501	3.7500
		ϵ (CA) [kJ·mol ⁻¹]	0.2930	0.4600
		σ (HP) [Å]	2.4200	-
		ϵ (HP) [kJ·mol ⁻¹]	0.1260	-
		σ (OH1) [Å]	3.0700	3.0700
		ϵ (OH1) [kJ·mol ⁻¹]	0.7110	0.7110
		σ (H) [Å]	0.0000	0.0000
		ϵ (H) [kJ·mol ⁻¹]	0.0000	0.0000

Table 8: Parameters used for Phenol simulations

6- Neopentane:

Neopentane was simulated using the OPLS-AA force-field. Neopentane is a large molecule similar to BPA and therefore of interest to study steric effects of molecules in silicalite. Our simulations were run with one molecule of neopentane per cell.

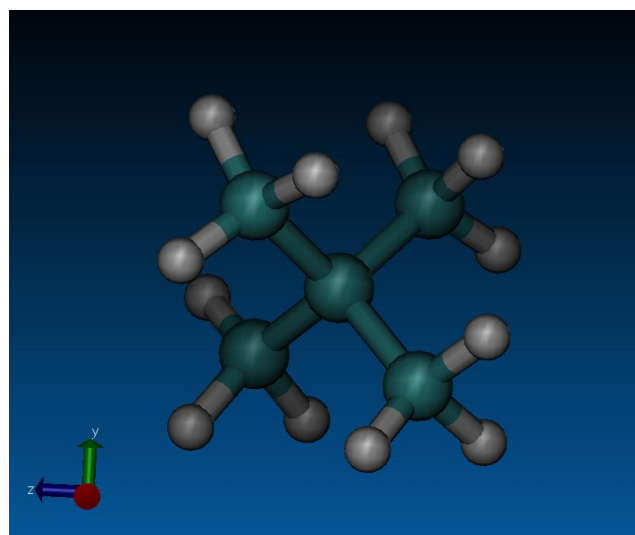


Figure 18: OPLS-AA neopentane

The following table is a collection of the parameters used for the neopentane simulations.

OPLS-AA		
Charge	CT1	0.0000
	CT3	-0.18000
	HA	0.06000
Bond	CT1-CT3	$r_0 [\text{\AA}]$ 1.5290 $K_r [\text{kJ} \cdot \text{\AA}^{-2}]$ 2242.62
	CT3-HA	$r_0 [\text{\AA}]$ 1.0900 $K_r [\text{kJ} \cdot \text{\AA}^{-2}]$ 2845.12
Angle	CT3-CT1-CT3	$\theta_0 [\text{deg}]$ 112.7000 $K_\theta [\text{kJ} \cdot \text{mol}^{-1} \cdot \text{rad}^{-1}]$ 488.2730
	CT1-CT3-HA	$\theta_0 [\text{deg}]$ 110.7000 $K_\theta [\text{kJ} \cdot \text{mol}^{-1} \cdot \text{rad}^{-1}]$ 313.8000
	HA- CT3-HA	$\theta_0 [\text{deg}]$ 107.8000 $K_\theta [\text{kJ} \cdot \text{mol}^{-1} \cdot \text{rad}^{-1}]$ 276.1440
Dihedral	HA-CT3-CT1-CT3	$V_0 [\text{kJ} \cdot \text{mol}^{-1}]$ 0.0000 $V_1 [\text{kJ} \cdot \text{mol}^{-1}]$ 0.0000 $V_2 [\text{kJ} \cdot \text{mol}^{-1}]$ 0.0000 $V_3 [\text{kJ} \cdot \text{mol}^{-1}]$ 1.2540 Angle [deg] 180.0000

LJ parameters	$\sigma(\text{CT1}) [\text{\AA}]$	3.5000
	$\varepsilon(\text{CT1}) [\text{kJ.mol}^{-1}]$	0.2760
	$\sigma(\text{CT3}) [\text{\AA}]$	3.5000
	$\varepsilon(\text{CT3}) [\text{kJ.mol}^{-1}]$	0.2760
	$\sigma(\text{HA}) [\text{\AA}]$	2.5000
	$\varepsilon(\text{HA}) [\text{kJ.mol}^{-1}]$	0.1260

Table 9: Parameters used for Neopentane simulations

7- Nonylphenol:

NP is described in the previous part of this report. OPLS-AA was used to simulate this molecule. It is important to note that we only simulated the most linear nonylphenol molecule branched at the 4-site. Most of the branched nonylphenol structures are too large to fit in the silicalite framework. We ran simulations with one molecule of nonylphenol per cell.

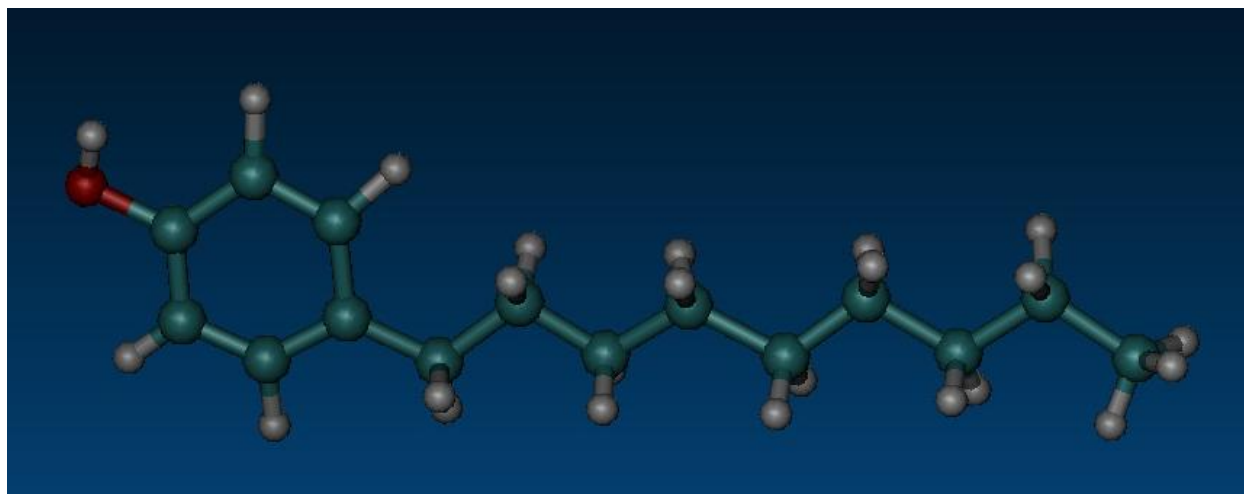


Figure 19: OPLS-AA linear Nonylphenol molecule

The following table summarizes the parameters used for our simulations.

OPLS-AA		
Charge	CA	-0.11500
	CA(OH)	0.15000
	HP	0.11500
	OH1	-0.58500
	H	0.43500
	CT2	-0.12000
	CT3	-0.18000
	HA	0.06000

Bond	CA-CA	r_0 [\AA]	1.4000
		K_r [$\text{kJ} \cdot \text{\AA}^{-2}$]	3924.59
	CA-HP	r_0 [\AA]	1.0800
		K_r [$\text{kJ} \cdot \text{\AA}^{-2}$]	3071.05
	CA-OH1	r_0 [\AA]	1.3800
		K_r [$\text{kJ} \cdot \text{\AA}^{-2}$]	2677.76
	OH1-H	r_0 [\AA]	0.9450
		K_r [$\text{kJ} \cdot \text{\AA}^{-2}$]	4627.50
	CA-CT2	r_0 [\AA]	1.5100
		K_r [$\text{kJ} \cdot \text{\AA}^{-2}$]	2652.65
	CT2/3-HA	r_0 [\AA]	1.0900
		K_r [$\text{kJ} \cdot \text{\AA}^{-2}$]	2845.12
	CT2-CT2/3	r_0 [\AA]	1.5290
		K_r [$\text{kJ} \cdot \text{\AA}^{-2}$]	2242.62
Angle	CA-CA-CA	θ_0 [deg]	120.000
		K_θ [$\text{kJ} \cdot \text{mol}^{-1} \cdot \text{rad}^{-1}$]	527.1840
	CA-CA-HP	θ_0 [deg]	120.000
		K_θ [$\text{kJ} \cdot \text{mol}^{-1} \cdot \text{rad}^{-1}$]	527.1840
	CA-CA-OH1	θ_0 [deg]	120.000
		K_θ [$\text{kJ} \cdot \text{mol}^{-1} \cdot \text{rad}^{-1}$]	585.2000
	CA-OH1-H	θ_0 [deg]	113.0000
		K_θ [$\text{kJ} \cdot \text{mol}^{-1} \cdot \text{rad}^{-1}$]	292.8800
	CT2-CA-CA	θ_0 [deg]	120.000
		K_θ [$\text{kJ} \cdot \text{mol}^{-1} \cdot \text{rad}^{-1}$]	585.7600
	CA-CT2-CT2	θ_0 [deg]	114.000
		K_θ [$\text{kJ} \cdot \text{mol}^{-1} \cdot \text{rad}^{-1}$]	527.1840
	CA-CT2-HA	θ_0 [deg]	109.500
		K_θ [$\text{kJ} \cdot \text{mol}^{-1} \cdot \text{rad}^{-1}$]	292.8800
	CT2-CT2-CT2	θ_0 [deg]	112.700
		K_θ [$\text{kJ} \cdot \text{mol}^{-1} \cdot \text{rad}^{-1}$]	488.2730
	CT2-CT2-HA	θ_0 [deg]	110.700
		K_θ [$\text{kJ} \cdot \text{mol}^{-1} \cdot \text{rad}^{-1}$]	313.8000
	HA-CT2-HA	θ_0 [deg]	107.800
		K_θ [$\text{kJ} \cdot \text{mol}^{-1} \cdot \text{rad}^{-1}$]	276.1440
Dihedral	X-CA-CA-X	V_0 [$\text{kJ} \cdot \text{mol}^{-1}$]	0.0000
		V_1 [$\text{kJ} \cdot \text{mol}^{-1}$]	0.0000
		V_2 [$\text{kJ} \cdot \text{mol}^{-1}$]	30.30500
		V_3 [$\text{kJ} \cdot \text{mol}^{-1}$]	0.0000
		Angle [deg]	180.0000
	CA-CA-OH1-H	V_0 [$\text{kJ} \cdot \text{mol}^{-1}$]	0.0000
		V_1 [$\text{kJ} \cdot \text{mol}^{-1}$]	0.0000
		V_2 [$\text{kJ} \cdot \text{mol}^{-1}$]	7.03076
		V_3 [$\text{kJ} \cdot \text{mol}^{-1}$]	0.0000
		Angle [deg]	180.0000
	CA-CA-CT2-CT2	V_0 [$\text{kJ} \cdot \text{mol}^{-1}$]	0.0000
		V_1 [$\text{kJ} \cdot \text{mol}^{-1}$]	0.0000

	V2 [kJ.mol-1]	0.0000
	V3 [kJ.mol-1]	0.0000
	Angle [deg]	180.0000
CA-CA-CT2-HA	V0 [kJ.mol-1]	0.0000
	V1 [kJ.mol-1]	0.0000
	V2 [kJ.mol-1]	0.0000
	V3 [kJ.mol-1]	0.0000
	Angle [deg]	180.0000
CA-CT2-CT2-CT2	V0 [kJ.mol-1]	0.00000
	V1 [kJ.mol-1]	5.43400
	V2 [kJ.mol-1]	-0.20900
	V3 [kJ.mol-1]	0.83600
	Angle [deg]	180.0000
CA-CT2-CT2-HA	V0 [kJ.mol-1]	0.00000
	V1 [kJ.mol-1]	5.43400
	V2 [kJ.mol-1]	-0.20900
	V3 [kJ.mol-1]	0.83600
	Angle [deg]	180.0000
CT2-CT2-CT2-CT2/3	V0 [kJ.mol-1]	0.0000
	V1 [kJ.mol-1]	5.4340
	V2 [kJ.mol-1]	-0.20900
	V3 [kJ.mol-1]	0.83600
	Angle [deg]	180.000
CT2-CT2-CT2/3-HA	V0 [kJ.mol-1]	0.0000
	V1 [kJ.mol-1]	0.0000
	V2 [kJ.mol-1]	0.0000
	V3 [kJ.mol-1]	1.2540

	Angle [deg]	180.000
HA-CT2-CT2-HA	V0 [kJ.mol-1]	0.0000
	V1 [kJ.mol-1]	0.0000
	V2 [kJ.mol-1]	0.0000
	V3 [kJ.mol-1]	1.2540
	Angle [deg]	180.000
LJ parameters	σ (CA) [\AA]	3.5501
	ϵ (CA) [kJ.mol-1]	0.2930
	σ (HP) [\AA]	2.4200
	ϵ (HP) [kJ.mol-1]	0.1260
	σ (OH1) [\AA]	3.0700
	ϵ (OH1) [kJ.mol-1]	0.7110
	σ (H) [\AA]	0.0000
	ϵ (H) [kJ.mol-1]	0.0000
	σ (CT2) [\AA]	3.5000
	ϵ (CT2) [kJ.mol-1]	0.2760
	σ (CT3) [\AA]	3.5000
	ϵ (CT3) [kJ.mol-1]	0.2760
	σ (HA) [\AA]	2.4200
	ϵ (HA) [kJ.mol-1]	0.1260

Table 10: Parameters used for Nonylphenol simulations

8- Bisphenol-A

An in-depth insight of BPA is given in the Background section of this thesis. We tried to use the OPLS-AA force-field to simulate the BPA molecule but encountered difficulty in formulating the correct parameters. Figure 20 shows what happened with the OPLS-AA force-field. Following the same methodology we considered only one molecule of BPA per cell for our simulations.

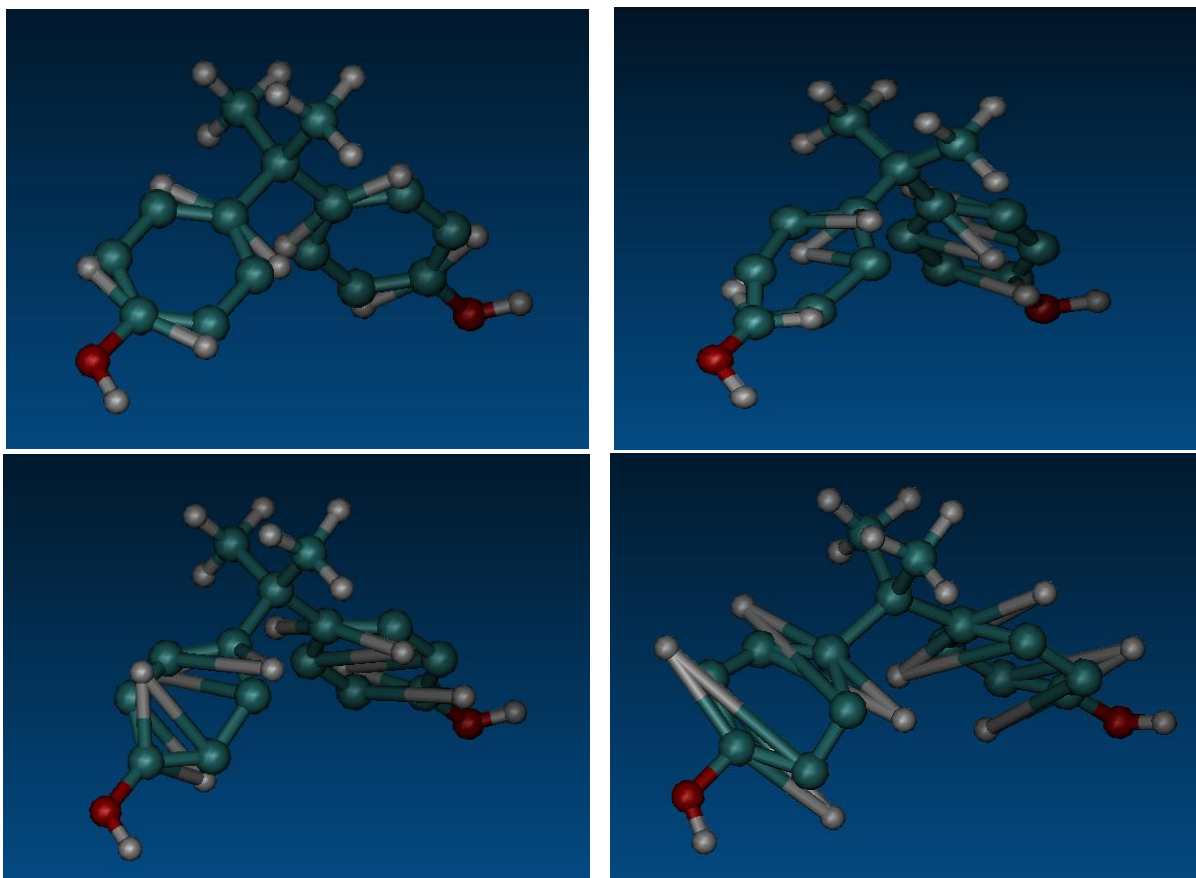


Figure 20: BPA molecule simulated using OPLS-AA Force field at various timesteps

As shown, the model is rather skewed and nonsensical. Likely the vibrations (similar to the toluene OPLS-AA model) led to the skewed BPA molecule. We believe that new parameters likely should be developed to describe this molecule. This was, however, beyond the scope of the current thesis. We therefore took a simplified approach, and modeled the phenol rings as rigid, but left the angle between the two rings, the methyl and alcohol groups as non-rigid. A second model used the OPLS-UA force field, and only the methyl and alcohol groups were allowed to move.

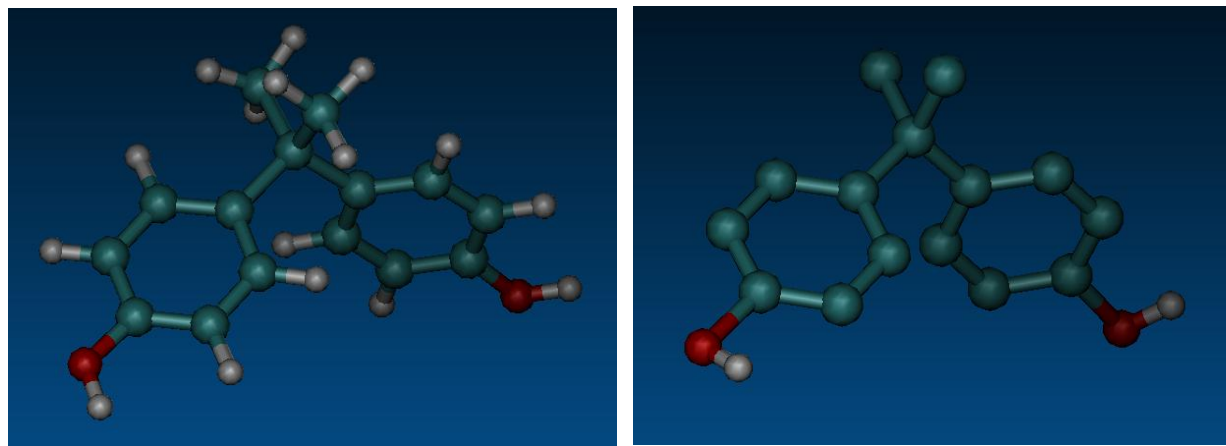


Figure 21: OPLS-AA BPA molecule (left) and OPLS-AA BPA molecule(right) with rigid rings

Table 11 shows the parameters used for our simulations.

			OPLS-AA	OPLS-UA
Charge	CA		-0.11500	0.00000
	CA(OH)		0.15000	0.26500
	HP		0.11500	-
	OH1		-0.58500	-0.70000
	H		0.43500	0.43500
	CT1		0.23000	0.00000
	CT3		-0.18000	0.00000
	HA		0.06000	-
Bond	CA-CA	r_0 [Å]	1.4000	1.3350
	CA-HP	r_0 [Å]	1.0800	-
	CA-OH1	r_0 [Å]	1.3800	1.3640
		K_f [kJ·Å ⁻²]	2677.76	3765.60
	OH1-H	r_0 [Å]	0.9450	0.9450
		K_f [kJ·Å ⁻²]	4627.50	4627.50
	CA-CT1	r_0 [Å]	1.5100	-
		K_f [kJ·Å ⁻²]	2652.65	-
	CT1-CT3	r_0 [Å]	1.52900	1.5260
		K_f [kJ·Å ⁻²]	2242.62	2175.68
	CT3-HA	r_0 [Å]	1.0900	-
		K_f [kJ·Å ⁻²]	2845.15	-
Angle	CA-CA-CA	θ_0 [deg]	120.000	-
		K_θ [kJ·mol ⁻¹ ·rad ⁻¹]	527.1840	-
	CA-CA-HP	θ_0 [deg]	120.000	-
		K_θ [kJ·mol ⁻¹ ·rad ⁻¹]	527.1840	-
	CA-CA-OH1	θ_0 [deg]	120.000	120.000

		K_θ [kJ.mol ⁻¹ .rad ⁻¹]	585.2000	585.2000
	CA-OH1-H	θ_0 [deg]	113.0000	113.0000
		K_θ [kJ.mol ⁻¹ .rad ⁻¹]	292.8800	292.8800
	CA-CA-CT1	θ_0 [deg]	120.000	-
		K_θ [kJ.mol ⁻¹ .rad ⁻¹]	585.7600	-
	CA-CT1-CT3	θ_0 [deg]	114.000	114.000
		K_θ [kJ.mol ⁻¹ .rad ⁻¹]	527.1840	527.1840
	CA-CT1-CA	θ_0 [deg]	120.000	-
		K_θ [kJ.mol ⁻¹ .rad ⁻¹]	710.6000	-
	CT1-CT3-HA	θ_0 [deg]	110.100	-
		K_θ [kJ.mol ⁻¹ .rad ⁻¹]	279.4748	-
	HA-CT3-HA	θ_0 [deg]	108.400	-
		K_θ [kJ.mol ⁻¹ .rad ⁻¹]	296.7800	-
	CT3-CT1-CT3	θ_0 [deg]	116.00	116.00
		K_θ [kJ.mol ⁻¹ .rad ⁻¹]	585.200	585.200
Dihedral	X-CA-CA-X	V0 [kJ.mol-1]	0.0000	-
		V1 [kJ.mol-1]	0.0000	-
		V2 [kJ.mol-1]	30.30500	-
		V3 [kJ.mol-1]	0.0000	-
		Angle [deg]	180.0000	-
	HA-CT3-CT1-CA	V0 [kJ.mol-1]	0.0000	-
		V1 [kJ.mol-1]	0.0000	-
		V2 [kJ.mol-1]	0.0000	-
		V3 [kJ.mol-1]	1.93116	-
		Angle [deg]	180.0000	-
	CT3-CT1-CT3-HA	V0 [kJ.mol-1]	0.0000	-
		V1 [kJ.mol-1]	0.0000	-
		V2 [kJ.mol-1]	0.0000	-
		V3 [kJ.mol-1]	1.25400	-
		Angle [deg]	180.0000	-
	CA-CA-OH1-H	V0 [kJ.mol-1]	0.0000	0.0000
		V1 [kJ.mol-1]	0.0000	0.0000
		V2 [kJ.mol-1]	7.03076	7.03076
		V3 [kJ.mol-1]	0.0000	0.0000
		Angle [deg]	180.0000	180.0000
LJ parameters	σ (CA) [\AA]	3.5501	3.7500	
	ϵ (CA) [kJ.mol-1]	0.2930	0.4600	
	σ (HP) [\AA]	2.4200	-	
	ϵ (HP) [kJ.mol-1]	0.1260	-	
	σ (CT3) [\AA]	3.5000	3.9100	
	ϵ (CT3) [kJ.mol-1]	0.2760	0.6690	
	σ (HA) [\AA]	2.5000	-	
	ϵ (HA) [kJ.mol-1]	0.1260	-	
	σ (OH1) [\AA]	3.0700	3.0700	

$\epsilon(\text{OH1})$ [kJ.mol-1]	0.7110	0.7110
$\sigma(\text{H})$ [\text{\AA}]	0.0000	0.0000
$\epsilon(\text{H})$ [kJ.mol-1]	0.0000	0.0000
$\sigma(\text{CT1})$ [\text{\AA}]	3.5000	3.8000
$\epsilon(\text{CT1})$ [kJ.mol-1]	0.2760	0.2090

Table 11: Parameters used for Bisphenol-A simulations

9- Simulation Controls:

All simulations ran with the NVT ensemble, using the velocity Verlet algorithm and temperatures ranged from 300K to 600K for water simulations and two temperatures, 300K and 400K were investigated for the other molecules. The time step was set to 5fs since it allows good energy conservation. The number of equilibration steps was typically set to 200,000 for each simulation.

Dynamical simulation parameters changed slightly between molecules. Water simulations lasted 6,000,000 steps for a total simulation time of 3ns. For the 7 other molecules the simulations lasted 20,000,000 steps for a total simulation time of 10 ns. The simulation time was increased because these molecules were expected to diffuse more slowly in silicalite and a longer simulation is should give a better statistical average of the MSD. We realized that the frequency of printing results in the output files had an impact on our results. We printed the positions at two different frequencies for benzene, phenol and toluene. The coordinates of the molecules were first printed every 500 steps and then every 200 steps to output file while for neopentane, nonylphenol, and bisphenol-A they were printed only every 500 steps to output file.

II- Simulations of interest

1- Self diffusivity versus transport diffusivity:

It is important to note the difference between these two types of diffusivity. Self-diffusion coefficient is the result of movement of molecules under macroscopic equilibrium⁵⁷ and can be related to Brownian motion. On the other hand, transport diffusivity or mass transfer is linked to a chemical potential gradient. Self-diffusion can be obtained by measuring the mean square displacement (MSD) of diffusing particles. It is however possible to relate these two diffusion coefficients using the Darken equation obtained for a “mixture of two identical species, distinguishable only by their labeling”⁵⁷.

$$Dt = Ds \frac{d \ln P}{d \ln q} \quad (23)$$

In this equation Dt is the transport diffusion coefficient, Ds the self-diffusion coefficient, P the total pressure and q the total concentration of the sorbate. The non linearity between activity and concentration is the reason why there is the $(d \ln P)/(d \ln q)$ term.⁴³

2- Mean Square displacement, Self-diffusion coefficient and Energy of activation:

In his thesis, Fleys⁵⁷ gives a detailed explanation of how the mean square displacement (MSD) can be related to Fick’s law. This is the random walk model. He also shows how MSD can also be related to the self-diffusion coefficient by using the ideal Einstein equation for a one dimensional system.

$$\langle z^2(t) \rangle = 2D * t \quad (24)$$

This ideal equation is valid under certain circumstances. First, diffusivity should be constant, more specifically it should not be a function of the concentration. Second, diffusing particles do not interfere with one another and can move in any direction with the same probability.

The general Einstein equation states that the displacement of a molecule is related to a power of time:

$$\langle z^2(t) \rangle = C * t^\alpha \quad (25)$$

where C and α are constants.

The constant α can be obtained by generating the theoretically linear plot of $\ln(\text{MSD})$ vs $\ln(t)$. If the constant α equals one, then this is the ideal case, also called normal diffusion case. If the value is equal to 0.5, this is the single-diffusion case. It means that molecules cannot pass one another in the channel.

A very important point is that it is meaningless to compare diffusion processes that are different in nature. In other words, the value of α has to be the same if one wants to compare the value of self-diffusion coefficient that is found.

We can now express the MSD as a function of time for anisotropic and isotropic systems.

$$\langle r^2(t) \rangle = 2k * D * t \quad (26)$$

In this equation $\langle r^2(t) \rangle$ is the mean square displacement, k is equal to the dimension of the system studied, D is the self-diffusion coefficient and t is time.

So for a 3-dimensional isotropic system we have:

$$\langle r^2(t) \rangle = 6 * D * t \quad (27)$$

Our system of interest, silicalite, is anisotropic; therefore we can define a self-diffusion coefficient in each direction. We used Cartesian coordinates to obtain:

$$\begin{cases} \langle x(t) \rangle^2 = 2D_x t \\ \langle y(t) \rangle^2 = 2D_y t \\ \langle z(t) \rangle^2 = 2D_z t \end{cases} \quad (28)$$

We can calculate the overall diffusion coefficient by taking the average of D_x , D_y and D_z .

$$D = \frac{1}{3}(D_x + D_y + D_z) \quad (29)$$

Once the self-diffusion coefficient is obtained, it is possible to calculate the activation energy. The self-diffusion coefficient can be expressed as follows, based on an Arrhenius-type law:

$$D = D_0 \exp\left(-\frac{E_a}{RT}\right) \quad (30)$$

In this equation D_0 is the pre-exponential constant, E_a the activation energy, R the gas constant, and T the temperature. We can access easily the activation energy in $\text{kJ} \cdot \text{mol}^{-1}$ by plotting the diffusion coefficient as a function of $1/1000 T$.

3- Diffusional Anisotropy

If one considers a Markovian process, i.e. the diffusion process is a sequence of random jumps between the intersections of the zeolite, then the random walk model gives the following relation:

$$\frac{c^2}{D_z} = \frac{a^2}{D_x} + \frac{b^2}{D_y} \quad (31)$$

where a , b and c are the unit cell dimensions of the system.

We can measure the discrepancy of the random walk model by calculating the parameter β defined as follows:

$$\beta = \frac{\frac{c^2}{D_z}}{\frac{a^2}{D_x} + \frac{b^2}{D_y}} \quad (32)$$

From the definition of β , 3 different cases can be observed^{33, 22}:

- $\beta=1$, the random walk model is valid.
- $\beta>1$, then it means that when a molecule gets to an intersection between straight and sinusoidal channels, it will continue to diffuse through the same channel.
- $\beta<1$, we have the reverse phenomenon. The molecule reaching an intersection will rather change channels and diffuse along the other type.

The other criterion that allows us to assess the anisotropy of our system is called diffusion anisotropy parameter and is defined as follows:

$$\delta = \frac{\frac{1}{2}(D_x + D_y)}{D_z} \quad (33)$$

The calculated values of δ should be equal to 4.4, if the diffusion follows the random walk model.

4- Mean-square displacement calculation:

The average mean square displacement of a molecule is the distance that it traveled during time t , squared, and is defined as follows:

$$MSD = \langle r(t) \rangle^2 = \left\langle \frac{1}{N} \sum_{i=1}^N (r_i(t) - r_i(0))^2 \right\rangle \quad (34)$$

where N is the number of molecule of interest, $r_i(0)$ is the coordinate (x, y or z) of molecule i at time 0, and $r_i(t)$ the same coordinate of the same molecule i at time t . We use a squared value of the displacement to take into account net movement.

The MSD was available through the STATIS file generated by DL_POLY but only the overall MSD, i.e. the sum of the MSD along the x, y and z axis was available. Parameters δ and β use D_x , D_y and D_z which are function of MSD_x , y and z , and not the total MSD. In order to calculate the mean square displacement along the different axis of a molecule in silicalite we created a program (see Appendix 3) that reads the coordinates of atoms from the simulation and then calculates an average MSD over time. This program considers all positions during the simulation as potential starting points and averages over several trajectories to get averaged MSD values over the simulation. We used the MSD available through the STATIS file to compare the results of our program with the ones given by DL_POLY.

5- Radial distribution functions (rdfs)

After simulations ran in DL_POLY it is possible to plot the radial distribution functions (rdfs) of the molecules that diffused through silicalite. These plots indicate average distances between atoms. We used these plots to understand the hydrogen bonding taking place within the zeolites.

These plots are especially important for water molecules because the hydrogen bonding that dictates the diffusion through the zeolite structure can be monitored. We plotted $g_{OO}(r_{OO})$ and $g_{OH}(r_{OH})$. $g_{OO}(r_{OO})$ is the probability of finding an oxygen atom near another oxygen from a different water molecule at a distance r_{OO} . Figure 22 shows the distance r_{OO} . $g_{OH}(r_{OH})$ is the probability of finding an H atom near an O atom at a distance r_{OH} .

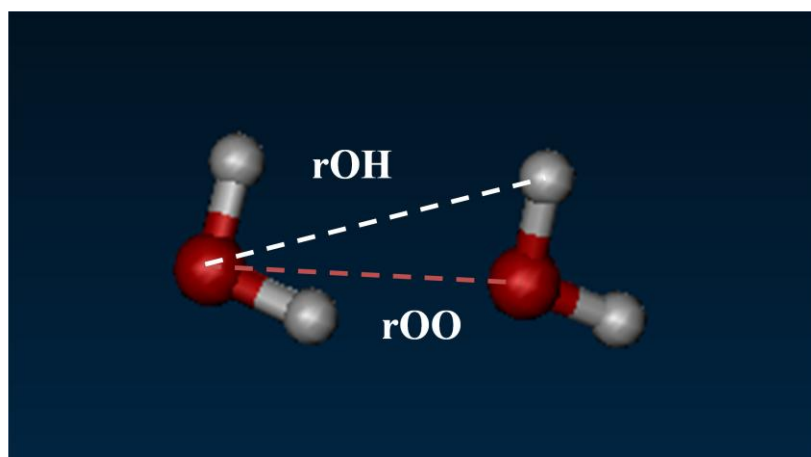


Figure 22: Distances r_{OO} and r_{OH} between two water molecules

Based on these functions, we can evaluate the number of hydrogen bonds per molecule of water. To do so we integrate the rdfs function and chose a maximum hydrogen acceptor distance (MAD). In order to compare the results we obtained to literature, we followed the methodology described by Fleys in his thesis. We have two peaks for g_{OH} and g_{OO} . The second peak for g_{OO} is much smaller and much broader than the first one. These maximums give us the distance where there are actual H-bonds. The first minimum for g_{OH} is found at 2.5\AA and is the limit where the H-bond is usually effective. In other words if the oxygen atom of water molecule X is more than 2.5\AA away from the H atom of molecule Y then the hydrogen bond is no longer taken

into account. The problem with this criterion is that hydrogen atoms are very mobile and using such a defined criterion might not allow us to take every H-bond into account. In order to solve this problem we decided to fix the MAD at the minimum of the g_{OO} function, around 3.5\AA . Then in order to calculate the actual number of H-bonds we calculate the integral of the g_{OH} rdf and we read the value of this integral at $r_{OH}=3.5\text{\AA}$. This gives us the number of H-bonds per water molecule for our simulation.

Radial distribution functions were also plotted for molecules that had an alcohol group, i.e. phenol, nonylphenol and bisphenol-A. The H-bonds are expected to play an important role in the diffusion of these molecules in silicalite. The alcohol group is expected to slow the diffusion by creating hydrogen-bonds with oxygen atoms of the framework. The rdf between the hydrogen atom of the alcohol group and the oxygen of the framework were plotted.

Results and Discussion

In this section we present results obtained for each molecule we simulated. We start with water, comparing the two models we used (SPC and TIP3P modified) to literature results^{22, 24, 33, 41, 44}. We plotted the mean square displacement (MSD) at different temperatures (300-600K) versus time which allowed us to calculate the self-diffusion coefficient, and the β and δ parameters. We then plotted the radial distribution functions g_{OO} and g_{OH} , and calculated the number of hydrogen-bonds at various temperatures. For neopentane and nonylphenol, we plotted the MSD, and calculated D, β and δ . For benzene, phenol, toluene and BPA, we plotted and calculated the same results but this time for both OPLS-UA and OPLS-AA. For the molecules containing at least one alcohol group, i.e. phenol, nonylphenol, and bisphenol-A, we plotted the radial distribution functions between the hydrogen of their alcohol group and the oxygen atom of silicalite to assess the importance of hydrogen bonding on the self-diffusion process. We compared our results to literature when possible.

I- Water

1- Diffusion

We start with the plots of the mean square displacement as a function of time at different temperatures. We explain the results obtained for these plots, i.e. what type of diffusion is present, and calculate the self-diffusion coefficients in the x, y and z directions. Finally, we obtained the β and δ parameters.

A- TIP3P water model

In this section we show the plots of the mean squared displacement (MSD) as a function of time at different temperatures for our non-rigid model. We had a total of 16 water molecules and our simulations ran for 6,000,000 steps (XYZ ps). The plots of MSD versus time based on our program give us the average MSD of water molecules in the x, y and z directions as well as the total mean square displacement. When the MSD plot appeared non-linear, we also compared

the MSD versus time as calculated by DL_POLY. DL_POLY determines the MSD over a longer time scale since it does not average the MSD. This may show long-term trends, but may lead to complications since the MSD values are not statistically averaged.

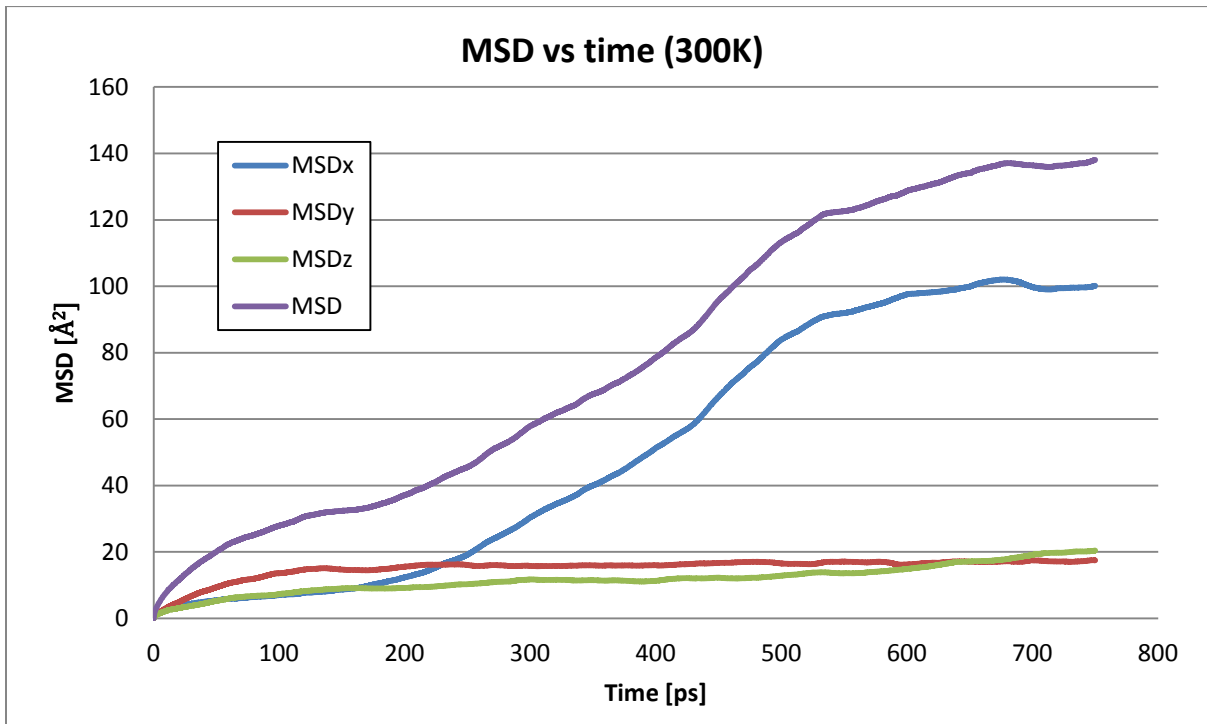


Figure 23: Average mean square displacement of water molecules in silicalite at 300K. MSDx is along the x-direction, MSDy is along the y-direction, and MSDz is along the z-direction. MSDs were calculated using the program described in the methodology section.

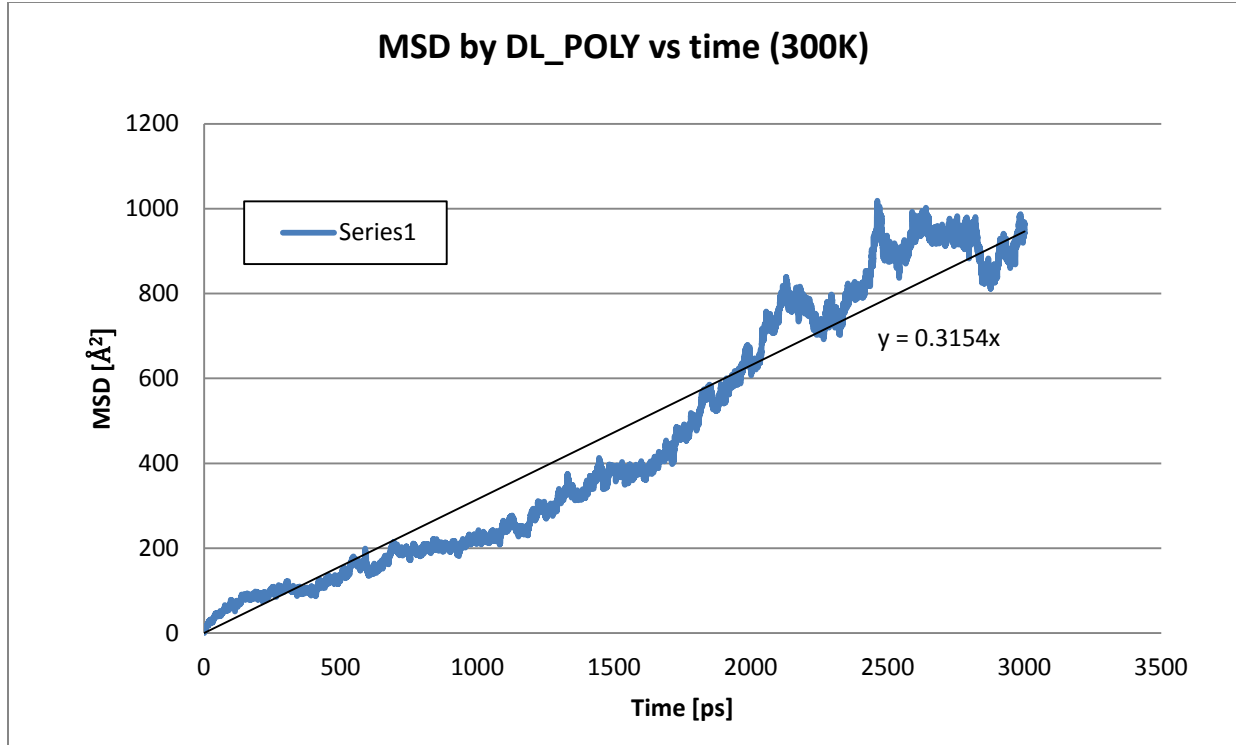


Figure 24: Mean square displacement calculated by DL_POLY for 16 water molecules in silicalite at 300K with trend line shown.

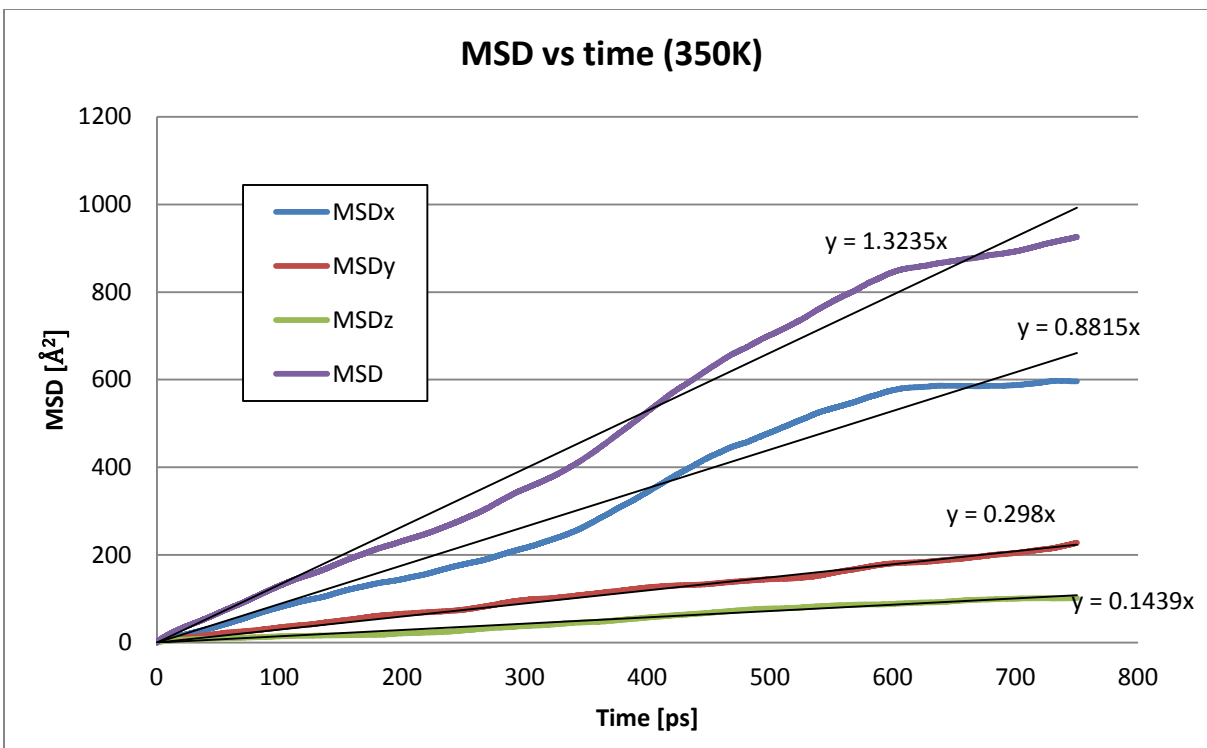


Figure 25: Average mean square displacement of water molecules in silicalite at 350K. MSDx is along the x-direction, MSDy is along the y-direction, and MSDz is along the z-direction. MSDs were calculated using the program described in the methodology section.

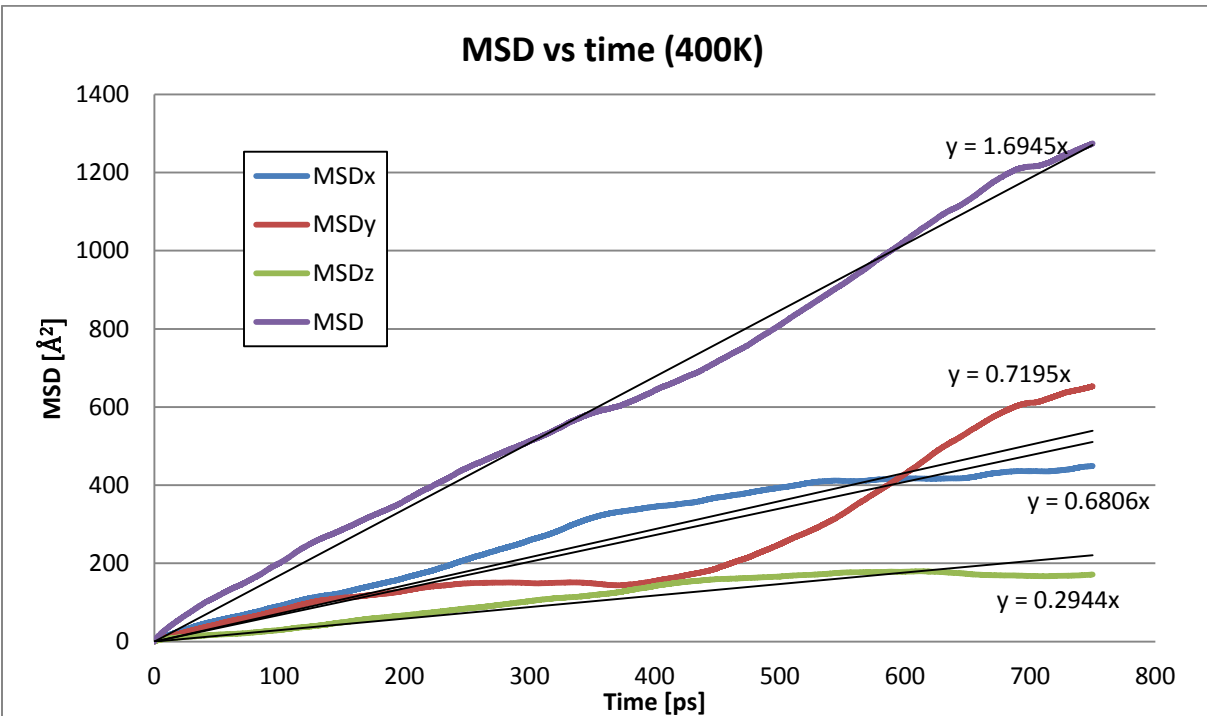


Figure 26: Average mean square displacement of water molecules in silicalite at 400K. MSDx is along the x-direction, MSDy is along the y-direction, and MSDz is along the z-direction.

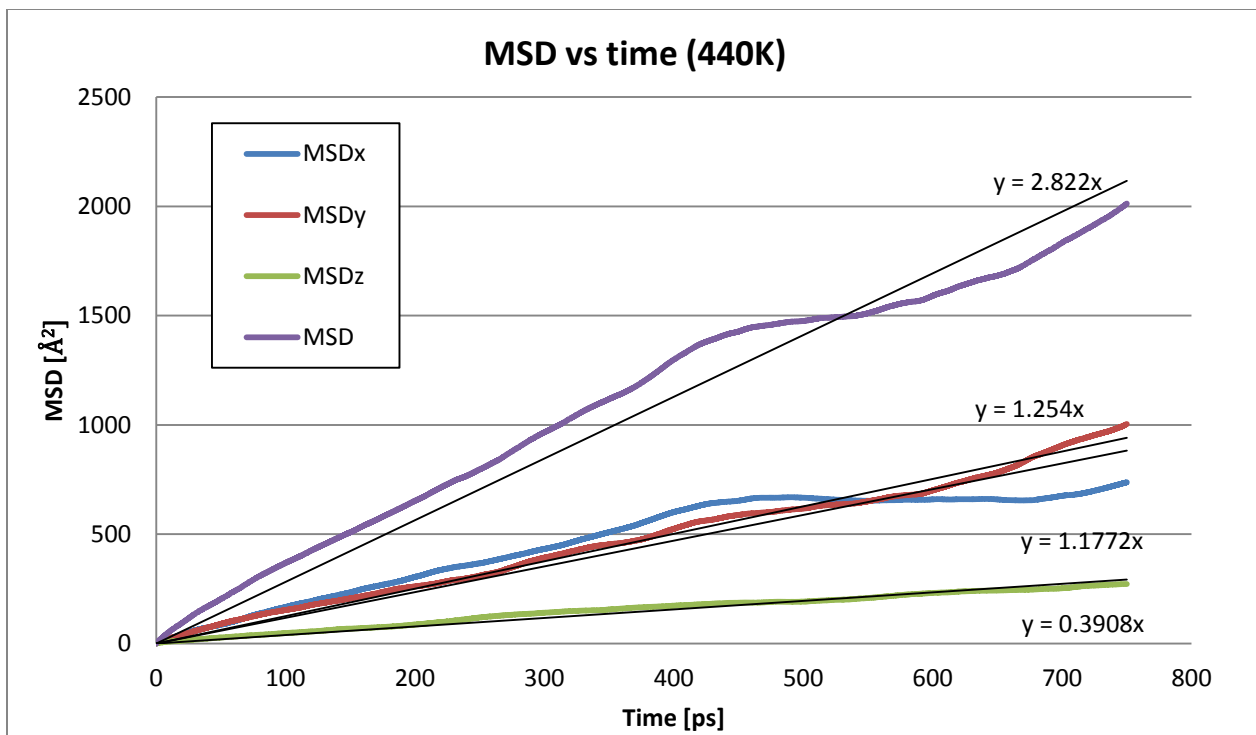


Figure 27: Average mean square displacement of water molecules in silicalite at 440K. MSDx is along the x-direction, MSDy is along the y-direction, and MSDz is along the z-direction.

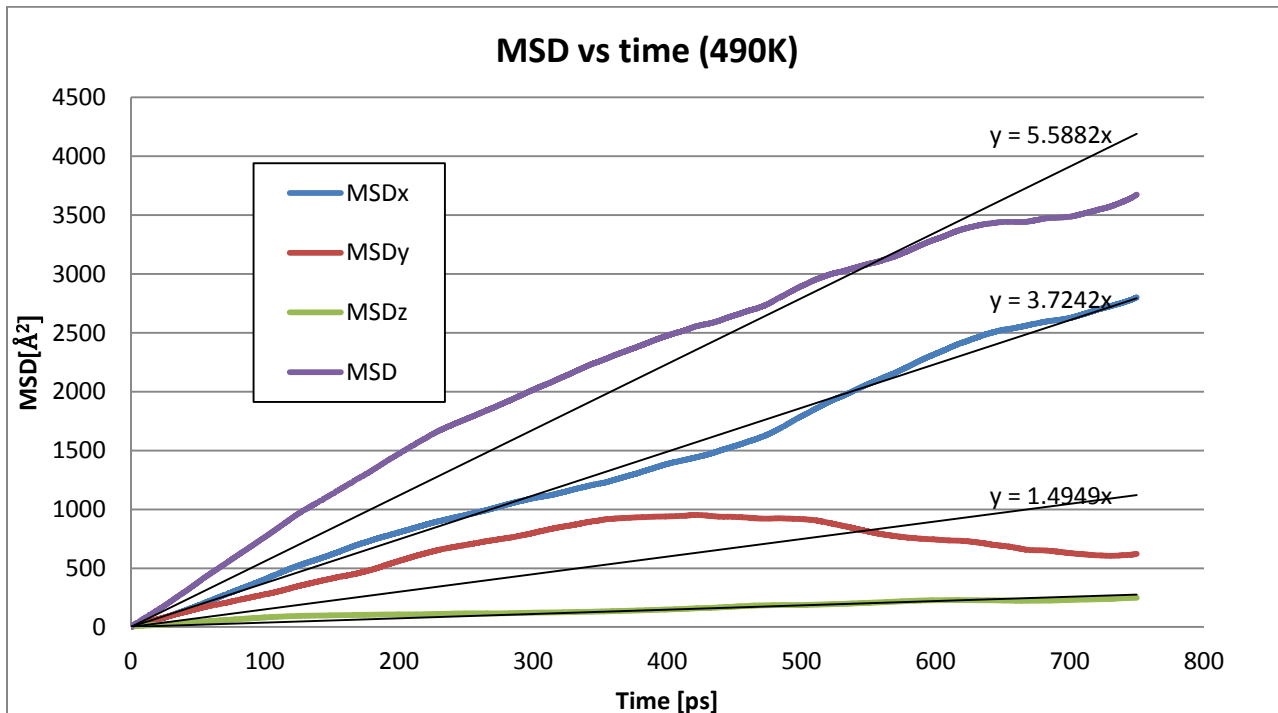


Figure 28: Average mean square displacement of water molecules in silicalite at 490K. MSDx is along the x-direction, MSDy is along the y-direction, and MSDz is along the z-direction.

MSD vs time (600K)

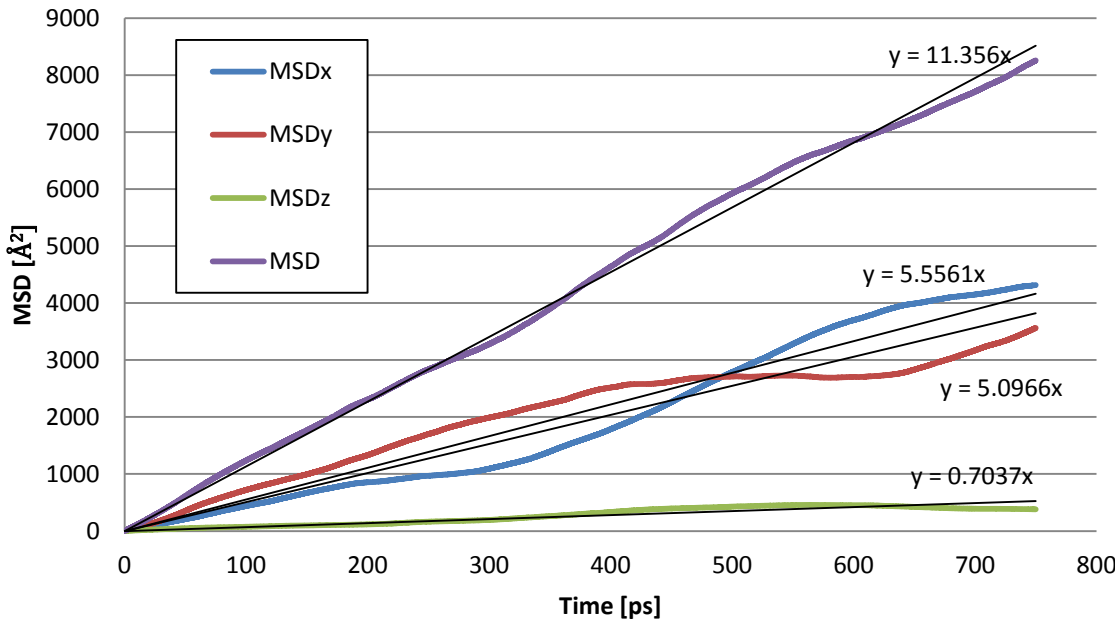


Figure 29: Average mean square displacement of water molecules in silicalite at 600K. MSDx is along the x-direction, MSDy is along the y-direction, and MSDz is along the z-direction.

Based on these plots, several comments can be made. Most of the diffusion is along the x-direction, or along the sinusoidal channels. It seems that the diffusion process is not always ideal, or that the average MSD line is not perfectly linear such as at 300K. This result is not in agreement with literature where diffusion is found to be ideal for temperatures above 220K^{22, 33}. The plots are usually linear, but deviations could be due to several reasons. Our force field for water may not be optimized for describing water in zeolites. Our simulation time may also not be long enough; longer simulation time may give better statistics that give a more linear MSD plot. Better algorithms to sample and average the atomic positions may also give more linear plots. In any case, the MSDs in x and z directions appear more linear while the y-direction MSD is not always linear (see Figure 23, 26, 28, 29). The diffusion along the y direction at 300 K appears to have a slight curve. Fitting the data to obtain a α constant of 0.5, implies single file diffusion process. We found that a value of $\alpha=0.46$ fits well the first 200 ps of simulation (Figure 30), suggesting single-file diffusion. Again, however we must acknowledge that the above-mentioned issues could be causing the appearance of single-file diffusion.

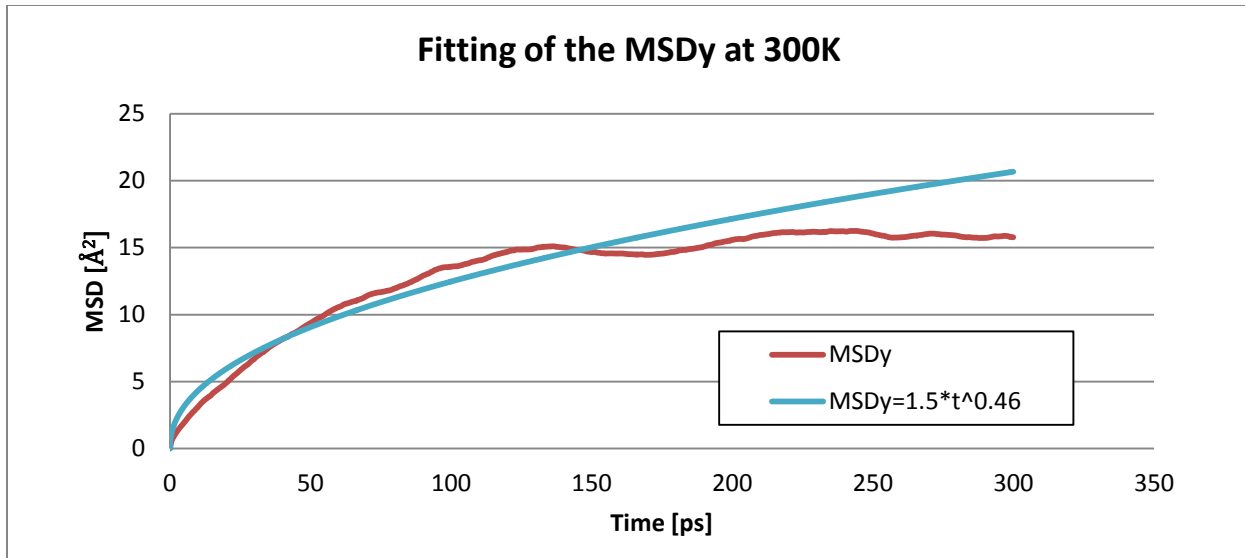


Figure 30: Fitting of α coefficient at 300K for MSDy

Another option is that clustering of water molecules in the straight channels is leading to single-file diffusion. We observed in the simulations that water molecules could move more easily in the sinusoidal channel. The majority of water molecules are stuck in a cluster and so when a water molecule is diffusing along the x-axis it has fewer chances of running into another molecule. We believe that is why MSDx is greater than MSDy. Also the values of the total MSD are much smaller than what was found in literature by almost a factor 10 for 300K and by a factor between 1.5 and 4 for other temperatures.

For temperatures between 350K and 600K the diffusion process seems to be ideal. The MSD vs time plots are almost linear meaning that α is equal to 1. MSDy is hard to interpret for most temperatures. We believe that this is because of the clustering effect that causes a complex behavior for diffusion in the y-direction even if it seems to be linear.

The MSD that we obtained for the z direction always seems to be much smaller than the ones in the x and y direction. This result is in good agreement with literature^{22, 33, 41}.

Nevertheless, we can observe a phenomenon that is not in agreement with previous studies. For this range of temperatures, the water molecules seem to move more easily in the sinusoidal channels than in the straight ones. Fleys found that the MSD in the y direction was almost twice as big as the MSD in the x-direction. For our simulations it is either the opposite case or the MSD is almost equal in both x and y directions. This phenomenon is most probably

due to the water clusters that are formed in the straight channel. In the following section we will calculate the number of H-bonds and we observe more H-bonding than Fleys had for his simulations. MSD_x is bigger or equal to MSD_y at nearly all temperatures. It is almost equal at 400K, 440K and 600K and almost twice as big for 350K and 490K. All these simulations were based on the same configuration, so we are not sure of why this phenomenon is not consistent with temperature. Further simulations may be needed to explore this.

Based on these plots we calculated the self-diffusion coefficients for water in silicalite, the β and δ parameters under ideal diffusion conditions at different temperatures.

T [K]	D	D _x	D _y	D _z	β	δ
350	2.2120	4.4075	1.49	0.7195	0.1219	4.0983
400	2.8241	3.5975	3.403	1.472	0.0777	2.3778
440	4.7033	6.27	5.886	1.954	0.0353	3.1105
490	9.3136	18.621	7.4745	1.8455	0.0128	7.0700
600	18.9273	27.78	25.483	3.5185	0.0045	7.5689

Table 12: Diffusion coefficients of TIP3P water in silicalite [$10^{-9} \text{ m}^2 \cdot \text{s}^{-1}$], β and δ parameters as function of T

Here we can see that the values of β are all inferior to one, meaning that water molecules will most likely change channel when they reach an intersection. The evolution of δ parameter does not seem to be consistent with temperature for our simulations. We can see that the value is higher than 4.4 for 490 and 600K and lower than 4.4 below 440K.

B- SPC water model

In this part we present results on the mean square displacement of water molecules for our second water model, the rigid SPC model. The same conditions were used for these simulations and the plots show the average MSD in the x, y and z directions as well as the total MSD. Plots based on the DL_POLY values of the actual total MSD are given when the linearity of the MSD is not clear for the results based on our program.

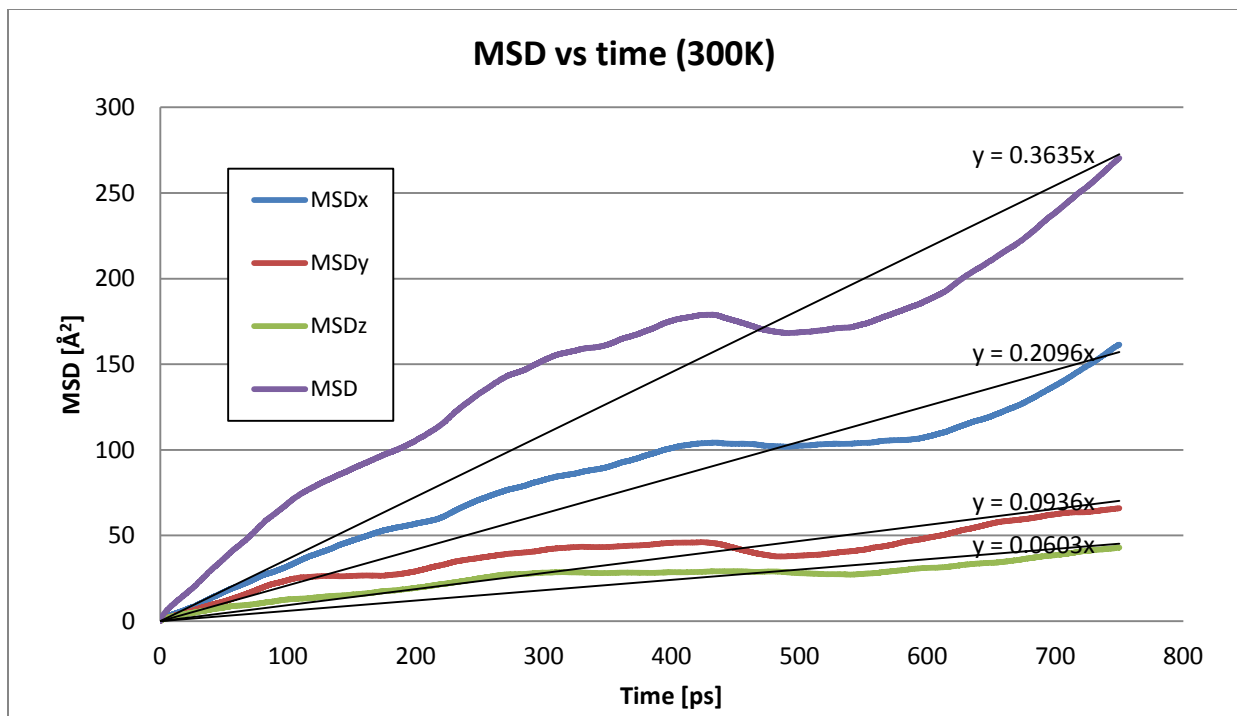


Figure 31: Average mean square displacement of rigid water molecules in silicalite at 300K. MSDx is along the x-direction, MSDy is along the y-direction, and MSDz is along the z-direction.

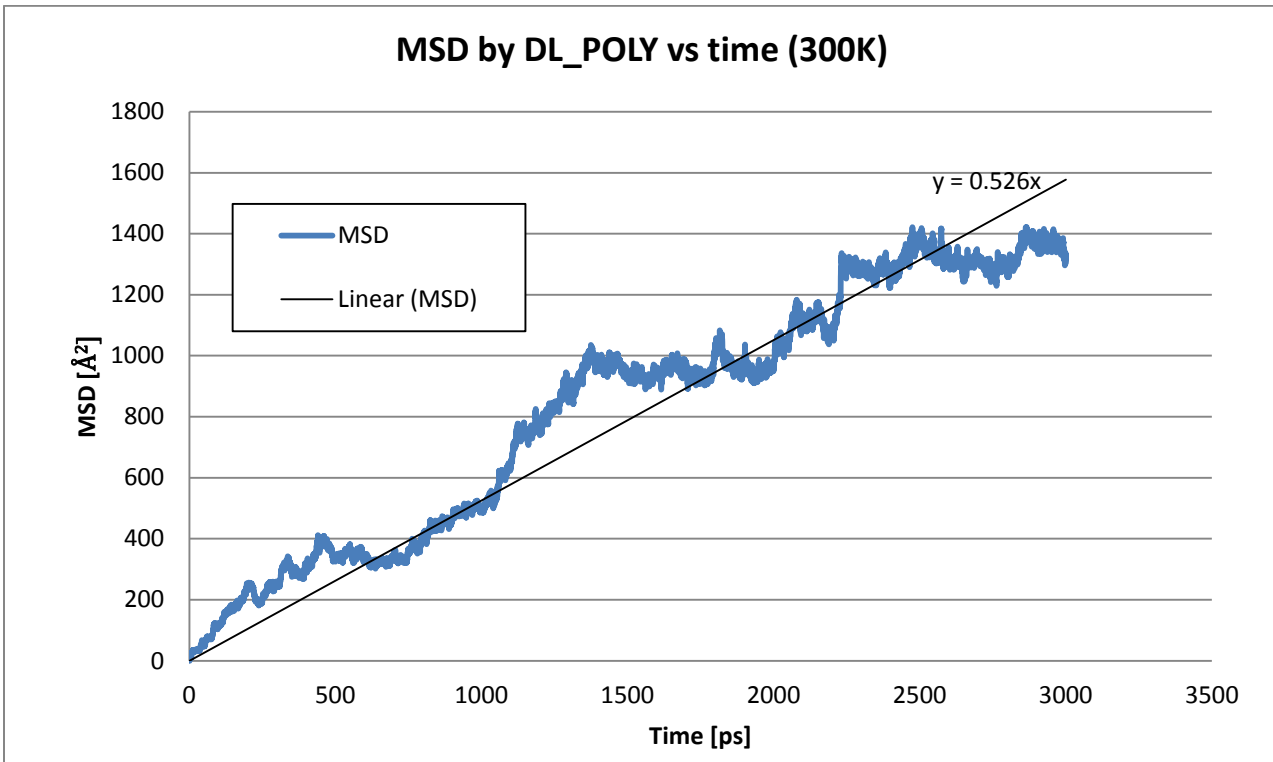


Figure 32: Mean square displacement calculated by DL_POLY of rigid water molecules in silicalite at 300K with trend line shown

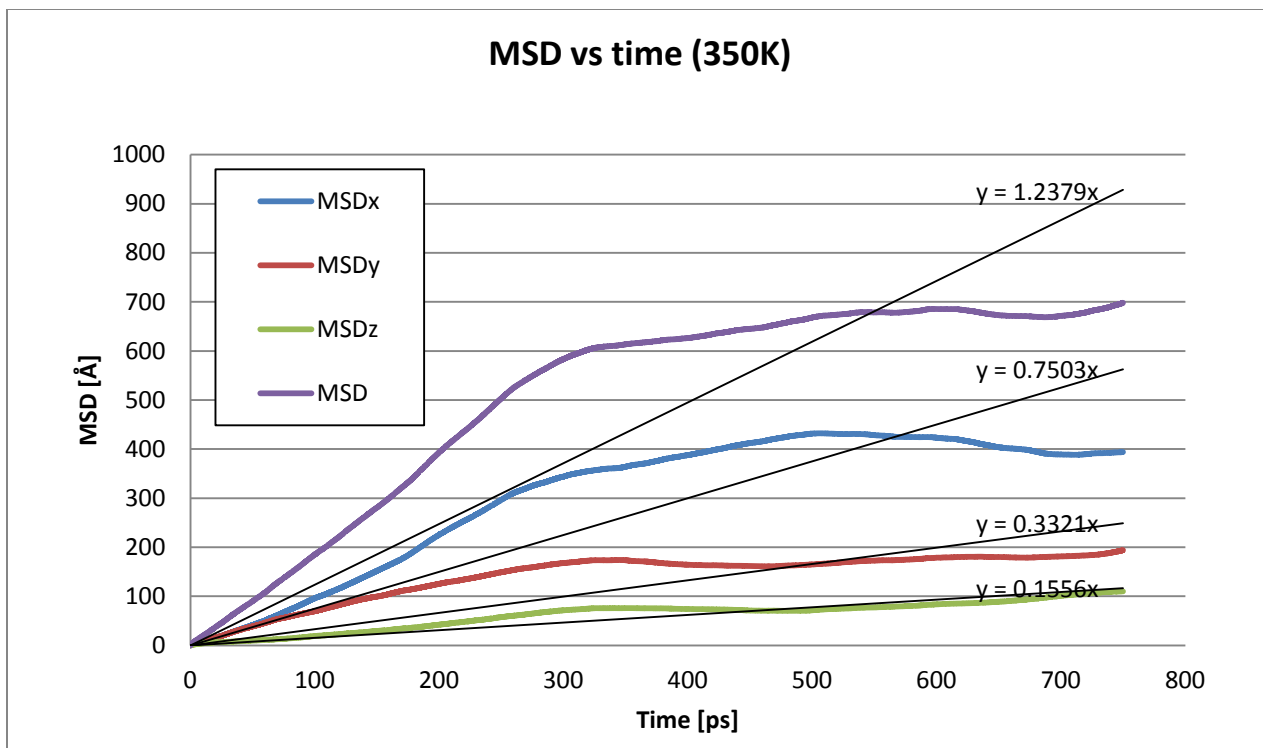


Figure 33: Average mean square displacement of rigid water molecules in silicalite at 350K. MSD_x is along the x-direction, MSD_y is along the y-direction, and MSD_z is along the z-direction.

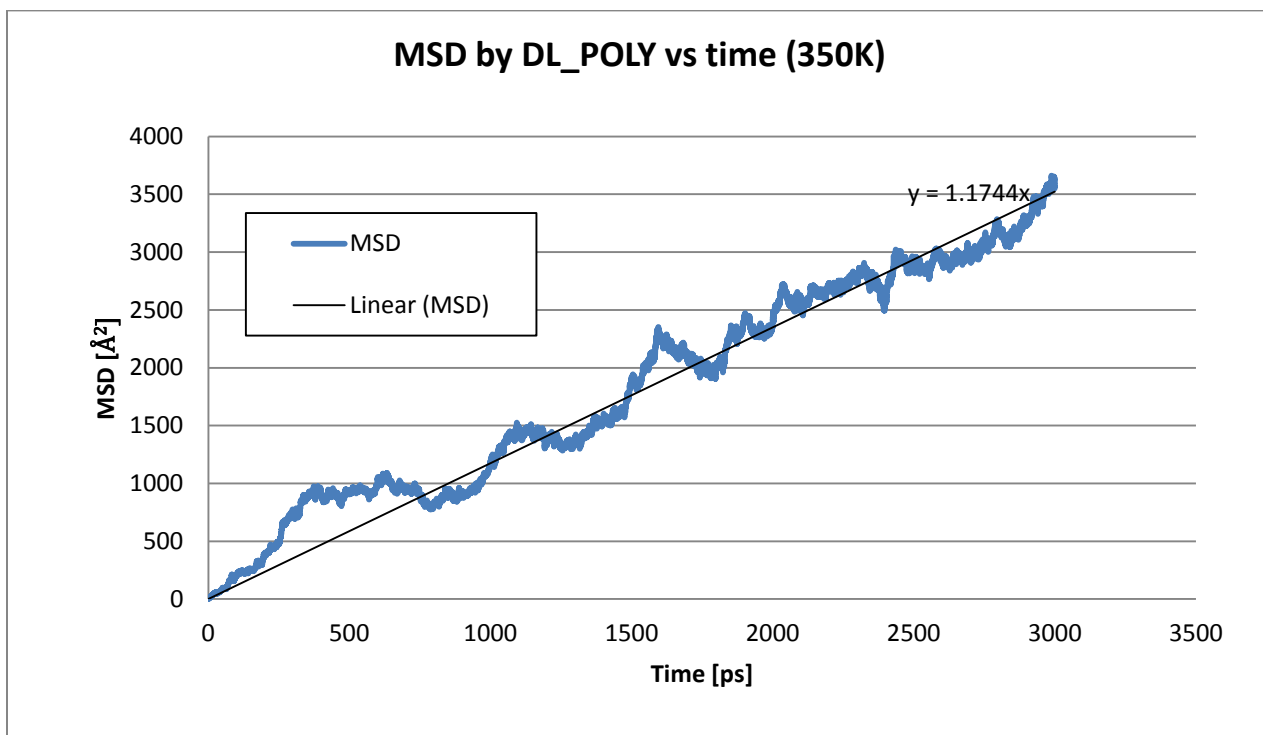


Figure 34: Mean square displacement calculated by DL_POLY of rigid water molecules in silicalite at 350K with trend line shown

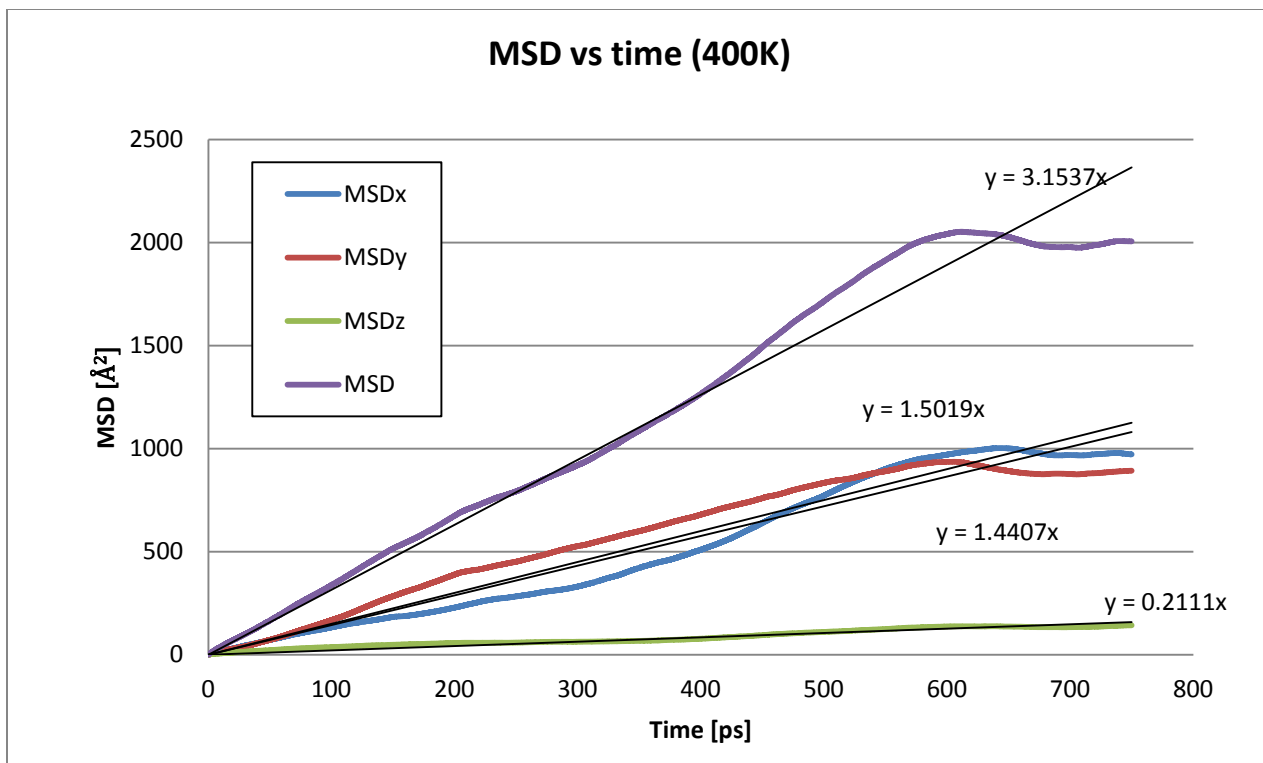


Figure 35: Average mean square displacement of rigid water molecules in silicalite at 400K. MSDx is along the x-direction, MSDy is along the y-direction, and MSDz is along the z-direction.

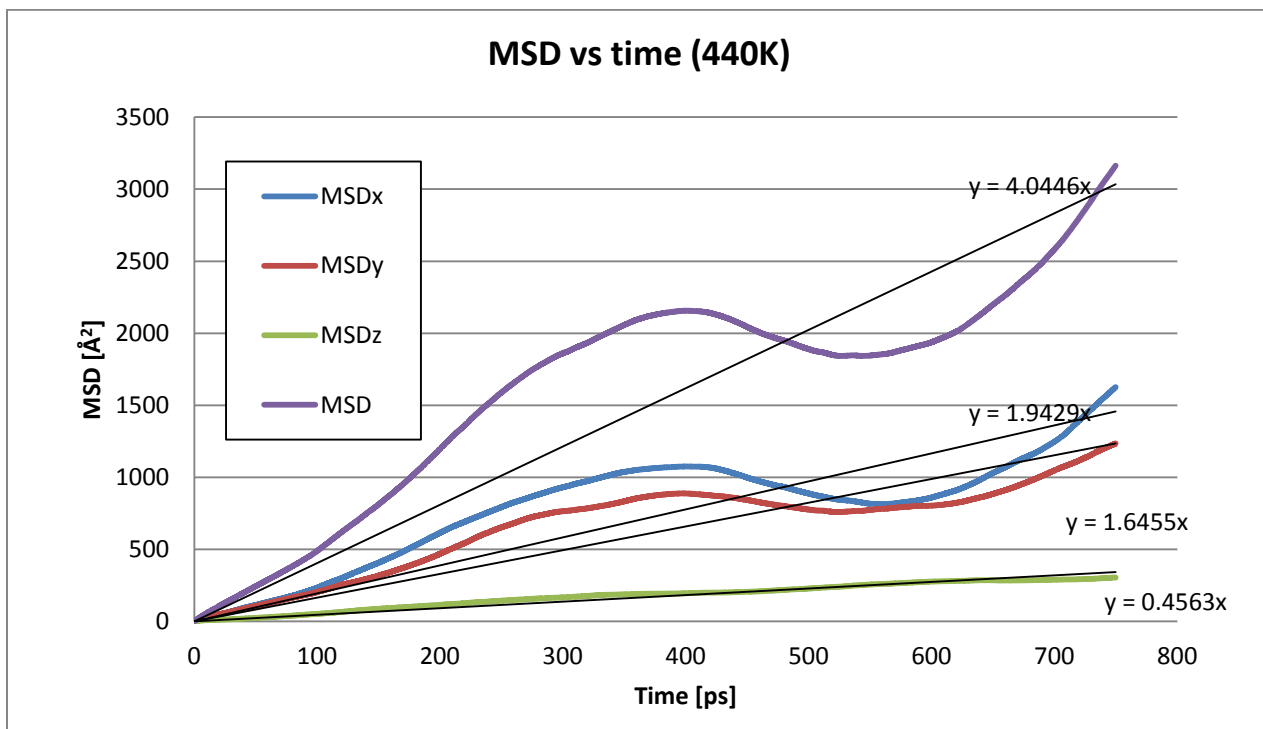


Figure 36: Average mean square displacement of rigid water molecules in silicalite at 440K. MSDx is along the x-direction, MSDy is along the y-direction, and MSDz is along the z-direction.

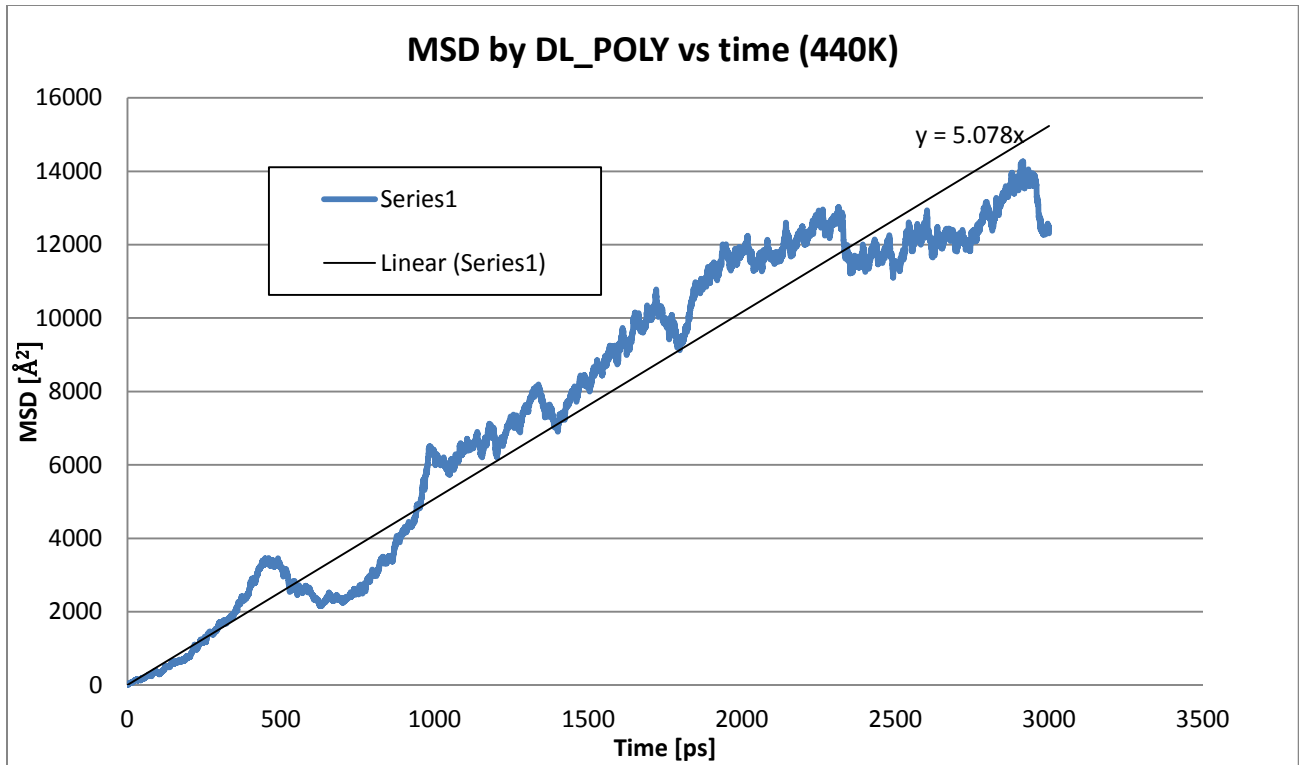


Figure 37: Mean square displacement calculated by DL_POLY of rigid water molecules in silicalite at 440K with trend line shown

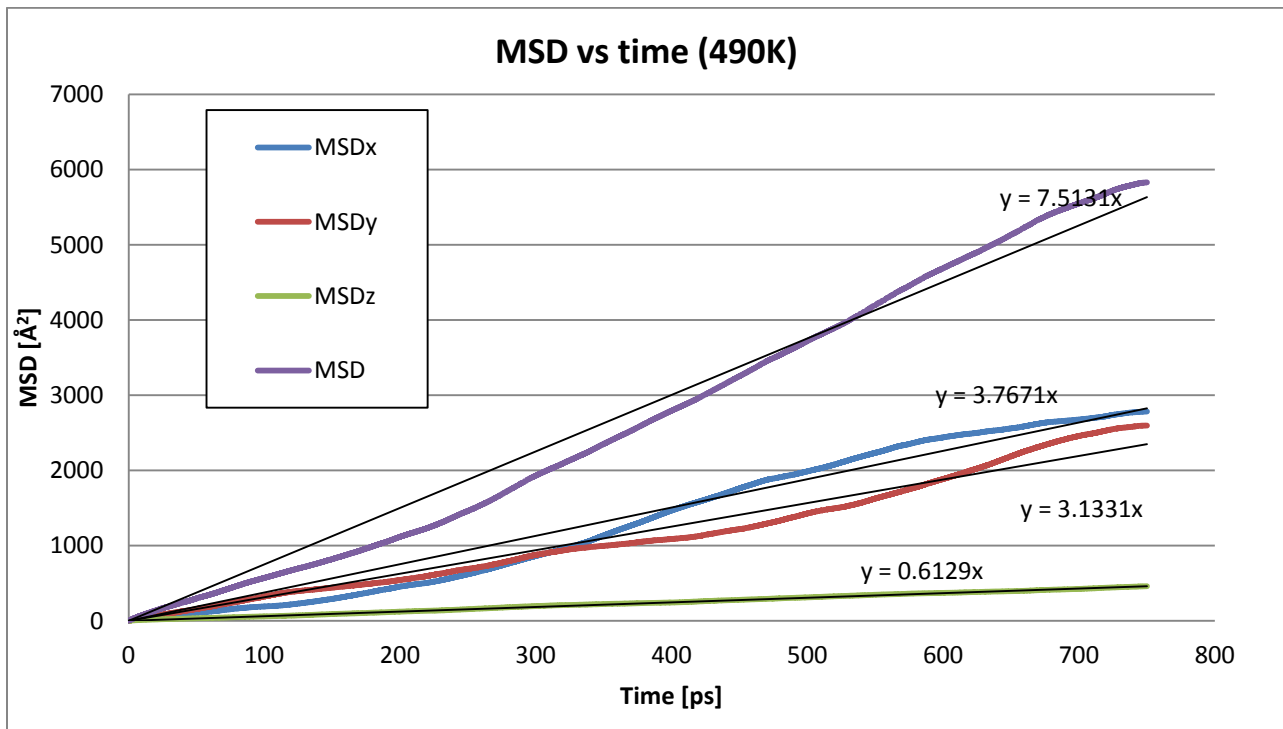


Figure 38: Average mean square displacement of rigid water molecules in silicalite at 490K. MSDx is along the x-direction, MSDy is along the y-direction, and MSDz is along the z-direction.

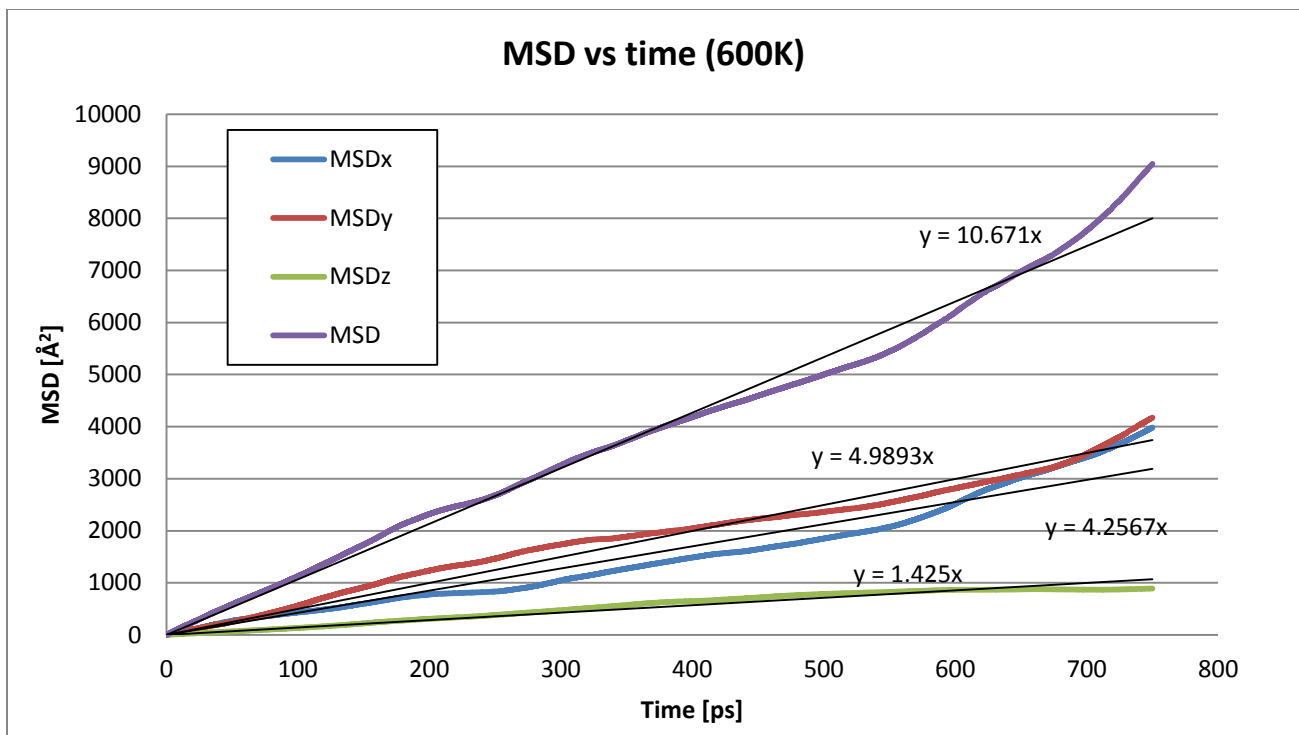


Figure 39: Average mean square displacement of rigid water molecules in silicalite at 600K. **MSDx** is along the x-direction, **MSDy** is along the y-direction, and **MSDz** is along the z-direction.

The rigid molecule gave comparable results to those using a non-rigid molecule (see above TIP3P results). An interesting result is the MSD at 300K appears to be more linear versus time. This implies we have an ideal diffusion for this temperature which was expected. It means that the α coefficient is equal to 1 and that the molecules can pass one another in the channels. For temperatures where the linearity was not clear based on the plots of the averaged MSD, we added the MSD calculated by DL_POLY in order to support our hypothesis, as shown in Figures 32, 34, 37. Another difference with the non-rigid water molecule is that the MSD in the x and y directions are more consistent with temperature. We have a greater MSD in the x direction for 300K and 350K while they are almost equal at higher temperatures. This could be explained by the relative smaller number of H-bonds that were found for the SPC water molecule compared to the non-rigid TIP3P model (see below for these results). Diffusion coefficients as well as β and δ parameters using the SPC model are given in Table 2.

T [K]	D	Dx	Dy	Dz	β	δ
300	0.605	1.048	0.468	0.3015	0.702198	2.514096
350	2.063	3.7515	1.6605	0.778	0.965518	3.478149
400	5.25	7.2035	7.5095	1.0555	0.057418	6.969683
440	6.654	9.7145	8.2275	2.021	0.022365	4.438892
490	12.52183	15.6655	18.8355	3.0645	0.009228	5.62914
600	17.785	21.2835	24.9465	7.125	0.002926	3.244211

Table 13: Diffusion coefficients of SPC water in silicalite [$10^{-9} \text{ m}^2 \cdot \text{s}^{-1}$], β and δ parameters as function of T

Almost the same conclusions can be drawn from this table compared to the TIP3P model. The β parameter is always inferior to 1, even if at 350 it is really close to 1, meaning that water molecules will rather change channels when they arrive at an intersection. The delta parameter values seem to also be quite random. A value of 4.4 is reached for 440K meaning that the random walk model is valid at that temperature.

2- Radial distribution functions

In this part we present the radial distribution functions g_{OO} and g_{OH} for both TIP3P and SPC water models at temperatures between 300 and 600K. We then calculate the number of H-bonds for each temperature based on the method explained in the previous section of this report, and compare our results with literature.

A- TIP3P water molecule:

In this part we show the plots (Figures 40-43) of $g_{\text{OO}}(r_{\text{OO}})$ and $g_{\text{OH}}(r_{\text{OH}})$ for the non-rigid water model TIP3P. Two different ranges of temperatures (300-400K and 440-600K) were investigated. We plotted them together because their values are close. Note that we kept the same scale for both ranges of temperature for the same rdf in order to see how different these plots are with temperature.

The trends of these different radial distribution functions are in very good agreement with literature. The values for this range of temperature are also very close to the values obtained by Fleys. We calculated the number of H-bonds for each temperature and the results are given in Figure 52 in order to compare our results with Fleys'.

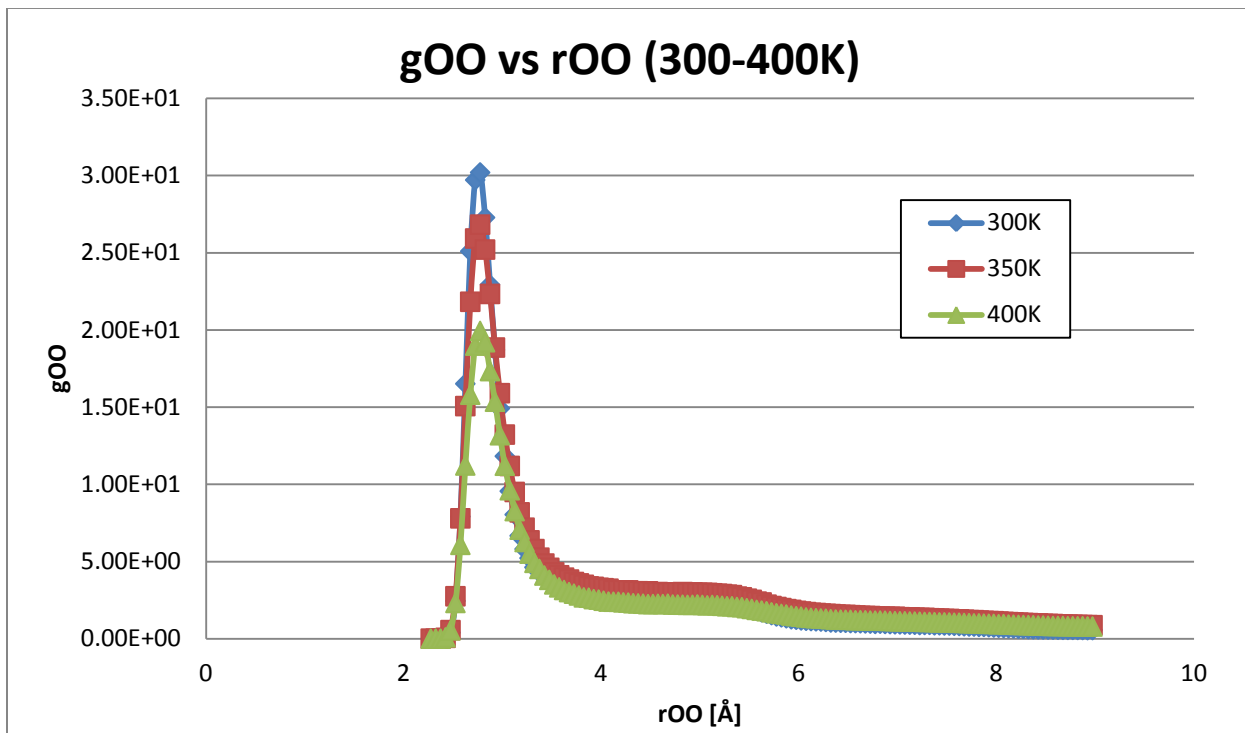


Figure 40: Radial distribution function g_{OO} versus r_{OO} at 300K, 350K and 400K for water

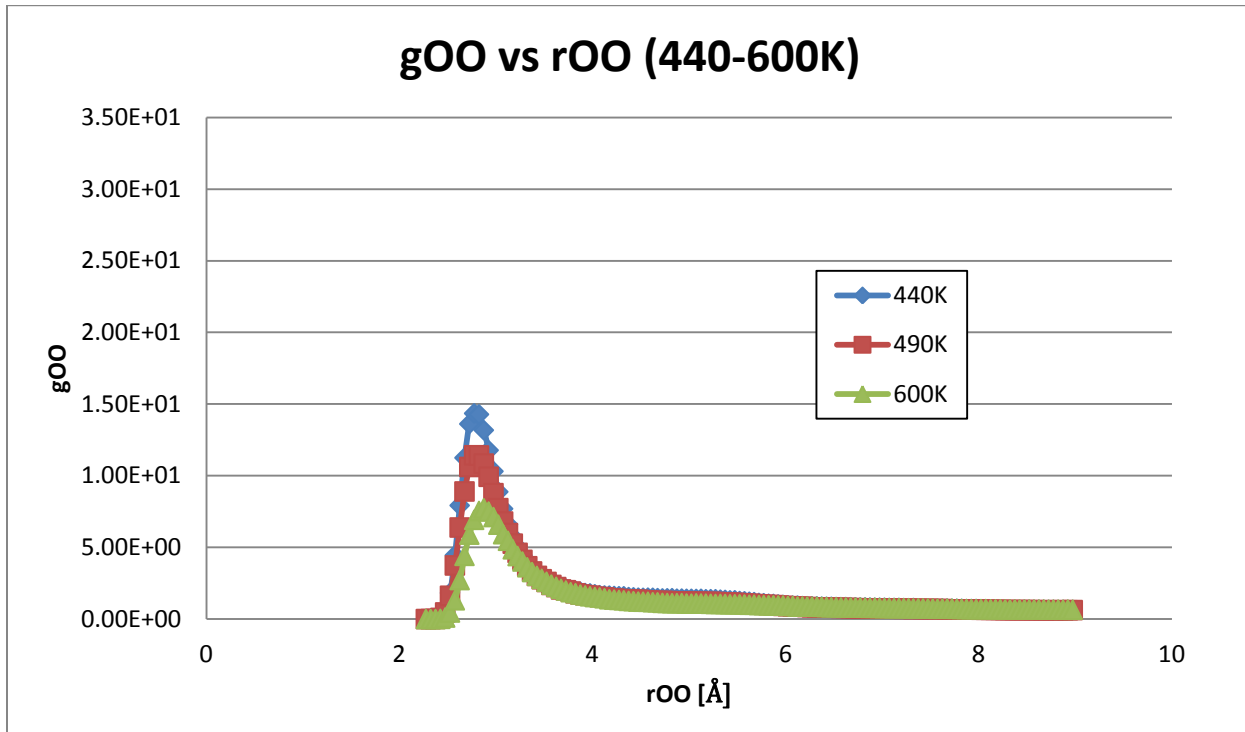


Figure 41: Radial distribution function g_{OO} versus r_{OO} at 440K, 490K and 600K for water

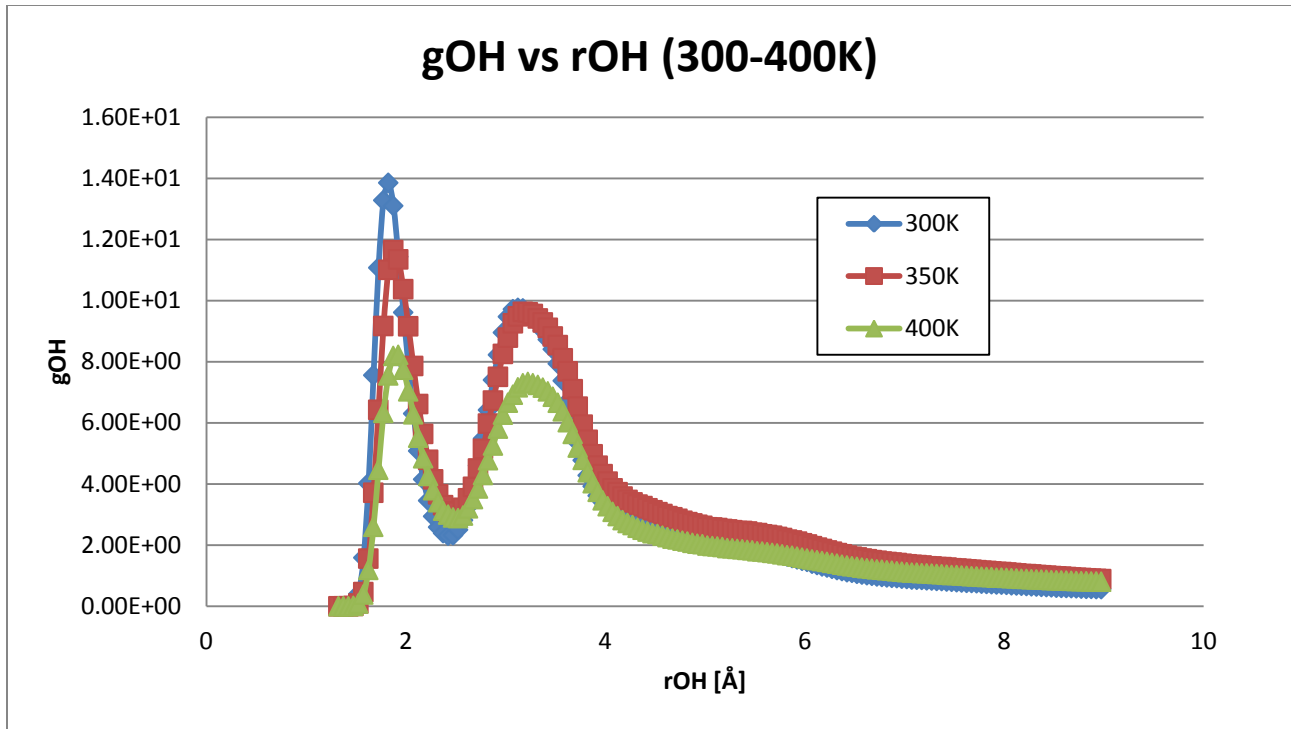


Figure 42: Radial distribution function gOH versus rOH at 300K, 350K and 400K for water

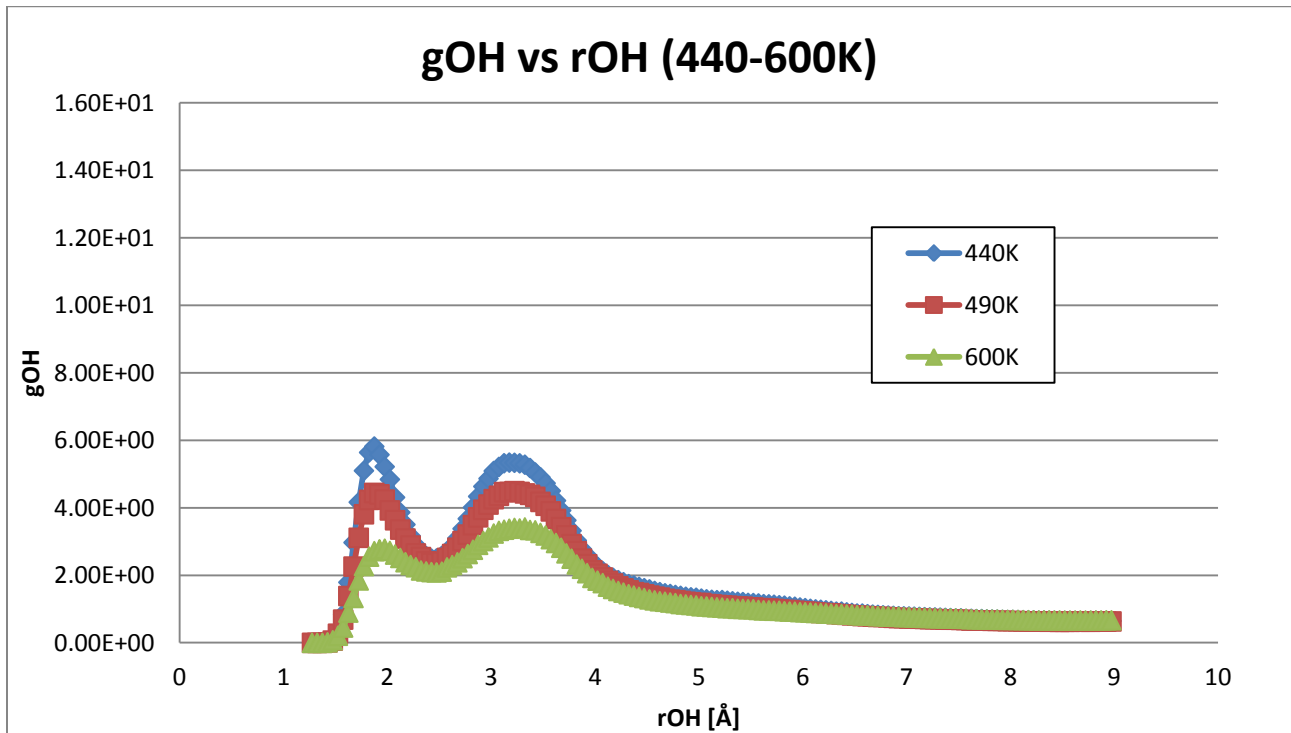


Figure 43: Radial distribution function gOH versus rOH at 440K, 490K and 600K for water

We also evaluated the importance of silicalite hydrophobicity by calculating the rdf between the oxygen of the framework and the hydrogen of the water molecules, as shown in Figure 44-45.

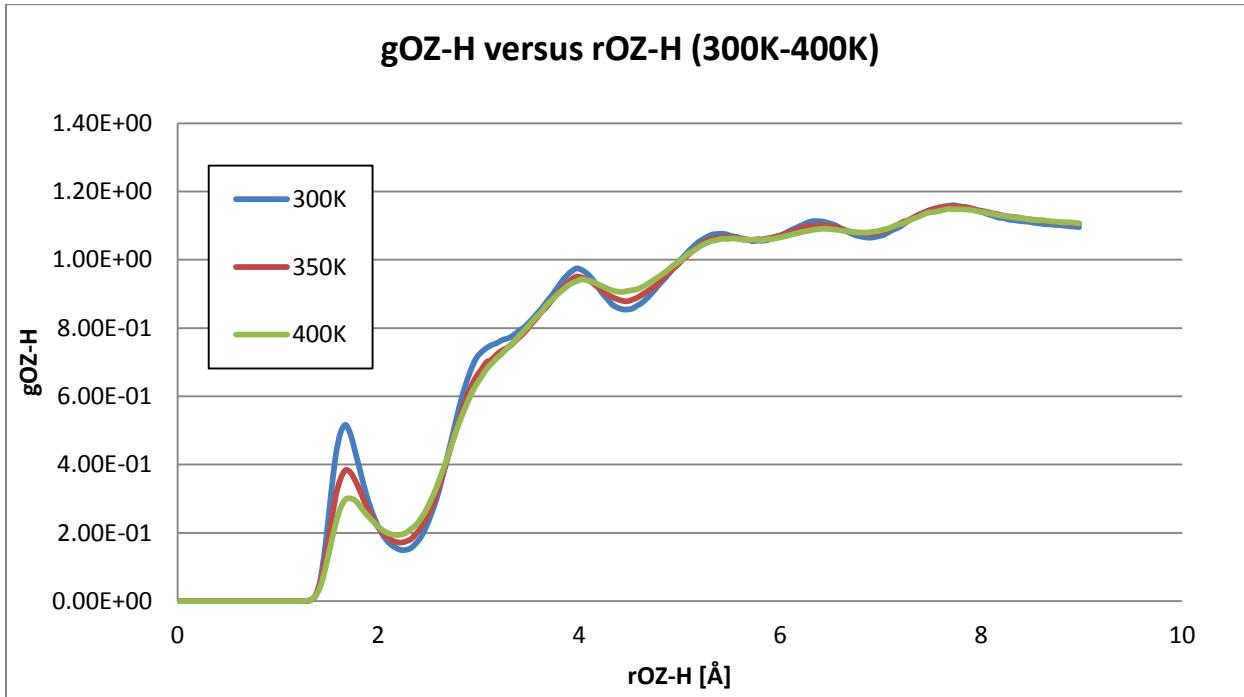


Figure 44: Radial distribution function g_{OZ-H} versus r_{OZ-H} at 300K, 350K and 400K for water

Hydrogen bonding between water and the hydrophobic zeolite is present due to the presence of negatively charged O atoms in the zeolite framework. We can see however on these plots that the values of the rdf's are much smaller than the ones between water molecules. Silicalite is hydrophobic and the diffusion process is mostly hindered due to water-water interactions.

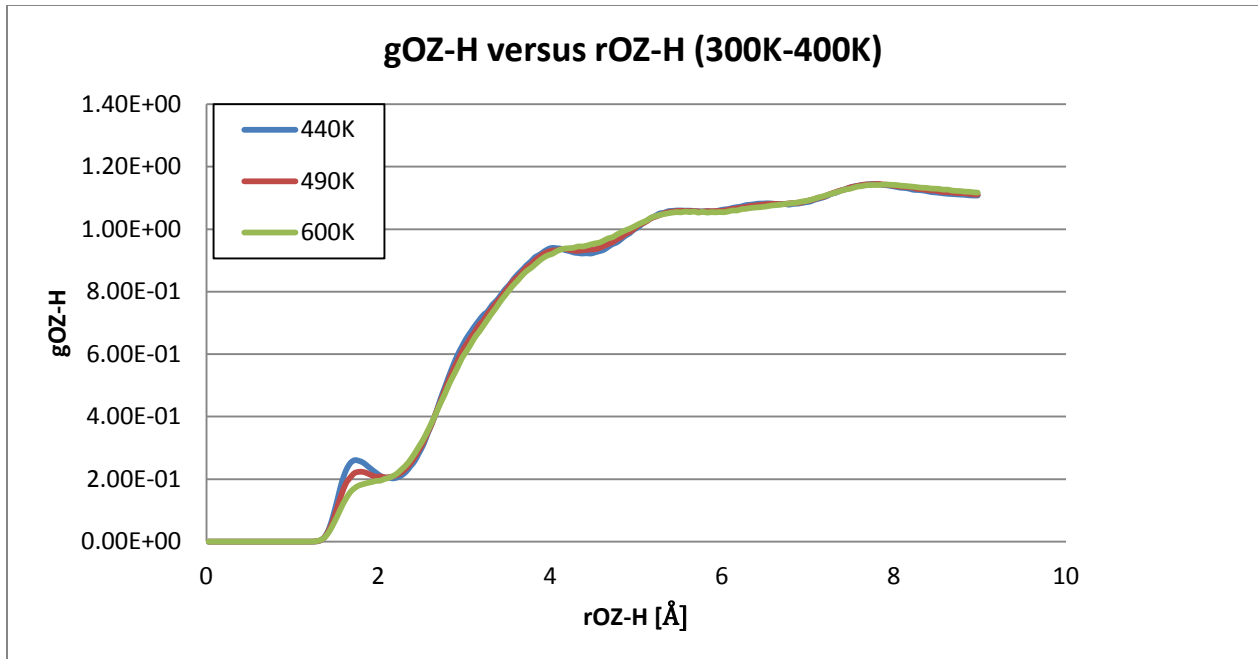


Figure 45: Radial distribution function g_{OZ-H} versus r_{OZ-H} at 440K, 490K and 600K for water

B- SPC water model

In this part we also show the plots (Figures X-Y) of $g_{OO}(r_{OO})$ and $g_{OH}(r_{OH})$ for the rigid water model SPC. The same two ranges of temperatures (300-400K and 440-600K) were investigated.

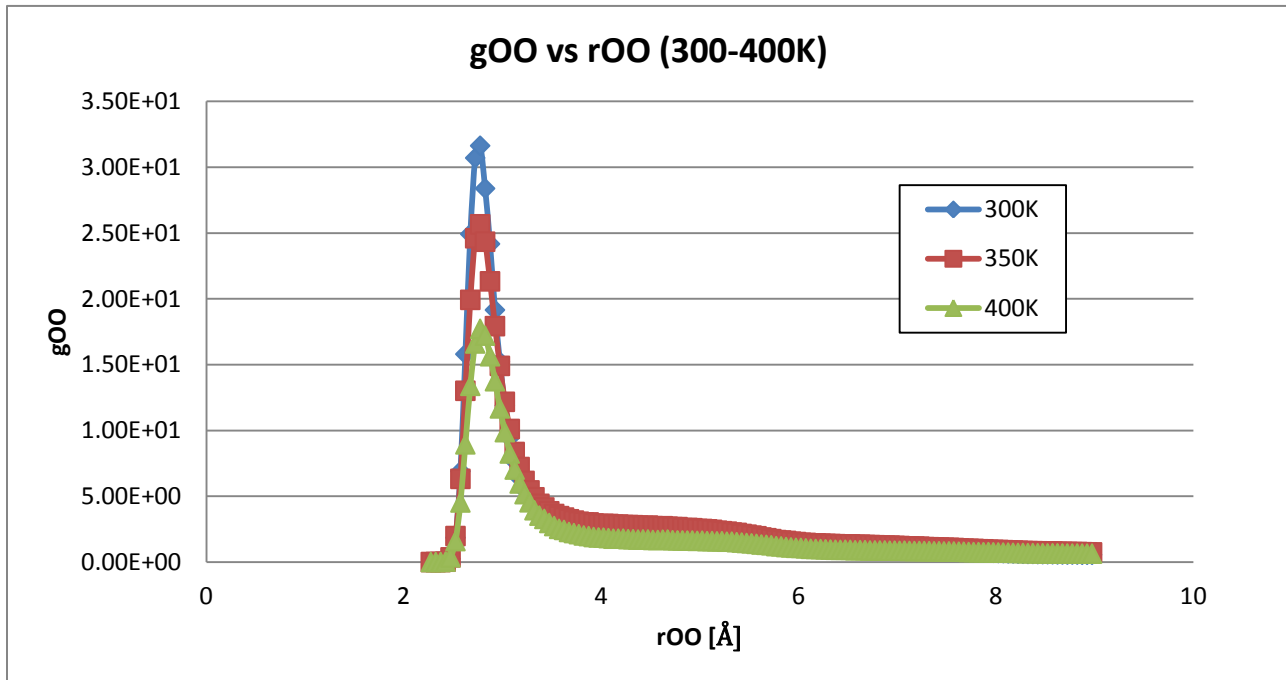


Figure 46: Radial distribution function g_{OO} versus r_{OO} at 300K, 350K and 400K for rigid water

The same conclusions can be drawn from these plots as for the previous section. The radial distribution functions obtained after our simulations are also in very good agreement with the ones calculated by Fleys. The trends are the same as the one found by Demontis et al. and the peaks are located at the same distance. The number of H-bonds is once again given in the following section where we will discuss these results.

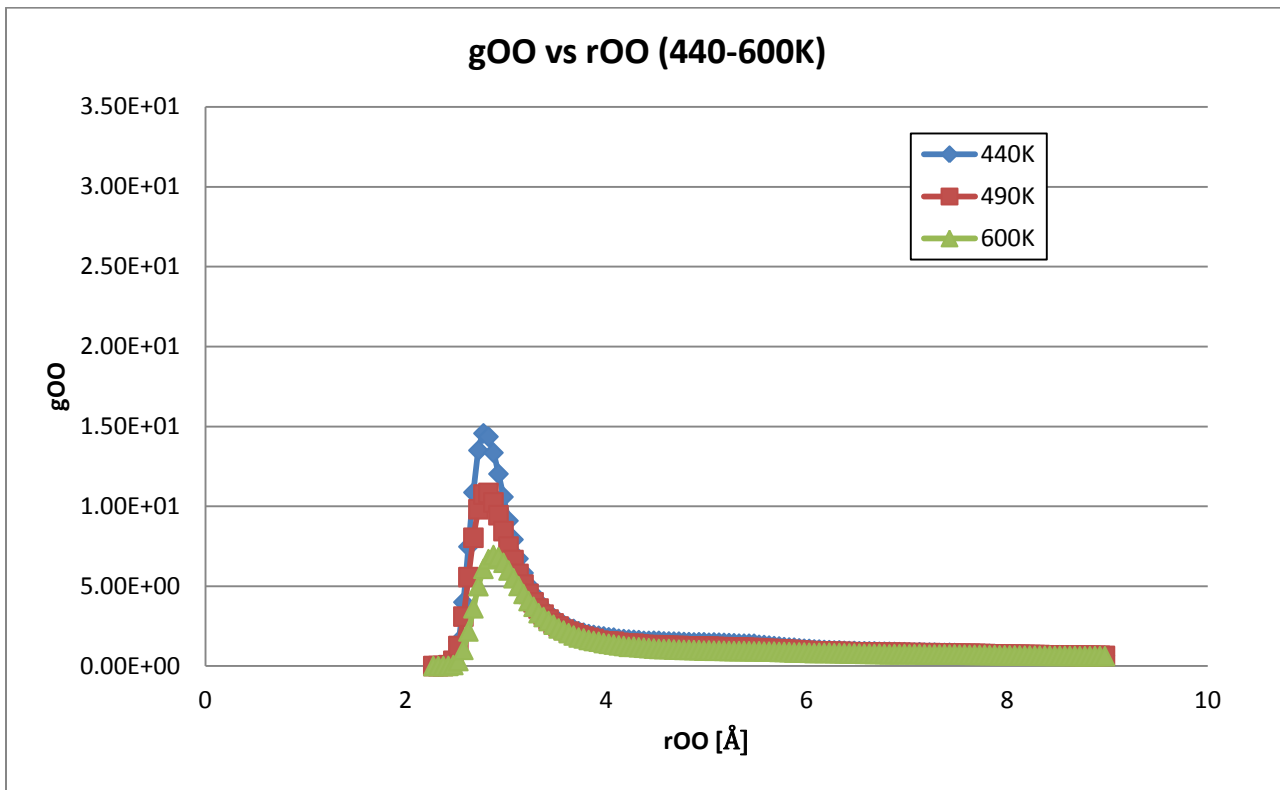


Figure 47: Radial distribution function g_{OO} versus r_{OO} at 440K, 490K and 600K for water

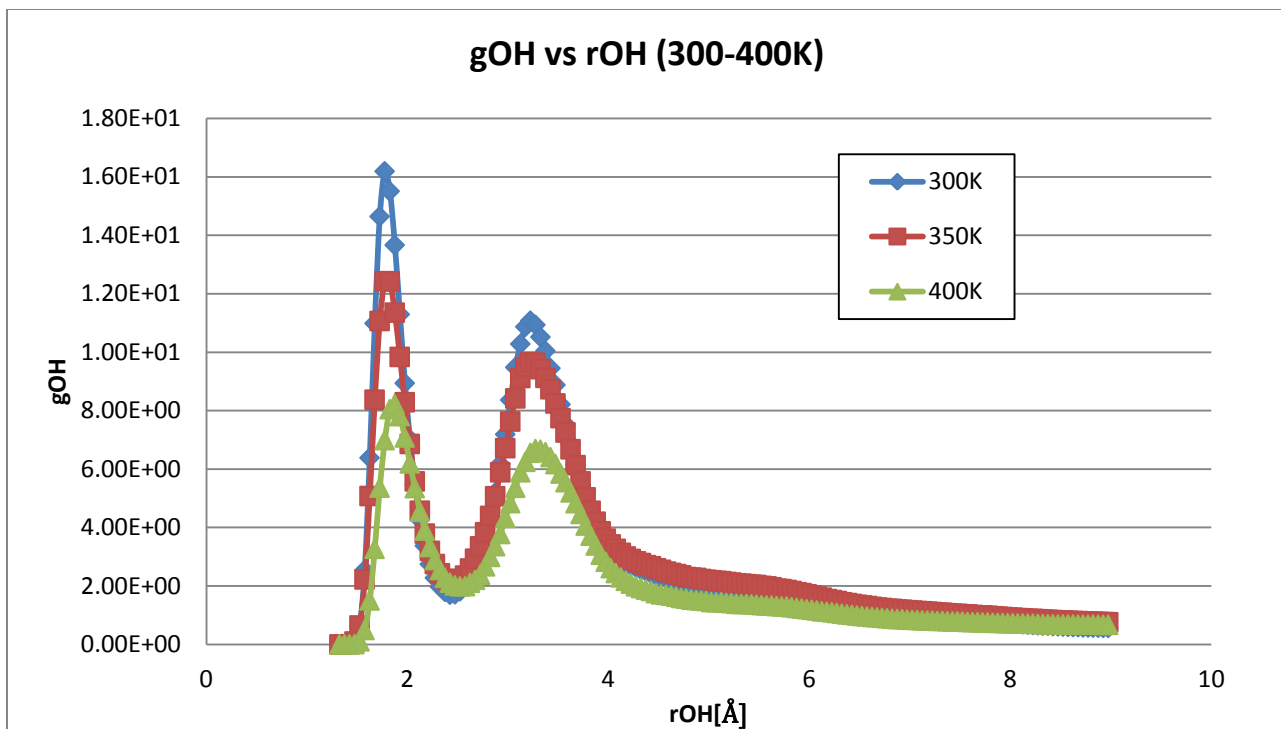


Figure 48: Radial distribution function gOH versus rOH at 300K, 350K and 400K for rigid water

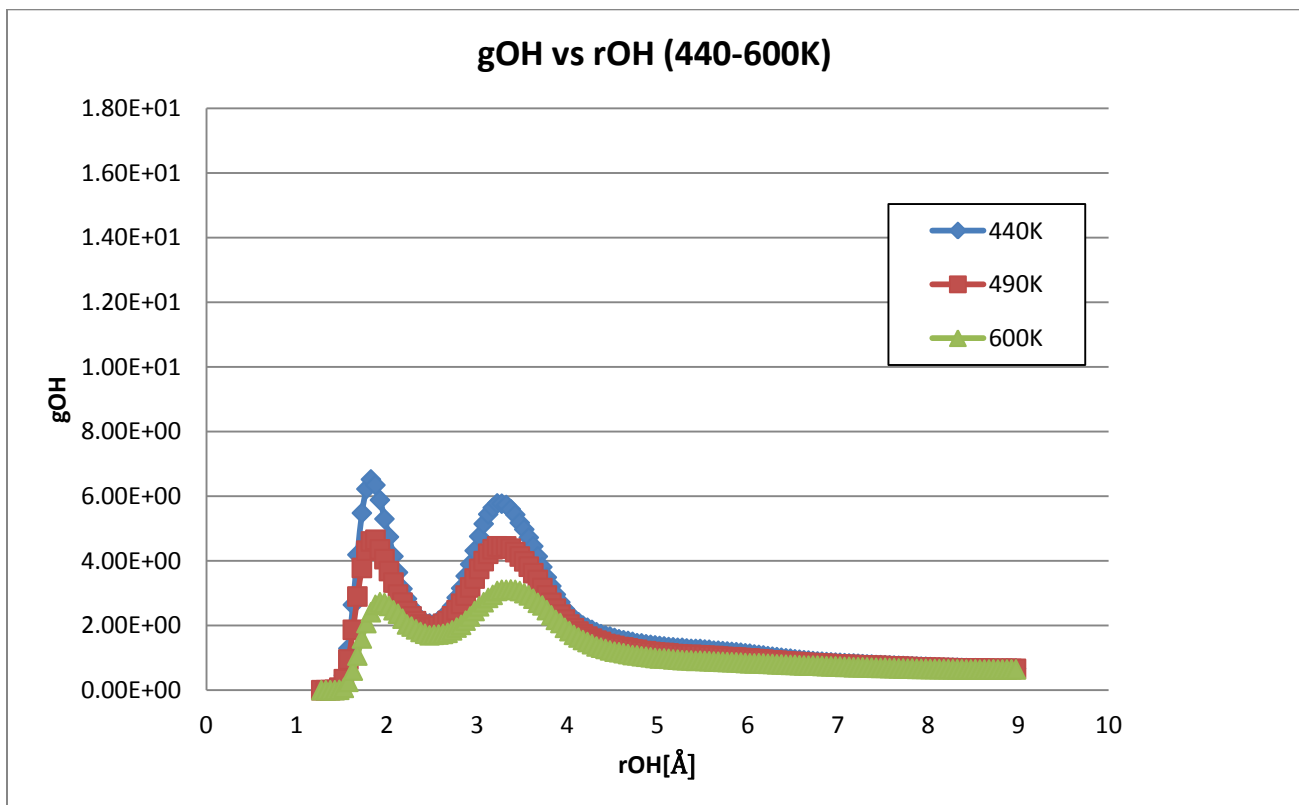


Figure 49: Radial distribution function gOH versus rOH at 440K, 490K and 600K for rigid water

The same rdf's can be evaluated to see if the rigid model interacts more with the framework than the TIP3P water model.

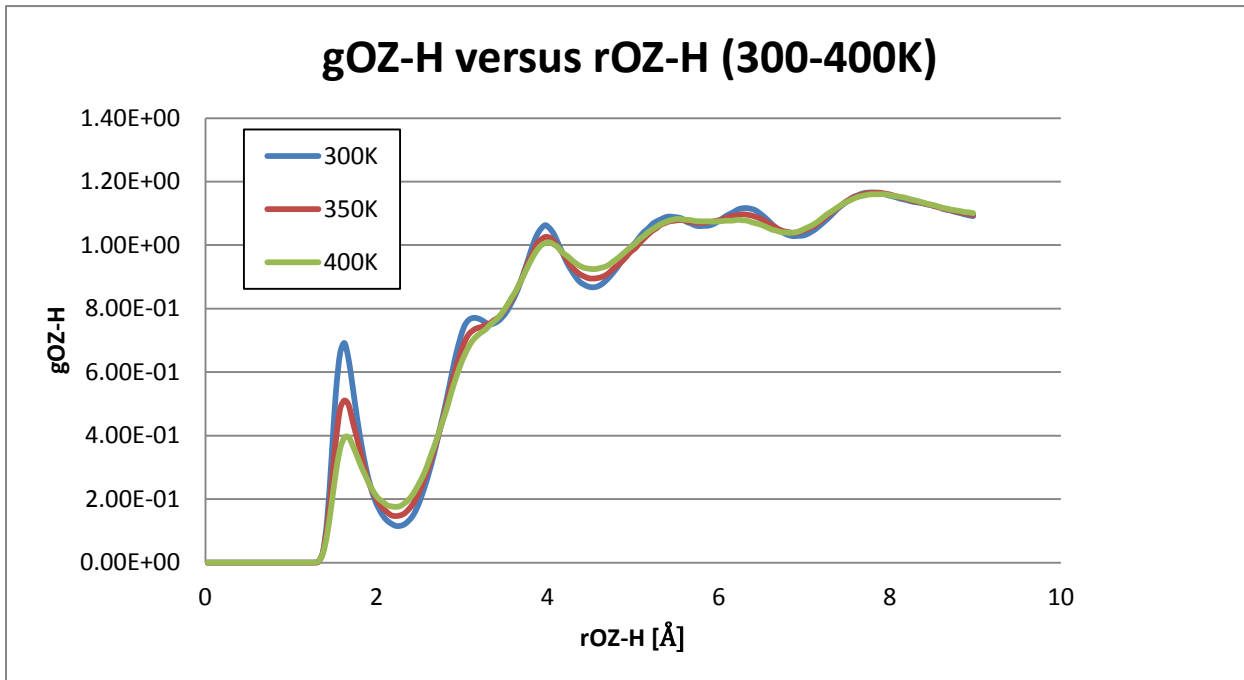


Figure 50: Radial distribution function gOZ-H versus rOZ-H at 300K, 350K and 400K for rigid water

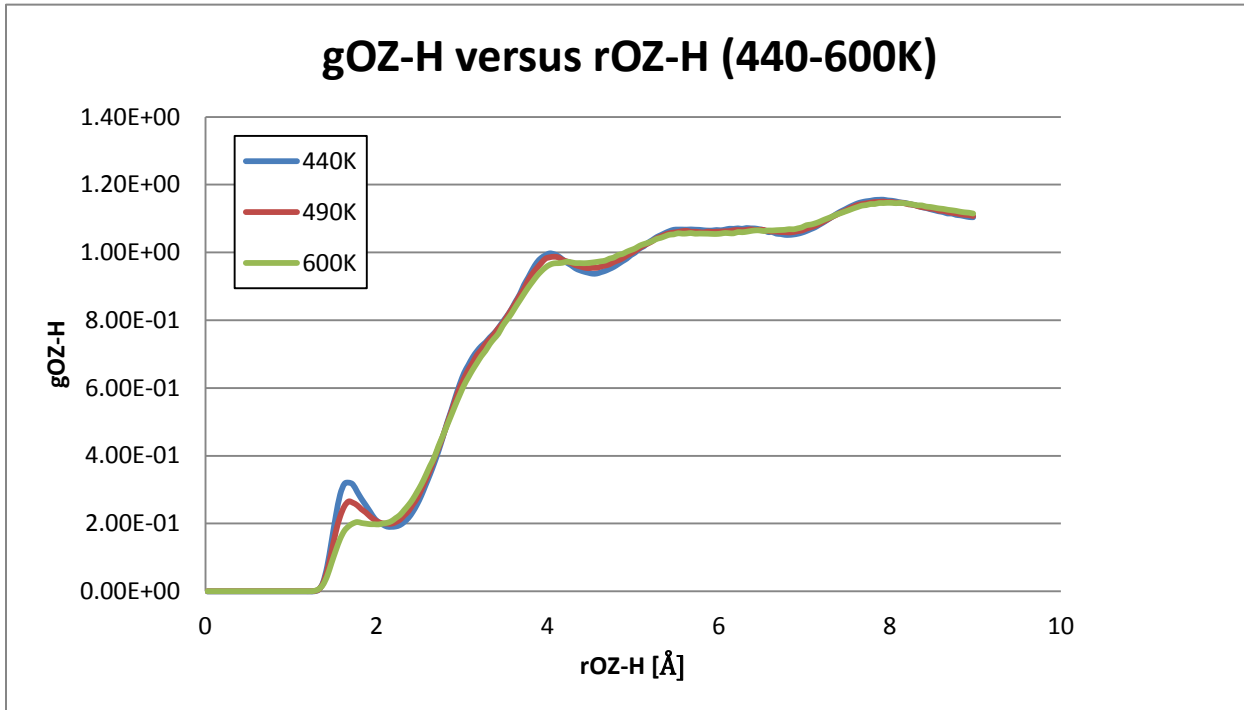


Figure 51: Radial distribution function gOZ-H versus rOZ-H at 440K, 490K and 600K for rigid water

The same conclusions can be drawn from these plots. Silicalite is highly hydrophobic, even if the values of gOZ-H for our rigid model are slightly higher than the ones seen for the TIP3P model. They are much smaller than the rdf between water molecules.

3- Discussion

Table 14 shows the different results found in literature next to the results of this thesis. As we can see in this table results found in literature vary quite a bit.

T [K]	Self-diffusion parameters [$10^{-9} \text{ m}^2.\text{s}^{-1}$]								
	300	350	400	440	450	490	500	580	600
TIP3P ^(This work)	-	2.2	2.8241	4.7033		9.313			18.927
SPC ^(This work)	0.605	2.063	5.25	6.654		12.521			17.785
Fleys ²²	8.83	10	10.55	13.11		16.53			26.13
Demontis et al. ³³	8.61	9.4	9.89		12.6		16.1	20.7	
Yang et al. ⁴¹	2.6								
Bussai et al. ⁴⁴	3.3		6.7						
Bussai PFG-NMR ⁴⁴	1.7		1.5						
Yazaydin et al. ²⁴	0.614	2.7	4.80						

Table 14: Summary of results for self-diffusion coefficient of water in silicalite found in literature

Fleys²² and Demontis³³ have very similar results working with different force-fields. Fleys worked with the Materials Studio® software and the COMPASS force-field water and silicalite and Demontis worked with a force-field that was developed in his group. Both worked with a flexible silicalite framework and a rigid water model. Yang⁴¹ and Bussai⁴⁴ found diffusion coefficients that are in the same order of magnitude but still much smaller than the ones found by Fleys and Demontis. Yang and Fleys used the force-field, but the main differences between their works are that Yang ran simulations under NVT conditions while Fleys used the NVE ensemble and Yang used the isotropic model in order to calculate the diffusion coefficient. The isotropic model states that the diffusion of molecules in silicalite is the same in every direction and the formula for the diffusion coefficient is calculated using the total MSD. (See the Methodology section for the formula) This is quite unexpected because it has been proven that silicalite has a strong anisotropic behavior. Bussai used a rigid silicalite structure with non-rigid water molecules for his calculations.

It is important to note that NMR experiments led by Bussai gave small diffusion coefficients.. First, the industrial zeolite might not be all-silica silicalite; defects, even in small numbers, could

have a great influence on the results found. Secondly, the presence of water in the zeolite pores or outer surface can also influence the results obtained. Finally, the signal treated by PFG-NMR for these experiments is very weak because of the high hydrophobicity of silicalite; that could imply a big error margin. This could explain the very small diffusion coefficient found at 400K from experiment.

Our results for the lower temperatures (300 and 350K) appear lower than other literature values. We found that for the TIP3P model at 300K water molecules were following a single-file diffusion process which is not what other groups observed. For the SPC model, we have an ideal-diffusion process, but our value of D is an order of magnitude smaller compared to other groups except for Yazaydin et al²⁴. They found a value for D that is really close to the one we found for the SPC water model. Their simulations parameters are also close to the ones we used. They worked with a NVT ensemble, simulated 8 water molecules per unit cell placed at intersections of straight and sinusoidal channel. They used a different rigid water model, the TIP4P water model but most importantly used different charges for his silicalite framework atoms. He used charges for Si that ranged from +1.167 to +1.314. The charge we decided to use for our simulations is +2.05. This is a major difference as molecules will not interact the same way with the framework. In his conclusions, Yazaydin points out the fact that the water model he used is probably not the reason why he had such small diffusion, but is most probably the fixed silicalite model that he used. We used a vibrating structure but still found very low diffusivities. If water models are not the cause, then it means that the charges used for the silicate and oxygen atoms are most probably the major issue. He also used an isotropic model to calculate the self-diffusion parameter that could lead to an error in the total diffusion coefficient.

At 350K, our results are a bit better. We have diffusion coefficients that are in the same order of magnitude but still much smaller. These values ($\sim 2.2 \cdot 10^{-9} \text{m}^2 \cdot \text{s}^{-1}$) are close to the one of bulk water.

For higher temperatures, our simulations are in fair agreement with literature. Our values of D are in the same order of magnitude, yet 1.5 to 2 times smaller. One important thing to note is that the mean square displacements, and therefore the diffusion coefficients, are calculated from averaged values. Our statistical method results in smaller values of the calculated MSD

compared to the one calculated by DL_POLY which are still significantly lower than the ones obtained by both Fleys and Demontis.

The number of H-bonds calculated after the rdf's is given in the following graph (Figure 52). As we can see, the number of H-bonds per molecule of water is much higher in our simulations compared to the work of Fleys²². Nevertheless, the three models follow the same trend; the number of hydrogen bonds reduces as temperature increases. The two models used for our simulations have almost the same number of H-bonds at each temperature while Fleys' values are almost twice as small. We had a diffusion coefficient that was about two times smaller than Fleys' which is very likely linked to the hydrogen bonding. Hydrogen bonding would tend to slow the water molecules in the channels as the water molecules cluster together. Our higher degree of hydrogen bonding is likely leading to our small diffusion coefficients.

Based on the theoretical results from literature^{22, 33, 44}, water molecules are expected to move more freely in the straight channel. Our simulations showed almost the opposite behavior, since MSDy was either smaller or equal to MSDx. The clusters of water molecules that hinder the diffusion of water molecules through the y-channel could be explained by these high numbers of H-bonds.

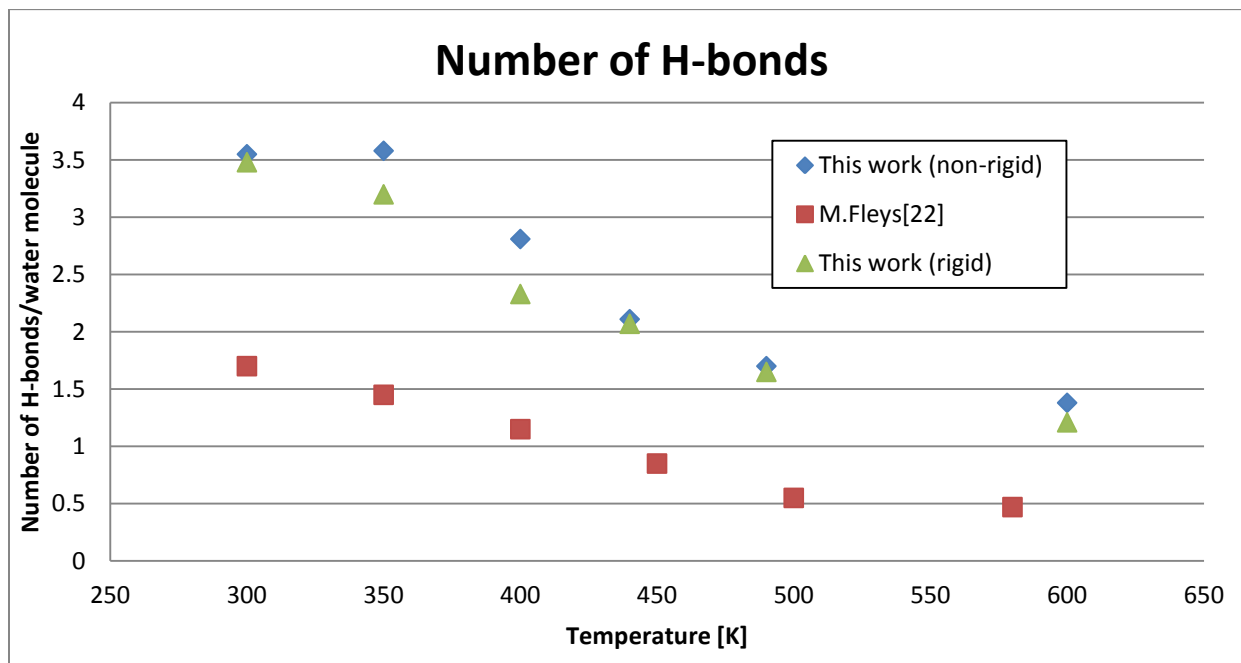


Figure 52: Number of Hbonds as a function of temperature for SPC and TIP3P models and Fleys results

Moreover, we found a diffusion coefficient of around $2.2 \cdot 10^{-9} \text{ m}^2 \cdot \text{s}^{-1}$ for 350K and we can see that the number of H-bonds is around 3.5 which is roughly the value in bulk water. From these results it looks like water is most probably in a liquid-like form. Based on our model, it looks like interactions between water molecules are too strong to allow them to move as much as they should. This is especially true for the TIP3P model, where charges and LJ parameters are put on the hydrogen atoms of water. The number of H-bonds is always slightly higher for TIP3P compared to SPC. An interesting point would be that we have almost the same rdfs as Fleys but our numbers of H-bonds per water molecule are higher than his. We used the integrated values given by DL_POLY to plot the integrals of the different rdf plots.

Our results can be used to calculate activation energy values. The following graph gives the activation energy of water in silicalite at various temperatures.

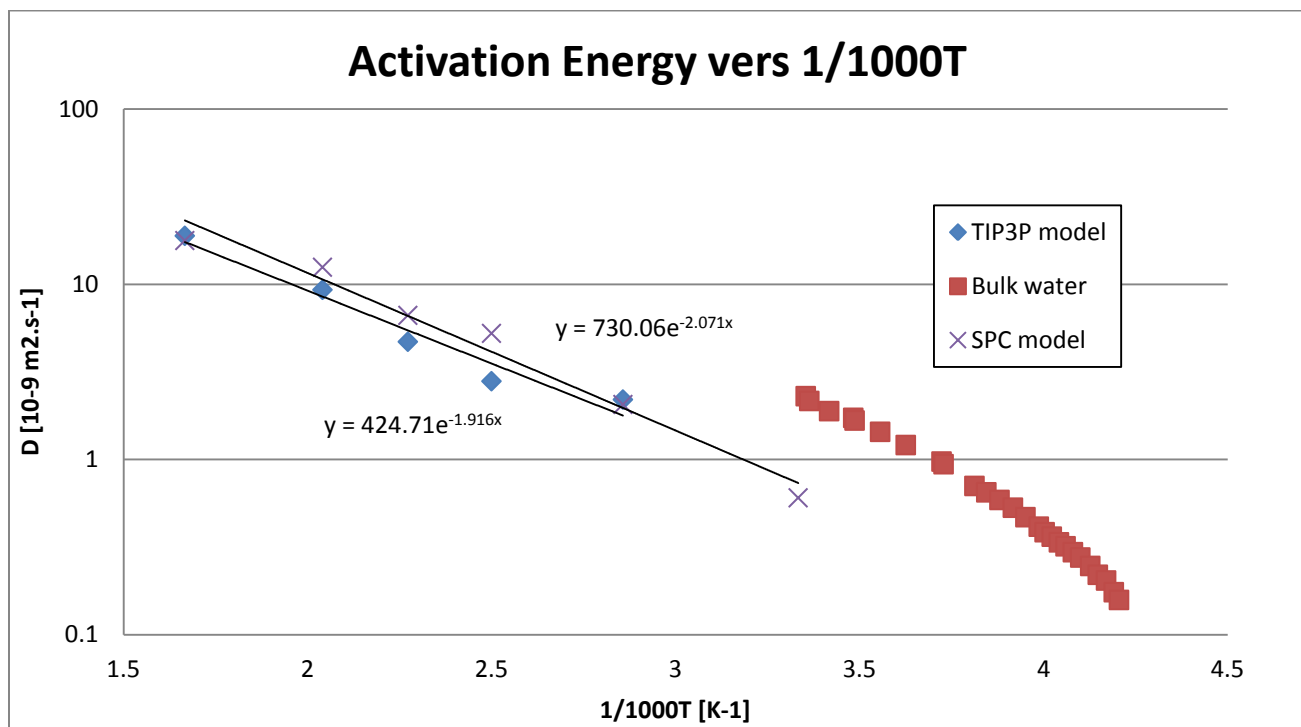


Figure 53: Activation energy of water molecule in silicalite versus temperature

Based on this graph we find only one value (or a linear curve) of the activation energy per model, although it is possible that better statistics may be needed to fully observe this premise. We do not see the same trend as Fleys and Demontis where their activation energy plots had 3 distinct sections. They argue that the first activation found between 250 and 300K is

smaller than bulk water because the number of hydrogen bonds is much smaller and so the movement of water molecules is faster compared to bulk water. Here we cannot compare this phase because we do not have an ideal diffusion below 300K. Their second phase is between 300 and 400K where the activation energy is very low ($\sim 1.5\text{kJ}\cdot\text{mol}^{-1}$). They explain that activation energy can be divided into 2 parts, one part for the translation, the other for the rotation of molecules. For this range of temperature they argue that only the translation barrier remains and that lattice vibration plays an important role in the diffusion of water. This also supports the idea that between 300 and 400K water is in a transition state between liquid and vapor phase. For temperatures above 400 K they find an activation energy of $8.5\text{kJ}\cdot\text{mol}^{-1}$ which seems to confirm the vapor state of water in silicalite. As mentioned earlier we found only one trend for the activation energy. The value is however different for the two models. We found $E_a = 1.916 * 8.314 = 15.93 \text{ kJ}\cdot\text{mol}^{-1}$ for the TIP3P model and $E_a = 2.071 * 8.314 = 17.22 \text{ kJ}\cdot\text{mol}^{-1}$ for the SPC rigid model. These values are close to the value reported by Yazaydin et al. which was $21.576 \text{ kJ}\cdot\text{mol}^{-1}$ for the TIP4P water model. These values are in the range of bulk water activation in a liquid-like state. This appears in disagreement with Fleys and Demontis.

We believe that these results could be explained by the water model we used in our simulations. SPC and TIP3P are great models for bulk water simulations but there are uncertainties concerning its ability to describe water in zeolites. Comparing our conclusions and Yazaydin et al. ones it seems that another possibility could be the charges used to describe our silicalite structure. Our results are close to theirs for the diffusivity of rigid water molecules in silicalite. He used a rigid framework with partial charges between +1.167 and +1.314 while we used a flexible framework with a partial charge for Si equal to +2.05. Further work should investigate how charges for Si could allow the self-diffusion coefficient of water molecules in silicalite to be closer to experimental values.

II- Benzene:

1- OPLS-AA and OPLS-UA results

We present the results we obtained for benzene. The mean square displacement of one benzene molecule in our 1 x 1x 2 silicalite cell is given in the following graphs. We simulated the diffusion of this molecule at two different temperatures, 300 and 400K with two different force fields the OPLS-AA and OPLS-UA. The OPLS-AA treats benzene as a vibrating molecule while the OPLS-UA keeps the ring rigid and implicitly takes the hydrogen atoms into account through the carbon atom parameters. How often the MSD was calculated influenced the determined MSD values. Therefore we present results when the MSD is calculated every 500 steps and every 200 steps for both temperatures. The averaged mean square displacement in the x (sinusoidal channel), y (straight channel) and z (mix of straight and sinusoidal channels) directions are given as well as the total averaged MSD for each case. Figures 54-60 show our MSD results.

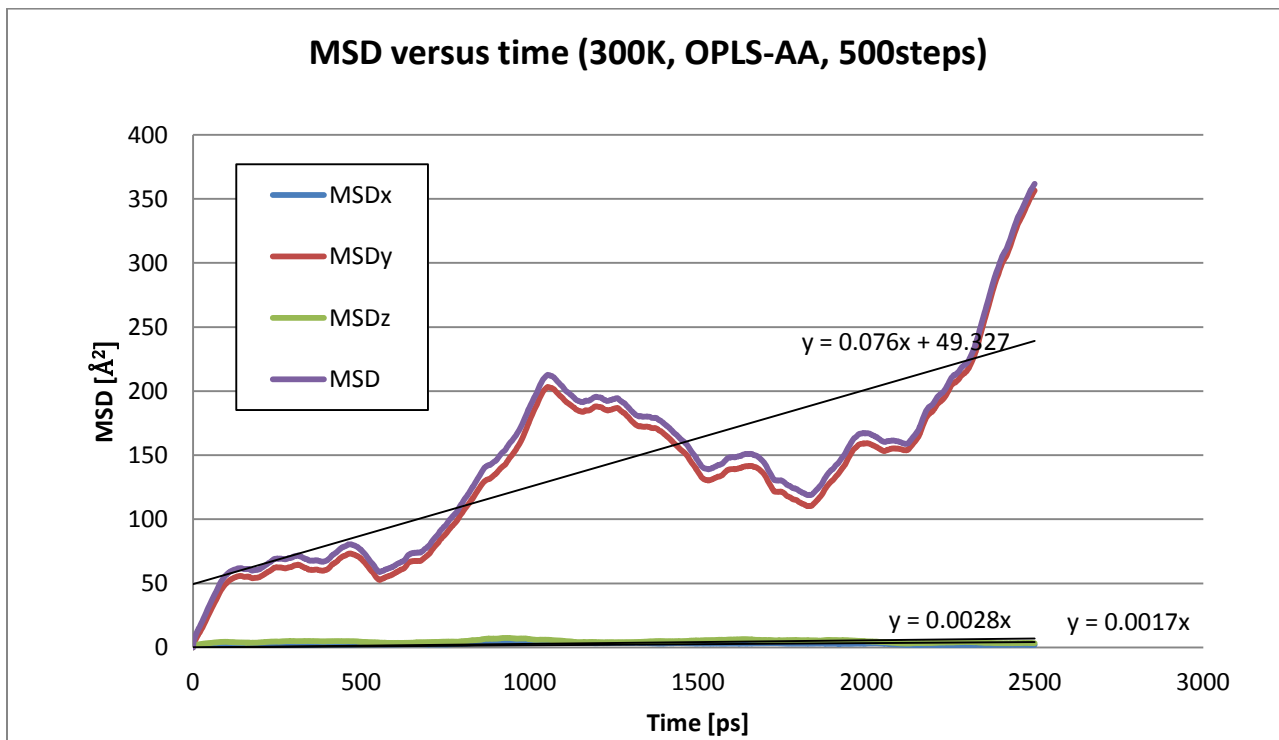


Figure 54: MSD of OPLS-AA benzene molecule at 300K, coordinates written every 500steps. MSDx is along the x-direction, MSDy is along the y-direction, and MSDz is along the z-direction.

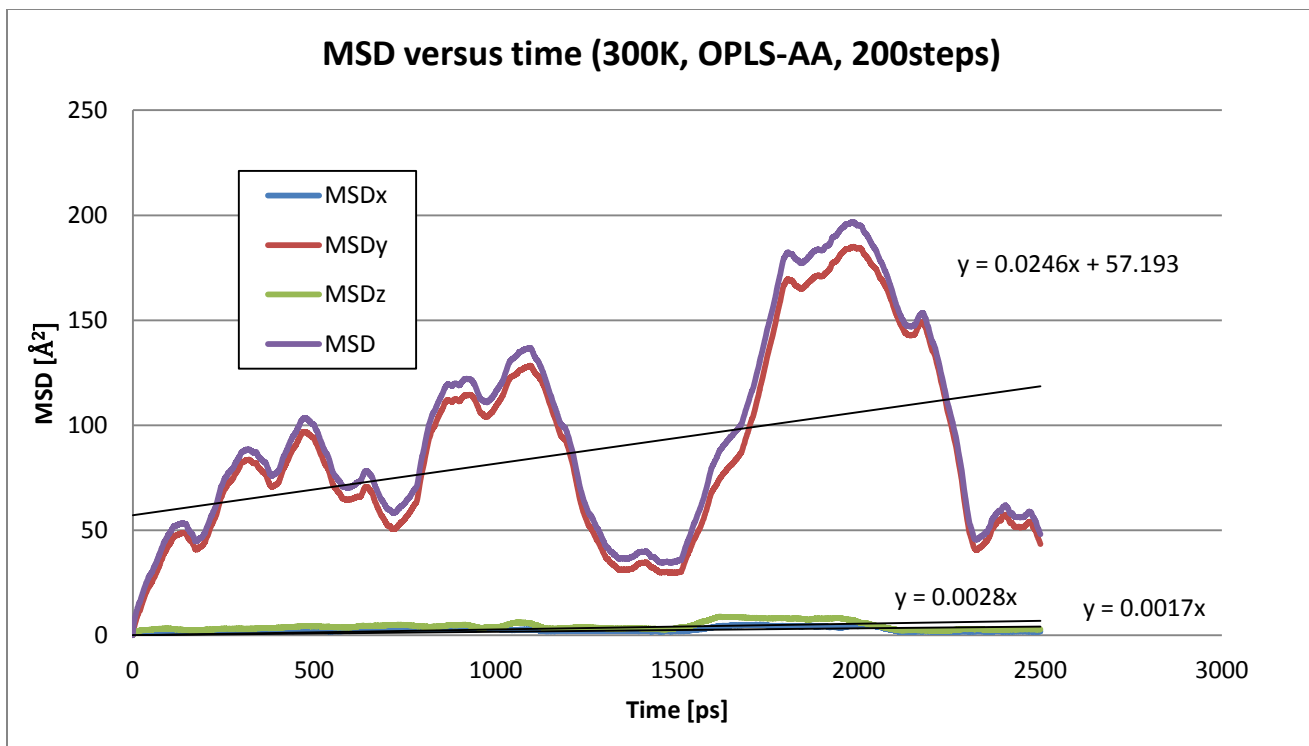


Figure 55: MSD of OPLS-AA benzene molecule at 300K, coordinates written every 200steps. MSDx is along the x-direction, MSDy is along the y-direction, and MSDz is along the z-direction.

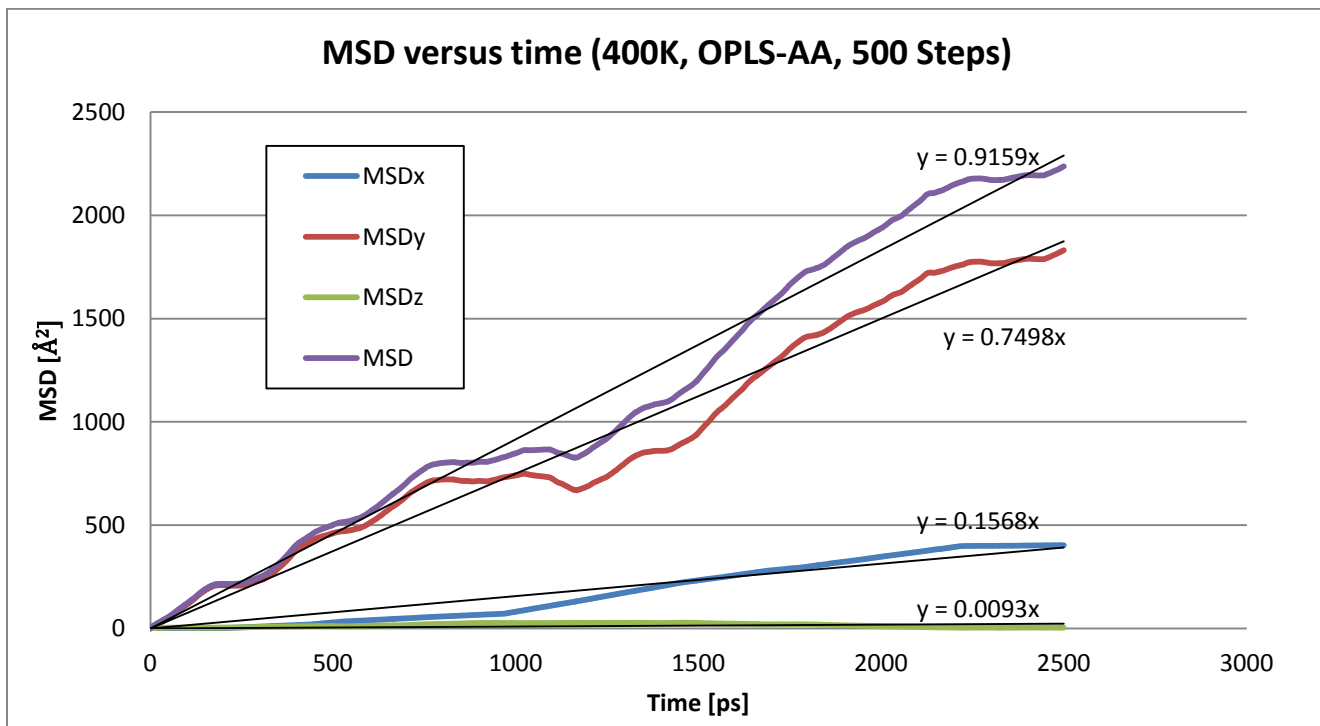


Figure 56: MSD of OPLS-AA benzene molecule at 400K, coordinates written every 500steps. MSDx is along the x-direction, MSDy is along the y-direction, and MSDz is along the z-direction.

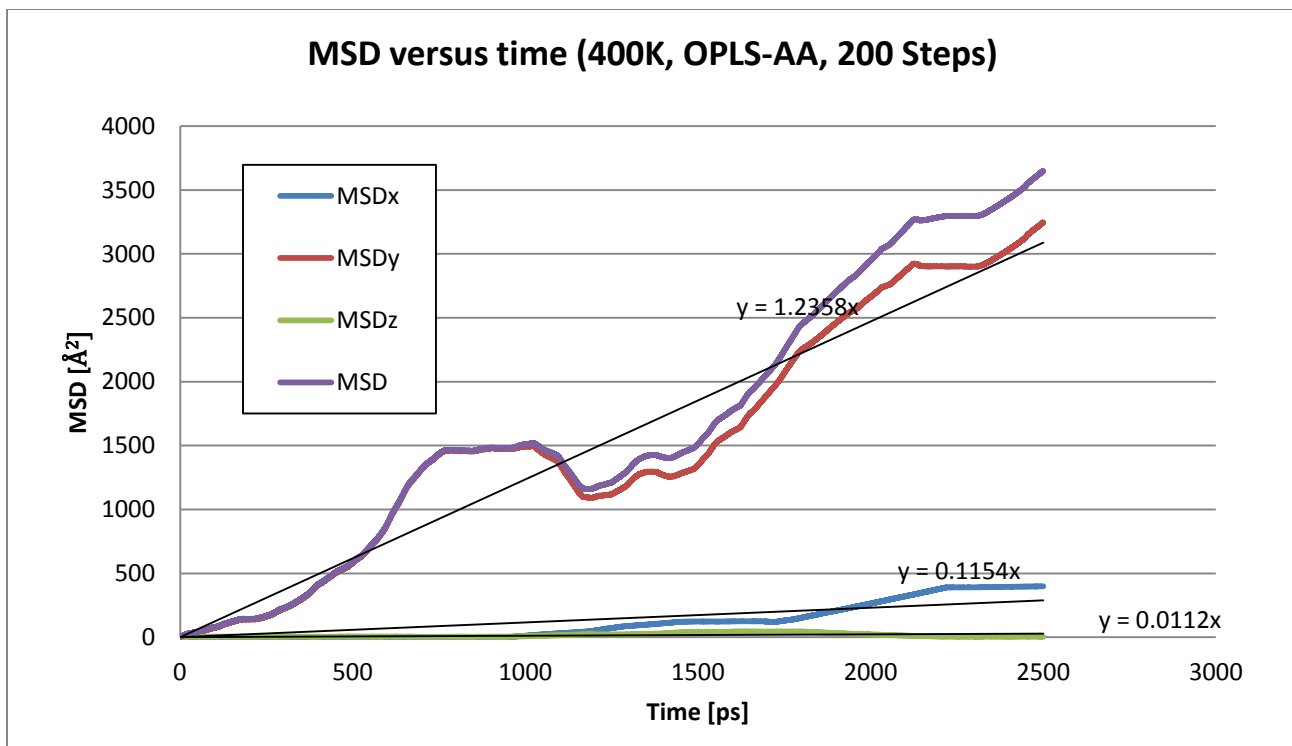


Figure 57: MSD of OPLS-AA benzene molecule at 400K, coordinates written every 200steps. MSDx is along the x-direction, MSDy is along the y-direction, and MSDz is along the z-direction.

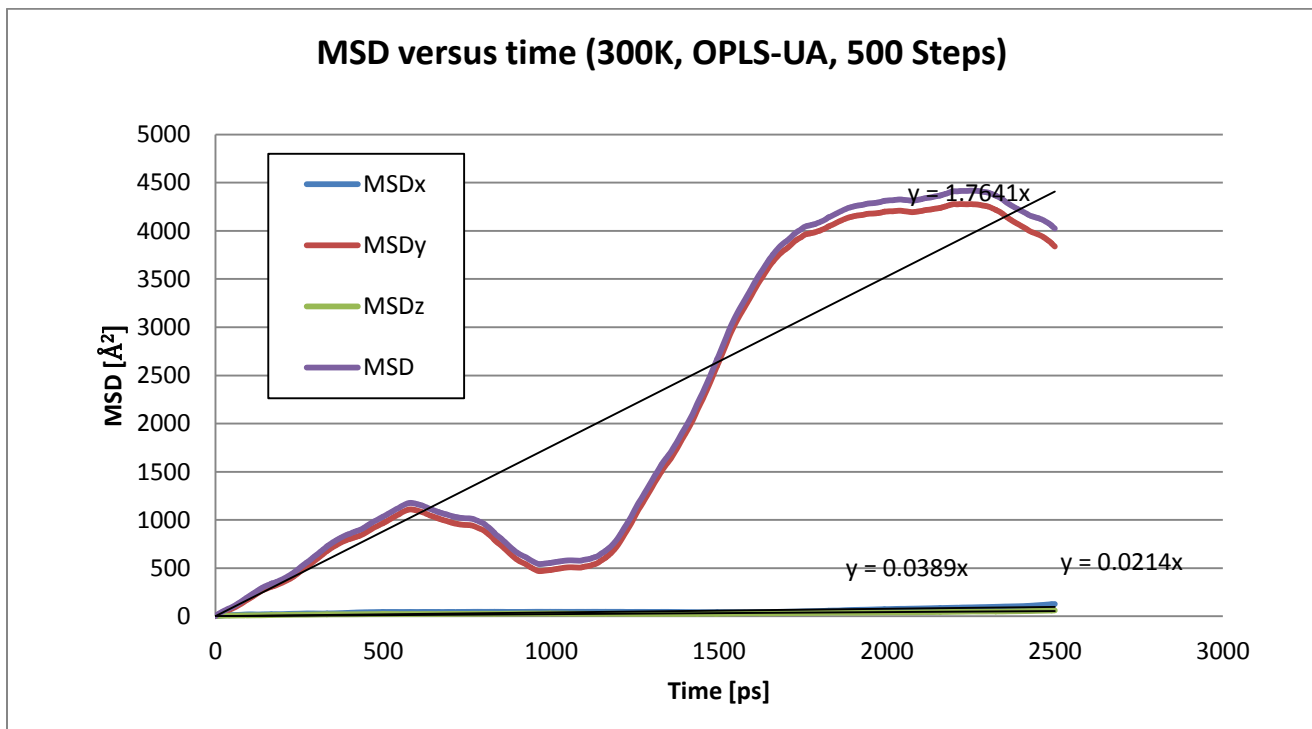


Figure 58: MSD of OPLS-UA benzene molecule at 300K, coordinates written every 500steps. MSDx is along the x-direction, MSDy is along the y-direction, and MSDz is along the z-direction.

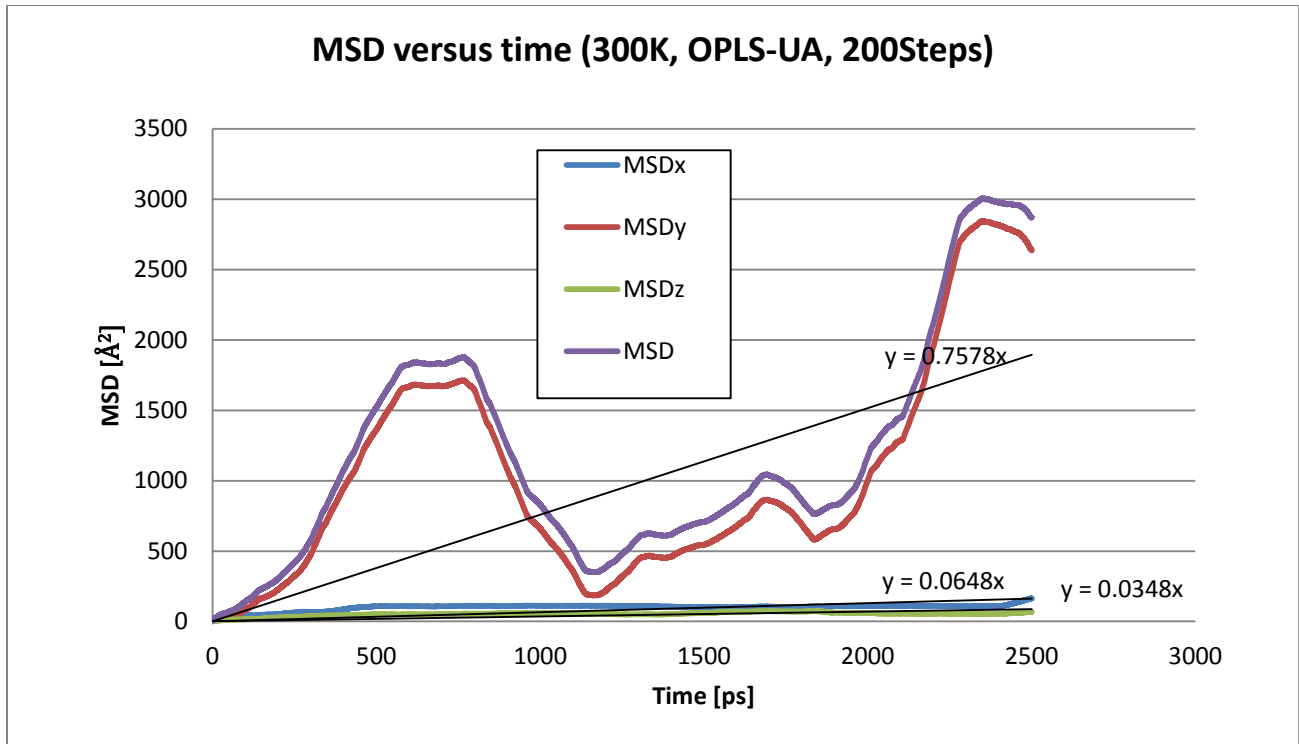


Figure 59: MSD of OPLS-UA benzene molecule at 300K, coordinates written every 200steps. MSDx is along the x-direction, MSDy is along the y-direction, and MSDz is along the z-direction.

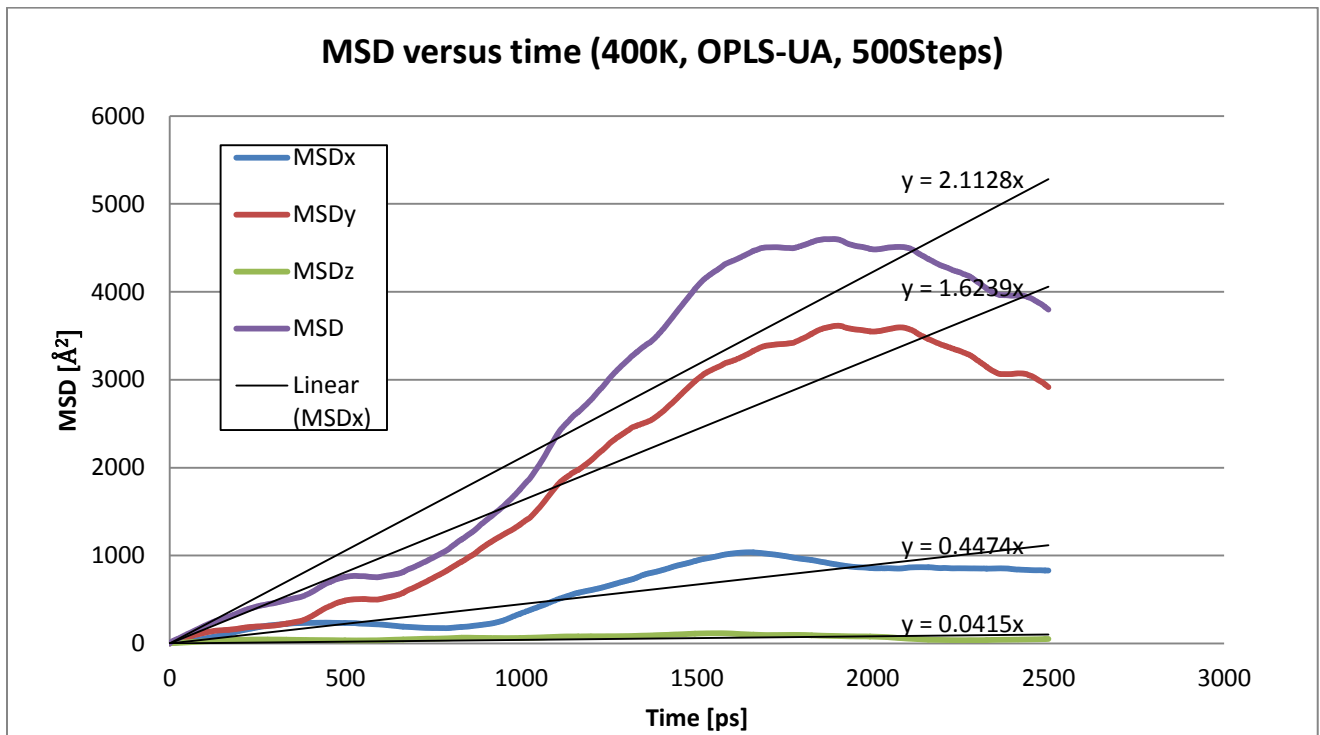


Figure 60: MSD of OPLS-UA benzene molecule at 400K, coordinates written every 500steps. MSDx is along the x-direction, MSDy is along the y-direction, and MSDz is along the z-direction.

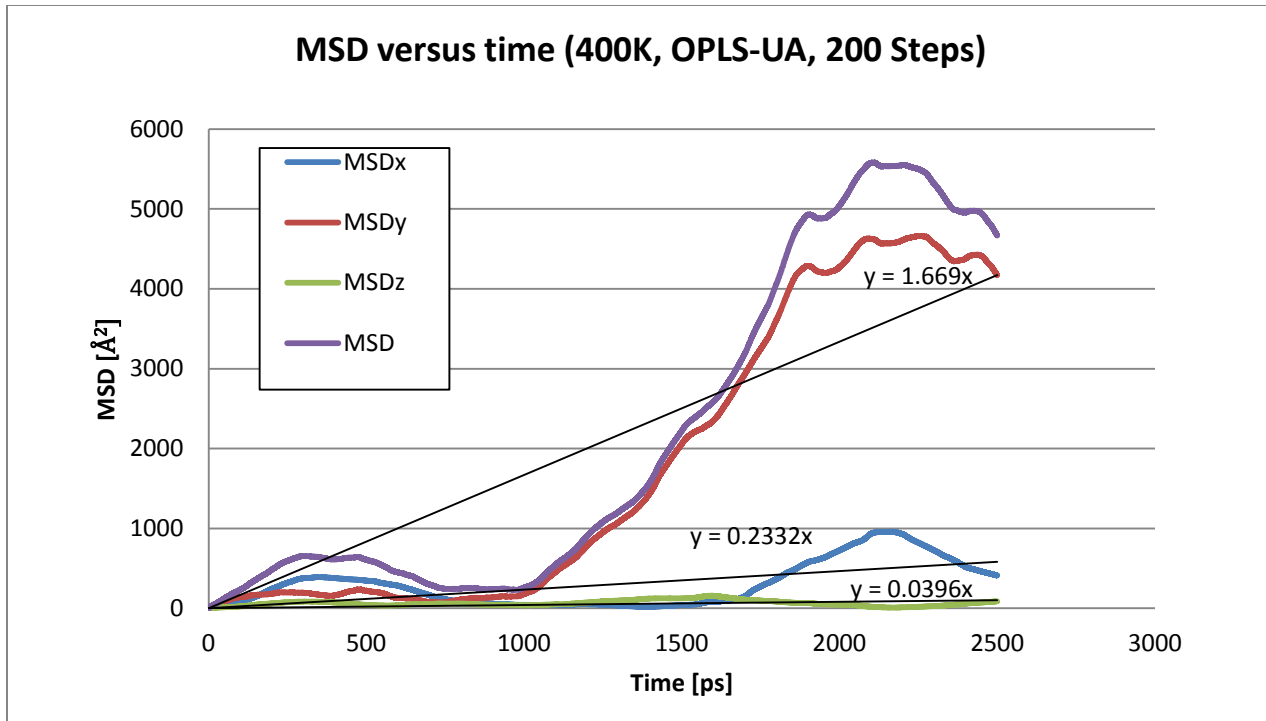


Figure 61: MSD of OPLS-UA benzene molecule at 400K, coordinates written every 200steps. MSDx is along the x-direction, MSDy is along the y-direction, and MSDz is along the z-direction.

On Figure 54 and 55 we observe a strange behavior for the MSD in the y direction and therefore in the total MSD. The process does not seem to be clearly linear; the MSD has an upward trend that is not strictly linear. The jump at the beginning on the simulation has been observed in literature for other molecules and is due to the vibrations of molecules. That is why the trend line for MSDy does not cross the y-axis at 0. We observed the same non-linearity using OPLS-AA at 300K for both sampling frequencies. At low temperatures the movement of benzene is slow. Benzene is such a large molecule that it may become trapped in the channels for significant time periods before it finally starts to diffuse. This trapping/diffusing behavior could explain the shapes of the MSD plots of benzene at 300 K. Moreover, the benzene molecule does not diffuse through the sinusoidal channel or in the z-direction at 300K. It seems that the energy barrier for diffusion in these directions is too high for the benzene molecule at this temperature. For the OPLS-AA at 400K the MSD is mostly linear for the 500 steps frequency. At higher temperatures benzene's movement is faster so the MSD starts to approach a linear curve.

We also observe that at 300K for the OPLS-UA it appears to be non-linear. The behavior of both the UA and AA force fields could be due to the simulation time that we used. In the literature³²,

⁴⁵ the simulation times vary from microseconds to seconds. We believe that these trends would vanish if we had longer simulations and the behavior would mostly be linear for the MSD of benzene in silicalite. The shapes of the averaged MSD plots, even if not perfectly linear make us believe we have an ideal-diffusion process for benzene at both temperatures and for both force fields. The same remark can be said about the 400K case. Future work should include longer simulations of benzene molecules in silicalite with a printing of coordinates more frequently. This will most probably take very long computation times to get results, and produce large output files.

2- Comparison with literature:

We have found very few papers that deal with separation of benzene using silicalite. Forester et al.³² used a Monte Carlo simulation technique in order to simulate the diffusion of benzene in silicalite. Snurr et al.⁴⁵ used dynamic Monte Carlo simulations to simulate the diffusion of benzene in silicalite. The results of their simulation and our simulations are given in Table 15. One experimental value was found in Forester's paper. Other experimental diffusivities are given in Snurr's paper and the values found by these groups^{46, 47, 48, 49, 50} are around 10^{-14} and $10^{-13} \text{ m}^2 \cdot \text{s}^{-1}$ at 300K and between 10^{-13} and $10^{-12} \text{ m}^2 \cdot \text{s}^{-1}$ at 400K, i.e. in good agreement with Forester's results.

T [K]	Self-diffusion parameters [$10^{-12} \text{ m}^2 \cdot \text{s}^{-1}$]							
	OPLS-AA, 500	OPLS-AA, 200	OPLS-UA, 500	OPLS-UA, 200	Forester et al. ³²	Experiment ³²	Snurr et al. [43] ⁴⁵	Rungsisirakun et al. ⁵¹
300	134.1	48.5	3040.66	1.43	3.36E-02	2.20E-02	1.10E-04	250 ^a
400	1565.25	2270.6	3521.3	3.23	-	-	4.00E-03	-

Table 15: Different results for the diffusion coefficient of benzene in silicalite found in literature. ^a Rungsisirakun et al. ran simulations with 2 benzene molecule per cell.

As we can see the values found in literature vary quite a lot. Forster found a value that is close to the experimental one. Snurr has a self-diffusion coefficient of 1 to 2 orders of magnitude smaller than experimental values. We found results that are 4 to 5 orders of magnitude higher compared to experiments. The results we obtained when MSD is calculated every 200 steps for our program are a little closer to experimental values indicating that better sampling frequency may

give better statistics when calculating the diffusion coefficient. Still a difference of several orders of magnitude is observed. Forester used a specific force-field to describe the zeolite-zeolite interaction that decomposes the oxygen atoms into two atoms, a core and a shell oxygen atom. The charges used for Si and O atoms change a lot, since he uses a +4.0 charge for Si. We used a +2.05 charge for the Si atom based on the reasoning explained earlier, in the Methodology part. These fundamental differences on the force-field used could explain why we have such different results.

Snurr et al. used a force-field described in their previous work^{52,53}. They simulated the silicalite structure as rigid and considered benzene as a rigid planar molecule. Vibrations of the lattice are supposed to play an important role in the diffusion of big molecules through silicalite and that could explain the very low values that the group found. Their values are closer to the ones found by Wu et al.⁴⁷ that are about $8.6 \times 10^{-12} \text{ m}^2 \cdot \text{s}^{-1}$ at 293K.

We used both OPLS force-fields to describe the diffusion of benzene through silicalite. We found that the OPLS-AA gives results that agree more with other results than the OPLS-UA force-field. We found smaller diffusion coefficients with the all-atom force-field.

Rungsirisakun et al.⁵¹ gave results that are close to the values we found. They used a force-field that is close to OPLS-AA to simulate the benzene molecule. They used harmonic potentials for bond and angle potentials, the LJ 12-6 law for intermolecular interactions and the partial charges for Si and O in the silicalite framework are almost the same ($q_{\text{Si}}=+2.0$). Their 3-body potential (Quartic), dihedral potential (cosine) and coulomb potential are different than the ones we used to describe our system. We used the screened Vessal potential, the OPLS potential, and the ewald sum respectively. They used the NVE ensemble while we used the NVT one. Another main difference is that they explicitly expressed the bond between oxygen and silicate atom in the silicalite structure. They use harmonic potentials for the bonds and angles between the framework atoms. They ran a much shorter simulations, around 100ps while ours were 10 times longer. Their result at 300K is given for 2 benzene molecules in the cell while we only ran one molecule per simulation. The main difference with our work is probably the way they decided to calculate the self-diffusion coefficient. They used the same hypothesis as Yang et al.⁴¹ and used the isotropic equation for linking the MSD and the self-diffusion coefficient. Silicalite is highly anisotropic so it might not be the best way to describe diffusion. Nevertheless, the MSD is

mostly due to the movement of benzene in the y-direction, so the total MSD could be approximated to the MSD in the y-direction leading to their equation. We have results in the same order of magnitude when we sampled the coordinates every 500 steps and have a one order of magnitude of difference when we printed them every 200 steps at 300K.

One should also keep in mind that experiments to obtain the self-diffusion coefficient of molecules in silicalite are very complicated. We gave some examples of problems that might occur in the discussion for water molecules. The main problem for benzene experiments is probably that silicalite obtained industrially may not be perfectly defect-free, and a few external framework cations can have a big effect on the diffusion coefficient of molecules.

It seems that OPLS-AA force-field describes the steric hindrance of benzene in silicalite since it takes the hydrogen atoms into account explicitly. Nevertheless it seems that the intermolecular parameters are not describing the interactions between benzene and silicalite in such a good way. Based on the experimental values given in Snurr's, the benzene molecule is expected to diffuse very slowly in silicalite, meaning that on top of the steric hindrance there must be important interactions between the benzene molecules and the atoms of the framework. Based on our results, benzene has a much higher diffusion coefficient meaning that these interactions are probably underestimated. It is probably even more significant with the OPLS-UA force-field. The benzene molecule could move very easily in the silicalite structure when we used this force-field. The change in the intermolecular parameters for this force-field does not seem to compensate the steric hindrance that OPLS-AA has. It may also be due to the charges used for our Si atom or the charges put on the carbon and hydrogen atoms of benzene. Yet it looks like both OPLS force-fields as well as the force-fields used by Snurr et al. Rungsirisakun et al. do not describe well the behavior of benzene in silicalite since the results obtained by these groups and the ones we obtained are either several orders of magnitude higher or smaller compared to experiments. Another potential problem is the sampling frequency of our simulations as well as simulation length. Better sampling and longer simulation times should allow us to calculate MSD values that average out any anomalies or strange behavior.

III- Phenol:

In this part, we show the plots obtained for the simulation of the diffusion of phenol in silicalite. We plotted the averaged MSD in the x, y and z-directions as well as the total averaged MSD for two temperatures, 300 and 400K. We used the program described in the methodology section to calculate these MSDs. Two force-fields were used during our simulations, the OPLS-AA and the OPLS-UA.

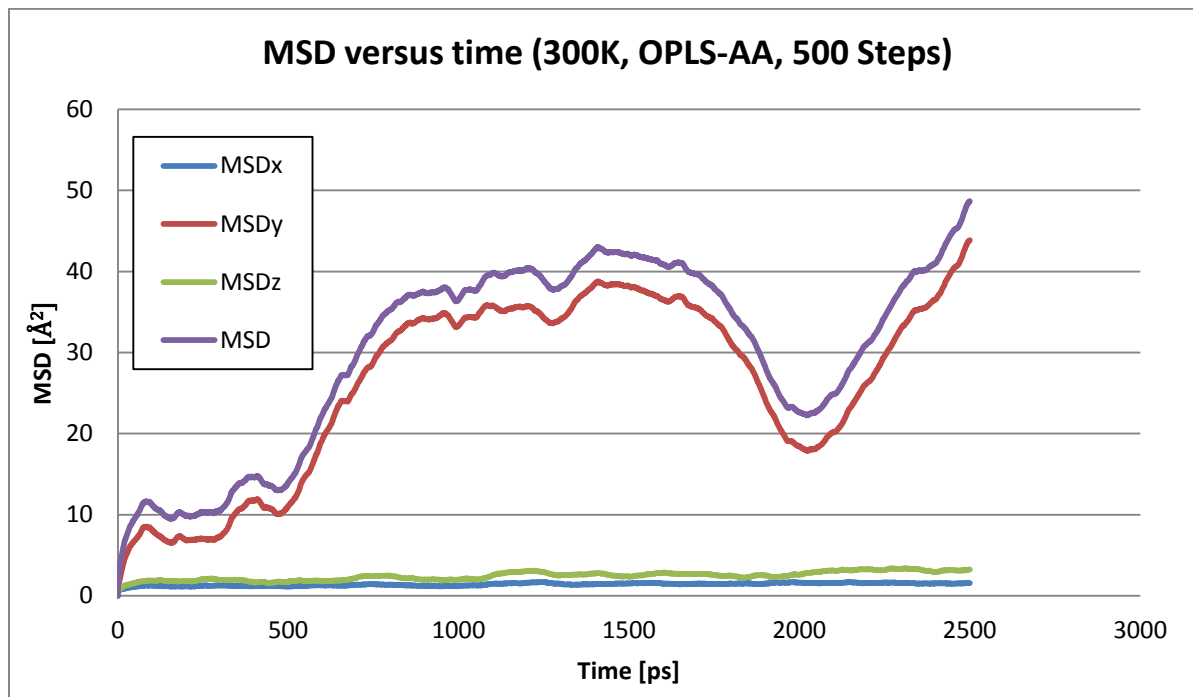


Figure 62: MSD of OPLS-AA phenol molecule at 300K, coordinates written every 500steps. MSDx is along the x-direction, MSDy is along the y-direction, and MSDz is along the z-direction.

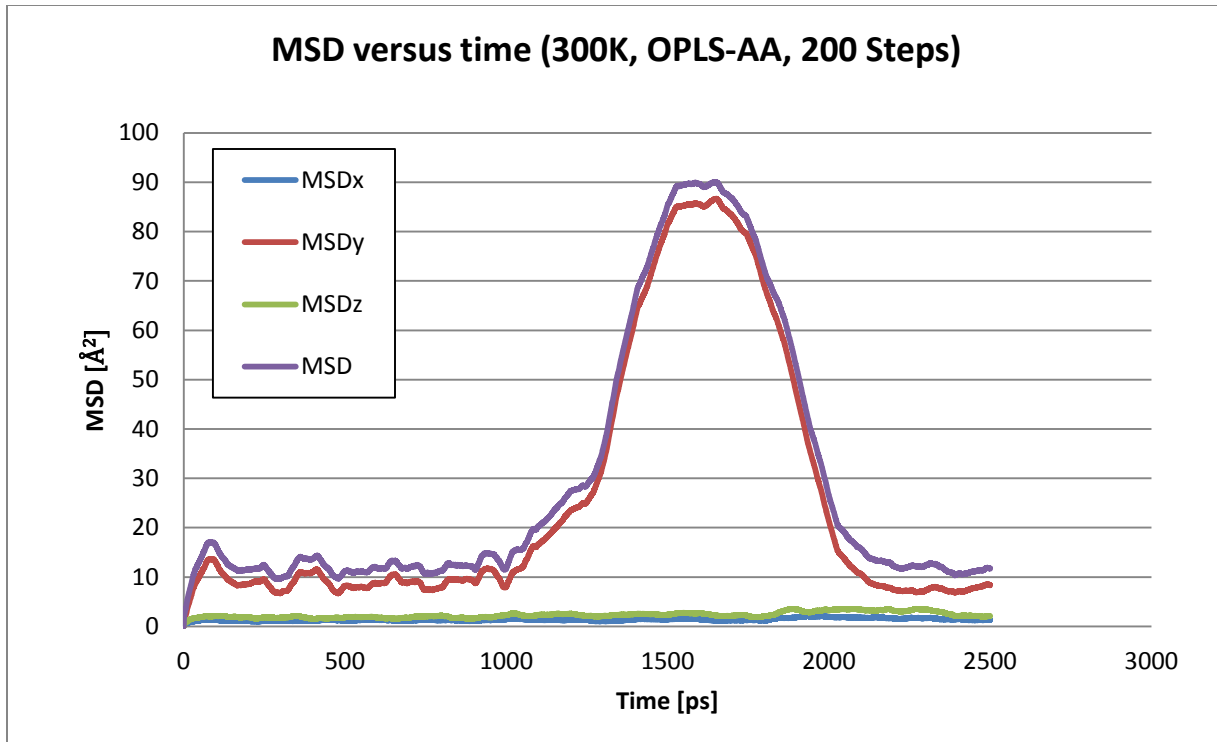


Figure 63: MSD of OPLS-AA phenol molecule at 300K, coordinates written every 200steps. MSDx is along the x-direction, MSDy is along the y-direction, and MSDz is along the z-direction.

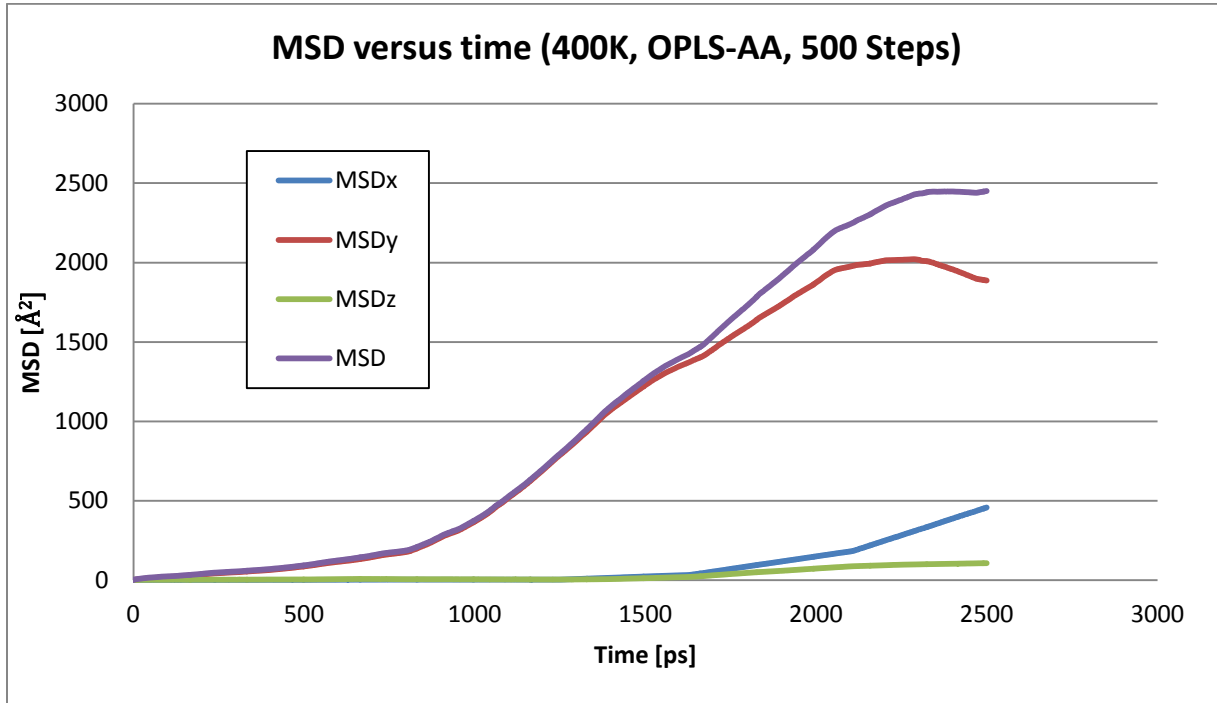


Figure 64: MSD of OPLS-AA phenol molecule at 400K, coordinates written every 500steps. MSDx is along the x-direction, MSDy is along the y-direction, and MSDz is along the z-direction.

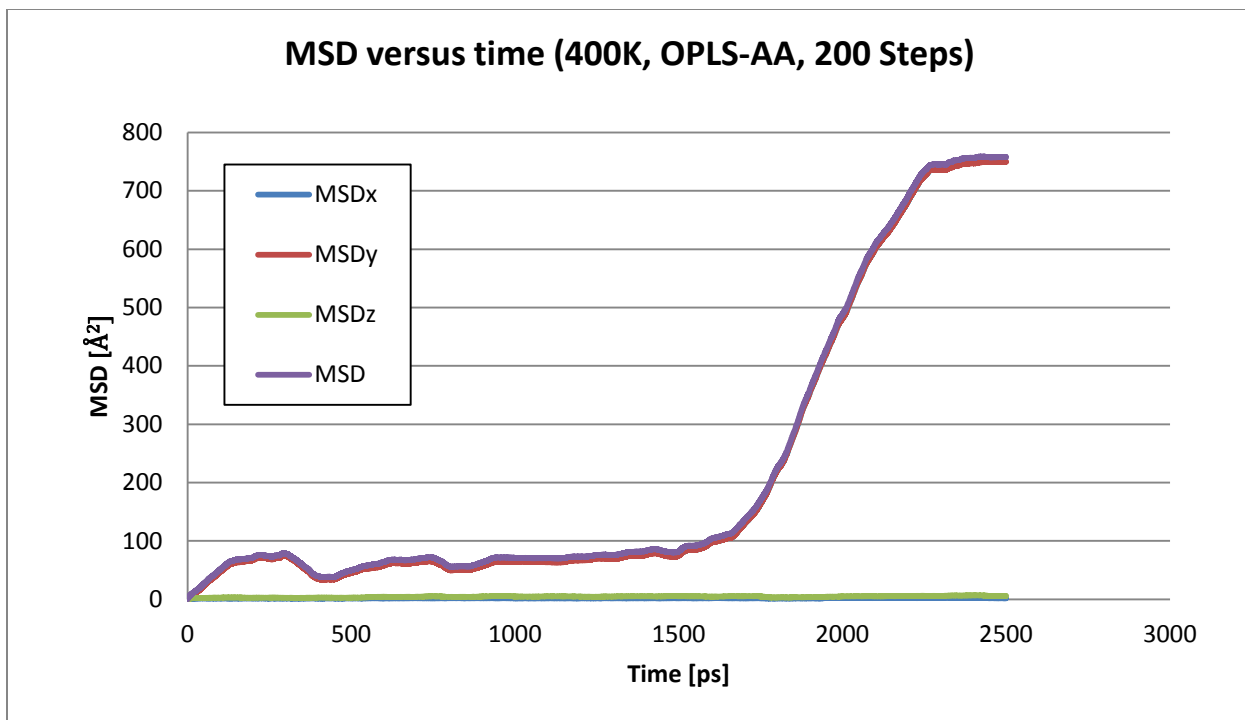


Figure 65: MSD of OPLS-AA phenol molecule at 400K, coordinates written every 200steps. MSDx is along the x-direction, MSDy is along the y-direction, and MSDz is along the z-direction.

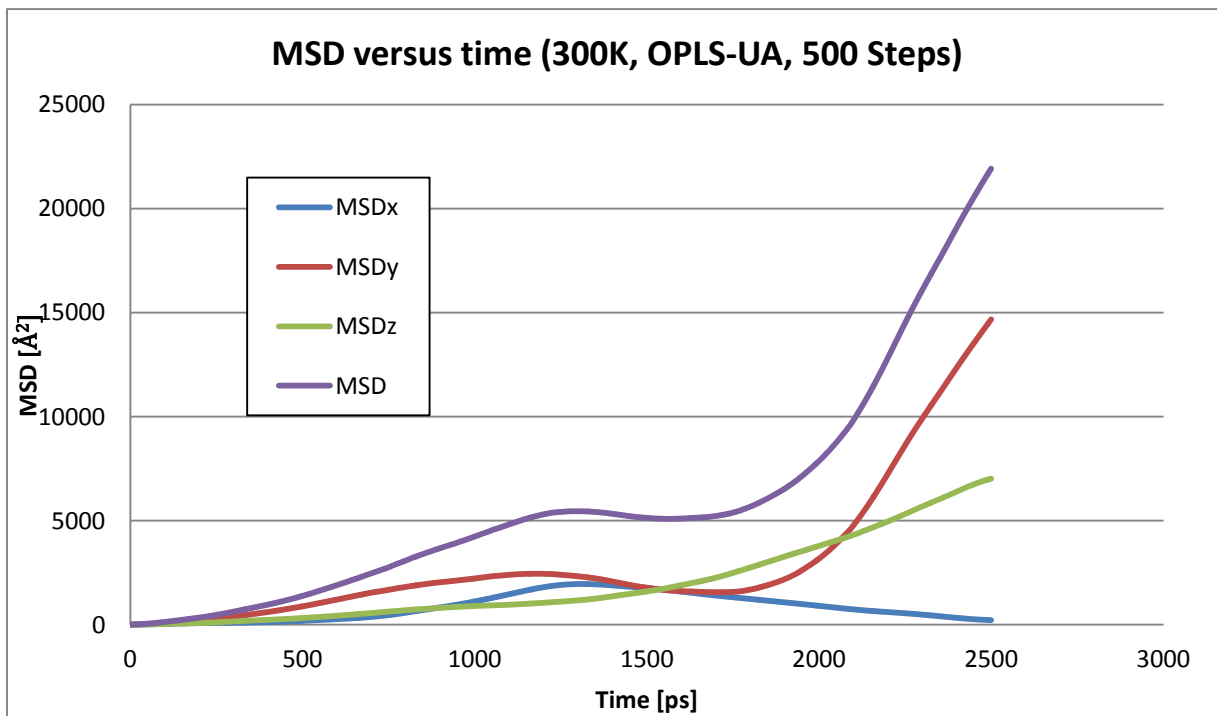


Figure 66: MSD of OPLS-UA phenol molecule at 300K, coordinates written every 500steps. MSDx is along the x-direction, MSDy is along the y-direction, and MSDz is along the z-direction.

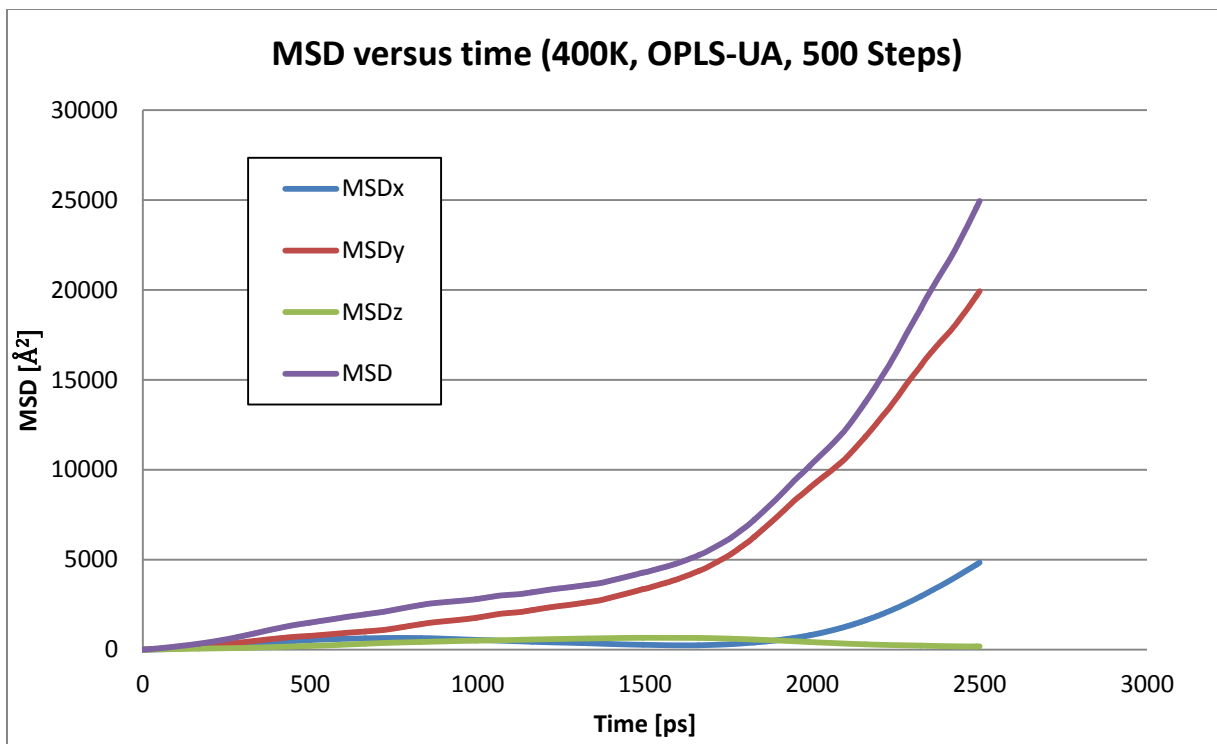


Figure 67: MSD of OPLS-UA phenol molecule at 400K, coordinates written every 500steps. MSDx is along the x-direction, MSDy is along the y-direction, and MSDz is along the z-direction.

At 300K, for OPLS-AA force field, we can see that the shape between the cases when coordinates are printed every 500 steps and every 200 steps are quite different. In the first case, one could assume that the MSD is linear, while in the second case it is clear that it is not linear. There is a sudden increase of the MSD in the y-direction followed by a decrease, meaning that the molecule moved along the straight channel and then came back to its original spot. In this case we do not know how to reach a meaningful diffusion coefficient. The diffusion of aromatic is usually done by consecutive jumps between adsorption sites. For phenol, we believe that the alcohol group plays a key role in its diffusion through silicalite. In order to assess the hydrogen bonding between the alcohol group and the framework we plotted the radial distribution functions (rdfs) between the oxygen atom of the alcohol group and the oxygen atom of the framework as well as the rdf between the H of the alcohol and the O of silicalite. (See Figure68)

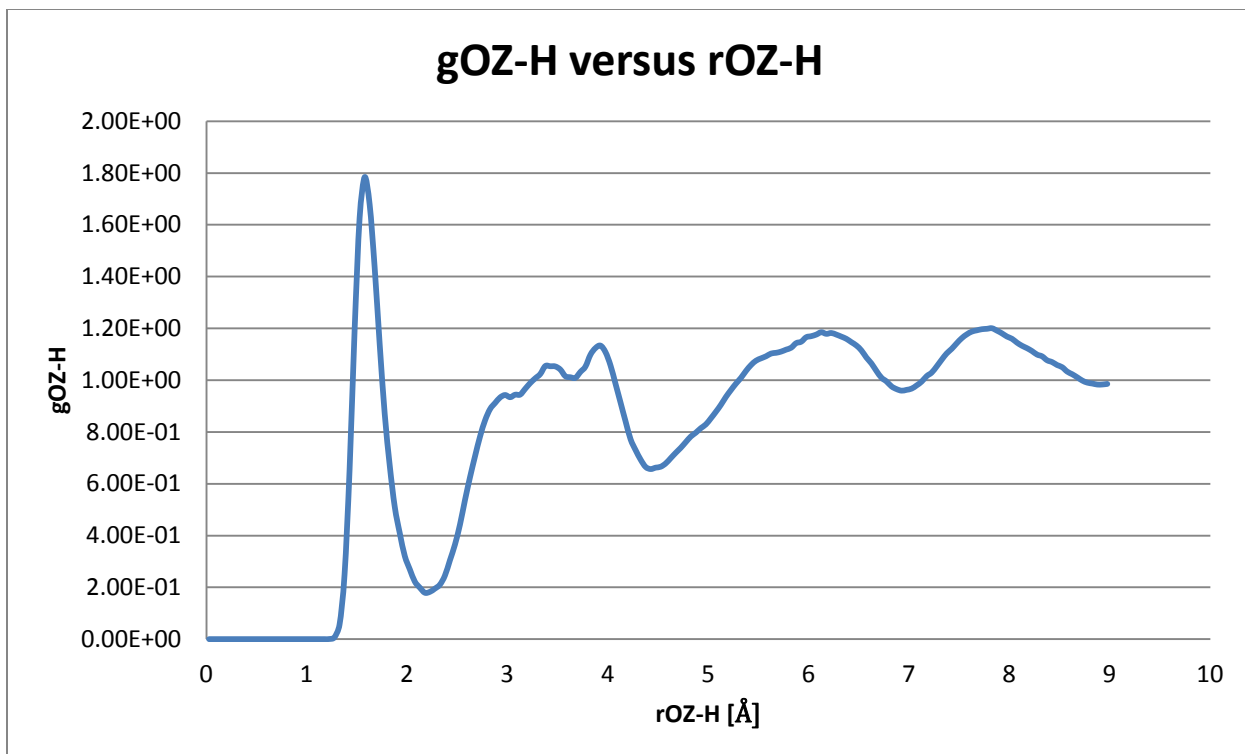


Figure 68: Radial distribution function between the hydrogen of the phenol alcohol group and the oxygen atom of the silicalite framework at 300K.

We can see a peak around 1.5 Å. This means that there is hydrogen bonding between the phenol molecule and the framework. The following peaks are less important as they are significantly longer in distance and do not represent real hydrogen bonding. The first peak has a magnitude around 1.8 which is around 6 times more than the rdf we saw for the water molecules. It means that phenol interacts a lot more with the framework atoms. This means that the diffusion of phenol in silicalite is linked with the hydrogen bonds that the alcohol group makes with the framework. As we can see on the following pictures (Figure 69) the phenol molecule is hydrogen bonding around its initial position. At that point it starts diffusing through the straight channel, until it anchors through hydrogen-bonding. The events are less comprehensible on Figure 62, where coordinates were printed every 500 steps, but the trend can be seen with a longer time where the molecule seems to be stuck in another adsorption site. Based on these results, no diffusion coefficient was calculated. This phenomenon might be buffered if longer simulations were run.

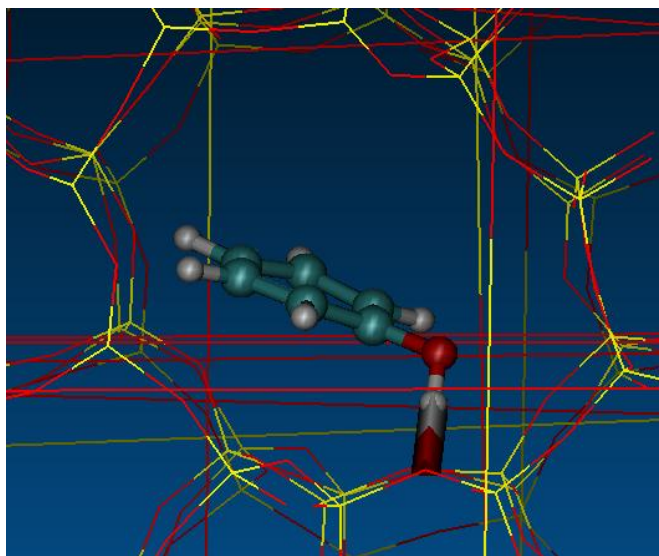


Figure 69: Example of hydrogen bond between hydrogen of the alcohol group of the phenol molecule and the oxygen of silicalite

At 400K, still for the OPLS-AA case, we have plots (Figure 63-64) that look more alike, with an upward trend, more sudden for the 200 steps case. There is still a doubt on the first one whether the MSD could be linear or not. When the coordinates are printed every 200 steps, the MSD is not linear and then starts increasing until it reaches a plateau. We have the same phenomenon described for 300K occurring at this temperature, i.e. the molecule rotates until it has a good alignment with one channel and diffuses through it. It seems harder for the phenol molecule to be in the right configuration to diffuse through a channel. The diffusion of phenol appears to have periods of movement and periods of inactivity, suggesting that only certain configurations of phenol allow it to diffuse through the pores. Therefore the time before it diffuses is more important. It is probably due to the higher temperature. The molecule being more excited, it rotates more and makes H-bonds with the O of the frameworks. When the molecule is in the right configuration, also due to the higher temperature, the molecule travels further in the silicalite structure until it reaches a new adsorption site where the H-bonds become once again more important and get the phenol molecule stuck.

For the OPLS-UA the diffusion seems to be following the same trends as the one we exposed for the OPLA-AA force-field. The mean square displacements calculated are not linear and have the same kind of very fast rise at some point. One difference seen at 300K for the OPLS-UA simulation compared to OPLS-AA ones is that the displacement in the z-direction is important. It could mean that the molecule just happened to end up in this direction and did not rotate to change diffusion channel. This result could be different for a different initial position but we unfortunately did not verify that. The main difference with the OPLS-AA is the value of MSDs. They are very high, around 2 orders of magnitude bigger than for the all-atom force-field. This is unexpected since the diffusion of phenol seemed to be mostly linked to the H-bonds done by the alcohol group with the framework. Changing the charges of carbons from the benzene ring does not seem to be enough to take into account the steric hindrance implied by the hydrogen atoms. These hydrogen atoms might induce small interactions with the framework atoms which slow the diffusion of both benzene and phenol molecules simulated with the OPLS-AA force-field. We note that increased simulation time could provide new details on the UA versus AA force fields for phenol.

IV- Toluene:

We will show the averaged MSD in the x, y and z-directions as well as the total averaged MSD for two temperatures, 300 and 400K, for three possible force-fields. The first case is for the OPLS-AA FF. For the second case we still use the OPLS-AA FF but this time we kept the benzene ring rigid for reasons explained in the methodology section. The third case is the OPLS-UA force-field.

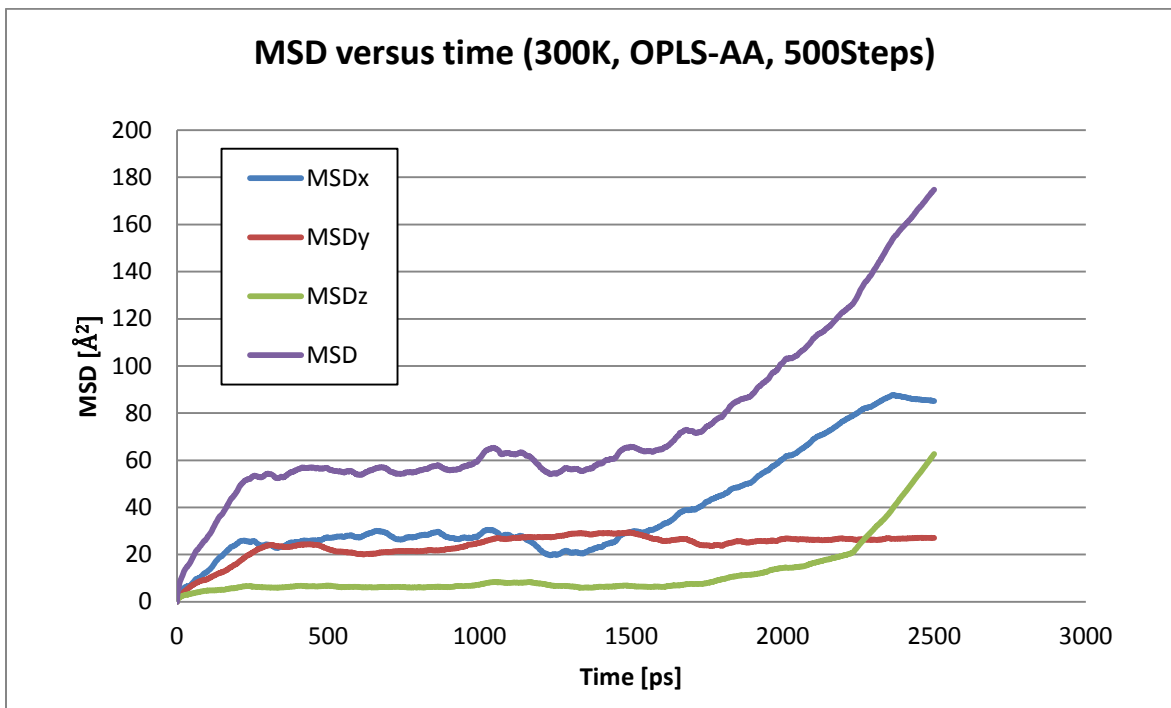


Figure 70: MSD of OPLS-AA toluene molecule at 300K, coordinates written every 500steps. MSDx is along the x-direction, MSDy is along the y-direction, and MSDz is along the z-direction

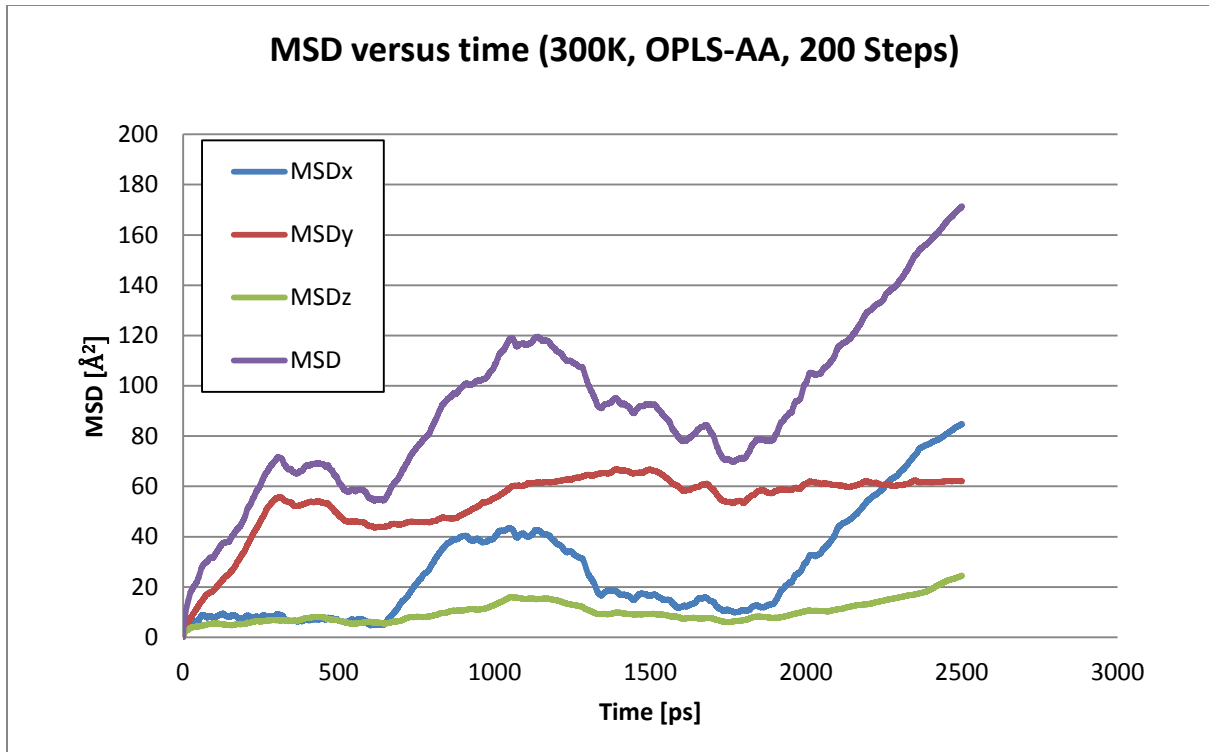


Figure 71: MSD of OPLS-AA toluene molecule at 300K, coordinates written every 200steps. MSDx is along the x-direction, MSDy is along the y-direction, and MSDz is along the z-direction

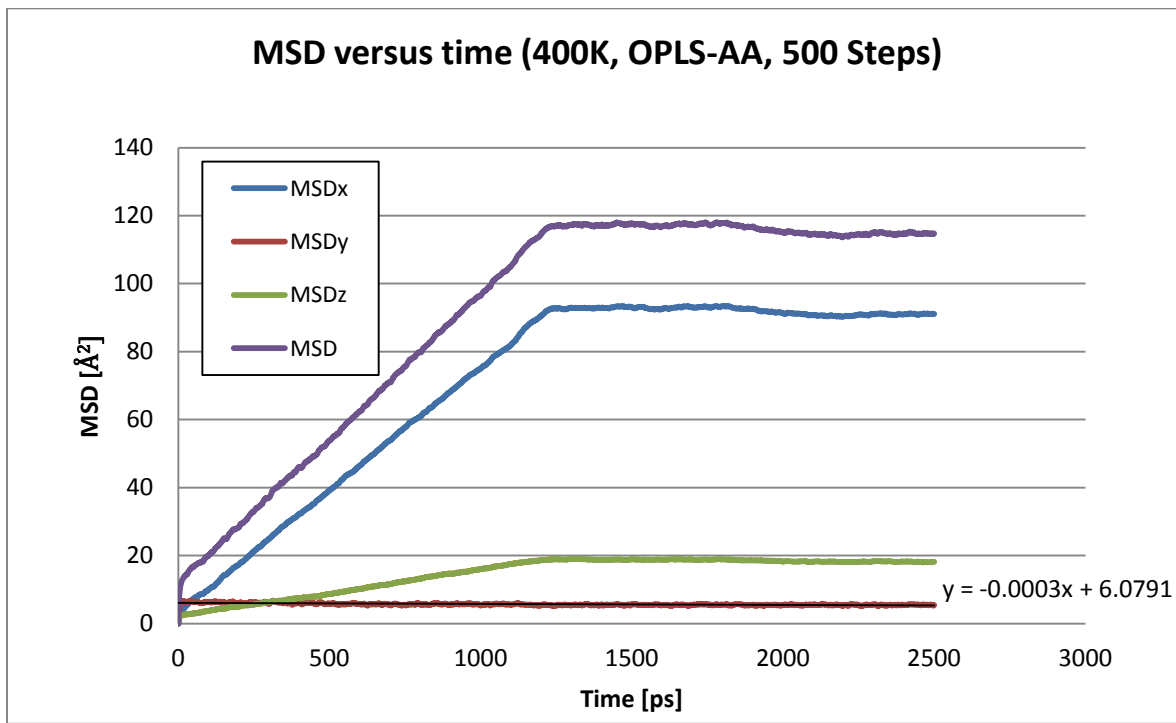


Figure 72: MSD of OPLS-AA toluene molecule at 400K, coordinates written every 500steps. MSDx is along the x-direction, MSDy is along the y-direction, and MSDz is along the z-direction.

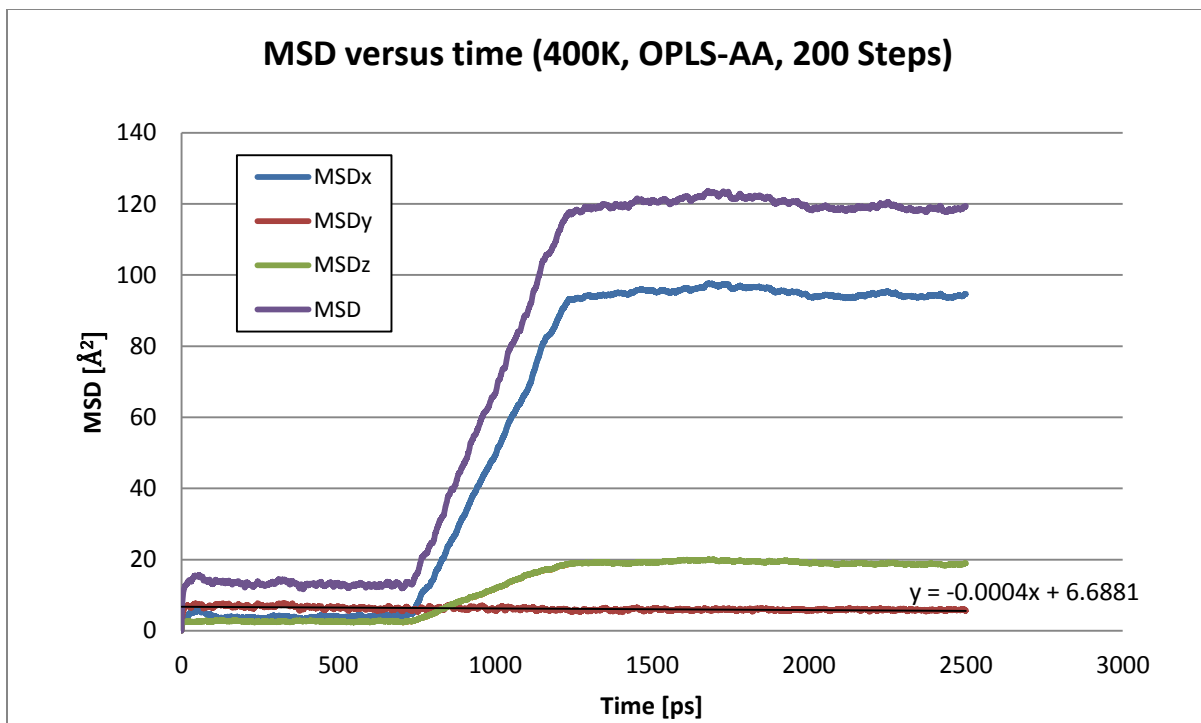


Figure 73: MSD of OPLS-AA toluene molecule at 400K, coordinates written every 200steps. MSDx is along the x-direction, MSDy is along the y-direction, and MSDz is along the z-direction.

The MSD plots for toluene OPLS-AA at 300K have similar shapes. Figure 70 where coordinates were printed every 200 steps is showing more bumps for the MSD in the three different directions. The diffusion of toluene seems to be following the same trend as for phenol. Nevertheless here, hydrogen bonds are not what explain the jumps in the MSD. Based on the work on Inui et al.⁵⁴ we can say that the energy barrier in one direction is lowered when the toluene molecule has its methyl group in this direction. Based on the plots we have at 300K it looks like the toluene molecule is vibrating early on and with our initial configuration ends up diffusing in the y-direction because the methyl group is in this direction. Then it rotates in the zeolite structure and diffuses along the x-axis more than the y-direction.

At 400K this is clearer as the vibrations of the molecule at the very beginning of the simulations do not seem to place the methyl group in line with any channel. The molecule rotates until its methyl group is in line with a channel, in our case the sinusoidal one and diffuses through. We hypothesis that the channel along which the molecule diffuses is a function of initial position. We believe that we could have had diffusion through the straight channel with a different initial configuration.

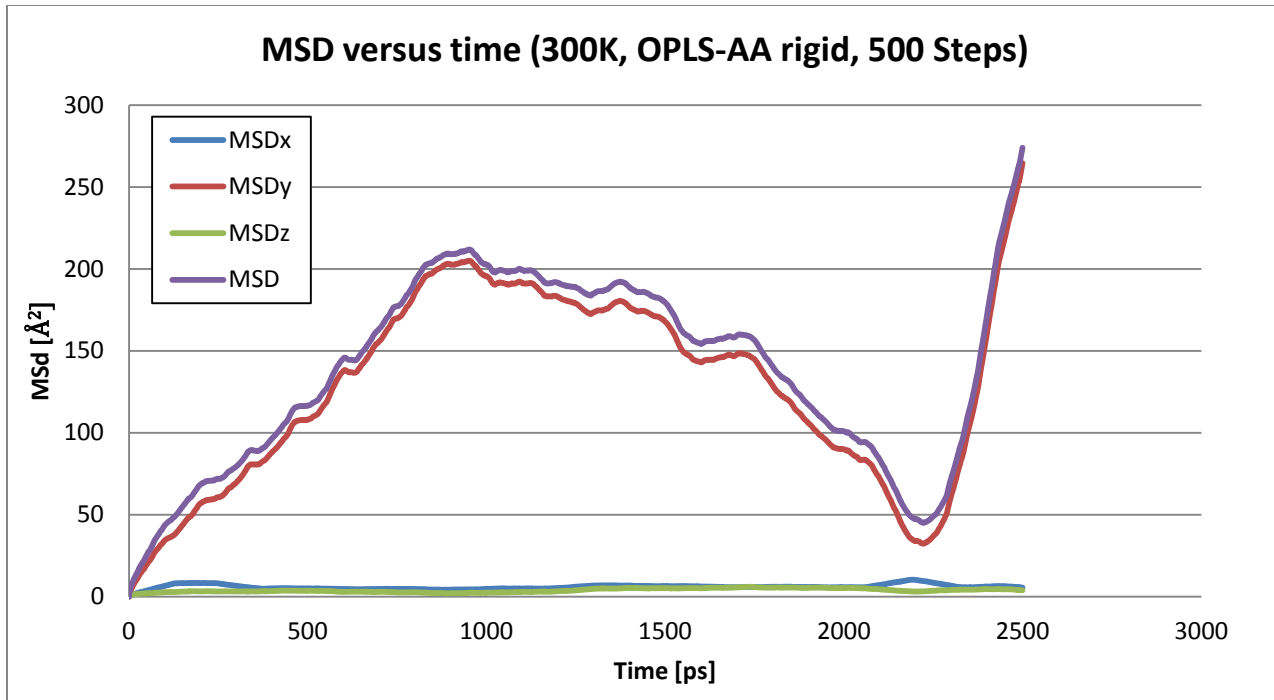


Figure 74: MSD of OPLS-AA rigid toluene molecule at 300K, coordinates written every 500steps. MSDx is along the x-direction, MSDy is along the y-direction, and MSDz is along the z-direction.

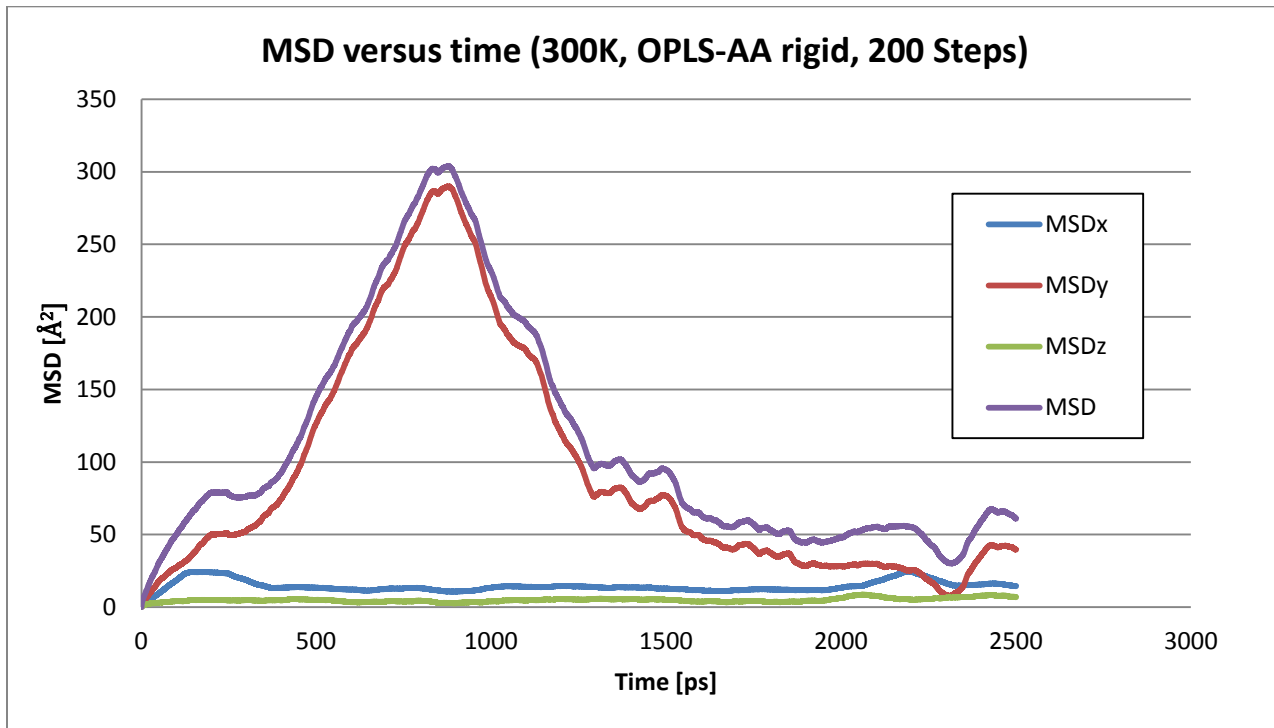


Figure 75: MSD of OPLS-AA rigid toluene molecule at 300K, coordinates written every 200steps. MSDx is along the x-direction, MSDy is along the y-direction, and MSDz is along the z-direction.

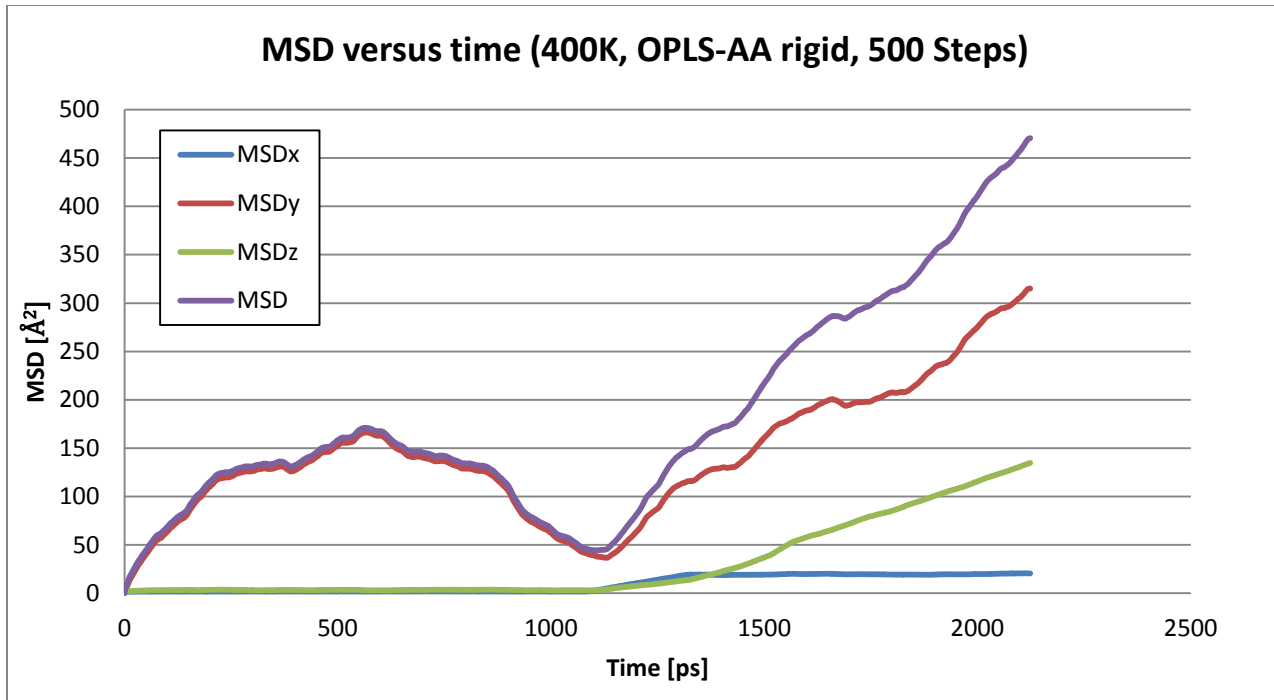


Figure 76: MSD of OPLS-AA rigid toluene molecule at 400K, coordinates written every 500steps. MSDx is along the x-direction, MSDy is along the y-direction, and MSDz is along the z-direction.

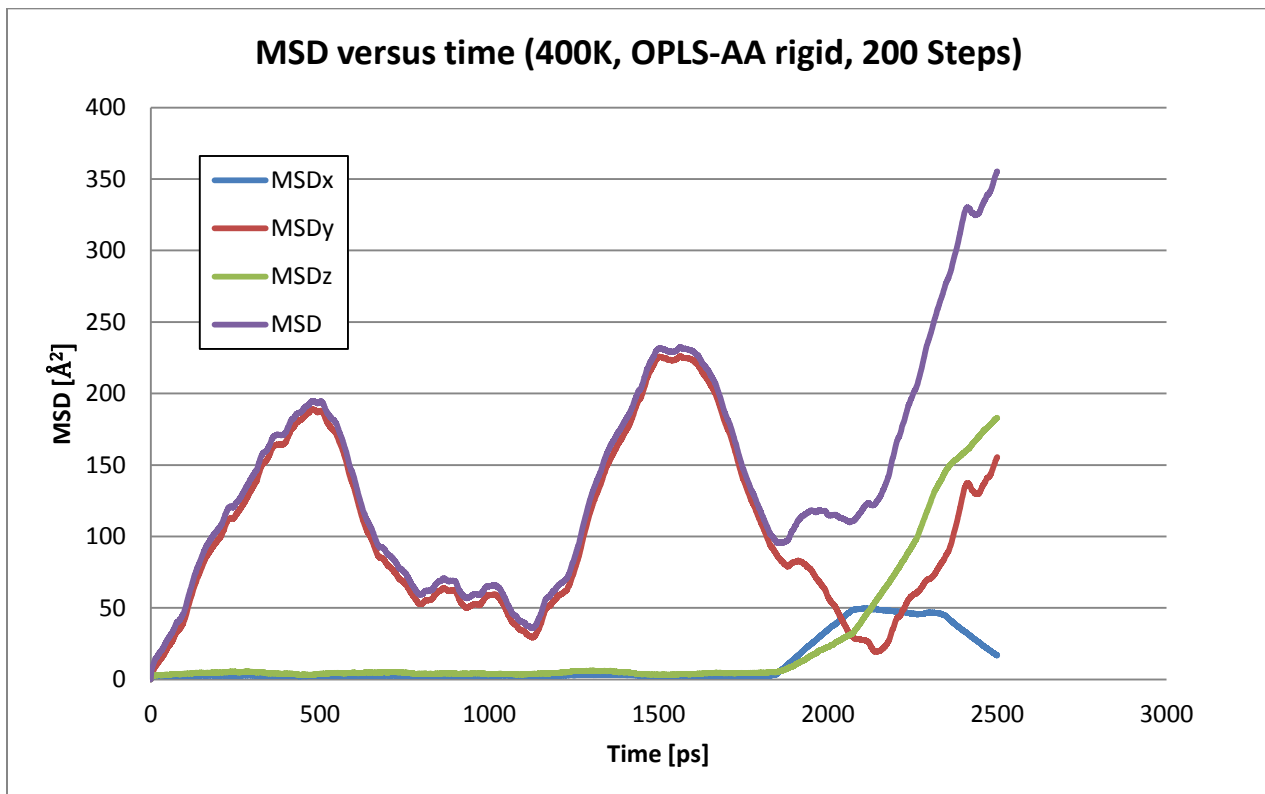


Figure 77: MSD of OPLS-AA rigid toluene molecule at 400K, coordinates written every 200steps. MSDx is along the x-direction, MSDy is along the y-direction, and MSDz is along the z-direction.

The results obtained when the ring was kept rigid are given in Figure 74 through Figure 77. In these graphs, the phenomenon we explained above where the methyl groups needs to be aligned with a channel seems to be true too. The molecule seems to move more easily in silicalite, and most importantly in the y-direction. Rotating when the ring is kept rigid seems to be easier. That is probably the reason why the UA molecule moves more in silicalite compared to the AA molecule, since the probability of aligning the molecule with one of the channels is higher. These very important vibrations could explain the slower diffusion for the AA model at both temperatures. When the ring is kept rigid the diffusion tends to look more like the one we described for phenol, with a somewhat more “random” diffusion.

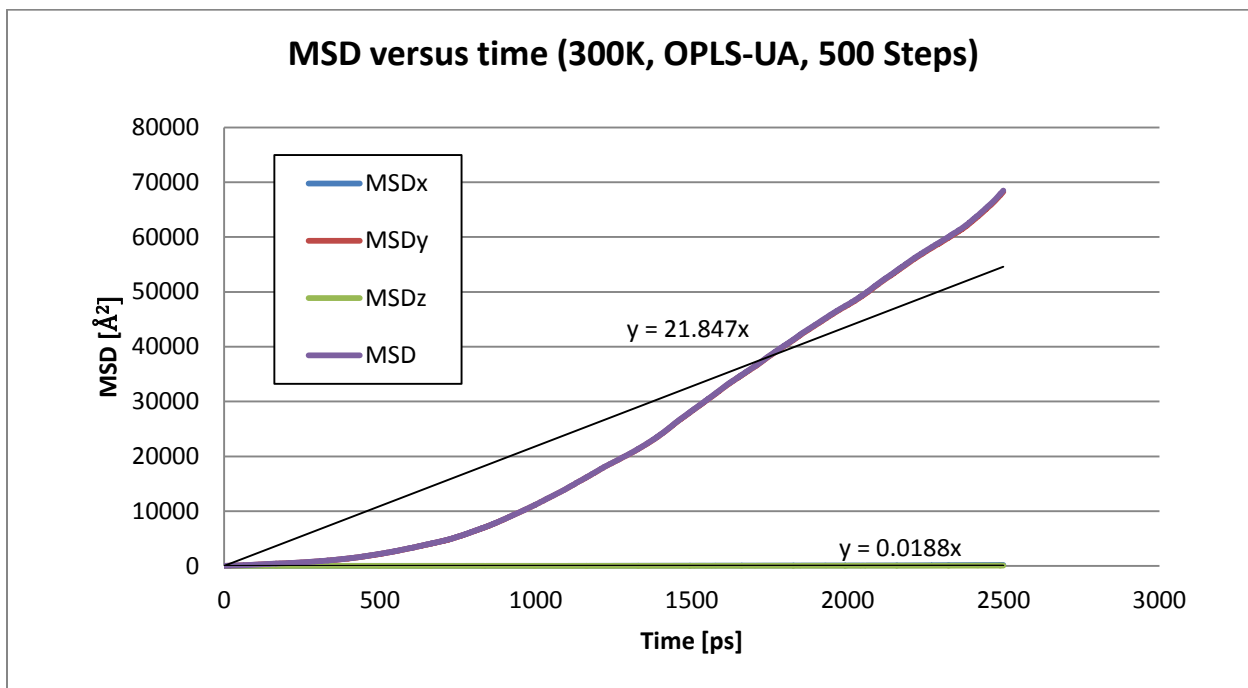


Figure 78: MSD of OPLS-UA toluene molecule at 300K, coordinates written every 500steps. MSDx is along the x-direction, MSDy is along the y-direction, and MSDz is along the z-direction.

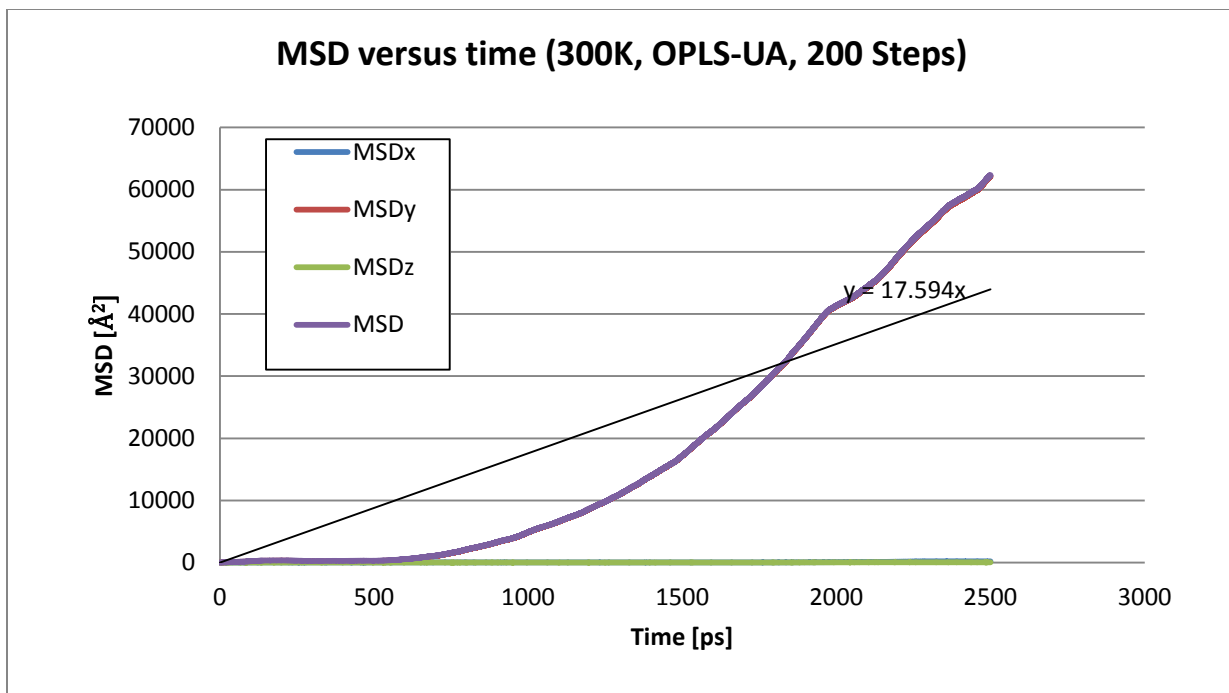


Figure 79: MSD of OPLS-UA toluene molecule at 300K, coordinates written every 200steps. MSDx is along the x-direction, MSDy is along the y-direction, and MSDz is along the z-direction.

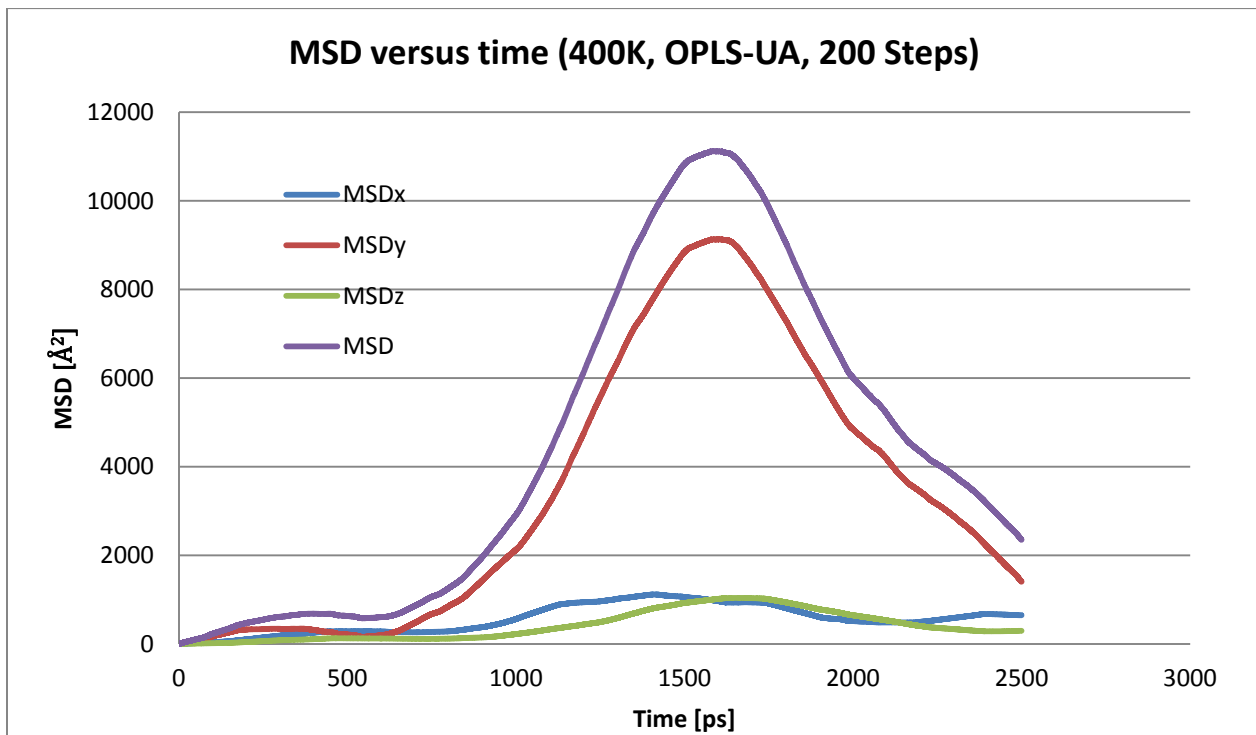


Figure 80: MSD of OPLS-UA toluene molecule at 400K, coordinates written every 500steps. MSDx is along the x-direction, MSDy is along the y-direction, and MSDz is along the z-direction.

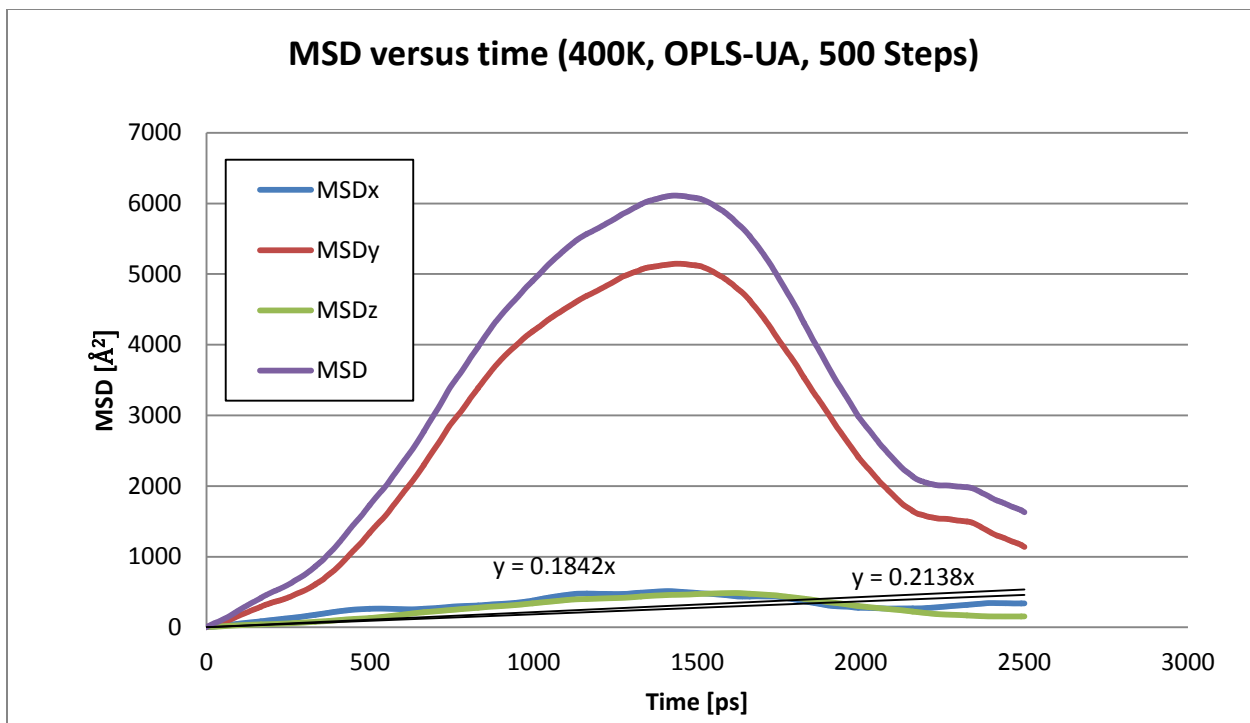


Figure 81: MSD of OPLS-UA toluene molecule at 400K, coordinates written every 500steps. MSDx is along the x-direction, MSDy is along the y-direction, and MSDz is along the z-direction.

The trends we have for our simulation using the OPLS-UA force field are similar to what we described for the OPLS-UA force-field at 400K. At 300K it seems to have a MSD that is almost linear. The very high values found for this temperature seems to indicate that there is a problem with the parameters used to describe either the molecule or the zeolite. Toluene should have a diffusion coefficient around $10^{-15} \text{ m}^2.\text{s}^{-1}$ at 300K. Based on these plots the diffusion coefficient of toluene would be much higher, around $10^{-8} \text{ m}^2.\text{s}^{-1}$ which is even faster than water diffusion through silicalite. This is too fast for such a big molecule.

At 400K, the trend seems to indicate that the OPLS-UA force field has the same property for the methyl group, allowing the molecule to diffuse through channel much more easily when this group is in line with a channel. Here again, the values of MSD found are much higher than expected. The same conclusions as for 300K can be drawn.

V- Neopentane:

We present our results for of MSD versus time for the neopentane molecule. We ran simulations at 300K and 400K using the OPLS-AA force-field. This molecule was thus allowed to vibrate in silicalite. For each graph, the averaged mean square displacement in the x (sinusoidal channel), y (straight channel) and z (mix of straight and sinusoidal channels)-directions as well as the total averaged mean squared displacement is given. One neopentane molecule was considered for each simulation. Figures 82-83 show our results at the different temperatures.

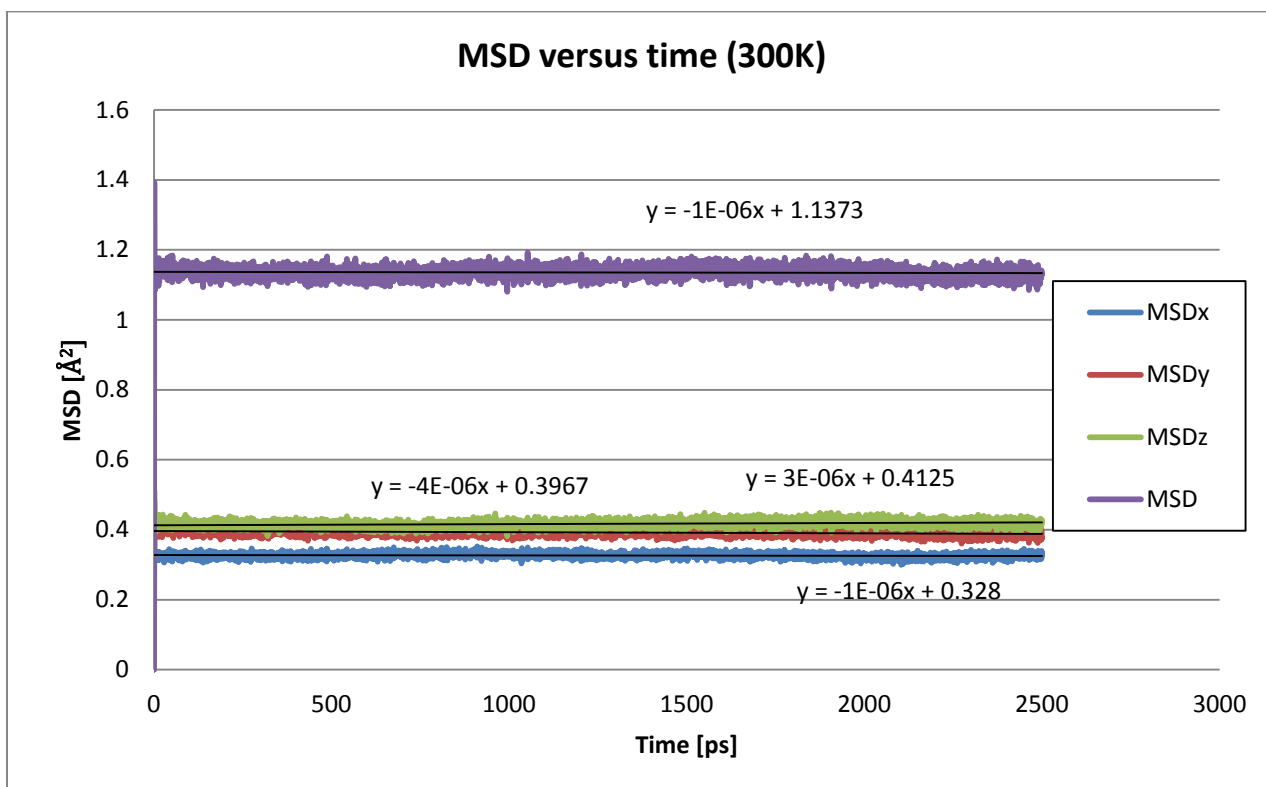


Figure 82: Mean square displacement of neopentane at 300K in silicalite. MSDx is along the x-direction, MSDy is along the y-direction, and MSDz is along the z-direction. These results were obtained using the program described in the methodology section.

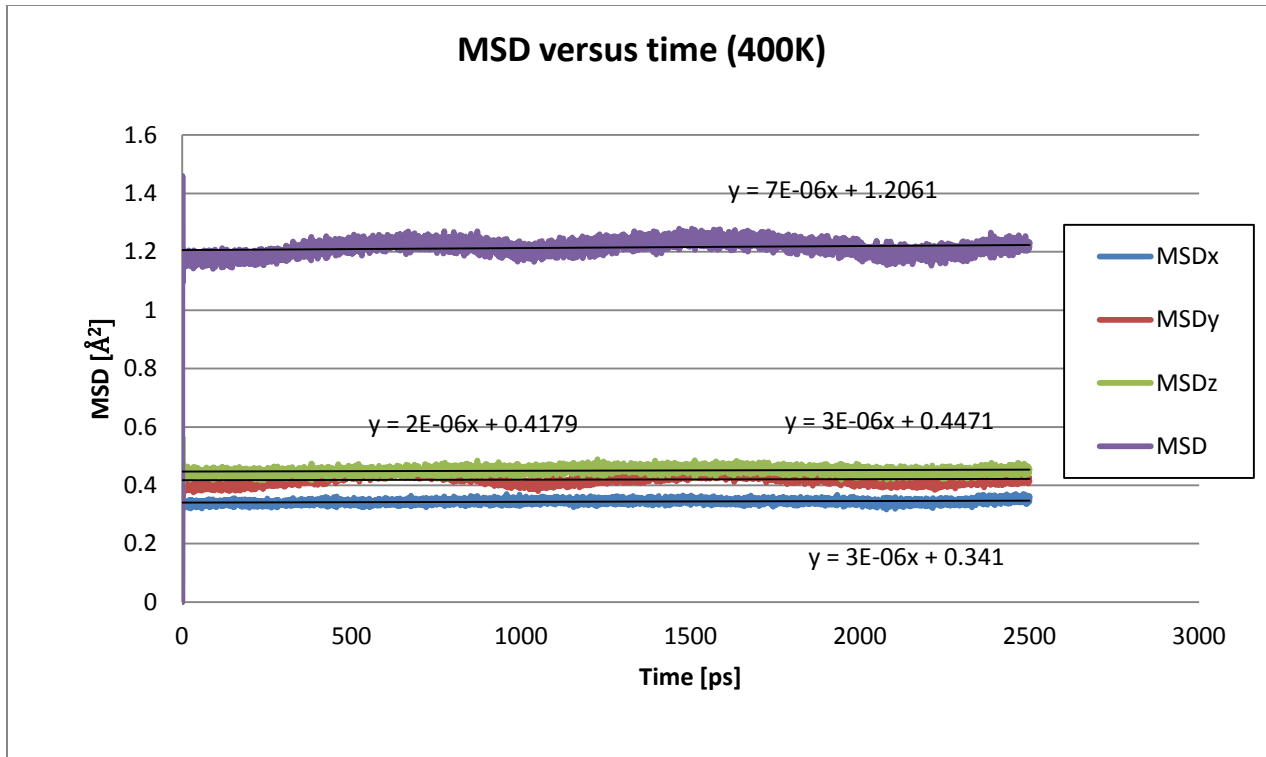


Figure 83: Mean square displacement of neopentane at 400K in silicalite. **MSDx** is along the x-direction, **MSDy** is along the y-direction, and **MSDz** is along the z-direction.

Based on these plots we can say that at both temperatures neopentane does not move considerably in silicalite. The neopentane molecule was initially placed at an intersection of straight and sinusoidal channels because intersections are supposed to have the lowest potential energy. The system is therefore supposed to be at a state that is close to a local equilibrium. Both plots have the same trends; the MSDs in every direction are nearly flat. The values of the different mean square displacements are very small, around 0.4 Å. For comparison, a unit cell of silicalite is 20.090 x 19.7938 x 13.142 Angstroms. The MSD in the z-direction seems to be the most important, because the jump at the beginning of the simulation is the most important. This jump in all three directions is due to the vibrations of the molecule and so has no real physical meaning. Also the diffusion constant calculated are so small that a slight change in the MSD linear trend line could give different results. Based on these simulations, it seems that neopentane is likely too big to diffuse significantly through silicalite. Nevertheless, it would be interesting to put the neopentane molecule at a location other than the intersection to see what the diffusion

pattern would be and if it would diffuse more in this case. Likely the molecule would diffuse until it reaches an intersection where it would be stuck for a longer time. There again, it should also be mentioned that the timescale for simulation of big molecules is very important, and running longer simulations might give us more precise self-diffusion coefficient and let us know if the molecule can diffuse or not through silicalite.

The different values of the self diffusion coefficients in the x, y and z directions, the total self-diffusion coefficient, the β and δ coefficients are given in the following table.

T [K]	D	Dx	Dy	Dz	β	δ
300	0.0000133	0.000005	0.00002	0.000015	0.603	0.8333
400	0.0000133	0.000015	0.00001	0.000015	0.3015	0.8333

Table 16: Diffusion coefficients of neopentane in silicalite [$10^{-9} \text{ m}^2 \cdot \text{s}^{-1}$], β and δ parameters as function of T

The β and δ parameters are given but do not really have a physical meaning because of the very small diffusion coefficients found for neopentane and because of our relatively small simulation time.

The self-diffusion coefficients that we found seem a little high and compare well with the experimental values for benzene. Running longer simulations might be a way to improve the error margin on these coefficients.

VI- Nonylphenol:

We show the plots of the mean square displacement of nonylphenol (NP) in silicalite at two different temperatures, 300 and 400K, in Figures 84 and 86. The averaged total MSD, and the averaged MSD in the x, y and z directions are shown. One molecule of a linear isomer of nonylphenol was simulated in silicalite. This NP was modeled using the OPLS-AA force-field parameters. The MSD was calculated for the phenol ring first, an averaged MSD for each carbon of this ring (Figure 84-86). We also calculated the average MSD for the carbons belonging to the linear chain (Figure 85-87).

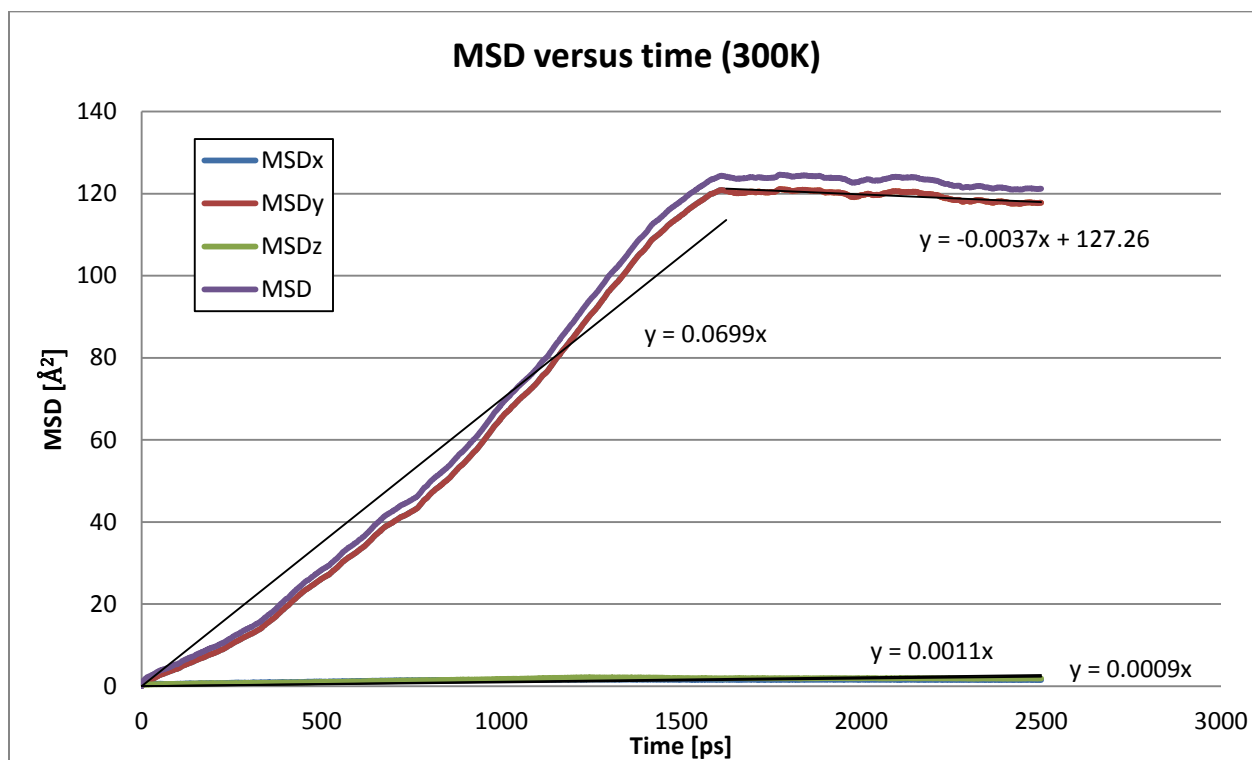


Figure 84: Mean square displacement of nonylphenol at 300K in silicalite. **MSDx** is along the x-direction, **MSDy** is along the y-direction, and **MSDz** is along the z-direction.

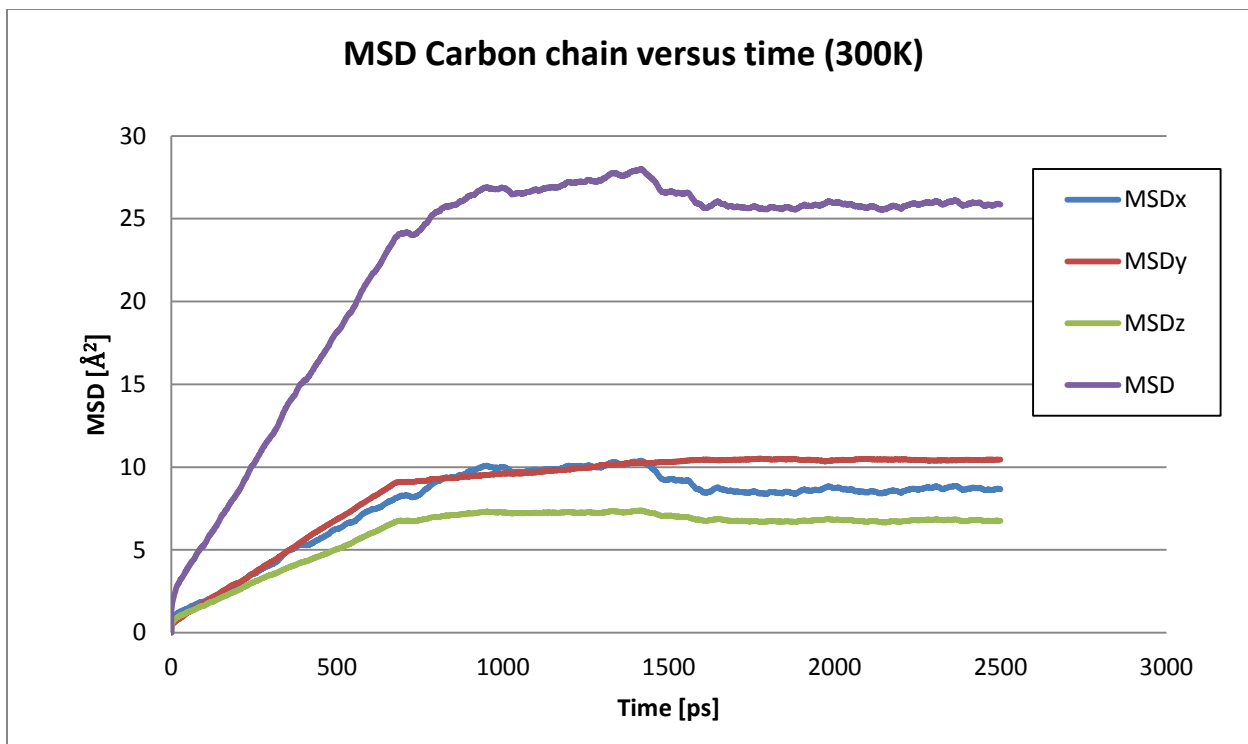


Figure 85: Mean square displacement of nonylphenol linear carbon chain at 300K in silicalite. MSDx is along the x-direction, MSDy is along the y-direction, and MSDz is along the z-direction.

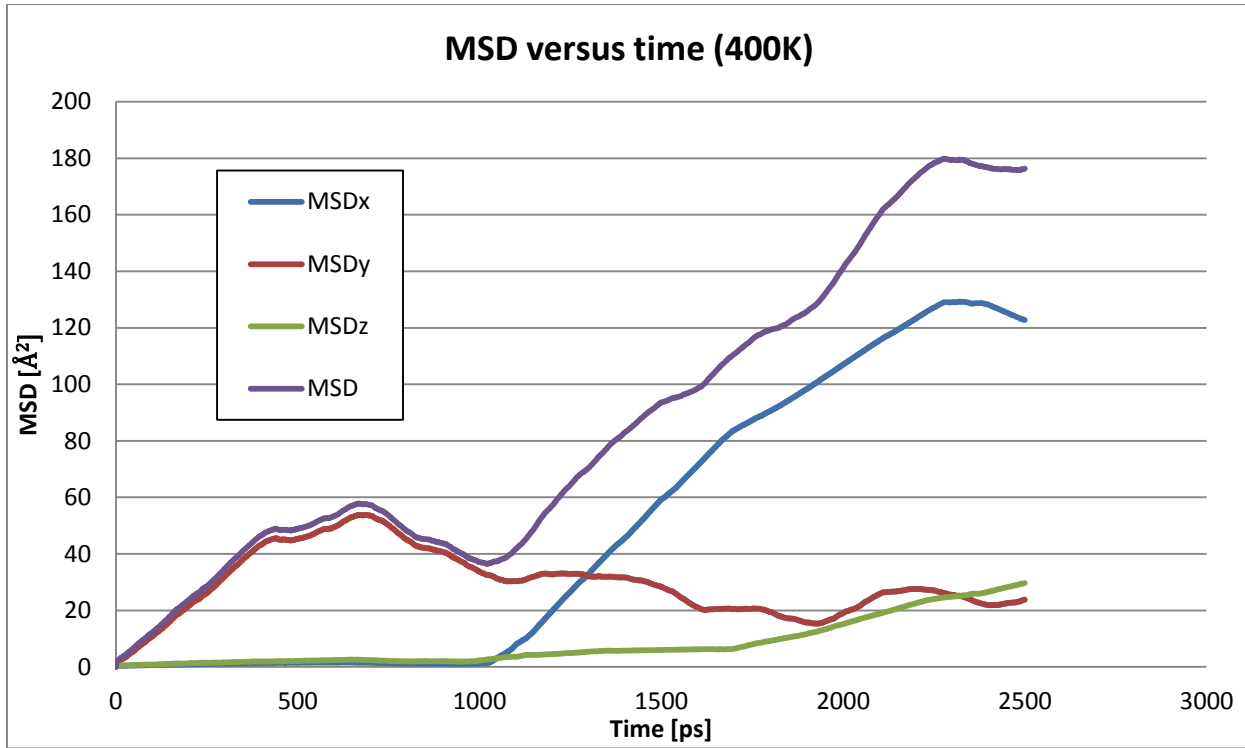


Figure 86: Mean square displacement of nonylphenol at 400K in silicalite. MSDx is along the x-direction, MSDy is along the y-direction, and MSDz is along the z-direction.

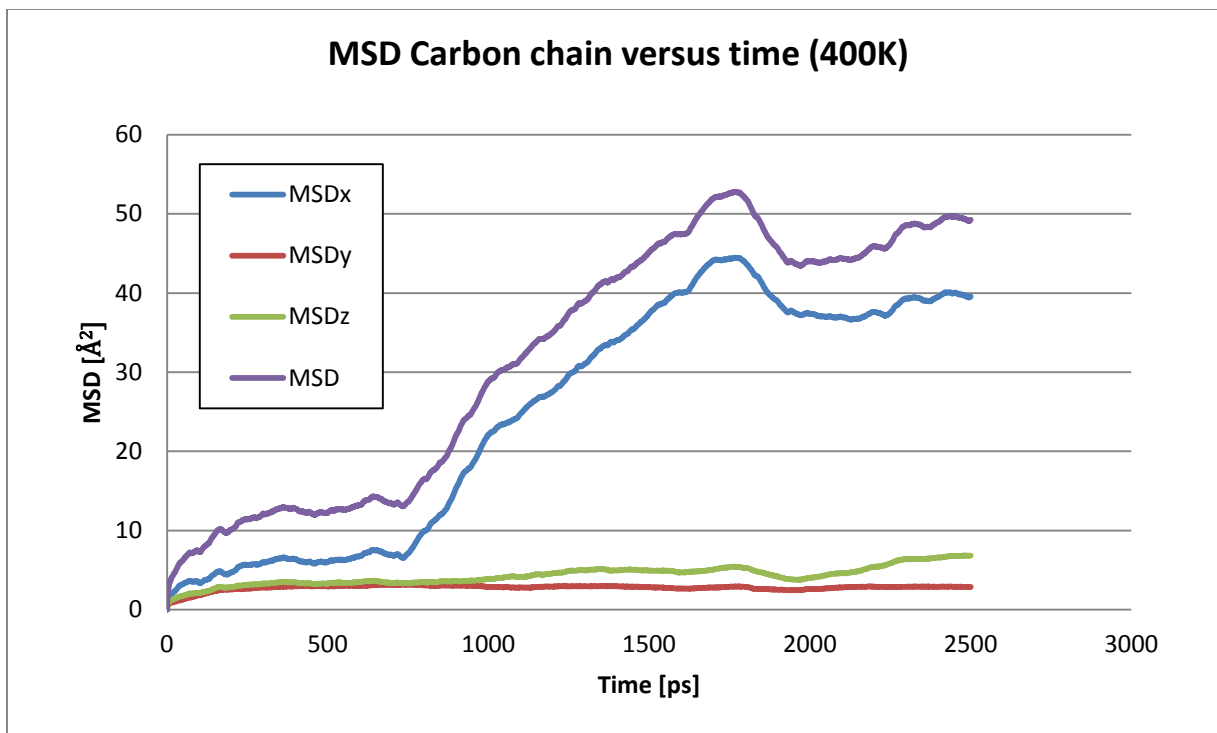


Figure 87: Mean square displacement of nonylphenol linear carbon chain at 400K in silicalite. **MSD_x** is along the x-direction, **MSD_y** is along the y-direction, and **MSD_z** is along the z-direction.

We initially expected that the linear carbonyl group could move more than the ring and so the MSD of the linear chain would not represent the actual movement of the molecule. We can see on figure 84 that the linear isomer of NP can indeed diffuse in silicalite at 300K. It diffuses through the straight channel for the first 1500 ps and then seems to be stuck as MSD_y reaches a constant value. MSD_x and MSD_z values are very small. These values of MSD were calculated for the phenol ring of NP. Looking at the coordinates of NP after the simulation it looks like the molecule's linear carbonyl group diffused through the sinusoidal channel. (See Figure 85) That is the reason why we decided to plot the MSD for the carbons of the linear chain of NP. We can see that these carbons move in the three directions almost at the same rate and at the same time. The fact that they move in the three directions "at the same time" seems bizarre, but is linked with our averaged MSDs. Here we averaged the displacement of the carbon atoms of the chain. While the edge of the chain is diffusing in the x and z direction, the carbons closer to the ring are dragged by these other carbons at the edge on the chain. The edge atoms go "up" in the zig-zag channel (see Figure 88) the others have to move along the y axis before being able to physically diffuse in the x direction. Therefore in average the carbons move in the x, y and z direction "at the same time".

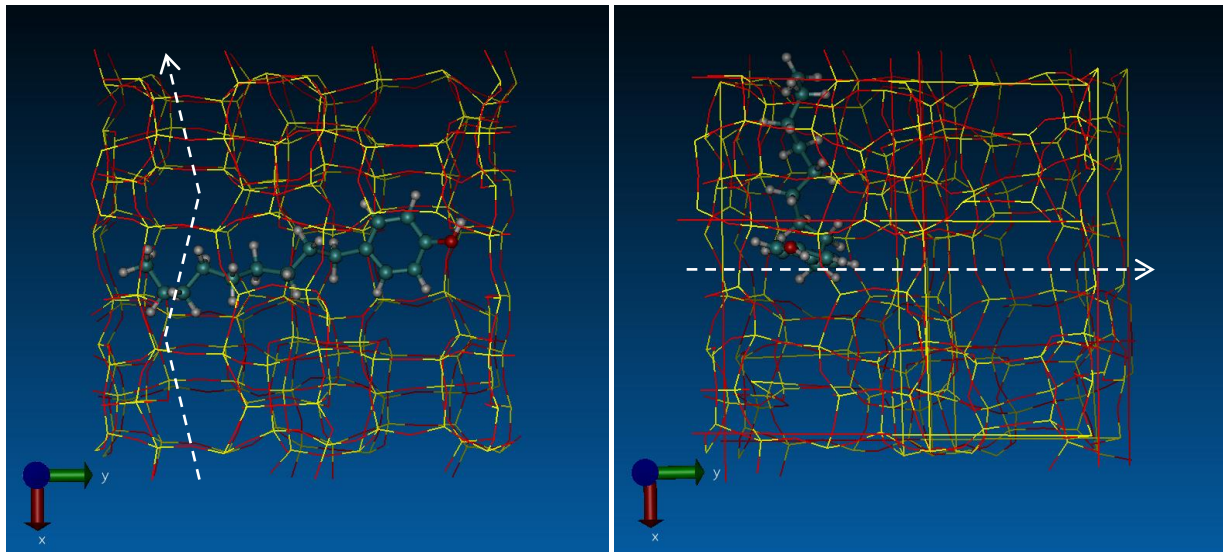


Figure 88: Movement of NP linear molecule in silicalite at 300K at $t=0$ (left, where the arrow shows the sinusoidal channel) and at $t=1500\text{ps}$ (right, where the arrow shows the straight channel)

At that point the molecule seems stuck in the sinusoidal channel which explains the almost constant MSD_y found for the benzene ring at that point. The ring is not in the right configuration to be able to diffuse through the zig-zag channel. It is the reason why the molecule becomes stuck in the silicalite structure. Figure 87 shows the averaged MSD for the carbon in the linear group. As we can see the same trend is observed, but the carbons also move in the x and z directions. After 1000 ps the linear chain becomes stuck in the sinusoidal channel.

The diffusion of NP in silicalite is also linked to the alcohol group at one end of the molecule. As we saw earlier with phenol, the diffusion of molecules with an alcohol group is linked with the hydrogen bonds that it could make with the framework. The following graph is the radial distribution of the hydrogen from the alcohol group and the oxygen of the framework.

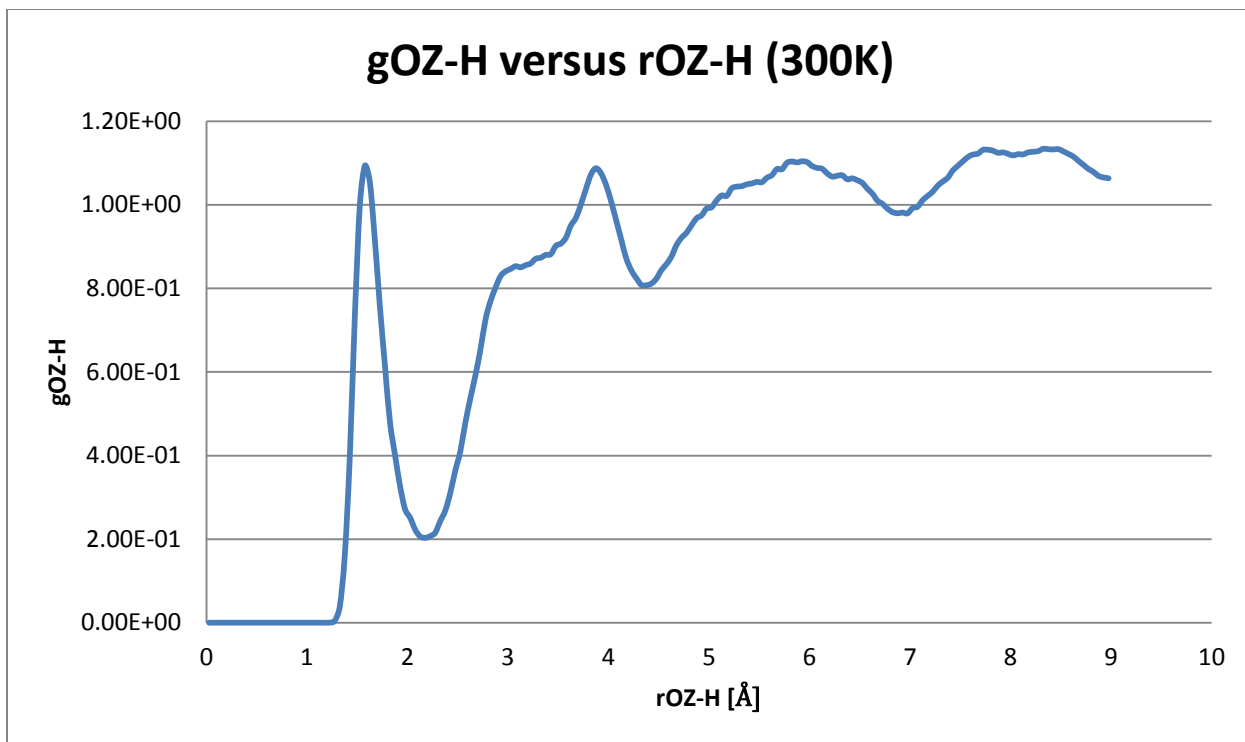


Figure 89: Radial distribution function between the hydrogen of the alcohol group of nonylphenol and the oxygen of the framework at 300K

As we can see there is a clear peak around 1.5 Å. The other peaks are probably due to the number of oxygen atoms in the framework. This means that the alcohol group is H-bonding with silicalite. As we saw for the phenol molecule earlier, the magnitude of the first peak is more important than for water meaning that there are more interactions between the alcohol group of NP and the atoms of silicalite. This could explain why the molecule is trapped at 300K. The vibrations of NP and silicalite are not important enough to allow the hydrogen to stop hydrogen bonding with the oxygen atoms at the intersection between straight and sinusoidal channels. The molecule is therefore likely to stay in this position for a long time, and thus hinder the diffusion of the molecule. We did not calculate a diffusion coefficient for phenol because of this.

At 400K, the plots (Figure86-87) are slightly different. The phenol ring seems to move at first along the y-axis more than the other two directions. After 1000 ps it starts to move a lot more along the x-axis and stops moving along the y-axis. This is the same phenomenon as for 300K. The linear chain starts to move along the x axis around 800 ps and so the ring follows the linear chain in the x-direction. After 1800 ps the linear chain seems to be stuck for the rest of the averaged time, and this trend is observed for the phenol ring in the x-direction around 2200 ps. It

means that the molecule was able to diffuse through the sinusoidal channel at 400K. The following plot is a plot of rdf at 400K.

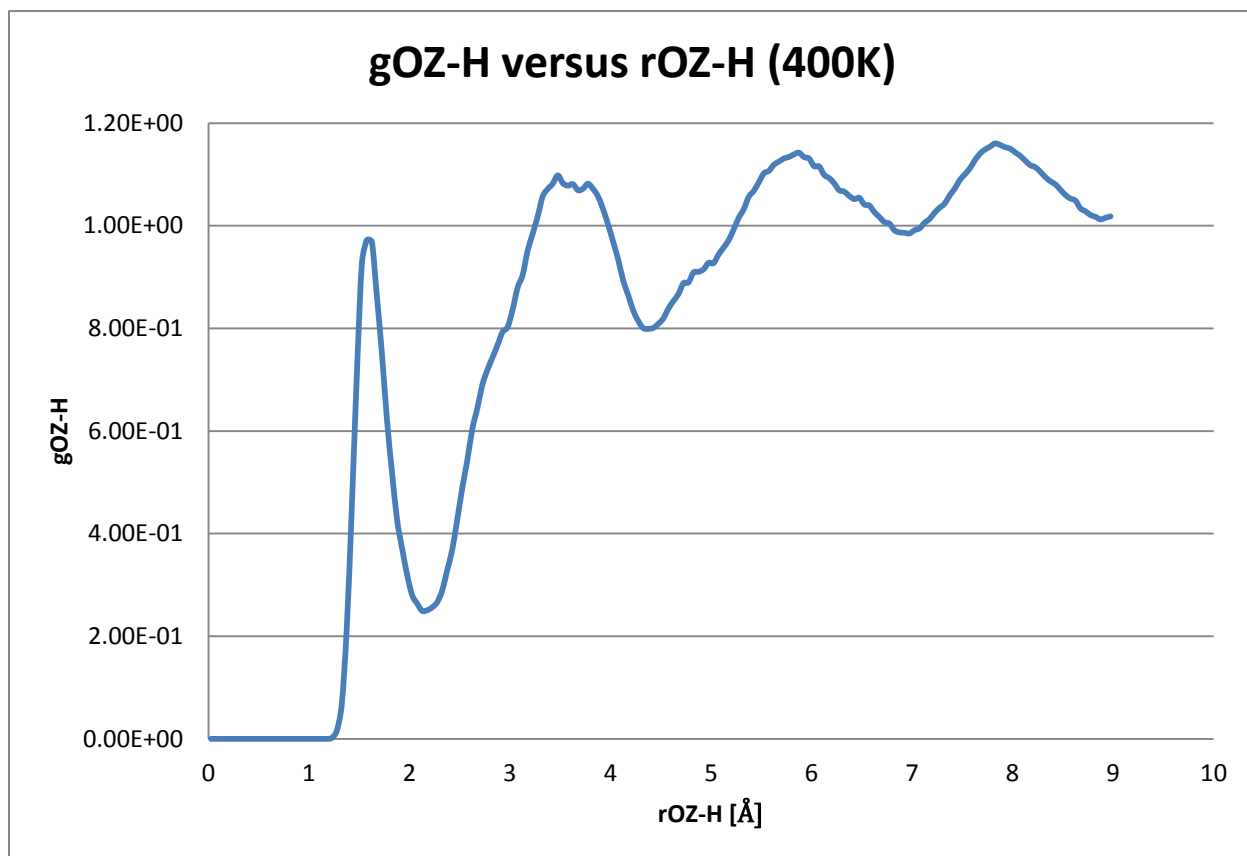


Figure 90: Radial distribution function between the hydrogen of the alcohol group of nonylphenol and the oxygen of the framework at 400K

The rdf shapes at 300 K and 400 K are almost identical. The values are also much larger than the ones saw for water molecules at the same temperatures, meaning that the molecule interacts with the framework. Note that the first peak is a slightly smaller than at 300K meaning that the hydrogen bonding is slightly weaker at 400K. This small change is probably what allowed the phenol ring to diffuse in the x-direction. H-bonds are a little weaker at higher temperature due to the increased molecular motion, allowing NP to diffuse. Nevertheless, the molecule seems stuck around the end of our simulation, which disrupts the diffusion of the molecule. Based on these plots it seems like nonylphenol can diffuse more easily at 400K in silicalite than at 300K, which was expected.

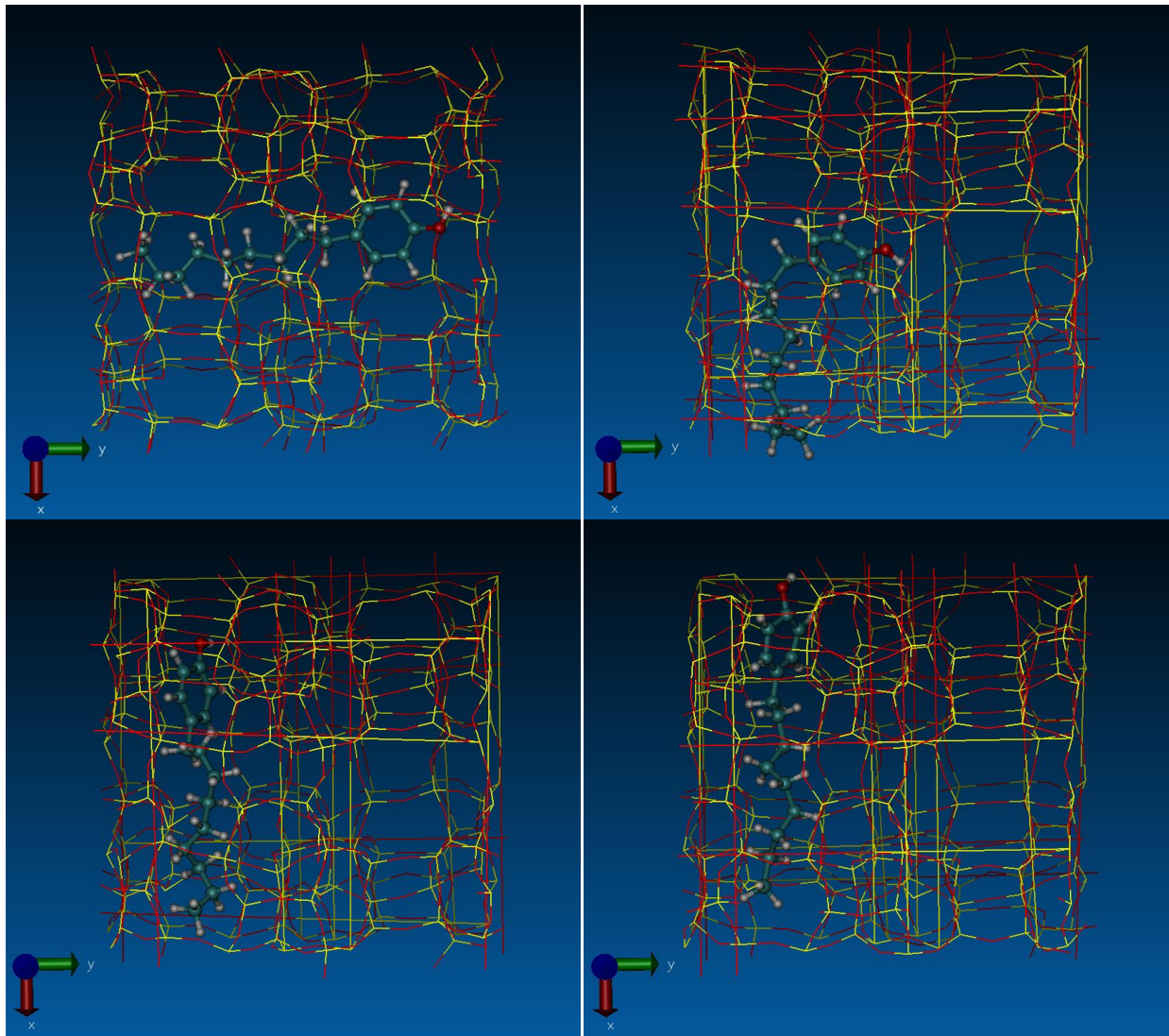


Figure 91: Movement of NP linear molecule in silicalite at 400K at $t=0$ (top left) and at different times. The molecule diffuses along the x axis in these pictures.

Another possible explanation of the increased MSD is the more important vibrations of the molecule and the framework. At 400K the vibrations are more important than at 300K and this allows the diffusion of the long nonylphenol molecule in the silicalite pores. Figure91 illustrates the diffusion of nonylphenol along the x axis.

VII- Bisphenol A:

We simulated bisphenol-A (BPA) in silicalite at two different temperatures, 300 and 400K, using the OPLS-AA and OPLS-UA parameters. We kept the phenol rings rigid for the OPLS-AA force-field but allowed the angle between these two rings, the methyl and alcohol groups to move. For the OPLS-UA we treated the molecule as rigid but allowed the alcohol and methyl groups to move. One molecule of BPA was simulated for each of these simulations. The following plots (Figures X-Y) give the averaged MSD values in the x, y and z directions, as well as the total averaged MSD.

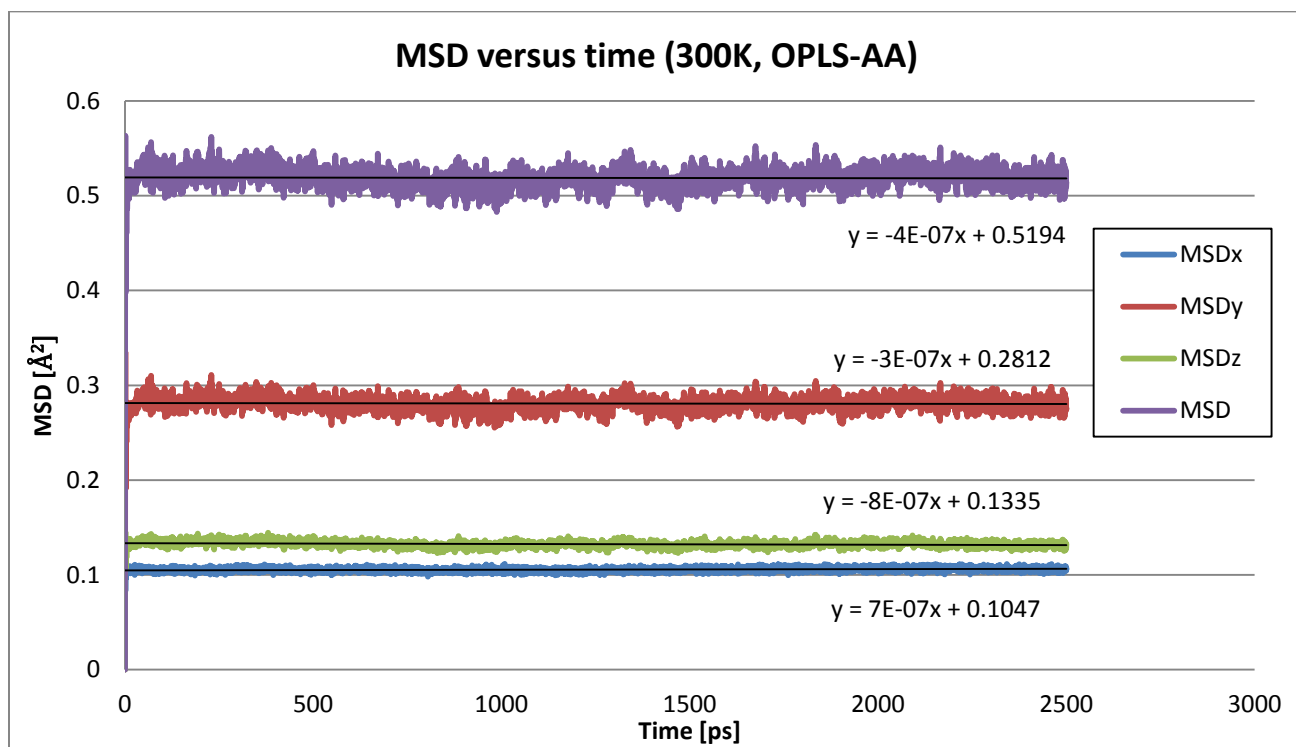


Figure 92: Mean square displacement of OPLS-AA BPA molecule at 300K in silicalite. MSDx is along the x-direction, MSDy is along the y-direction, and MSDz is along the z-direction.

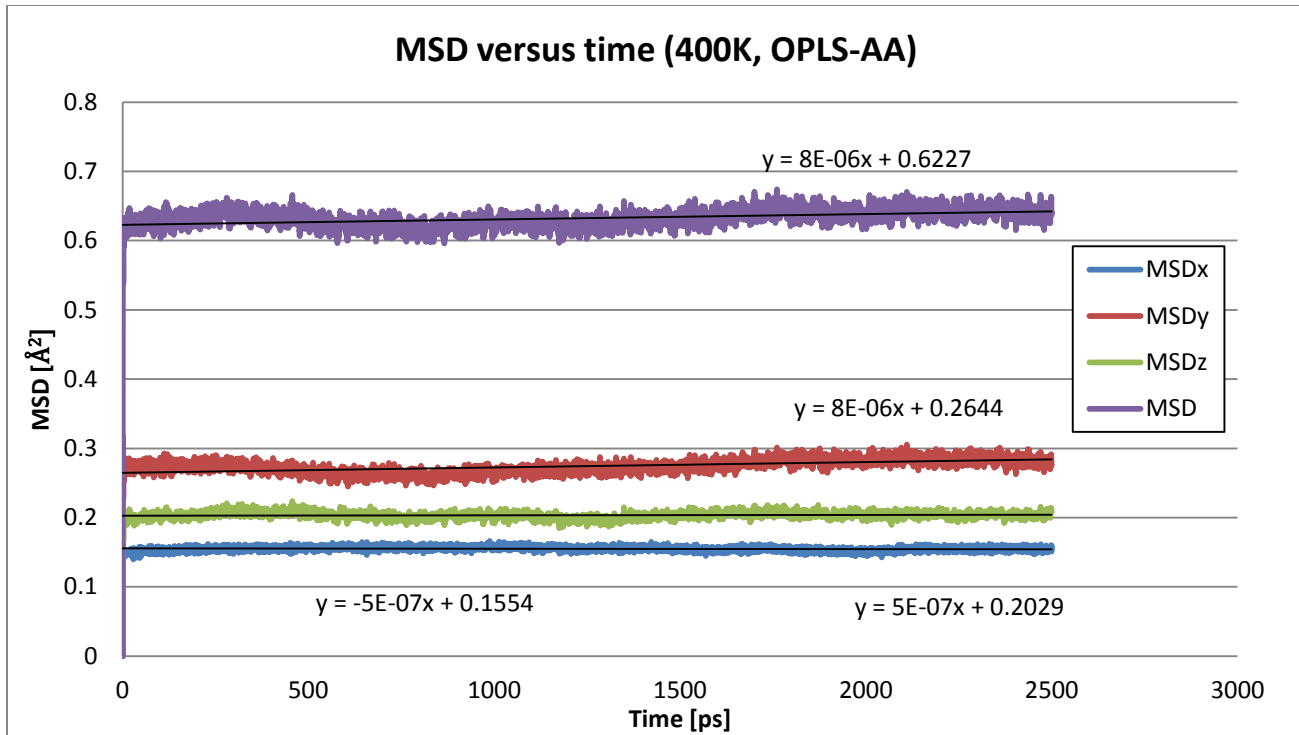


Figure 93: Mean square displacement of OPLS-AA BPA molecule at 400K in silicalite. MSDx is along the x-direction, MSDy is along the y-direction, and MSDz is along the z-direction.

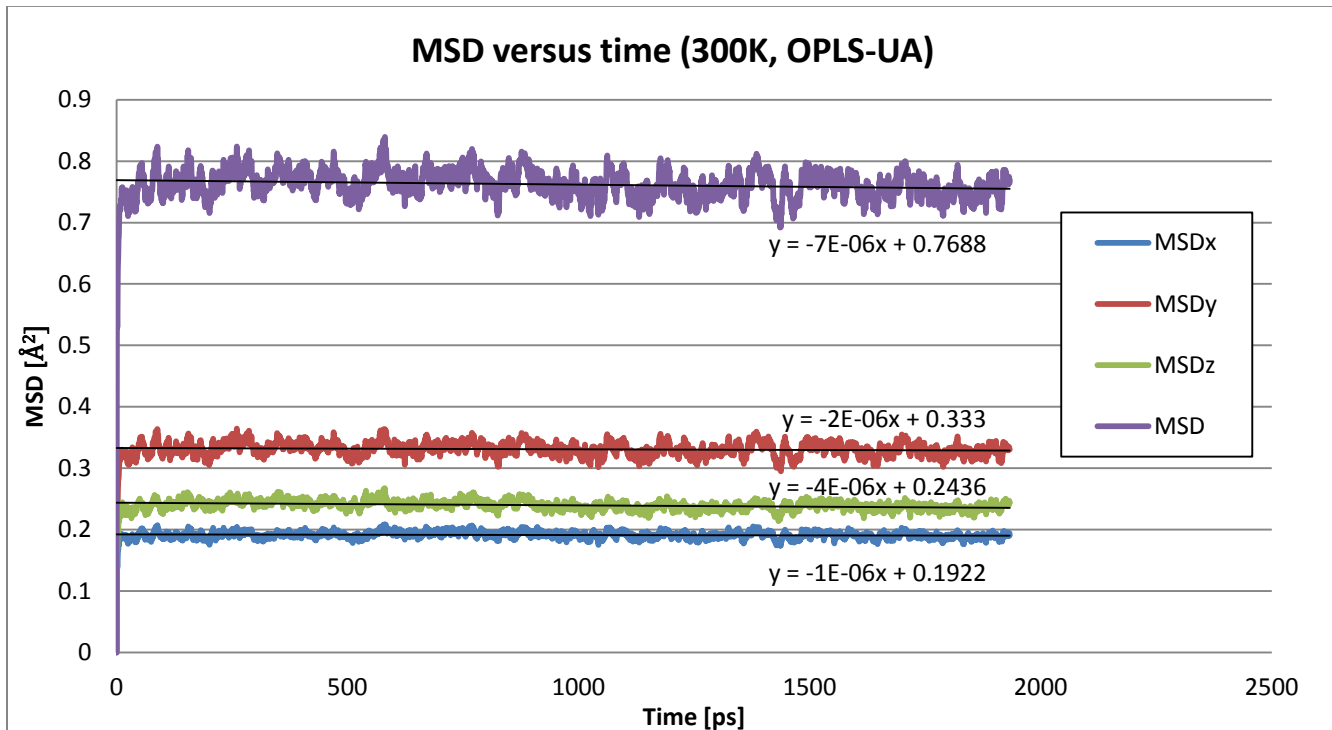


Figure 94: Mean square displacement of OPLS-UA BPA molecule at 300K in silicalite. MSDx is along the x-direction, MSDy is along the y-direction, and MSDz is along the z-direction.

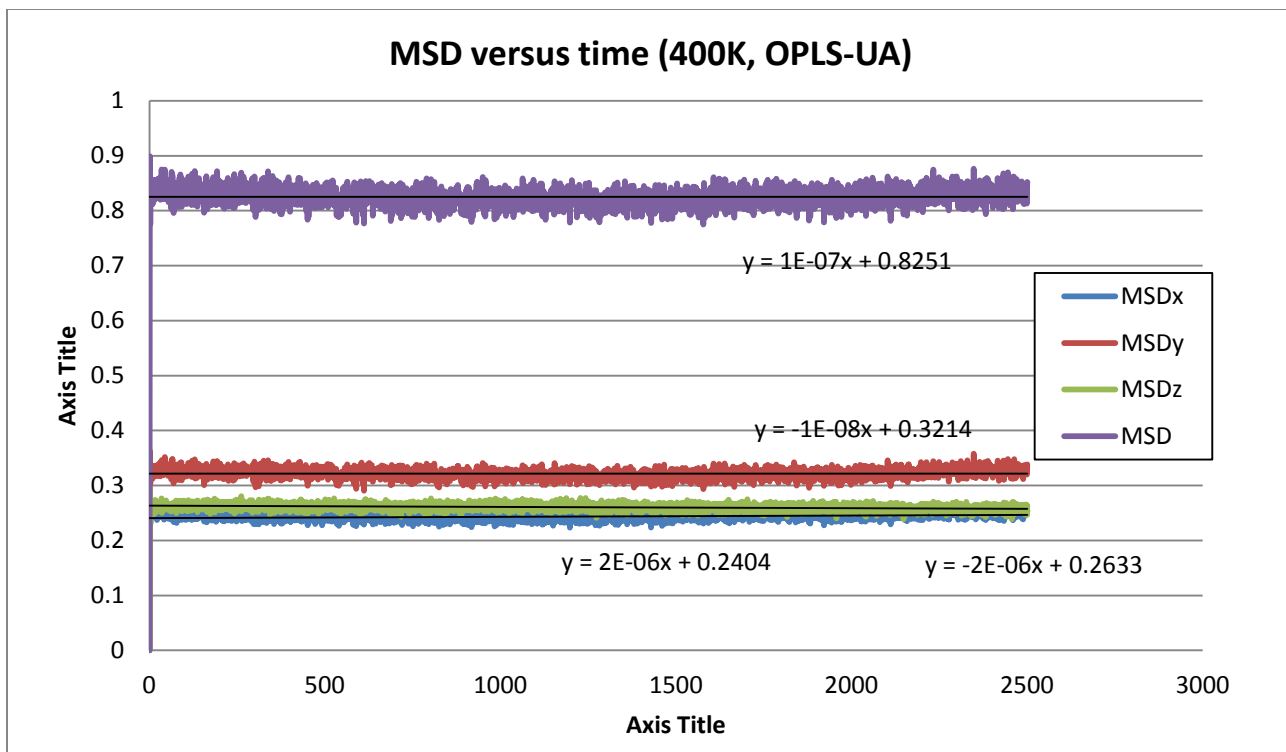


Figure 95: Mean square displacement of OPLS-UA BPA molecule at 400K in silicalite. **MSDx** is along the x-direction, **MSDy** is along the y-direction, and **MSDz** is along the z-direction.

The results obtained for BPA are very similar to the ones obtained for neopentane. The MSD plots are very flat. The same plots are observed for both force-fields, with very slight differences in the values reached. It seems that BPA moves slightly more in the y direction, which is what we expected because of the size of this molecule. The MSD values in the x and z directions are closer together compared to MSDy. Still, these values of MSD are very small, in the order of 0.4 \AA^2 . This means that even though BPA fits in the silicalite pores, it diffuses very slowly through the zeolite structure, if at all. The difference between OPLS-UA and OPLS-AA does not seem to be very important. As mentioned earlier, BPA barely fits in the silicalite structure and so the diffusion process is hindered mostly because of the molecular size. Using the OPLS-UA force field did not seem to change the results as much compared to smaller molecule such as benzene, phenol or toluene. (See previous sections) The general structure of BPA can also explain why the diffusion process is very slow. As we saw in the previous section, the nonylphenol molecule we simulated was linear. This allowed it to diffuse through the straight channel, although it became stuck in the zig-zag channel. BPA has a large size and can barely fit in the silicalite structure. We

initially believed that the movement of the angle between the two phenol rings would be important for the diffusion of BPA as it makes the molecule more planar and able to fit better in the zeolite. We expected the OPLS-AA force-field to move more freely because this angle was allowed to vibrate but the very small MSD seems to suggest that the large size still prevents diffusion despite any conformational changes of BPA.

Another reason of the poor displacement of BPA in silicalite is linked with the two alcohol groups it has at both ends. As we saw for phenol and nonylphenol in the previous sections, the hydrogen bonding of these groups influences the diffusion of the guest molecules. The following graph is the radial distribution between the hydrogen from the alcohol group and the oxygen from silicalite. The rdfs were almost the same between the OPLS-UA and OPLS-AA force-fields so we decided to show only the plots we obtained for the all-atom force-field.

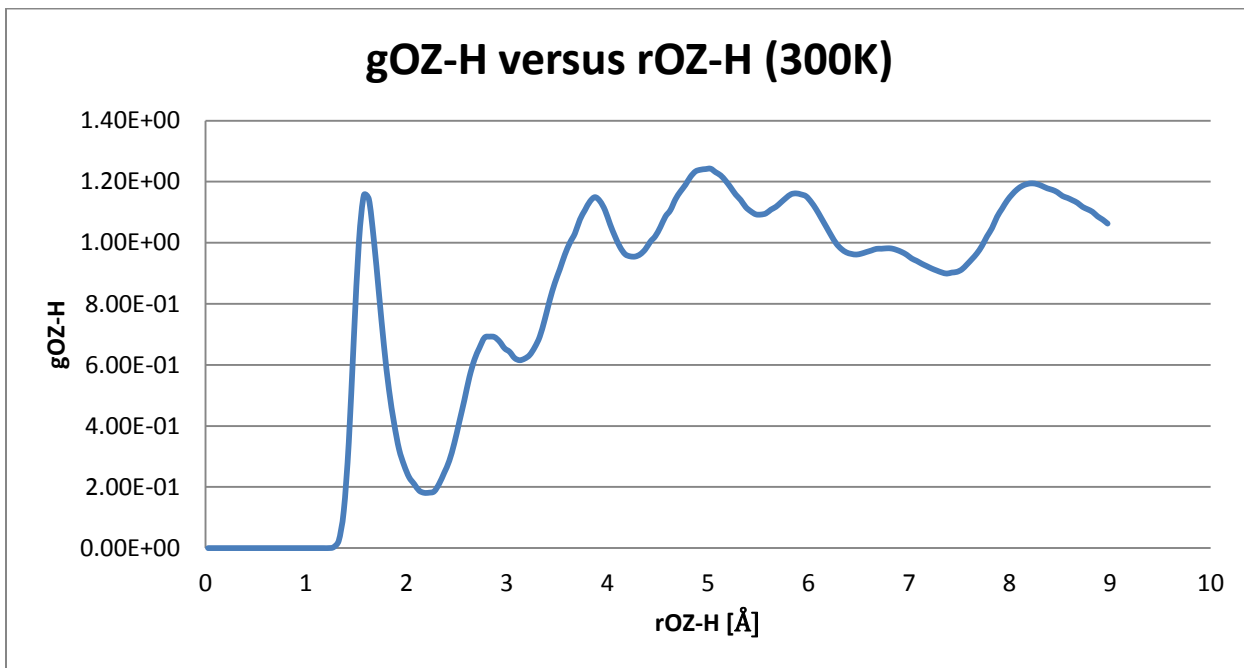


Figure 96: Radial distribution function between the hydrogen of the alcohol group of bisphenol-A and the oxygen of the framework at 300K

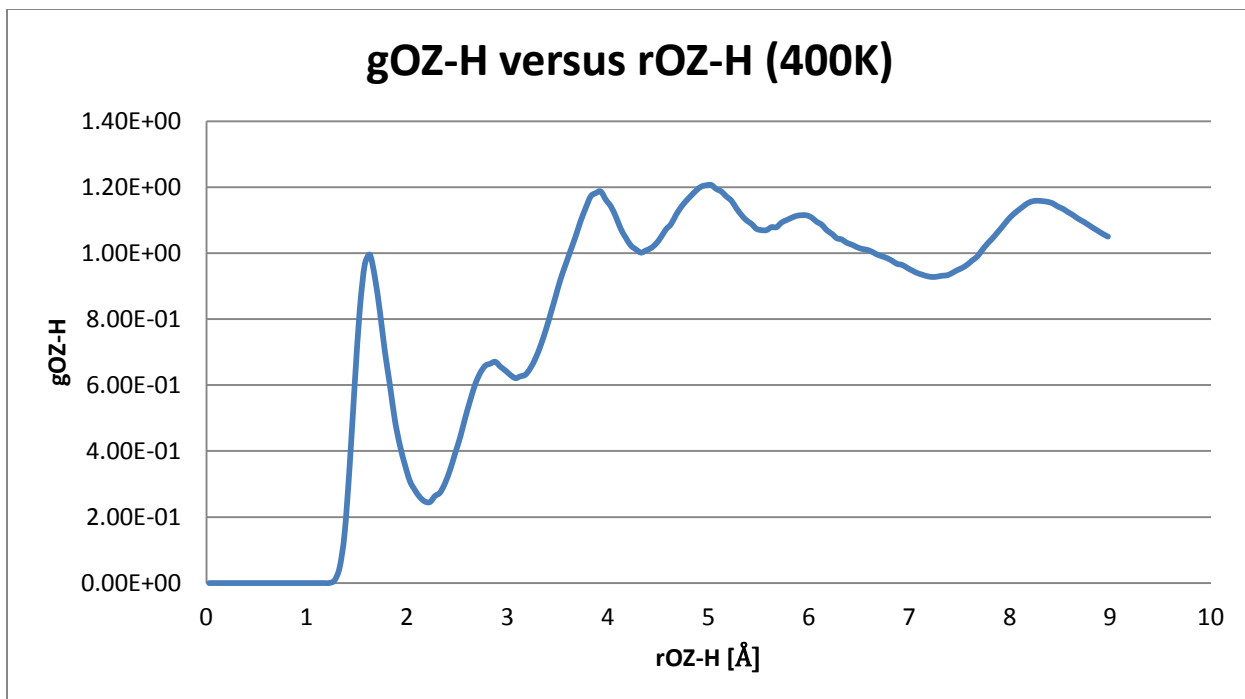


Figure 97: Radial distribution function between the hydrogen of the alcohol group of bisphenol-A and the oxygen of the framework at 300K

Here we can see the same trends for both temperatures with slightly smaller values for the rdf at 400K as expected. The first peak has a magnitude of 1.15 at 300K and 1.0 at 400K. We can say that the molecule interacts with the framework, based on the values seen for water. Also the peak is a little less important at 400K meaning that the hydrogen bonding is slightly less important. This is probably why the molecule moved a little bit more at the very start of the simulation at 400K compared to the simulation at 300K. We have a clear peak at around 1.5-1.6 \AA meaning we have hydrogen bonding. Here we have to remember that both ends of the BPA molecule has alcohol groups so the diffusion in silicalite must be very difficult. In the case of nonylphenol, the carbon chain moved while the hydrogen bonding at the other edge was slowing the diffusion process. Here we have hydrogen bonding at both ends so even if the molecule is trying to diffuse at one end, the other edge could be hydrogen bonded resulting in a very slow diffusion.

The following table summarizes the values we calculated for the self-diffusion coefficients of BPA. As for neopentane, the beta and delta parameters do not have a meaningful physical sense because of the very small diffusion coefficient that we found.

OPLS	T [K]	D	Dx	Dy	Dz	β	δ
AA	300	0.000003	0.0000015	0.0000035	0.000004	0.3958	0.625
	400	0.000015	0.0000025	0.00004	0.0000025	7.2380	8
UA	300	0.0000116	0.000005	0.00001	0.00002	0.2261	0.375
	400	0.0000066 8	0.0001	0.0000000 5	0.00001	0.00226	5.0025

Table 17: Diffusion coefficients of bisphenol-A in silicalite [$10^{-9} \text{ m}^2 \cdot \text{s}^{-1}$], β and δ parameters as function of T

These self-diffusion coefficients are very small as expected. The value found for the OPLS-UA force-field at 400K is smaller than the one at 300K which was not foreseen. We believe that longer simulations should be able to reduce these error margins by having a bigger sample of coordinates over time.

Conclusions

In this report, we studied the diffusion of different molecules in silicalite.

The results obtained for water molecule using two different famous bulk water models were in general agreement with previous literature values, although at low temperature (300 K), we obtained diffusion coefficients smaller than other reports. The mean-square displacement (MSD) was more important in the x-direction (sinusoidal channel) than in the expected y-direction (straight channel). The results obtained for self-diffusion coefficients for both models were in agreement with work by Yazaydin et al.²⁴ but around an order of magnitude smaller than experimental values. The results tended to improve with higher temperatures. We believe these results could be explained by the high number of hydrogen bonding that we found for our water molecules. These hydrogen bonds indicate the presence of clusters of water molecules in the straight channel. The activation energies that we found for both models were unique on the 300-600K interval. The values were around $16\text{kJ}\cdot\text{mol}^{-1}$ which is close to the value of bulk water.

The results obtained for benzene were in the same order of magnitude as the work done by Rungsirisakun et al.⁵¹ when the coordinates of our system was printed every 200 steps at 300K. Yet these values are several orders of magnitude higher than the experimental values found in literature. It is possible that longer simulation times may give average diffusion coefficients that are in better agreement with experiment. We also believe that the partial charges of the molecule and of silicalite have a very important impact on the diffusion. Forester et al.³² for example used charges that were very different for the silicate atom of the framework (+4.0 compared to our +2.05).

The shape of the different MSD for phenol was not linear for our simulation times. We believe that the diffusion on phenol in silicalite is mostly linked to the hydrogen bonding that happens between the alcohol group and the framework. These hydrogen bonds hinder the diffusion of phenol until a particular configuration of phenol is reached in the pores allowing it to diffuse through the channels. This phenomenon was observed for both OPLS-AA and UA force-fields.

Simulations of toluene had similar shapes for the MSD compared to phenol. The methyl group of toluene, when in line with a channel reduces the energy barrier for diffusion and allows it to move through the channel. Otherwise the molecule is stationary for a long time until it aligns with the channel. Therefore we believe that the molecule rotates in the zeolite until the methyl group is in line with one channel, and then diffuses through. No self-diffusion coefficients were calculated because our simulation time does not allow us to see a straight line for the MSDs. Values found for the OPLS-UA were much higher than expected so we believe that the steric hindrance of hydrogen atoms for toluene is also playing an important role in slowing the diffusion of the molecule in silicalite.

Neopentane simulations led to the calculation of a self-diffusion coefficient. We saw a very small displacement of neopentane as a function of time and believe that longer simulations could allow us to calculate a more precise coefficient. The rigid structure of neopentane and its size are the main reason for its very slow diffusion through silicalite.

Nonylphenol was able to diffuse through silicalite. The carbon chain seemed to drag the phenol ring in channels, while the alcohol group was slowing down the diffusion by making hydrogen-bonds with the framework. These hydrogen bonds resulted in the molecule being stuck in the channels for long times relative to our simulation time. The relative big size of this molecule implied steric hindrance from the hydrogen that was also slowing down the diffusion. Therefore no self-diffusion coefficients were calculated.

The results obtained for bisphenol-A indicate that the molecule is small enough to fit in silicalite, but the steric hindrance due to its size is important. The two alcohol groups at both ends of the molecule make hydrogen-bonds with the oxygen atoms of the framework leading to an anchoring of the molecule in the pores of silicalite. We believe that this is the main reason for the very slow diffusion observed for BPA. Longer simulations could lead to a better calculation of the self-diffusion coefficient for this molecule.

Our results are summed up in the following table.

Self-diffusion coefficients [$10^{-9} \text{ m}^2 \cdot \text{s}^{-1}$]		
T [K]	300	400
TIP3P Water	-	2.82
SPC Water	0.605	5.25
Benzene OPLS-AA	0.0485	2.27
Benzene OPLS-UA	1.43	3.23
Neopentane OPLS-AA	0.0000133	0.0000133
BPA OPLS-AA	0.000003	0.000015
BPA OPLS-UA	0.0000116	0.00000668

Table 18: Summary of the most important self-diffusion coefficients obtained throughout this report

References

1. Caliman, F. A.; Gavrilescu, M., Pharmaceuticals, Personal Care Products and Endocrine Disrupting Agents in the Environment - A Review. *Clean-Soil Air Water* **2009**, 37 (4-5), 277-303.
2. Kolpin, D. W.; Furlong, E. T.; Meyer, M. T.; Thurman, E. M.; Zaugg, S. D.; Barber, L. B.; Buxton, H. T., Pharmaceuticals, hormones, and other organic wastewater contaminants in US streams, 1999-2000: A national reconnaissance. *Environmental Science & Technology* **2002**, 36 (6), 1202-1211.
3. Stahlhut, R. W.; Welshons, W. V.; Swan, S. H., Bisphenol A Data in NHANES Suggest Longer than Expected Half-Life, Substantial Nonfood Exposure, or Both. *Environmental Health Perspectives* **2009**, 117 (5), 784-789.
4. Tsai, W. T., Human health risk on environmental exposure to bisphenol-A: A review. *Journal of Environmental Science and Health Part C-Environmental Carcinogenesis & Ecotoxicology Reviews* **2006**, 24 (2), 225-255.
5. Krishnan, A. V.; Stathis, P.; Permuth, S. F.; Tokes, L.; Feldman, D., BISPHENOL-A - AN ESTROGENIC SUBSTANCE IS RELEASED FROM POLYCARBONATE FLASKS DURING AUTOCLAVING. *Endocrinology* **1993**, 132 (6), 2279-2286.
6. Stackelberg, P. E.; Furlong, E. T.; Meyer, M. T.; Zaugg, S. D.; Henderson, A. K.; Reissman, D. B., Persistence of pharmaceutical compounds and other organic wastewater contaminants in a conventional drinking-water treatment plant. *Science of the Total Environment* **2004**, 329 (1-3), 99-113.
7. Calafat, A. M.; Ye, X. Y.; Wong, L. Y.; Reidy, J. A.; Needham, L. L., Exposure of the US population to bisphenol A and 4-tertiary-octylphenol: 2003-2004. *Environmental Health Perspectives* **2008**, 116 (1), 39-44; Calafat, A. M.; Kuklenyik, Z.; Reidy, J. A.; Caudill, S. P.; Ekong, J.; Needham, L. L., Urinary concentrations of bisphenol A and 4-nonylphenol in a human reference population. *Environmental Health Perspectives* **2005**, 113 (4), 391-395.
8. Vandenberg, L. N.; Hauser, R.; Marcus, M.; Olea, N.; Welshons, W. V., Human exposure to bisphenol A (BPA). *Reproductive Toxicology* **2007**, 24 (2), 139-177.
9. Heindel, J. J.; vom Saal, F. S., Role of nutrition and environmental endocrine disrupting chemicals during the perinatal period on the aetiology of obesity. *Molecular and Cellular Endocrinology* **2009**, 304 (1-2), 90-96.
10. Howdeshell, K. L.; Hotchkiss, A. K.; Thayer, K. A.; Vandenberghe, J. G.; vom Saal, F. S., Environmental toxins - Exposure to bisphenol A advances puberty. *Nature* **1999**, 401 (6755), 763-764.
11. Kim, Y. H.; Lee, B.; Choo, K. H.; Choi, S. J., Selective adsorption of bisphenol A by organic-inorganic hybrid mesoporous silicas. *Microporous and Mesoporous Materials* **2011**, 138 (1-3), 184-190.
12. Zhang, H. F.; Zuehlke, S.; Guenther, K.; Spiteller, M., Enantio selective separation and determination of single nonylphenol isomers. *Chemosphere* **2007**, 66 (4), 594-602.
13. Sun, C.; Baird, M.; Anderson, H. A.; Brydon, D. L., Separation of broadly distributed nonylphenol ethoxylates and determination of ethylene oxide oligomers in textile lubricants and emulsions by high-performance liquid chromatography. *Journal of Chromatography A* **1996**, 731 (1-2), 161-169.
14. Gundersen, J. L., Separation of isomers of nonylphenol and select nonylphenol polyethoxylates by high-performance liquid chromatography on a graphitic carbon column. *Journal of Chromatography A* **2001**, 914 (1-2), 161-166.
15. Babay, P. A.; Gettar, R. T.; Silva, M. F.; Thiele, B.; Batistoni, D. A., Separation of nonylphenol ethoxylates and nonylphenol by non-aqueous capillary electrophoresis. *Journal of Chromatography A* **2006**, 1116 (1-2), 277-285.
16. Moeder, M.; Martin, C.; Schlosser, D.; Harynuk, J.; Gorecki, T., Separation of technical 4-nonylphenols and their biodegradation products by comprehensive two-dimensional gas

- chromatography coupled to time-of-flight mass spectrometry. *Journal of Chromatography A* **2006**, *1107* (1-2), 233-239.
17. Vermeire, T.; Bontje, D.; Hermens, J., Global relevance of integrated risk assessment (IRA), a case study. *Toxicology and Applied Pharmacology* **2004**, *197* (3), 143-144.
 18. Smit, B.; Maesen, T. L. M., Molecular simulations of zeolites: Adsorption, diffusion, and shape selectivity. *Chemical Reviews* **2008**, *108* (10), 4125-4184.
 19. Smit, B.; Maesen, T. L. M., Towards a molecular understanding of shape selectivity. *Nature* **2008**, *451* (7179), 671-678.
 20. Zhu, W.; Kapteijn, F.; Moulijn, J. A.; den Exter, M. C.; Jansen, J. C., Shape selectivity in adsorption on the all-silica DD3R. *Langmuir* **2000**, *16* (7), 3322-3329.
 21. Murugavel, R.; Walawalkar, M. G.; Dan, M.; Roesky, H. W.; Rao, C. N. R., Transformations of molecules and secondary building units to materials: A bottom-up approach. *Accounts of Chemical Research* **2004**, *37* (10), 763-774.
 22. Fleys, M.; Thompson, R. W.; MacDonald, J. C., Comparison of the behavior of water in silicalite and dealuminated zeolite Y at different temperatures by molecular dynamic simulations. *Journal of Physical Chemistry B* **2004**, *108* (32), 12197-12203.
 23. Fleys, M.; Thompson, R. W., Monte Carlo simulations of water adsorption isotherms in silicalite and dealuminated zeolite Y. *Journal of Chemical Theory and Computation* **2005**, *1* (3), 453-458.
 24. Yazaydin, A. O.; Thompson, R. W., Molecular simulation of water adsorption in silicalite: Effect of silanol groups and different cations. *Microporous and Mesoporous Materials* **2009**, *123* (1-3), 169-176.
 25. Yazaydin, A. O.; Thompson, R. W., Molecular simulation of the adsorption of MTBE in silicalite, mordenite, and zeolite beta. *Journal of Physical Chemistry B* **2006**, *110* (29), 14458-14462; Kotdawala, R. R.; Yazaydin, A. O.; Kazantzis, N.; Thompson, R. W., A molecular simulation approach to the study of adsorption of hydrogen cyanide and methyl ethyl ketone in silicalite, mordenite and zeolite beta structures. *Molecular Simulation* **2007**, *33* (9-10), 843-850.
 26. Trzpit, M.; Soulard, M.; Patarin, J.; Desbiens, N.; Cailliez, F.; Boutin, A.; Demachy, I.; Fuchs, A. H., The effect of local defects on water adsorption in silicalite-1 zeolite: A joint experimental and molecular simulation study. *Langmuir* **2007**, *23* (20), 10131-10139.
 27. Degnan, T. F., The implications of the fundamentals of shape selectivity for the development of catalysts for the petroleum and petrochemical industries. *Journal of Catalysis* **2003**, *216* (1-2), 32-46.
 28. Mravec, D.; Hudec, J.; Janotka, I., Some possibilities of catalytic and noncatalytic utilization of zeolites. *Chemical Papers-Chemicke Zvesti* **2005**, *59* (1), 62-69.
 29. Huang, H. J.; Ramaswamy, S.; Tscherner, U. W.; Ramarao, B. V., A review of separation technologies in current and future biorefineries. *Separation and Purification Technology* **2008**, *62* (1), 1-21.
 30. Bejblova, M.; Zilkova, N.; Cejka, J., Transformations of aromatic hydrocarbons over zeolites. *Research on Chemical Intermediates* **2008**, *34* (5-7), 439-454.
 31. Kerby, M. C.; Degnan, T. F.; Marler, D. O.; Beck, J. S., Advanced catalyst technology and applications for high quality fuels and lubricants. *Catalysis Today* **2005**, *104* (1), 55-63.
 32. Forester, T. R.; Smith, W., Bluemoon simulations of benzene in silicalite-1 - Prediction of free energies and diffusion coefficients. *Journal of the Chemical Society-Faraday Transactions* **1997**, *93* (17), 3249-3257.
 33. Demontis, P.; Stara, G.; Suffritti, G. B., Behavior of water in the hydrophobic zeolite silicalite at different temperatures. A Molecular Dynamics Study. *Journal of Physical Chemistry B* **2003**, *107* (18), 4426-4436.
 34. Hoover, W. G., CANONICAL DYNAMICS - EQUILIBRIUM PHASE-SPACE DISTRIBUTIONS. *Physical Review A* **1985**, *31* (3), 1695-1697.

35. Jorgensen, W. L.; Maxwell, D. S.; TiradoRives, J., Development and testing of the OPLS all-atom force field on conformational energetics and properties of organic liquids. *Journal of the American Chemical Society* **1996**, *118* (45), 11225-11236.
36. Jorgensen, W. L.; Chandrasekhar, J.; Madura, J. D.; Impey, R. W.; Klein, M. L., COMPARISON OF SIMPLE POTENTIAL FUNCTIONS FOR SIMULATING LIQUID WATER. *Journal of Chemical Physics* **1983**, *79* (2), 926-935.
37. Jorgensen, W. L.; Tiradorives, J., THE OPLS POTENTIAL FUNCTIONS FOR PROTEINS - ENERGY MINIMIZATIONS FOR CRYSTALS OF CYCLIC-PEPTIDES AND CRAMBIN. *Journal of the American Chemical Society* **1988**, *110* (6), 1657-1666.
38. Mark, P.; Nilsson, L., Structure and dynamics of the TIP3P, SPC, and SPC/E water models at 298 K. *Journal of Physical Chemistry A* **2001**, *105* (43), 9954-9960.
39. Auerbach, S. M.; Henson, N. J.; Cheetham, A. K.; Metiu, H. I., TRANSPORT-THEORY FOR CATIONIC ZEOLITES - DIFFUSION OF BENZENE IN NA-Y. *Journal of Physical Chemistry* **1995**, *99* (26), 10600-10608.
40. Smith, W.; Todorov, I. T., A short description of DL_POLY. *Molecular Simulation* **2006**, *32* (12-13), 935-943.
41. Yang, J. Z.; Liu, Q. L.; Wang, H. T., Analyzing adsorption and diffusion behaviors of ethanol/water through silicalite membranes by molecular simulation. *Journal of Membrane Science* **2007**, *291* (1-2), 1-9.
42. Desbiens, N.; Boutin, A.; Demachy, I., Water condensation in hydrophobic silicalite-1 zeolite: A molecular simulation study. *Journal of Physical Chemistry B* **2005**, *109* (50), 24071-24076.
43. Schemmert, U.; Karger, J.; Krause, C.; Rakoczy, R. A.; Weitkamp, J., Monitoring the evolution of intracrystalline concentration. *Europhysics Letters* **1999**, *46* (2), 204-210.
44. Bussai, C.; Vasenkov, S.; Liu, H.; Bohlmann, W.; Fritzsche, S.; Hannongbua, S.; Haberlandt, R.; Karger, J., On the diffusion of water in silicalite-1: MD simulations using ab initio fitted potential and PFG NMR measurements. *Applied Catalysis a-General* **2002**, *232* (1-2), 59-66.
45. Snurr, R. Q.; Bell, A. T.; Theodorou, D. N., INVESTIGATION OF THE DYNAMICS OF BENZENE IN SILICALITE USING TRANSITION-STATE THEORY. *Journal of Physical Chemistry* **1994**, *98* (46), 11948-11961.
46. Ruthven, D. M.; Eic, M.; Richard, E., DIFFUSION OF C-8 AROMATIC-HYDROCARBONS IN SILICALITE. *Zeolites* **1991**, *11* (7), 647-653.
47. Wu, P. D.; Debebe, A.; Yi, H. M., ADSORPTION AND DIFFUSION OF C-6 AND C-8 HYDROCARBONS IN SILICALITE. *Zeolites* **1983**, *3* (2), 118-122.
48. Shah, D. B.; Hayhurst, D. T.; Evanina, G.; Guo, C. J., SORPTION AND DIFFUSION OF BENZENE IN HZSM-5 AND SILICALITE CRYSTALS. *Aiche Journal* **1988**, *34* (10), 1713-1717.
49. Shen, D. M.; Rees, L. V. C., DIFFUSIVITIES OF BENZENE IN HZSM-5, SILICALITE-1, AND NAX DETERMINED BY FREQUENCY-RESPONSE TECHNIQUES. *Zeolites* **1991**, *11* (7), 666-671.
50. Vandenbegin, N.; Rees, L. V. C.; Caro, J.; Bulow, M., FAST ADSORPTION-DESORPTION KINETICS OF HYDROCARBONS IN SILICALITE-1 BY THE SINGLE-STEP FREQUENCY-RESPONSE METHOD. *Zeolites* **1989**, *9* (4), 287-292.
51. Rungsisakun, R.; Nanok, T.; Probst, M.; Limtrakul, J., Adsorption and diffusion of benzene in the nanoporous catalysts FAU, ZSM-5 and MCM-22: A molecular dynamics study. *Journal of Molecular Graphics & Modelling* **2006**, *24* (5), 373-382.
52. Snurr, R. Q.; Bell, A. T.; Theodorou, D. N., PREDICTION OF ADSORPTION OF AROMATIC-HYDROCARBONS IN SILICALITE FROM GRAND-CANONICAL MONTE-CARLO SIMULATIONS WITH BIASED INSERTIONS. *Journal of Physical Chemistry* **1993**, *97* (51), 13742-13752.
53. Snurr, R. Q.; Bell, A. T.; Theodorou, D. N., A HIERARCHICAL ATOMISTIC LATTICE SIMULATION APPROACH FOR THE PREDICTION OF ADSORPTION THERMODYNAMICS OF BENZENE IN SILICALITE. *Journal of Physical Chemistry* **1994**, *98* (19), 5111-5119.

54. Inui, T.; Nakazaki, Y., SIMULATION OF DYNAMIC BEHAVIORS OF BENZENE AND TOLUENE INSIDE THE PORES OF ZSM-5 ZEOLITE. *Zeolites* **1991**, *11* (5), 434-437.
55. <http://www.bisphenol-a.org/>
56. <http://www.panna.org/>
57. Fleys, M., WATER BEHABIOR IN HYDROPHOBIC POROUS MATERIALS. COMPARISON BETWEEN SILICALITE AND DEALUMINATED ZEOLITE Y BY MOLECULAR SIMULATIONS.
58. Yazaydin, A.O., MOLECULAR SIMULATION OF THE ADSORPTION OF ORGANICS FROM WATER.
59. Ban, S., COMPUTER SIMULATION OF ZEOLITES: ADSORPTION, DIFFUSION AND DEALUMINATION.
60. Smith, W.; Forester T.R.; Todorov, I.T.; Leslie, M., THE DL_POLY_2 USER MANUAL
61. <http://cccbdb.nist.gov/>
62. http://www.stfc.ac.uk/CSE/randd/ccg/software/DL_FIELD/36156.aspx

Appendices

Appendix 1: Examples of input files for DL_POLY

CONTROL:

```
#####
temperature          300 kelvin
steps                20000000
equilibration        10000
timestep             0.0005 ps
multiple timestep    1
scale every          1
integrator           velocity
cutoff               9.00 angstroms

delr                 .50 angstroms

print every          100
#mxlist              2.5
rdf                  100
print rdf

job time             10000000 seconds
close time            100 seconds
ewald precision       1d-8
cap forces in equilibration mode 1000 kT/A

ensemble      nvt hoover 0.5

trajectory nstraj=0 istraj=500 keytrj=0
stats          200
stack          100
#restart
finish
#####
```

CONFIG:

In this section we will give a few examples of CONFIG files used in our simulations. The first system will show an entire CONFIG file while the rest will just give the coordinates of the molecules diffusing through silicalite.

TIP3P water/silicalite

```
#####
DL_POLY CONFIG
      2      2      624 -83063693.7962
 20.051100000000 0.000000000000 0.000000000000
 0.000000000000 19.875700000000 0.000000000000
 0.000000000000 0.000000000000 26.736400000000
OZ      1
 9.743549373 0.9393098220 9.156173496
 -0.378291704719E-03 -0.207451265352E-03 0.394950087977E-04
 -0.380671701600 -0.258503127092 0.501577390085E-01
OZ      2
 7.132136028 1.495945109 9.522974483
 -0.652699334997E-04 -0.479727169754E-04 0.221692809528E-04
 -0.460210307970 -0.355463129825 0.168328140187
OZ      3
 8.371845768 2.474531366 7.423832098
 -0.391114858113E-03 -0.821187933815E-03 0.185024215556E-03
 -0.290063821558 -0.524117140165 0.583637381569E-01
OZ      4
 7.895734208 -0.9540312443E-01 7.648425975
 -0.220588666310E-03 -0.570756174575E-03 -0.316767075501E-03
 -0.412933618549 -1.07171090252 -0.560650812518
OZ      5
 5.622795269 1.278767053 11.69848522
 0.730891606921E-04 -0.456624691437E-03 0.138484913532E-03
 0.504179185982E-01 -0.388623142995 0.129947583264
OZ      6
 6.299807068 -0.8767294027 10.40274237
 -0.31481786274747E-04 -0.421258256548E-03 0.312772985620E-04
 -0.152740156429 -1.76810790456 0.905107199433E-01
OZ      7
 4.644488394 0.7385009465 9.259036899
 0.340238456614E-04 -0.109912634550E-03 0.124212695558E-03
 0.306004378838E-01 -0.215303699631 0.223948642100
OZ      8
 5.934122053 2.986196802 0.5909632351
 -0.133891327339E-03 0.171675153421E-03 0.380360966152E-04
 -0.353231750778E-01 0.252984596373E-01 -0.678660093399E-03
OZ      9
 4.062229535 1.159020216 0.4142638559E-01
 -0.824003180634E-03 -0.658959277305E-03 0.784469571389E-03
 -0.445500441407 -0.456760314632 0.604880621469
OZ      10
 6.431119146 0.4447878218 0.7166032427
 0.510877935745E-03 0.532010261771E-03 -0.433048864630E-04
 0.394162782759E-01 -0.406564517471E-02 0.804899600553E-02
OZ      11
 1.977582529 2.701475510 0.2505217510
 0.418743276374E-05 -0.163515946053E-05 -0.322870296837E-05
 0.737752713194E-01 0.750049752241E-02 -0.428507108300E-01
OZ      12
 2.249169163 1.052762542 11.66137966
 0.844955185148E-04 -0.156908914083E-04 -0.264085443874E-04
 0.233717510695 -0.168292947565E-01 -0.549969935564E-01
OZ      13
 2.077238511 0.9743094470 9.020338523
 0.619052361443E-04 0.186055543825E-03 -0.192968913822E-03
 0.154901095500 0.417972193582 -0.455917816704
OZ      14
```

	1.233770548	-1.016244114	10.46627012
	0.267313573338E-03	-0.110661254301E-04	-0.205589728842E-03
	0.113354568179	-0.269956962438E-01	-0.894191970692E-01
OZ	15		
	3.778067843	2.234884216	7.327962096
	0.218220822537E-02	-0.425826594614E-03	0.792558911929E-03
	-0.264901229821E-02	-0.123385421975E-01	0.325941063056E-02
OZ	16		
	9.695622961	-3.285255490	9.066070403
	0.600113501459E-03	-0.439584397500E-04	-0.770715958520E-03
	-0.794058678512E-01	-0.246220903518E-01	-0.109749087639
OZ	17		
	7.042534662	-3.106353023	9.247514332
	-0.133743661842E-03	-0.418774467923E-03	-0.304431915695E-03
	-0.859931563382E-01	-0.318475686333	-0.228758458231
OZ	18		
	8.161637187	-5.147080137	8.053255984
	-0.887320448889E-07	-0.100413821823E-04	0.243343614639E-05
	0.860996129632E-03	-0.189436542519	0.389118084222E-01
OZ	19		
	5.975348208	-3.200495982	11.65890193
	-0.153084218648E-04	-0.322424921500E-04	-0.947753429259E-04
	-0.961121362780E-01	-0.219840025946	-0.486676159926
OZ	20		
	4.478866608	-2.583999169	9.618698207
	-0.437061207419E-04	-0.217721753358E-04	-0.200121371196E-04
	-0.563662966764	-0.279064779432	-0.253777537728
OZ	21		
	5.623243053	-4.828749938	0.5660030572
	-0.269909761732E-02	0.119315406885E-02	0.986221833546E-03
	-0.175869377661	-0.439726696618E-02	0.972604046437E-01
OZ	22		
	3.787953567	-2.993159759	0.1661100833
	-0.137414043437E-02	0.236817041080E-02	0.172887298399E-02
	-0.277724102493	0.864824251559	0.594496045112
OZ	23		
	2.067507367	-4.940983983	0.2597218845
	-0.138051577810E-02	0.115410798927E-02	0.199881418665E-02
	-0.420740547643	0.248309953601	0.714698044554
OZ	24		
	1.326662665	-3.246566818	11.84965031
	0.310068548548E-03	0.187860050489E-03	0.257499567799E-03
	0.687227797212	0.430691874595	0.496931960461
OZ	25		
	1.956421820	-3.227522400	9.320124029
	-0.749131986427E-03	-0.662425041427E-03	-0.652597010383E-03
	-0.107923174444	-0.931619678995E-01	-0.848670480984E-01
OZ	26		
	3.880098756	-5.022595555	9.006863991
	-0.777970628887E-03	-0.411235902928E-03	-0.909897610256E-03
	-0.199066616538	-0.100432713371	-0.230318555503
OZ	27		
	0.4263711671E-02	-9.126956000	2.573852142
	0.403118800625E-03	-0.362329003005E-04	0.134832316031E-04
	1.02976105738	-0.116084748975	0.637706784860E-01
OZ	28		
	2.385127939	-8.426516015	3.646345521
	0.118528892879E-03	0.371158538322E-04	0.271510835884E-04
	0.386364501408	0.112354562792	0.696567630794E-01
OZ	29		
	1.560832089	-7.420136829	1.278111811
	-0.675593568658E-03	0.612390594292E-03	0.236238808956E-03
	-0.150160893365	0.142035025792	0.713066708522E-01
OZ	30		
	2.213529528	-9.903095431	1.532253421
	0.198007234576E-03	0.318688037006E-04	-0.159938758913E-03
	0.148929355395	0.370760267024E-01	-0.982586988184E-01
OZ	31		
	3.710835084	-8.794234332	6.022806788
	0.296021666849E-05	0.178562902591E-06	0.645534031201E-05
	0.781332158772E-01	-0.386998945578E-02	0.140563705433

OZ	32		
	3.387742091	9.082967698	4.371852346
-0.605690530992E-03	-0.660274313163E-03	0.406488885968E-03	
-0.642197746870	-0.543167253830	0.415148042098	
OZ	33		
	4.931785937	-8.797105697	3.705313778
0.297256264678E-03	-0.254233994052E-02	-0.106329755897E-03	
0.378007166000E-01	-0.394593478094	-0.522617817478E-02	
OZ	34		
	4.509816618	-7.627955440	8.375923278
0.429859492322E-03	-0.157610598952E-03	-0.322851609772E-03	
0.147636471524	-0.443116476745E-01	-0.737639828694E-01	
OZ	35		
	6.067124131	-9.252038287	7.051628835
0.435412355654E-04	-0.233262661801E-04	-0.579365272456E-05	
0.324105968481	-0.174524727765	-0.468496269459E-01	
OZ	36		
	3.979761229	9.685333726	8.257902492
0.528354361110E-05	-0.117246049908E-03	0.671108476294E-04	
0.212905590997E-01	-0.411915528035	0.243279028065	
OZ	37		
	8.090676605	-7.765660531	7.862446240
-0.441247042225E-04	-0.367909395250E-03	0.788771681217E-04	
-0.103025279750E-01	-0.515810731686E-01	0.102516377501E-01	
OZ	38		
	8.320533597	-9.251866517	5.680033295
0.386248467815E-04	0.695920365247E-04	-0.368953357609E-04	
0.796649829172E-01	0.141814250355	-0.776319462930E-01	
OZ	39		
	7.438009977	-9.137211997	3.198970744
0.296396843453E-03	0.155923003406E-02	-0.454731814494E-03	
0.608454832545E-01	0.375727030639	-0.104561567368	
OZ	40		
	8.984918260	8.767905197	3.996846720
-0.381803130972E-02	-0.153191542832E-03	-0.816076979459E-03	
-0.206247678107	0.434993766976E-02	-0.644546603799E-01	
OZ	41		
	6.089541498	-7.226725228	1.851174158
-0.133480088842E-02	0.415330601414E-03	0.205741974055E-03	
-0.359180483681	0.103514965860	0.129469900363	
OZ	42		
	-0.2725125975	6.217162264	2.450937135
-0.775122712001E-03	-0.461003205439E-03	0.886523346985E-03	
-0.148963411149	-0.110575369181	0.215273265596	
OZ	43		
	2.130775450	6.866101510	3.663239158
-0.304326043280E-03	-0.195647027221E-03	0.117544661371E-02	
-0.435688669304	-0.277168289296	1.33049084460	
OZ	44		
	1.943741188	4.900541371	1.843352090
-0.405801162316E-03	0.866924758111E-04	0.119624072933E-02	
-0.163179827968	-0.304949178026E-01	0.526464833549	
OZ	45		
	3.319526932	7.084981502	6.103490372
0.638793035449E-05	-0.320197031070E-05	0.178160353083E-04	
0.110649466060	-0.651474375927E-01	0.295260556348	
OZ	46		
	4.725376884	6.843461127	3.977529602
-0.450824162831E-03	0.559920776261E-04	0.426422690617E-03	
-1.09845541824	0.109322359712	1.06286530951	
OZ	47		
	4.356606766	4.894675387	7.066062307
-0.776023310931E-05	0.990241579193E-05	0.333983719972E-05	
-0.616687960901E-01	0.948192878459E-01	0.534328910453E-01	
OZ	48		
	5.860593212	7.006624722	7.000410106
0.138260428182E-04	0.694494578126E-06	0.181287734723E-06	
0.223181794504	0.832986195564E-02	0.885051500700E-02	
OZ	49		
	7.606490239	5.048681047	6.872944046
0.702973597651E-05	-0.898909109385E-04	-0.855368789309E-05	

	0.243406639584E-01	-0.349124022829	-0.140688186730E-02
OZ	50		
	8.327815069	7.370335282	6.082522252
	0.162438535011E-02	-0.750119461226E-03	0.132447231486E-03
	0.205707533087E-02	-0.577604055325E-01	0.124303703466
OZ	51		
	7.353930586	6.689736992	3.819625530
	-0.693284475931E-04	-0.397099333872E-03	0.494102835111E-03
	-0.112880518751	-0.604551332480	0.692285587985
OZ	52		
	5.900745132	5.010116985	2.425809195
	-0.170835383921E-02	0.394899598412E-03	-0.998198773059E-04
	-0.209658486128	0.475256963982E-01	-0.171173654826E-01
OZ	53		
	-9.776936335	8.346927327	9.058567462
	0.818306440942E-03	0.376528100569E-04	0.207485830241E-03
	0.223103116329	-0.765123920451E-02	0.768711803944E-01
OZ	54		
	8.106122078	8.879855945	10.58525076
	0.374846383542E-03	0.296265527497E-03	0.627044652373E-04
	0.257562304692	0.184110463998	0.210996308415E-01
OZ	55		
	7.951311274	7.053532568	8.635249616
	0.172489496101E-03	0.243040933150E-03	0.221310580687E-03
	0.499732505112	0.692804930590	0.614836784662
OZ	56		
	8.194655622	9.546982255	8.126823597
	0.283352741927E-03	-0.143077788789E-03	-0.654655051399E-04
	0.245424291774	-0.125672657381	-0.376656263625E-01
OZ	57		
	6.250641458	9.150314310	12.52882307
	0.124700770774E-02	0.873042756824E-04	0.483343543565E-03
	0.311136364035	0.271303308091E-01	0.120251859240
OZ	58		
	6.586133727	-8.828960482	10.75084002
	0.470757931700E-05	0.967067922111E-04	0.126954188100E-04
	0.196391942627E-01	0.434225915375	0.512524167680E-01
OZ	59		
	5.596588901	8.747089080	10.01888824
	0.209906362594E-03	0.167045635700E-03	0.242902119917E-03
	0.151309885237	0.125477144746	0.192933852264
OZ	60		
	5.884348135	7.605006861	1.824448900
	0.13941323441E-02	0.225144463150E-02	0.323865676083E-02
	0.879851308564E-01	0.157466333796	0.221936781607
OZ	61		
	3.901640349	8.451296900	0.3352155776
	0.605756688065E-03	-0.168264199675E-03	0.359514475256E-03
	1.02832106142	-0.294620612438	0.632702472980
OZ	62		
	5.595447139	-9.729371638	1.399532586
	0.931535022789E-04	0.433682015602E-03	-0.422507267576E-03
	0.364094311740E-01	0.123361148133	-0.971529247254E-01
OZ	63		
	1.616934177	7.453872357	1.255534592
	-0.196748650478E-03	-0.429258721157E-03	0.126362754596E-02
	-0.183072349424	-0.405509476233	1.41732821547
OZ	64		
	1.680857589	9.116563899	12.71282652
	-0.724509676227E-04	-0.358857886222E-04	0.443520839310E-03
	-0.473321577638E-01	-0.462689349188E-01	0.354853628902
OZ	65		
	3.027210718	8.739855153	10.51967147
	-0.228850560352E-04	0.108901321463E-02	0.676822995500E-03
	0.102136218662	0.335667336940E-01	-0.296323353796E-01
OZ	66		
	1.323399467	-9.183855798	10.62271097
	-0.304825906373E-03	0.284505188509E-03	0.798372897012E-03
	-0.157618609148	0.857297094917E-01	0.356123048457
OZ	67		
	3.921690060	7.100875542	8.663841969

-0.734866007992E-06	-0.622416312057E-05	0.818207403873E-05
-0.330248647151E-02	0.789164303569E-03	0.141386210758
OZ 68		
-9.825010848	-6.623056267	8.830201061
-0.136118088871E-04	-0.176127277199E-03	-0.171497609261E-03
-0.291746679795E-01	-0.196457913480	-0.184414300636
OZ 69		
7.955533288	-6.670298941	10.22738710
-0.375434632483E-04	0.948075901594E-04	-0.957493892032E-04
-0.181791634604E-01	0.354518393469E-01	-0.440219247212E-01
OZ 70		
6.597732470	-7.067634323	12.66567461
-0.477546364351E-05	0.577192531826E-05	0.796351383141E-05
-0.814442030201E-01	0.959455939919E-01	0.101574017746
OZ 71		
5.404895582	-6.485223213	10.48791773
-0.260914359880E-04	0.254161328592E-04	-0.322554878116E-04
-0.183404520481	0.188349871656	-0.203973984742
OZ 72		
3.944293151	-6.794971277	0.4090165354
-0.491676328359E-04	-0.184261870253E-05	-0.181295159701E-04
-0.820885862869	-0.334114743355E-01	-0.292978042256
OZ 73		
1.586371810	-7.535046805	12.58019700
0.141538925833E-04	0.469082427403E-04	-0.282568358016E-05
0.944422939101E-01	0.288015104576	0.296349803684E-01
OZ 74		
2.887842731	-7.056713975	10.40931914
0.448004123230E-04	-0.609345565725E-04	-0.210059674195E-04
0.370127049537E-01	-0.295631096787E-01	-0.170110966155E-01
OZ 75		
-0.5963735492E-01	-0.6275782672	2.402217165
-0.727760545674E-03	0.445048754487E-03	0.299768410903E-03
-1.00673338261	0.668282225976	0.458909277333
OZ 76		
2.580526919	-0.9227764590	2.822553114
-0.112728278385E-03	0.718998152025E-03	-0.212196444121E-03
-0.145682200328	0.699377740090	-0.166128456127
OZ 77		
1.381119524	-2.375635620	0.9685905895
-0.905637189128E-04	0.223143821821E-03	0.193103560129E-03
-0.509559706973	1.17421064244	1.03265878027
OZ 78		
1.693335240	0.1663326497	0.6365436800
-0.682382443806E-05	0.120036495088E-04	-0.403493189975E-05
-0.175516322528	0.261845173940	-0.750653668729E-01
OZ 79		
4.064583604	-1.640777877	4.958858536
-0.308297136682E-04	0.426379569180E-05	-0.577511050770E-04
-0.227938253065	0.281795315938E-01	-0.374286866051
OZ 80		
3.941750978	0.8237454935	4.243017239
-0.329857845911E-04	0.113780341823E-03	0.667758343006E-04
-0.198924178177	0.721554851342	0.429872675940
OZ 81		
5.193486666	-0.8028936416	2.665304589
-0.153684993006E-03	0.769951883037E-03	0.136045162023E-02
0.174197542772	0.874191537423E-02	-0.109436357881
OZ 82		
3.669804488	-3.037426440	7.232356006
-0.232752825169E-03	-0.185212474715E-03	-0.297802552883E-03
-0.235145459297	-0.180702219623	-0.236293025337
OZ 83		
5.804469234	-1.502737327	6.885806022
-0.662970281685E-03	-0.459898055163E-03	-0.846242558316E-03
-0.165310376649	-0.150833999912	-0.275089503877
OZ 84		
3.489218547	-0.4227689905	7.260730556
-0.118631932642E-03	0.240126463587E-05	-0.506915951687E-04
-0.239044071088	-0.439742786693E-02	-0.867433226231E-01
OZ 85		

	8.185518695	-2.612292002	7.031465577
-0.463557697783E-03	-0.413457045631E-03	-0.646085931105E-03	
-0.217934247470	-0.213216688371	-0.268011453685	
OZ	86		
7.659441873	-0.7782893911	5.154009559	
0.214724339684E-05	0.319229631197E-05	-0.621853702164E-05	
0.338727769886E-01	0.415840319238E-01	-0.760103688553E-01	
OZ	87		
7.785959790	-0.9208171228	2.540388931	
0.748431418288E-04	-0.115460496666E-03	-0.168607801410E-04	
0.256591281868E-01	-0.528258826371E-01	-0.119882458785E-01	
OZ	88		
8.706243616	1.188966406	3.761361960	
-0.122477501293E-04	0.302530554147E-04	0.503793438655E-06	
-0.143390005014	0.363472645869	0.173597468338E-01	
OZ	89		
6.217820637	-2.188996619	0.7292380065	
-0.142922425290E-02	0.376991218271E-03	0.602620333540E-03	
-0.316053276416	0.105747220534	0.141050741891	
OZ	90		
0.2067598788	2.948339494	2.114201050	
-0.324731903165E-03	-0.485147017007E-04	0.610917678326E-04	
-0.811776997623	-0.129090468522	0.136885509153	
OZ	91		
2.845888323	2.571756667	2.647578485	
-0.114346280088E-03	-0.928973850200E-04	0.564864457259E-03	
-0.157263084149	-0.674672540426E-01	0.654424913686	
OZ	92		
3.942207461	3.373932556	4.966012526	
-0.741303750098E-03	0.934310899102E-03	0.936117855390E-03	
-0.409898464161	0.474937060011	0.461136874230	
OZ	93		
5.451014559	2.543851167	3.029029455	
-0.293431472462E-03	0.442719889992E-04	0.188236540510E-03	
-0.835396925122	0.156223736547	0.559212908571	
OZ	94		
6.071093996	3.017245715	6.336276632	
0.256102610495E-04	0.496970521237E-04	-0.482409989836E-04	
0.146610280781	0.213625871835	-0.221945951278	
OZ	95		
8.281520173	3.433147416	4.967542194	
0.447674851640E-03	0.656917196776E-03	0.224157696234E-03	
0.213443108049	0.286762185437	0.106285834405	
OZ	96		
7.887943890	3.294657263	2.418165828	
-0.567883314330E-04	0.170151204717E-04	-0.187935171241E-04	
-0.540157298070	0.167727405193	-0.154206140755	
OZ	97		
-10.02331635	-1.030326069	4.112988732	
0.533463250309E-03	0.167376601242E-02	-0.185098293208E-03	
-0.272631840256E-01	0.107011138738	-0.132648174572E-01	
OZ	98		
-7.482840705	-1.003831371	3.249087255	
-0.624023903742E-04	0.577406070058E-03	-0.143658565461E-02	
-0.130752505267	0.212288630299	-0.476496685877	
OZ	99		
-8.156616633	-2.598288020	5.271908687	
-0.348718629961E-03	0.452295236568E-03	-0.749394622021E-03	
-0.697865414480	0.890322982621	-1.54758176101	
OZ	100		
-8.089394526	-0.1692316594E-01	5.548480110	
0.543049449873E-03	-0.793177482030E-04	-0.919462840981E-03	
0.672289559996E-01	0.253158656369E-01	-0.427904672101E-01	
OZ	101		
-5.776611248	-1.700292416	1.287837710	
0.191422490110E-03	0.550720549062E-03	-0.563128612497E-03	
0.121050076753	0.328313786679	-0.277810853665	
OZ	102		
-5.813771251	0.7459580466	2.115176525	
-0.104514464804E-03	0.689680486873E-03	-0.206223200512E-02	
-0.306814960832E-01	0.119350169869	-0.604149519787	

OZ	103		
	-4.946625641	-1.046812545	3.744221490
	-0.470431764438E-03	0.984661458387E-03	-0.499938548940E-03
	-0.194791589308E-03	0.160218261382	0.327873117922E-01
OZ	104		
	-6.034119113	-2.836870550	12.23397951
	-0.739001677213E-05	-0.131616167039E-04	-0.158813565292E-04
	-0.200177967617	-0.370013742013	-0.458796900530
OZ	105		
	-4.038468906	-1.161483953	12.73767607
	-0.400425296337E-04	-0.205104841097E-05	-0.230356503969E-04
	-0.519876156892	-0.317651294308E-01	-0.303917837460
OZ	106		
	-6.464441259	-0.2911396202	12.40721063
	-0.555783270477E-03	0.281072973227E-03	-0.163701741876E-03
	-0.217887462139	0.703012592348E-01	-0.114030059580
OZ	107		
	-1.819445169	-2.527781258	12.52636626
	-0.308172192982E-05	-0.353674091169E-04	-0.137037608538E-04
	-0.449053643788E-01	-0.487557267079	-0.173898097466
OZ	108		
	-2.297569478	-1.055487908	1.180632707
	0.147134862756E-03	0.230944236432E-03	0.158325696265E-02
	0.605048167836E-01	0.102028582025	1.16399321672
OZ	109		
	-2.392246028	-0.6502200830	3.785117295
	-0.625740215039E-03	0.565115552089E-03	0.103745311146E-02
	-0.598373735481	0.722471231698	1.08112350532
OZ	110		
	-1.793521503	1.319093869	2.192341788
	-0.218265696061E-02	0.117821798812E-02	-0.574046067423E-03
	-0.438672754814	0.990822454187E-01	-0.973190015411E-01
OZ	111		
	-3.525962327	-2.525108433	5.376171474
	-0.821638625420E-03	-0.230654001544E-03	-0.192594589632E-02
	-0.187185423103	-0.424549103263E-01	-0.409779149322
OZ	112		
	-9.621167113	3.119598254	3.505570112
	-0.787589767361E-03	0.667453791871E-04	-0.120213918383E-02
	-0.447464541325	0.849702816995E-01	-0.856240669145
OZ	113		
	-6.996590849	2.559202018	3.543334461
	-0.623483914753E-03	0.465369453361E-04	-0.101303028516E-02
	-0.229592162511	0.262929125483E-02	-0.318808295966
OZ	114		
	-7.917544083	4.877964469	4.353894314
	-0.173064950562E-03	-0.300250022022E-03	-0.112900241572E-03
	-0.336546125762	-0.576658603308	-0.219892517662
OZ	115		
	-5.912894668	3.247911465	1.246908679
	-0.149218048014E-05	0.383685117795E-04	-0.116808353461E-03
	-0.107885352190E-02	0.352751588796	-1.04712128935
OZ	116		
	-4.380083977	2.597130011	3.290243665
	-0.144868638443E-03	0.204371123241E-02	-0.164797074925E-02
	-0.263229772027E-01	0.163562330534	-0.110611545802
OZ	117		
	-5.689746328	4.926126707	12.49000489
	-0.679548741399E-03	0.278465294195E-03	0.106962176878E-02
	-0.138824659508	0.588610567802E-01	0.235320178670
OZ	118		
	-3.979052336	3.073117701	13.18301731
	-0.827968624241E-03	-0.125038943720E-03	-0.232360810515E-03
	-1.65157934295	-0.324299342123	-0.542171525483
OZ	119		
	-2.511802348	5.195900617	12.93696262
	0.357607691913E-05	0.564165578068E-05	-0.706683441782E-04
	0.134335087164E-01	-0.653444296452E-01	-0.508927674544
OZ	120		
	-2.138158139	3.668298342	1.176193027
	-0.116704918482E-04	0.233423229898E-04	-0.213171443990E-04

-0.202025574861	0.426932225047	-0.355759169233
OZ 121		
-1.948157664	3.378532099	3.785807136
-0.416900667688E-04	-0.857571476458E-04	-0.555575571253E-04
-0.988636112888E-01	-0.169701686982	-0.116463183989
OZ 122		
-4.050826019	4.897241385	4.376938468
0.361246938160E-03	0.167594847594E-03	0.610612423628E-03
0.198903436158	0.117190868421	0.367432118252
OZ 123		
0.4486412416	8.197275450	10.51147931
0.132011834709E-03	0.310607908123E-05	-0.355758532493E-04
0.158721788064	-0.113571023039E-01	-0.642261855764E-01
OZ 124		
-1.897636663	8.718143373	9.144881885
0.293137569062E-03	0.190236580560E-03	-0.742526076780E-03
0.142558696233	0.595359264394E-01	-0.376102573971
OZ 125		
-1.941441363	7.216809823	11.30769932
-0.116526267884E-05	-0.480466871936E-05	-0.114374154664E-04
0.693152174681E-01	-0.187006465367E-01	-0.344744782749
OZ 126		
-1.378454672	9.685466066	11.46202098
-0.137945807104E-03	-0.270525369077E-03	-0.288008523240E-03
-0.262249991243	-0.533649223267	-0.596749141592
OZ 127		
-3.539950781	9.035097252	7.007881666
-0.153968153586E-04	-0.112156493743E-03	-0.354044577271E-03
-0.154335558632E-01	-0.155201398414	-0.495575933996
OZ 128		
-3.460494616	-9.065747596	8.959120838
0.159113215421E-04	-0.156737697895E-03	-0.770859324936E-04
0.801195150425E-01	-0.598608054840	-0.324768394607
OZ 129		
-4.511602178	8.453771138	9.346005899
0.183976913754E-03	0.235147430331E-04	-0.108792689167E-03
0.832372917808	0.918000384336E-01	-0.506108899252
OZ 130		
-4.155825606	7.549343004	4.806382787
-0.590698674885E-03	0.718139748807E-03	-0.141156050223E-02
-0.108875323138	0.116529779028	-0.241570443017
OZ 131		
-5.939424769	9.068386583	5.974683674
0.474810297443E-04	0.748414028429E-04	-0.204618811438E-04
0.789063479315E-01	0.760429338006E-01	-0.153861342988E-01
OZ 132		
-3.953015733	-9.737710453	4.659805375
0.735958261787E-03	-0.163632008113E-03	-0.401100092827E-03
0.663280405315E-01	0.438875423424E-02	-0.211483555795E-01
OZ 133		
-7.804658283	7.478206973	5.024603634
-0.450924542491E-05	-0.237929563436E-04	-0.120159324059E-04
-0.536208948561E-01	-0.366659097439	-0.168698308453
OZ 134		
-8.432943903	9.176022243	6.928406630
0.653609209704E-04	-0.648663843925E-04	-0.206584076928E-03
0.142879006351	-0.138798655541	-0.412766468884
OZ 135		
-7.134922372	8.859483333	9.142319556
0.384184150240E-04	-0.142041462793E-04	0.188091883712E-04
0.382835442015	-0.139724189181	0.168387318417
OZ 136		
-8.882138048	-9.074925208	8.925020188
0.796133023178E-03	-0.285249307058E-05	-0.716399713292E-03
0.179637854006	0.385662920598E-02	-0.170685675163
OZ 137		
-6.207986135	7.157075870	10.98843083
0.373384816202E-05	-0.380334121496E-06	-0.102428638843E-04
0.623506649249E-01	-0.155386337246E-02	-0.164202131498
OZ 138		
0.2293888827	-6.748462617	10.49266561

	0.110478480845E-03	0.503098229987E-04	-0.181700457027E-03
	0.231434705464	0.118151502723	-0.365671172000
OZ	139		
	-2.235752218	-6.768839994	9.457615684
	-0.283942051950E-04	-0.284749451525E-04	-0.692266379172E-04
	-0.162522647087	-0.179271794256	-0.446325944667
OZ	140		
	-1.561866723	-5.024475750	11.37003975
	-0.434552308854E-03	-0.504685506468E-03	-0.928471513846E-03
	-0.488334725044	-0.412812814317	-0.953960874248
OZ	141		
	-3.326382033	-7.318120786	7.020643147
	-0.241729687507E-03	0.192439334016E-03	-0.717376450888E-03
	-0.385078191483	0.294608603208	-1.30316533667
OZ	142		
	-4.793886955	-6.791583906	9.090085839
	0.873452995100E-03	-0.582399483861E-04	-0.109926137847E-02
	0.650740360757	-0.121039125261E-01	-0.921982159907
OZ	143		
	-4.121213714	-5.068454577	5.999937570
	-0.217422607319E-05	0.102849576551E-03	-0.748370514240E-04
	-0.148285534406E-01	0.307141101614	-0.206644705821
OZ	144		
	-5.695726923	-7.106758097	5.898055513
	-0.192516593936E-03	0.100072460317E-03	-0.233742205961E-03
	-0.345687531153	0.196490381544	-0.486950168941
OZ	145		
	-7.422403181	-5.127843722	6.020006314
	-0.793040087183E-03	-0.667335138004E-03	-0.290520658465E-02
	-0.107322795535	0.166533702839	-0.344337073257
OZ	146		
	-7.962150000	-7.401567401	7.168631377
	0.183737049751E-03	0.247372843264E-03	-0.985782694708E-03
	0.168131213562	0.303176365713	-1.16714964410
OZ	147		
	-7.303732564	-7.084962787	9.673227847
	-0.282272620507E-04	-0.292112987611E-04	-0.633686356621E-03
	0.235004831156E-01	-0.188169716148E-02	-0.736484887660
OZ	148		
	-5.983070551	-5.072419298	10.71003863
	0.386768672491E-03	0.336170848114E-03	-0.160206681506E-02
	0.151738404078	0.138926941640	-0.611345335510
OZ	149		
	10.01058650	-8.694737148	3.732152639
	0.112900109806E-03	-0.924852047420E-03	-0.397038919502E-03
	0.410089723931E-01	-0.323949403815	-0.123918932873
OZ	150		
	-7.772758365	-8.732292341	2.242136994
	0.173139128563E-03	-0.975633297435E-04	-0.114424886696E-03
	0.633789449465	-0.382710181564	-0.406764162463
OZ	151		
	-7.931931875	-7.280605323	4.522039207
	-0.220309232875E-03	-0.245184651159E-03	-0.459974782917E-03
	-0.367795742641	-0.452441592158	-0.761927206020
OZ	152		
	-7.872196407	-9.821521301	4.540134030
	-0.316281936015E-03	-0.135286750337E-02	-0.683755892470E-03
	-0.447273031459E-01	-0.391104500131E-01	-0.924005312754E-01
OZ	153		
	-5.935893537	-9.120309726	0.2644360370
	0.604241375798E-06	-0.717718924924E-05	0.258417706851E-05
	0.417507007514E-01	-0.184667068430	0.748737304093E-02
OZ	154		
	-6.359262975	8.923733578	2.095758704
	0.625457842556E-03	-0.780934609931E-03	0.550694150435E-03
	0.176647500979	-0.192777315238	0.117172410703
OZ	155		
	-5.239145910	-8.657979556	2.732533820
	-0.193689816184E-04	-0.502622813059E-04	-0.170786644352E-03
	-0.573766012785E-01	-0.239724604545	-0.607863790706
OZ	156		

	-5.384564088	-7.627322018	11.45073841
0.399757347439E-03	-0.550438404877E-03	-0.204851418109E-02	
0.769824551735E-01	-0.869206952084E-01	-0.275011188052	
OZ	157		
	-3.616299492	-9.325766439	12.49763875
-0.260339937357E-04	0.517742321605E-04	-0.129044389929E-04	
-0.189715372371	0.348227073222	-0.896216509464E-01	
OZ	158		
	-5.736228257	9.697167745	11.18897721
-0.967612620301E-05	-0.139499814466E-04	-0.153431762227E-04	
-0.607758828592E-01	-0.100219150845	-0.117848889849	
OZ	159		
	-1.770000041	-7.639964971	11.82092413
0.106415622762E-03	-0.217460159159E-03	-0.137474640191E-02	
0.350727820155E-01	-0.184007550753	-0.721653670905	
OZ	160		
	-1.321199751	-9.598394811	0.3566700459
0.107222366323E-02	-0.326380386460E-03	0.204093060448E-03	
0.593030992487	-0.196307562084	0.859044423041E-01	
OZ	161		
	-2.648580041	-8.987387200	2.533454888
0.170859694958E-02	0.805511000508E-03	-0.323678095118E-03	
-0.143675017189	0.642922332381E-01	0.104614239299	
OZ	162		
	-1.445381433	8.553732100	2.285901817
-0.979986542311E-07	0.604422597285E-05	-0.275545549671E-06	
-0.247242036176E-02	0.835646995265E-01	-0.497828333710E-02	
OZ	163		
	-3.651976281	-7.211407980	4.351419369
-0.440035009280E-03	0.744120488869E-03	-0.13299925342E-02	
-0.186343615689	0.273513459240	-0.371004384007	
OZ	164		
	10.00495015	6.388086782	4.266590957
0.235912181902E-03	0.541317238379E-03	-0.211056086577E-03	
0.627227573395E-01	0.108374588537	-0.558550483602E-01	
OZ	165		
	-8.021714385	6.868597336	2.573575583
-0.778753599231E-04	0.109339215414E-04	-0.800217140528E-04	
-0.213609983146	0.232691030506E-01	-0.249859210380	
OZ	166		
	-6.389019825	6.951810499	0.3983867600
-0.302482325358E-03	0.150161256283E-03	-0.342943831062E-03	
-0.164105870845E-01	0.254971679597E-01	-0.297772422650E-01	
OZ	167		
	-5.519518618	6.557950079	2.845010131
0.309831700103E-04	-0.504660834962E-04	0.138595170345E-04	
0.113392590221	-0.304357530895	0.314133260927E-01	
OZ	168		
	-4.254964897	7.096453400	12.61404759
0.207645906944E-04	-0.897813102279E-05	-0.129155426067E-04	
0.305998095966	-0.133106013738	-0.199015847000	
OZ	169		
	-1.759238615	6.839225072	0.3478142984
0.253959862526E-04	0.332507563694E-04	0.103133637684E-04	
0.129310131953	0.161370597923	0.466469802268E-01	
OZ	170		
	-2.943777229	6.490396616	2.678209935
-0.463538080961E-05	-0.947939459474E-05	-0.205939974875E-04	
-0.671892344471E-01	-0.771905342299E-01	-0.138709298637	
OZ	171		
	-0.1250197597	1.190823447	10.65780532
0.595241862071E-03	-0.168264160989E-03	0.220200599118E-04	
0.508524030294	-0.148071812085	0.489606812498E-01	
OZ	172		
	-2.786702939	1.288788727	10.44291542
-0.242680900103E-03	0.109088552665E-02	0.259109970673E-03	
-0.376409193805E-01	0.151132502078	0.402370045867E-01	
OZ	173		
	-1.575001386	2.696694689	12.35089477
-0.566645890275E-05	-0.221941614803E-06	0.302305014294E-04	
-0.430754568188E-01	-0.944726395610E-01	0.287738840831	

OZ	174		
	-1.710976515	0.7920640790E-01	12.40786733
	0.284289533642E-03	-0.205463284213E-02	-0.122504847757E-02
	0.174613566094	-0.821085452568	-0.670571578299
OZ	175		
	-4.119118200	1.345656214	8.106586428
	-0.928472003028E-03	0.270214166276E-02	0.724623571871E-03
	-0.180891305226	0.494570648456	0.131742334518
OZ	176		
	-3.682340453	-0.9297192033	9.318465882
	-0.171600486012E-02	0.154237028663E-02	0.562046313637E-03
	-0.305668558575	0.100409451659	0.624379719602E-01
OZ	177		
	-5.365621015	0.7514579451	10.33765524
	-0.169441243826E-03	0.214874461863E-02	0.881681031250E-03
	0.497052985738E-01	0.739800428047	0.284697907278
OZ	178		
	-3.691827238	2.605495565	5.742002131
	0.831072580580E-05	-0.876234676236E-03	-0.887917306245E-03
	-0.921819522796E-02	-0.308819099537	-0.334563787910
OZ	179		
	-6.012769208	1.450404188	6.294526179
	-0.974605017824E-03	0.131112793781E-02	0.386253944442E-03
	-0.236599552243	0.426968667191	0.120204554688
OZ	180		
	-3.904617625	0.1646883543E-01	5.857548323
	-0.323983341870E-04	0.437055673057E-04	0.612358695990E-04
	-0.331595930964	0.397149273980	0.628719570494
OZ	181		
	-8.329166282	2.559554743	5.717666758
	-0.554199167053E-04	0.715348007888E-04	-0.188888627145E-03
	-0.351803173942	0.405638317530	-1.00233732097
OZ	182		
	-8.035286695	1.006557203	7.921239325
	-0.592900866730E-05	-0.273863461576E-05	0.206672090315E-05
	-0.132354319423	-0.599622769846E-01	-0.141212796734E-01
OZ	183		
	-7.959411763	0.8753389883	10.54855080
	-0.170969329137E-04	-0.751866954821E-04	-0.151345117606E-03
	-0.550198195415E-01	-0.224772105767	-0.423976416274
OZ	184		
	-8.773648453	-1.190157267	9.150434310
	-0.933419182678E-05	0.215980534093E-04	-0.541202369851E-05
	-0.492048090541E-01	0.117622215799	-0.409546364467E-01
OZ	185		
	-6.306851204	2.325743409	12.17306961
	-0.447871885960E-02	0.769068437502E-03	0.190541351964E-02
	-0.140784737647	0.131698772093E-01	0.690074979734E-01
OZ	186		
	-0.6195384919	-2.885359627	10.24210759
	-0.851367309337E-04	0.535521846462E-06	0.892743409402E-03
	-0.932762296361E-02	0.292600344811E-01	0.421711948169
OZ	187		
	-3.211889539	-3.217005057	10.47644761
	-0.567198898705E-03	0.140608015272E-03	-0.603168825451E-03
	-0.985403193754	0.301275666174	-1.07211677622
OZ	188		
	-3.796450539	-3.219784349	7.909670590
	0.604286871325E-05	0.659856500752E-04	-0.311322955734E-03
	0.411398267806E-02	0.296751462942	-1.19616153040
OZ	189		
	-5.609210768	-2.668994758	9.720148455
	-0.626376674209E-03	0.454143277148E-04	-0.196090866156E-02
	-0.254331742493	0.106339616668E-01	-0.590027443890
OZ	190		
	-5.845953679	-3.131270592	6.379998865
	-0.384504793632E-03	-0.199249691120E-03	-0.330719059321E-03
	-0.787016098137	-0.389539682310	-0.712265729459
OZ	191		
	-8.093000016	-3.331648128	7.792587203
	0.317373906132E-03	-0.445667484088E-03	-0.141534638839E-02

	0.311098966871	-0.550641015451	-1.72550948388
OZ	192		
	-7.974481125	-3.365754002	10.40239715
	-0.325097982997E-03	-0.551670724224E-03	-0.219665173562E-02
	0.427877271050E-01	-0.307553975862	-0.773955656850
OZ	193		
	9.762804457	0.6244439463	-4.267854649
	-0.291279717765E-02	-0.243868258083E-02	0.474742483491E-02
	0.462159676613E-01	-0.780937007703E-01	0.155204602280
OZ	194		
	7.141416517	1.005350611	-4.043750352
	-0.184012506058E-03	0.737893603728E-04	0.113239519130E-03
	-1.34451956877	0.499099635564	0.820634106498
OZ	195		
	8.488889284	2.315980311	-5.941037530
	0.653985193373E-04	-0.230837070572E-03	0.297707515168E-05
	0.907382070582E-01	-0.353732615804	0.455513119596E-01
OZ	196		
	8.113085281	-0.2588604422	-6.072714277
	-0.550226041505E-03	-0.136866045616E-02	0.431273408193E-02
	-0.599446473489E-01	-0.243048873400	-0.216954492566E-01
OZ	197		
	5.941110167	1.519421928	-1.685706515
	-0.325134705197E-02	0.418612961242E-03	-0.284979590429E-03
	-0.379805319059	0.638475607393E-01	-0.568983133307E-01
OZ	198		
	6.013501242	-0.8935571230	-2.591270232
	-0.350334729473E-04	0.354681111226E-03	0.829877577102E-04
	-0.240396709269E-01	0.338044201422	0.114914442074
OZ	199		
	4.569193540	0.7615482808	-3.901810674
	-0.127624612159E-02	-0.167619314778E-02	0.486053077697E-04
	-0.139140120297	-0.196069918100	-0.675677402523E-02
OZ	200		
	6.004873368	2.756943248	-12.80994107
	0.165937941277E-03	0.150914044675E-02	-0.194632391808E-02
	0.911138984520E-02	0.112676401073	-0.964623867112E-01
OZ	201		
	3.942427755	1.091836609	-13.06480623
	0.324155571097E-03	0.632296930860E-04	0.128923635787E-03
	0.140693586149	0.530850939831E-01	0.640065729858E-01
OZ	202		
	6.339386402	0.1822018933	-12.74336978
	0.123897952092E-03	0.124036900401E-02	0.185421797738E-02
	0.375418178965E-01	0.284952517803	0.412023451943
OZ	203		
	1.708936859	2.396658684	-12.80824792
	0.435944228087E-04	0.199856878453E-03	-0.249622760610E-03
	0.699414277860E-01	0.390141841275	-0.455324704213
OZ	204		
	2.177778319	0.9108979605	-1.793248402
	0.136682274159E-03	0.225068078693E-03	0.201130357682E-03
	0.256039185524	0.394274966522	0.344349072333
OZ	205		
	2.051279583	1.087489274	-4.455352728
	-0.477166832228E-05	0.221925958013E-04	0.325102513686E-05
	-0.691034553111E-01	0.224545467639	0.454874386378E-01
OZ	206		
	1.427781296	-1.128913729	-3.237984343
	0.961975434174E-04	0.153241328699E-03	0.123314126987E-05
	0.445728126419	0.719486960956	-0.102283154938E-01
OZ	207		
	4.051505894	2.122530821	-6.059641644
	-0.248534671086E-04	-0.160612196258E-03	0.864554967991E-04
	-0.907948649292E-01	-0.660900717819	0.339159572377
OZ	208		
	9.676405905	-3.333606935	-4.198771483
	0.721701059402E-03	-0.752678965174E-03	-0.130517905807E-02
	0.258927022813	-0.350613291263	-0.503891657627
OZ	209		
	7.069409583	-2.928884243	-3.832888850

	0.126102979193E-03	-0.474352446117E-04	0.150957727734E-03
	0.231974925233	-0.930168892894E-01	0.402319604509
OZ	210		
	7.960467659	-5.188597204	-4.804859590
	0.373472744833E-05	-0.300234777185E-03	0.158205453432E-03
	-0.114389351470E-01	-0.972985377211	0.557906590923
OZ	211		
	5.658156341	-3.314899081	-1.587557140
	-0.193908035744E-03	0.364644357187E-04	0.367960945748E-03
	-0.688686978709	0.119291951085	1.29962146241
OZ	212		
	4.497757373	-2.659070009	-3.828488956
	0.194628023760E-04	0.346213687952E-05	0.108150118588E-04
	0.333877402756	0.581761616583E-01	0.194860586442
OZ	213		
	5.419649061	-4.956400215	-13.12412442
	0.129494143752E-03	0.285990386117E-03	0.116228211589E-02
	0.315129835781E-01	0.698560323381E-01	0.320730384274
OZ	214		
	3.717418929	-3.106598843	12.89692234
	0.704235734848E-03	0.153008328627E-02	0.143355190471E-02
	0.158776525408	0.513271590662	0.502882640729
OZ	215		
	2.263766052	-5.169982647	-13.33447073
	0.171533379864E-03	0.107056094360E-02	0.126632445038E-03
	0.101645449324	0.274494508940	0.563164132745E-01
OZ	216		
	1.815567990	-3.078311652	-1.536846453
	-0.204478683838E-02	0.299994408477E-02	0.178780588021E-02
	-0.219349849958	0.352282294538	0.234644848473
OZ	217		
	2.090322204	-3.522690166	-4.100202624
	-0.258828309189E-04	0.823990938165E-05	0.889663784774E-04
	-0.239639551909	0.750034329808E-01	0.815960531771
OZ	218		
	4.180945254	-5.117633114	-4.638141327
	0.459459239975E-05	-0.108103189240E-03	0.599132683368E-04
	0.331538494136E-01	-0.741756801574	0.421236240800
OZ	219		
	-0.8115105097E-01	-8.434971628	-10.65723383
	0.201470405767E-03	-0.155720386093E-02	-0.819117933362E-03
	0.212708303884	-1.11052753820	-0.566142721830
OZ	220		
	2.224440711	-8.644068569	-9.294427611
	0.385567428471E-05	0.196182648938E-05	0.974465074972E-05
	0.164997261968E-01	0.569762908288E-01	0.117937912792
OZ	221		
	2.081813275	-7.149585751	-11.57000197
	-0.788784968159E-03	0.108024079660E-02	0.304110804736E-03
	-0.203529755364	0.323368304726	0.690342653670E-01
OZ	222		
	1.934308988	-9.674284765	-11.62489269
	0.221131484133E-02	0.215606346459E-02	0.535682911841E-03
	0.231531402722	-0.145902968826	-0.182355015972
OZ	223		
	3.899746647	-9.504115828	-7.388013859
	-0.113009522923E-03	0.126033259832E-03	0.196450299647E-03
	-0.159153353480	0.172620623256	0.296524246600
OZ	224		
	3.266178368	8.732080855	-9.273457268
	-0.426343133790E-03	-0.290798466636E-03	0.960150426447E-03
	-0.472007966924E-01	0.103317797913	0.909192384077E-01
OZ	225		
	4.681036518	-9.070365945	-9.932190722
	0.239663049767E-03	0.255870826084E-03	0.579120826394E-03
	0.169790256521	0.186864820867	0.409844554677
OZ	226		
	4.717201422	-7.518842155	-5.744215193
	-0.581784727253E-04	-0.516631061182E-05	0.190448500764E-03
	-0.363647659200	-0.201764181020E-01	1.11708765698
OZ	227		

	6.405579503	-9.446640131	-6.528474265
-0.882562192514E-03	-0.340322580223E-03	-0.180728521731E-03	
-0.236187742452	-0.132663181601	-0.357125248902E-01	
OZ 228			
4.481237127	-9.935076896	-4.882190192	
0.562237683059E-03	-0.158747483937E-02	0.916081728440E-03	
0.140431756929	-0.168177333310	0.622527888918E-01	
OZ 229			
8.024165453	-7.803091080	-5.328124833	
-0.475580188106E-03	-0.428106555875E-03	0.167649312236E-04	
-0.455929661948	-0.331160618132	0.732770096001E-01	
OZ 230			
8.773021177	-9.089999680	-7.527351621	
-0.838310438919E-04	0.312517740137E-04	0.163364603774E-03	
-0.328930307172	0.111328567054	0.662777103843	
OZ 231			
7.224165464	-8.510113843	-9.623811743	
0.460630028996E-03	-0.281211072083E-03	0.169457812204E-03	
0.461972614266	-0.280148355938	0.142302614667	
OZ 232			
8.493024197	9.109660476	-9.465560451	
-0.154381119301E-05	-0.277804683030E-04	0.346598939038E-05	
-0.182774270104E-01	-0.387762148113	0.594505257802E-01	
OZ 233			
5.809043883	-7.105798422	-11.48277791	
0.615384516783E-03	-0.351817339907E-03	0.149384096725E-03	
0.118886816048	-0.332184812887E-01	-0.310288128458E-01	
OZ 234			
-0.1083299711	6.553533001	-11.29215741	
0.120745924526E-02	-0.118081045083E-02	-0.428614657397E-04	
1.28319685616	-1.24979072895	-0.647809796835E-01	
OZ 235			
2.004712786	6.447423207	-9.660409238	
0.616599468239E-03	0.619333706688E-03	0.791057203983E-03	
0.460294540196	0.476571373419	0.695385706134	
OZ 236			
1.888319113	4.942274854	-11.83648109	
0.4686686924545E-02	-0.332823899036E-03	0.131170177300E-02	
0.941209068010	-0.659397815471E-01	0.275863534769	
OZ 237			
3.799165098	6.807925109	-7.596904480	
-0.194149603334E-03	0.960416819436E-03	0.167265719578E-03	
0.427401731104E-01	-0.109950385267E-01	0.134614022787	
OZ 238			
4.571118561	6.592587919	-10.05753335	
-0.198492595660E-03	0.714281106740E-03	0.698883872390E-03	
-0.556913180153E-01	0.588194920525	0.522744462167	
OZ 239			
4.505479748	4.837444226	-5.995976991	
0.438470495688E-04	-0.211411967698E-03	-0.612620216583E-04	
0.202709398141	-1.00200613509	-0.301270914061	
OZ 240			
6.178017446	6.739097596	-6.468972229	
0.124487859880E-03	-0.288247512883E-04	-0.152642422467E-04	
0.413207767788	-0.115898442595	-0.332186617431E-01	
OZ 241			
8.079497983	4.952576946	-6.568255520	
0.171216660125E-04	-0.208022344130E-03	0.693712910730E-05	
0.684995303163E-01	-0.859704562881	0.548000407571E-01	
OZ 242			
8.462936361	7.356955605	-7.532797566	
0.120382353483E-04	-0.565994799893E-03	0.408826937528E-03	
0.280537272120E-01	-0.814773285186	0.561345049040	
OZ 243			
7.173391727	6.859950225	-9.761533739	
0.124243226241E-04	-0.395960996944E-05	0.118131789444E-04	
0.117461012738	-0.475515152916E-01	0.111610753779	
OZ 244			
6.235799624	5.047713654	-11.40043360	
-0.127023649155E-04	-0.301740889413E-04	0.346023240225E-04	
-0.563878538906E-01	-0.137717287027	0.143065897049	

OZ	245		
	-9.603926717	8.387265190	-4.007449296
	0.142717643253E-04	-0.155479809786E-04	0.295563719673E-05
	0.520134453441E-01	-0.101427602253	0.227367694484E-01
OZ	246		
	8.108453062	8.632742792	-2.734071991
	0.596470385165E-03	0.939218359297E-04	0.869248656850E-03
	0.144923433650	0.257228762601E-01	0.216540216779
OZ	247		
	8.290392316	7.040282483	-4.904392651
	-0.841062733241E-04	-0.759558769129E-04	0.235682257057E-03
	-0.675320249647E-01	-0.767816612699E-01	0.248446625235
OZ	248		
	8.454167684	9.544331391	-5.141174640
	-0.247905463429E-03	-0.220606090466E-03	0.851240661617E-04
	-0.421066282295	-0.359435914089	0.138104238633
OZ	249		
	6.369114036	8.682029238	-0.6090873375
	0.772898966314E-03	-0.204568217594E-02	0.818535411910E-03
	0.192943708589	-0.478785233870	0.172136549276
OZ	250		
	6.577405203	-9.161817995	-2.242617064
	-0.212037943285E-04	0.231840557466E-04	0.824057658439E-04
	-0.140179039823	0.383392763288E-01	0.517351891544
OZ	251		
	5.576208854	8.473472238	-3.098024937
	0.345595578607E-03	-0.670219470658E-04	0.267647322176E-03
	0.898514981669	-0.188575492271	0.725925729996
OZ	252		
	5.955538872	7.696352789	-11.94042294
	0.636381932932E-03	-0.462475007342E-03	0.588429083825E-03
	0.362867236243	-0.174474643201	0.255564278745
OZ	253		
	4.044384610	9.249373194	-12.81541826
	0.457746338923E-03	-0.157808802943E-03	-0.808347596531E-04
	0.950408004122	-0.348933336139	-0.198119490814
OZ	254		
	6.244807483	-9.580626057	-11.82975128
	0.102321401990E-03	-0.512591767787E-03	0.601807435580E-03
	0.254463303099E-01	-0.207175569387	0.231092570051
OZ	255		
	2.173049740	7.603903229	-11.94908709
	0.100956049260E-02	0.134398778006E-03	0.110246104073E-02
	0.107419721429	0.529800582174E-01	0.589068331647E-01
OZ	256		
	1.606747189	9.076451555	-0.8566752180
	0.843991115522E-04	-0.128289301690E-03	0.310132264220E-03
	0.571642088717	-0.908971077750	2.04611714028
OZ	257		
	2.965734551	8.827475566	-3.058812120
	0.591762347993E-03	-0.394026743944E-03	-0.847972751737E-04
	1.35700210184	-0.976126567371	-0.172984569352
OZ	258		
	1.319900425	-9.038994609	-2.767737019
	0.222383806351E-02	-0.130739798048E-02	0.286351224032E-02
	0.476280936159	-0.294268497894	0.548845994215
OZ	259		
	4.134070092	7.373102049	-5.023474313
	0.716929700375E-03	-0.121512388897E-02	0.628646890406E-03
	0.289719008037	-0.492113603495	0.348997682577
OZ	260		
	-9.921836862	-6.632251941	-4.422746777
	-0.734558503034E-03	-0.672085421482E-03	-0.480425796794E-03
	-0.347383709318	-0.406267664011	-0.249603795105
OZ	261		
	7.961128336	-6.998817769	-2.879050684
	-0.165204192747E-03	-0.123123896911E-02	0.146837045819E-02
	0.218284532893E-01	-0.125335321454	0.112169352244
OZ	262		
	6.245832621	-6.993255794	-0.7716842332
	-0.478506617040E-03	0.758228144103E-03	0.141356844401E-02

	-0.229796702490	0.356783346069	0.666652210050
OZ	263		
	5.457809456	-7.030867956	-3.288443376
	0.379819497986E-03	-0.316585561316E-03	0.706286818248E-03
	0.738997879860	-0.625991441753	1.48082940903
OZ	264		
	4.038141346	-7.121873051	-13.31350101
	-0.225293895604E-04	0.102021778428E-04	0.901831688602E-05
	-0.233406896659	0.129300255836	0.989517860035E-01
OZ	265		
	2.041237150	-7.010359435	-1.308111408
	-0.361012739196E-02	0.388843486489E-02	-0.584393255163E-04
	-0.602731238516	0.722802778713	-0.388899020436E-01
OZ	266		
	2.919672432	-7.201417893	-3.774415524
	-0.335490187616E-03	-0.181043235406E-03	0.910697860527E-03
	-0.853941068635E-02	-0.174831352679E-01	0.958214407419E-01
OZ	267		
	0.6536336903E-01	-1.037128262	-10.96792283
	-0.341168290122E-03	0.146723775317E-03	-0.648262293009E-05
	-1.91407763150	0.854423851199	-0.600455479384E-01
OZ	268		
	2.692397684	-0.8990798516	-10.61514724
	-0.164344634980E-03	-0.194864925137E-03	0.948813084276E-04
	-0.702312154765E-01	-0.872758921114E-01	0.887143136588E-01
OZ	269		
	1.678277567	-2.730884621	-12.29973529
	-0.210876928527E-04	0.459787453467E-04	0.413580463948E-04
	-0.264547229184	0.564919463181	0.485973181640
OZ	270		
	1.656518446	-0.2086754385	-12.86903725
	0.335355468486E-03	0.414348459764E-03	0.675980165337E-04
	0.647292864669E-01	0.114187502382	0.204152798287E-01
OZ	271		
	3.993403089	-1.459879973	-8.360225517
	-0.266970359763E-03	-0.113024884992E-02	0.734936599671E-03
	-0.415119975687	-1.61942572438	1.03398781526
OZ	272		
	3.995863446	0.9990213424	-9.243632568
	-0.430768065986E-04	-0.499311366265E-03	0.436515063560E-04
	-0.188206051060	-2.28994852742	0.248322175542
OZ	273		
	5.291102011	-0.7911069439	-10.59402284
	-0.340362536808E-03	-0.557560748317E-03	0.347710349116E-04
	-0.590249929228	-1.01375856492	0.560792155011E-01
OZ	274		
	3.678197119	-3.049742726	-6.232859767
	-0.186633009287E-02	-0.136884867682E-02	0.782130922642E-03
	-0.539467599276	-0.376039998298	0.163290165317
OZ	275		
	5.850337413	-1.534500315	-6.542721136
	-0.204094645907E-03	-0.192287717212E-04	-0.114780834508E-04
	-1.70091003865	-0.168982302122	-0.569760821420E-01
OZ	276		
	3.562679030	-0.4324693777	-5.968912226
	-0.173519396043E-02	-0.538389613803E-03	0.892888934571E-05
	-0.566535926102	-0.202494251149	-0.521601328546E-02
OZ	277		
	8.072823351	-2.856091043	-6.198263868
	0.122920172487E-05	-0.146737957267E-04	0.131117152568E-04
	0.329350314896E-01	-0.356479427823	0.339853005436
OZ	278		
	7.717210041	-1.317938499	-8.397467014
	-0.170177174281E-02	-0.426305761245E-03	0.237673934500E-02
	-0.821399891665	-0.139841127742	1.06225023505
OZ	279		
	7.796995288	-1.253808068	-11.03371148
	0.385164973408E-03	0.493438959999E-03	0.158706959274E-02
	0.235489429226	0.434300884355	1.43192766253
OZ	280		
	8.415932332	0.8674978214	-9.690798761

-0.483544140862E-03	-0.107201591665E-03	0.103341249780E-02
-0.271085390627	-0.780791746176E-01	0.614320464529
OZ 281		
5.888010003	-2.381882842	-12.58564615
0.111824866809E-02	0.367240735621E-03	-0.673203030863E-03
0.259904204089	0.815036421282E-01	-0.136980245332
OZ 282		
0.3685721226	3.171657636	-10.71398578
-0.450151194594E-03	0.244214038670E-03	-0.460347678780E-03
-0.710370146939	0.476866358958	-0.889421210541
OZ 283		
3.017113443	2.935000160	-10.64524383
-0.930341273991E-03	-0.162050375891E-02	0.804453362568E-03
-0.625352159057	-1.18525384074	0.563961162115
OZ 284		
4.109929243	3.506434784	-8.285939076
0.426874860680E-04	-0.949969015505E-04	-0.588704775318E-04
0.260121810413	-0.657083485170	-0.415759321393
OZ 285		
5.596549686	2.782204762	-10.29739454
-0.696328490501E-03	-0.560699385865E-03	-0.523622874236E-03
-0.183805726279	-0.171020164507	-0.174211692236
OZ 286		
6.259459580	3.171101272	-6.944967949
0.301531750017E-03	-0.466966382638E-03	0.178768308827E-04
0.225051892066	-0.407887124502	0.102250413929E-01
OZ 287		
8.412356948	3.164606908	-8.453663509
0.671660183220E-04	0.311121995706E-03	0.284963817359E-03
0.903022703797E-01	0.448927095276	0.407311148156
OZ 288		
8.025384816	3.093933977	-11.04772738
-0.615895154954E-04	-0.100319910106E-02	0.529616078669E-03
-0.186059908177	0.187975455783E-01	-0.875092419456E-01
OZ 289		
-9.993112014	-1.148561696	-9.512913988
-0.647426257989E-04	0.211829889397E-04	0.195485413547E-03
-0.341186496623	0.833165306545E-01	0.895430678204
OZ 290		
-7.340819891	-1.124934342	-9.919324101
-0.220421925981E-03	0.249728289934E-03	-0.803991059919E-03
-0.265618125974	0.307197333092	-0.832897100528
OZ 291		
-8.381525809	-2.702776027	-8.051702701
0.426578236752E-02	0.281009786486E-02	0.132832579239E-02
0.193811620608	0.199164248655	0.539488062256E-01
OZ 292		
-8.364673952	-0.1009650030	-7.776872720
0.106484386908E-02	0.227511641318E-02	0.170517372944E-03
0.321568768039	0.685823509045	-0.186227038423
OZ 293		
-5.797323759	-1.536301144	-12.10844246
0.904273384367E-04	-0.135161339178E-02	-0.170573120133E-02
0.533326812547E-02	-0.877088514129	-1.03570741567
OZ 294		
-6.112672906	0.8629104728	-11.15462917
0.242816857779E-02	-0.716192413660E-03	-0.271354830637E-02
0.366147199717	-0.111507726233	-0.350106875428
OZ 295		
-4.759617510	-0.8282003347	-9.748078230
-0.944404657097E-03	-0.179809210391E-02	-0.180981340889E-03
-0.284210937464	-0.491722769764	-0.349059439344E-02
OZ 296		
-6.165052215	-3.014414176	-1.034039454
0.710211121785E-03	0.708230296311E-03	-0.679023154140E-03
0.743364022521	0.715326145483	-0.725063401318
OZ 297		
-4.064937182	-1.475304542	-0.6789373615
0.559832128965E-03	0.262993661902E-03	-0.606667711021E-04
0.622241067656	0.310276146767	-0.257163404622E-01
OZ 298		

	-6.427245167	-0.4282692813	-0.9235493538
OZ	0.148183469581E-03	0.221573940977E-03	-0.279108719372E-03
	0.599247141563E-01	0.862932971140E-01	-0.143425454204
OZ	299		
	-1.830494175	-2.871228649	-0.8020399443
	-0.126575740155E-03	0.285948429539E-03	0.790446827183E-03
	-0.888985136289E-01	0.159860497964	0.622629146103
OZ	300		
	-2.289685458	-0.9834881725	-12.04882556
	-0.126878985757E-02	-0.903243689391E-04	-0.731466397312E-03
	-0.439026767148	0.338598921035E-01	-0.244518185489
OZ	301		
	-2.179205888	-0.7787914392	-9.440261620
	-0.210894693790E-02	0.450412159861E-02	-0.188478942963E-02
	-0.307022638571	0.710185136844	-0.333760217265
OZ	302		
	-1.301557184	1.180575388	-10.93772551
	-0.120287018014E-03	0.153658769904E-02	-0.547198873368E-03
	-0.209013113498	2.52845624564	-1.04916050375
OZ	303		
	-3.731987739	-2.453114046	-7.983379033
	-0.739723215686E-05	-0.363291619745E-05	0.134112332903E-04
	-0.411346526788E-02	0.174920634744	0.159757471793E-01
OZ	304		
	-9.614732424	2.560365168	-9.889148514
	-0.289697813420E-05	0.100718959009E-05	0.200980459723E-06
	-0.161000168075	0.111747907558E-01	-0.116904624183E-01
OZ	305		
	-6.989368136	2.866458820	-9.717626542
	-0.979909470800E-03	-0.524890487189E-02	0.555005531799E-04
	-0.124533815509	-0.632265229979	0.517304777914E-02
OZ	306		
	-8.602993992	4.812362113	-9.022029096
	0.333592663508E-04	0.710244425417E-04	-0.690987893976E-04
	0.377870175714	0.576673248527	-0.681473673060
OZ	307		
	-6.069544459	3.327330177	-12.13806694
	-0.181157773973E-04	0.525969856318E-04	0.275927105713E-03
	-0.425661384616E-01	0.197504571544	0.999121948978
OZ	308		
	-4.431669051	2.597908057	-10.18598649
	-0.290007453309E-04	-0.133476552739E-03	0.422157151679E-04
	-0.163638658373E-01	-0.166408949556	0.906825120396E-01
OZ	309		
	-5.699850257	4.788062446	-0.8889595705
	0.553351310210E-04	0.373631830599E-03	-0.217367617838E-03
	0.156811866167	1.10753867931	-0.646256675689
OZ	310		
	-4.041303273	2.826966883	-0.4281482290
	0.467544205524E-04	0.638134777337E-04	-0.189515384079E-04
	0.117506448762	0.158862213321	-0.860240186666E-01
OZ	311		
	-2.476317467	4.798418287	-1.113008173
	-0.149939167484E-04	0.140014253200E-03	-0.485002948623E-04
	-0.793653151504E-01	0.821467364634	-0.268077474067
OZ	312		
	-1.922516590	3.515615746	-11.91287307
	-0.223911639517E-02	0.242834049242E-02	-0.923942056067E-03
	-1.37002565775	1.46531239130	-0.344422029973
OZ	313		
	-2.034152142	3.133921567	-9.363429243
	0.160158570676E-03	0.332688523868E-03	-0.755373406154E-03
	0.655954791283E-01	0.224433385584	-0.443947302771
OZ	314		
	-3.960436453	4.939498308	-9.222321641
	-0.139738660687E-05	0.386915706196E-04	-0.152586470315E-03
	-0.266244471097E-01	0.243612706634	-0.676478064624
OZ	315		
	0.3092509059	8.435247249	-3.069057412
	0.605236753076E-04	-0.358776455362E-04	0.148190219439E-04
	0.444010877107	-0.311129627416	0.108539381451

OZ	316		
	-1.947723306	8.577762077	-4.562683735
	0.270540090546E-03	0.537744406197E-03	-0.311225662783E-04
	0.666876488107E-01	0.778309930799E-01	0.400625657374E-02
OZ	317		
	-1.893861440	7.139335354	-2.291791885
	-0.534520426223E-03	0.999439255486E-03	0.484363133210E-03
	0.111999909514E-01	0.794096281134E-01	-0.264101324492E-01
OZ	318		
	-1.740312762	9.675298762	-2.201757049
	0.154139898854E-03	0.852622403026E-03	0.484576051882E-03
	0.454114746386E-01	-0.959190395007E-01	-0.917484962317E-01
OZ	319		
	-3.907685765	8.732656389	-6.480931576
	0.108056721493E-03	-0.559565459014E-05	-0.172043122328E-03
	0.405805524340	-0.308588480271E-01	-0.693756349755
OZ	320		
	-3.632152385	-9.285053244	-4.671088271
	-0.751442321466E-03	0.431246665659E-04	-0.100490813270E-02
	-0.121665734590	-0.183568928978E-01	-0.208313406999
OZ	321		
	-4.466422133	8.241721055	-3.969846373
	0.138744678890E-03	0.386615656302E-04	-0.183309815115E-03
	0.199838758985	0.529335785395E-01	-0.216297955110
OZ	322		
	-4.552618868	7.529309335	-8.795339987
	0.532557626860E-03	-0.538380957168E-03	-0.643334064264E-03
	0.952435207453	-0.898502972361	-1.14111139641
OZ	323		
	-6.286991937	9.060284696	-7.593675089
	0.358190469232E-03	-0.177357058851E-02	0.453661561807E-03
	0.134227833223	-0.792085577994	0.203840412392
OZ	324		
	-4.171783347	-9.746237303	-8.677320139
	-0.162397302912E-03	0.488194372626E-03	-0.408180571377E-03
	-0.519719143495E-01	-0.129170494984E-01	0.270394442487E-01
OZ	325		
	-8.185357502	7.288891496	-8.096050453
	-0.105532246550E-03	-0.124360363178E-02	-0.174163035706E-03
	-0.803005255129E-01	-1.19893841245	-0.871160533115E-01
OZ	326		
	-8.494450236	9.163913621	-6.223677783
	0.372108165266E-03	-0.919298770957E-03	-0.603591056514E-04
	0.564574349228E-01	-0.209182810447	-0.157579731822E-01
OZ	327		
	-6.991976078	8.949636117	-4.072339691
	0.850703806813E-03	0.937471079501E-03	-0.637326712941E-03
	-0.321182757871E-01	0.371241328148E-01	-0.316711492144E-01
OZ	328		
	-8.777731671	-8.999432921	-4.282691032
	-0.608760394080E-03	-0.104874818265E-02	-0.357557946330E-03
	-0.299845654156E-01	0.146765491516	-0.125074398579E-01
OZ	329		
	-6.172094910	7.112652410	-2.260680586
	-0.187864704169E-05	0.703639896457E-05	-0.869182672611E-05
	-0.440734522545E-01	0.170251782944	-0.208548292900
OZ	330		
	0.3282294421	-6.644262167	-3.207527043
	-0.163990353210E-02	-0.232656063110E-02	-0.142178987016E-02
	-0.567578769119	-0.814710628142	-0.490915610637
OZ	331		
	-2.197160648	-7.212157223	-3.882813541
	-0.135457106862E-02	-0.415899050721E-04	-0.765282255914E-04
	-2.17590069779	-0.250584457952E-01	-0.143523538526E-01
OZ	332		
	-1.661935067	-5.190891999	-2.252721955
	0.124780194352E-04	0.161009456920E-03	0.344941860318E-04
	0.894832039994E-01	0.877314057232	0.179854142652
OZ	333		
	-3.318004143	-7.321906498	-6.372873275
	0.129212190419E-04	0.481176550977E-05	0.159233083169E-04

0.106554947721	0.465140756496E-01	0.665116414930E-01
OZ 334		
-4.729812086	-6.910246395	-4.283782380
-0.990792929849E-03	-0.308490888879E-03	-0.390082106508E-03
-0.376904099230	-0.118881584840	-0.145353660878
OZ 335		
-4.228270325	-5.047963247	-7.352972307
0.113466846962E-02	0.356663071771E-03	-0.885095911410E-03
0.804936366570	0.218248228870	-0.681329595565
OZ 336		
-5.775502833	-7.134960920	-7.311767505
-0.400308376005E-04	0.242889362642E-04	-0.395587584850E-04
0.291655392348	0.170066293029	-0.167388678693
OZ 337		
-7.564272317	-5.272756380	-7.582447021
0.455382131230E-03	0.110341979017E-02	-0.649618612792E-03
0.179041256957	0.321764673112	-0.159350447639
OZ 338		
-8.162902142	-7.411853971	-6.236874622
0.502747282431E-04	0.454555428368E-04	0.165538679121E-03
0.485442105921	0.437653381854	1.21733780197
OZ 339		
-7.300268703	-6.878917276	-3.854165420
-0.143819211740E-02	-0.236244404225E-03	0.428717675487E-02
-0.706478283315	-0.107234949971	2.03237170803
OZ 340		
-5.813944440	-5.085975069	-2.698762575
0.751644803435E-03	0.287402907715E-03	-0.243282847294E-03
0.308873734885	0.118956024078	-0.108645112616
OZ 341		
9.880509444	-8.544370648	-9.846989924
0.502625982966E-03	-0.217626690204E-02	0.524415838212E-03
0.495737828678E-01	-0.245761015791	0.710707445229E-02
OZ 342		
-7.812332290	-9.050896796	-11.10432754
0.175267199497E-03	0.329935030614E-03	0.879761853562E-04
0.185501909028	0.291916360497	0.794602229895E-01
OZ 343		
-7.866788280	-7.651150248	-8.840963616
-0.185321338106E-02	-0.342618251284E-03	0.283427336419E-02
-0.151437143635	-0.255063603604E-01	0.243733974077
OZ 344		
-8.461046180	9.734785606	-8.835608576
0.677177964070E-03	-0.887023295764E-03	-0.204604268942E-04
0.546720552233	-0.631825729693	-0.879484302804E-01
OZ 345		
-5.989372005	-9.183496713	-13.14572223
0.428861201790E-05	0.778459602665E-04	-0.812625118719E-04
0.590597089422E-01	0.499992483095	-0.522007888547
OZ 346		
-6.155294925	8.833979317	-11.27177241
0.562784410210E-05	0.402956528965E-04	-0.140965220856E-04
0.108696320414	0.722732431190	-0.205204211216
OZ 347		
-5.298069916	-8.644404660	-10.69088294
0.956217869865E-03	0.670538144686E-03	0.165126639362E-03
1.28198435843	0.994864738220	0.153503789067
OZ 348		
-5.569963868	-7.673816582	-1.989793596
0.164662931634E-02	0.109330547322E-03	0.990319428316E-03
0.954659677160	0.767963622675E-01	0.531569920240
OZ 349		
-3.557684284	-8.944592809	-0.8715035471
0.639243312258E-04	-0.197101239953E-04	0.156078967368E-04
0.808282578357	-0.247093569804	0.208860214406
OZ 350		
-5.488158297	9.603565331	-2.036613246
0.196410727187E-03	0.644859426872E-04	-0.578964699108E-03
0.352341222689	0.976171706570E-01	-0.927322873621
OZ 351		
-1.316861579	-7.720237360	-1.523403690

-0.471579939798E-03	-0.804523128417E-04	0.393879335214E-03
-0.744427462558	-0.919407170290E-01	0.631952992519
OZ 352		
-1.328988342	-9.208579515	-12.84164691
0.196829529024E-05	0.390615541712E-03	-0.504426028147E-03
-0.104998900009E-01	0.166113236086	-0.159174336236
OZ 353		
-2.708668415	-8.934475783	-10.67599141
0.125092563868E-02	-0.300943915876E-02	-0.105494703723E-02
0.290287547774	-1.58055709811	-0.313086091330
OZ 354		
-1.013874545	8.969331522	-10.89722531
0.474526902597E-02	-0.124484365640E-02	-0.444692146152E-02
0.422620287304	-0.125639831337	-0.391042767991
OZ 355		
-3.838838478	-7.188931770	-8.974985679
0.107281886161E-03	0.690416611372E-04	0.337172821616E-04
0.610319492684	0.279732137271	0.559945932764E-02
OZ 356		
9.855243329	6.828017217	-9.654510790
-0.337713382491E-04	-0.880551168169E-03	-0.218478596747E-05
-0.123685119855E-01	-0.134489352093	-0.761113652320E-02
OZ 357		
-7.662054219	6.769557380	-10.55780114
-0.625248701995E-03	0.583329364580E-02	0.667841883407E-03
0.227443424956E-02	0.117646647945	-0.144758782699E-01
OZ 358		
-6.642892999	7.040083725	-13.07724940
0.417971218158E-03	0.116311449030E-02	-0.39922235816E-03
0.271778894168	0.847952912566	-0.286770312450
OZ 359		
-5.122803894	6.430852428	-11.05935036
0.140617645529E-02	0.183899433973E-02	-0.227096675615E-02
0.164184241693	0.163366172517	-0.316005119099
OZ 360		
-4.074318498	6.814068384	-0.8222573314
0.115426078626E-04	0.379726109837E-05	0.235152294775E-05
0.139612072406	0.718434284845E-01	0.361458205862E-01
OZ 361		
-1.988501121	7.558944613	-12.84222569
0.347358628967E-05	-0.101684367574E-03	-0.941408509277E-04
-0.325571386202E-01	-0.900887049935	-0.886797943684
OZ 362		
-2.627209325	6.876224857	-10.44932239
0.216000006630E-03	0.161782705594E-04	-0.153216323905E-03
1.21883827022	0.149348571432	-0.788474719202
OZ 363		
-0.1561905501	0.9266365342	-2.872193548
0.330879686706E-03	-0.141946149772E-03	0.791802563070E-03
0.250813509712	-0.542661091739E-01	0.534447025786
OZ 364		
-2.803000318	1.255127431	-3.041207058
0.739113755509E-03	-0.276610940651E-02	0.268691465870E-02
-0.341715434020E-01	-0.896931855218	0.702432106602
OZ 365		
-1.550082724	2.262055511	-0.9867975016
0.910615907655E-03	0.112908526556E-02	0.103401652188E-02
0.397528984991	0.321100121932	0.277990688017
OZ 366		
-1.774512098	-0.3266358311	-1.258659574
0.799947793358E-04	-0.816476605402E-04	0.227637008106E-03
0.394816960285	-0.358859394400	1.09882454718
OZ 367		
-4.328325903	1.430251603	-5.297133084
0.334778504952E-03	0.211983595182E-03	0.797135763215E-03
0.582539843339	0.374934359115	1.19499645785
OZ 368		
-3.799427189	-0.8507500583	-4.198862845
0.175657874354E-02	-0.246672142219E-03	-0.842895664889E-03
0.428897413403	-0.842417760609E-01	-0.266898824901
OZ 369		

	-5.392548013	0.7815554189	-2.963878179
0.194557488208E-03	-0.889800256178E-04	-0.368834122374E-03	
0.183357818380	-0.695262193931E-01	-0.350571095103	
OZ 370			
-4.066956031	2.723704589	-7.656099806	
0.274379826325E-03	0.149649185259E-02	0.167397693844E-03	
0.294896752204	1.65145626690	0.282779386904	
OZ 371			
-6.139124577	1.169870721	-7.192781919	
-0.120436253044E-03	0.169220265451E-02	0.211995492821E-02	
-0.715304692512E-01	1.49219660252	1.83081556221	
OZ 372			
-3.799548930	0.1407650509	-7.548342728	
-0.156994767817E-03	0.259361344364E-03	0.568783143192E-04	
-0.822513319730	1.33044526245	0.302041707007	
OZ 373			
-8.384636690	2.483060359	-7.595902013	
-0.117639076164E-02	0.213354501542E-02	-0.824316337353E-03	
-0.544011743386	0.877901133026	-0.130868828865	
OZ 374			
-8.011373357	0.9104835069	-5.405166210	
-0.148814448942E-03	0.966291971077E-04	-0.864742226671E-04	
-0.693082924252	0.323177548977	-0.200089540636	
OZ 375			
-7.982395437	0.6108902589	-2.789995685	
0.300845688490E-04	-0.395610580178E-04	-0.154487556286E-03	
0.377348745242E-01	-0.402283004223E-01	-0.248975270410	
OZ 376			
-8.625866797	-1.405288247	-4.346476410	
-0.183232286384E-03	0.381210776967E-03	-0.305928136452E-03	
-0.435458268604E-01	0.174248180004E-01	-0.733972517903E-01	
OZ 377			
-6.502573759	2.202199080	-1.113361509	
0.437863602375E-05	-0.375336743948E-04	-0.180392810659E-03	
0.293444482013E-01	-0.812134286571E-01	-0.587067756148	
OZ 378			
-0.3399643520	-3.070447949	-2.950240837	
-0.113566038311E-03	0.250488604949E-02	0.119649837256E-02	
-0.476515947994E-01	0.150513653114	0.963470862407E-01	
OZ 379			
-2.990238104	-3.067854001	-3.058470264	
0.485442968001E-03	-0.172020985476E-03	0.590816835622E-03	
0.576526092301	-0.214042440792	0.732234148880	
OZ 380			
-3.997715742	-3.181408569	-5.481131926	
0.347632671873E-02	-0.252787577507E-02	-0.229470624274E-04	
0.472465519010	-0.343183315617	0.320839004053E-02	
OZ 381			
-5.555891610	-2.629304704	-3.475002230	
0.509401083179E-03	0.122235055583E-04	-0.510782947853E-03	
0.387978396684	-0.799031704446E-03	-0.376875373086	
OZ 382			
-6.051189461	-3.227345798	-7.050671188	
0.457848282212E-03	0.223704820482E-05	-0.448605426039E-05	
2.27177030009	0.473893973667E-01	0.612361859730E-01	
OZ 383			
-8.192063921	-3.672942404	-5.603683355	
0.329108159569E-04	-0.256287672095E-05	-0.285600090853E-04	
0.251548515538	-0.196647529119E-01	-0.220655628094	
OZ 384			
-7.931175351	-3.544418720	-3.012473452	
0.106870837757E-02	0.672123371715E-03	-0.422005504984E-03	
0.293880815666	0.244734868507	-0.180460958381	
Si 385			
8.332254252	1.237192003	8.452685688	
0.976022331971E-06	0.379058415060E-05	-0.567387749739E-08	
-0.172123240845E-01	0.492439192371E-01	0.123083309254E-01	
Si 386			
5.915251675	0.6834551923	10.23609917	
-0.222554301381E-03	-0.833058729269E-03	0.249727995671E-03	
-0.315072228982	-1.33880861106	0.389488594882	

Si	387		
	5.618326559	1.572453569	-0.1140062243
	-0.873416167440E-04	0.324901637652E-05	0.594063951010E-04
	-1.01773149033	0.298760063218E-01	0.657353853730
Si	388		
	2.480946137	1.259003671	-0.2586615611
	-0.202995115904E-03	0.157075839202E-03	0.114351070576E-03
	-0.976997563658	0.687965615418	0.556823723979
Si	389		
	1.348900301	0.5951864509	10.39793778
	0.916755128948E-03	-0.346643436385E-04	-0.219501278922E-03
	-0.441285961642E-03	-0.122848945538E-01	0.114653422777E-01
Si	390		
	3.446400787	0.9120522051	8.175819755
	0.786344354852E-04	-0.163704111117E-03	0.680648663106E-04
	0.327186777508	-0.551823222093	0.232760889870
Si	391		
	8.288029848	-3.555783062	8.337867747
	-0.221785947884E-03	-0.224753227059E-03	-0.252065373198E-03
	-0.770017417188	-0.822330183630	-0.985719655856
Si	392		
	5.967196379	-2.446632549	10.23908984
	-0.866661105919E-03	-0.183314947363E-02	-0.900644014283E-03
	-0.223576040294	-0.533344459573	-0.278850550839
Si	393		
	5.362123269	-3.341357600	0.6056836352E-02
	-0.143789339523E-04	0.167065789376E-04	0.379375549388E-05
	-0.607052454383	0.610558083172	0.163610379775
Si	394		
	2.215328690	-3.356948752	0.4021832836E-02
	-0.206167110890E-03	0.166269704723E-03	0.224103253687E-03
	-1.43672791110	1.23396492507	1.60013919872
Si	395		
	0.9559619167	-2.597570795	10.41337532
	-0.164276819498E-04	-0.206131276981E-04	0.401831996285E-05
	-0.139246988540	-0.195637169963	0.444425646715E-01
Si	396		
	3.441164107	-3.500851923	8.773059879
	-0.160952662091E-03	-0.839429078470E-04	-0.102232115351E-03
	-0.885284722426	-0.447721725397	-0.580203328633
Si	397		
	1.515259583	-8.663005880	2.293964525
	-0.220177301205E-04	0.867037009460E-05	0.189301797606E-05
	-0.187033669826	0.123762171869	-0.662753200658E-02
Si	398		
	3.569911621	-9.183649659	4.467021434
	-0.292100522087E-04	-0.109711345711E-03	0.389183201060E-04
	-0.231582662135	-0.858898782891	0.296554196603
Si	399		
	4.519370137	-8.919766825	7.410605486
	0.554741875394E-03	-0.702369489498E-03	0.994207498791E-04
	0.253088495489	-0.350027227520	0.208554758566E-01
Si	400		
	7.673703221	-9.159501713	7.150952987
	0.145349370784E-04	-0.142831474957E-03	-0.391444215909E-04
	0.604871905081E-01	-0.516184202387	-0.142571474189
Si	401		
	8.692923930	-9.523257510	4.126929944
	-0.346919106681E-03	0.235963761680E-04	-0.217335932434E-03
	-0.969187373750	0.937196078190E-01	-0.595152221292
Si	402		
	6.040227125	-8.677506351	2.544457826
	-0.246813782844E-03	0.661355979948E-04	-0.279952550849E-04
	-0.665468159690	0.196398757241	-0.108890906883
Si	403		
	1.340850494	6.293107628	2.370994147
	-0.380664349112E-04	0.168890021123E-05	0.543671736661E-04
	-0.648213522593	0.559437571530E-02	0.973960930171
Si	404		
	3.340029074	7.472899184	4.524431091
	-0.137800032233E-04	-0.663194174766E-05	0.389963774627E-04

	-0.231028470043	-0.131441225658	0.619733712449
Si	405		
	4.339661475	6.488466073	7.218529886
	0.230547793185E-03	-0.550878202750E-04	0.608110355509E-03
	0.771442647460	-0.188887713803	2.05531528176
Si	406		
	7.421592244	6.613284165	7.180658148
	0.188731901911E-03	-0.111938046621E-03	0.298696893471E-03
	0.748907243719	-0.383661695781	1.08203840724
Si	407		
	8.688042273	7.268863897	4.512693348
	-0.107877529552E-03	-0.609774296691E-04	0.157859815928E-03
	-0.568895821430	-0.357678221109	0.778622356142
Si	408		
	5.970273253	6.507721319	3.005005872
	-0.257318791333E-03	0.139243587151E-03	0.921804355718E-03
	-0.237643461311	0.128495195764	0.979944055918
Si	409		
	8.675051467	8.393424945	9.160861446
	0.117623808086E-02	0.162700134660E-03	0.337711816301E-03
	0.898466629496E-01	0.395966092583E-02	0.282382360783E-01
Si	410		
	6.663295063	9.452349954	11.00862636
	0.574286739235E-03	0.413451080943E-03	0.328926853978E-03
	0.357993791457	0.218612075570	0.201704908013
Si	411		
	5.455087521	8.690079221	0.7121363543
	0.125780931347E-02	-0.197559773757E-03	0.167166849167E-02
	0.804877701994E-01	-0.184503905512E-01	0.675103136018E-01
Si	412		
	2.318674628	8.705652287	0.5360370698
	0.470317296717E-03	-0.612230917524E-03	0.862445041588E-03
	0.589513180691	-0.773860441296	1.09117491576
Si	413		
	1.594542325	9.183896662	11.10930542
	-0.752641906765E-05	0.671476509415E-04	0.461910689161E-04
	-0.105293029984	0.529374223134	0.426785235221
Si	414		
	4.141093430	8.539848169	9.377108539
	0.227911140433E-03	0.179245631122E-03	0.394826110960E-03
	0.553519783802	0.461310401370	1.04585547340
Si	415		
	8.621473126	-6.538292575	8.762655869
	-0.946511914606E-04	-0.432972824518E-03	-0.290247320055E-03
	-0.215138279988E-01	-0.111494654415	-0.879414488400E-01
Si	416		
	6.700839638	-7.244156012	11.06582940
	-0.171177120779E-03	0.321927028497E-03	-0.668145263119E-04
	-0.113323178296	0.226892287184	-0.430755513153E-01
Si	417		
	5.513743391	-6.440592527	0.5676817629
	-0.151071159155E-02	0.139395310651E-02	0.127390763429E-02
	-0.142886818537	0.185697274566	0.191030534104
Si	418		
	2.362623952	-6.527334654	0.2047644012
	-0.184371120322E-03	0.187632857811E-03	-0.152096657092E-04
	-1.63749821230	1.69938016863	-0.388268578827E-01
Si	419		
	1.491313196	-7.618540398	10.95846224
	-0.132578074715E-05	0.238250912027E-04	0.130227994597E-04
	-0.156657843399E-01	0.262653366830	0.152476326115
Si	420		
	4.115305452	-6.535160520	9.501079705
	0.610500942620E-05	-0.695437114661E-04	-0.693116381513E-04
	0.237229767627E-01	-0.428833506627	-0.440117166550
Si	421		
	1.373463456	-0.9603367574	1.751636590
	-0.117116261988E-02	0.11305269778E-02	0.448704847669E-03
	-0.871960027402	0.834367591866	0.309754148317
Si	422		
	3.933043725	-0.6883154740	3.664277520

-0.115874125904E-03	0.598392264422E-03	0.335309544684E-03
-0.255253697281	0.961486216607	0.528333075667
Si 423		
4.228999379	-1.669260835	6.555966901
-0.841157698967E-03	-0.167152931367E-03	-0.413692278277E-03
-0.500195156420	-0.105534696382	-0.264442454503
Si 424		
7.379223709	-1.257525448	6.656810321
-0.704473581278E-04	-0.246396506333E-04	-0.359305284984E-04
-0.723785611491	-0.277144420442	-0.377350265146
Si 425		
8.555390337	-0.4130845594	3.857312425
-0.231753667890E-03	0.512248239168E-03	0.546972402829E-05
-0.409088774362	0.920311368374	-0.118362271678E-03
Si 426		
6.449097819	-0.8792890204	1.639847762
-0.431011773227E-04	0.254153784279E-03	0.136198057271E-03
-0.295894991135	1.23868144459	0.708444917349
Si 427		
1.732644283	3.311471440	1.733372395
-0.162165435836E-05	0.407590191641E-07	0.243810789683E-05
-0.697511130247E-01	-0.177657101399E-01	0.116172499367
Si 428		
4.009079123	2.349501146	3.734042269
-0.580633463694E-03	0.887501053716E-03	0.150563709409E-02
-0.766174396822E-01	0.126217698558	0.214919555096
Si 429		
4.498935551	3.398245174	6.484027524
0.883681666264E-04	0.400298414620E-04	0.139022307252E-03
0.548762257104	0.251844399281	0.844988369994
Si 430		
7.611857425	3.501088118	6.430370355
0.273957133290E-03	0.660677707804E-04	0.239885960435E-03
0.586434627813	0.105517871369	0.533967056663
Si 431		
8.855005197	2.789585934	3.603150541
-0.266715499630E-03	0.163630576530E-03	0.281392977339E-04
-0.956673448985	0.558101145820	0.836068396097E-01
Si 432		
6.327832088	3.501440141	2.060926606
-0.535829815161E-03	0.343985990876E-03	0.100723148697E-03
-1.27404886907	0.820895783403	0.253137712349
Si 433		
-8.472354741	-1.204257577	4.511304497
0.133877303255E-04	0.275182766902E-04	-0.555012781092E-04
0.223871053683	0.403187470991	-0.892990695888
Si 434		
-6.031105006	-0.7895114874	2.582020909
0.300808877083E-04	0.746161740580E-04	-0.872598235304E-04
0.336789920264	0.977550045330	-1.17210269960
Si 435		
-5.600483376	-1.502544869	13.02991569
-0.112117477386E-02	-0.611709335991E-03	-0.201073877931E-02
-0.289988436860	-0.849337619111E-01	-0.585212789931
Si 436		
-2.463332407	-1.164487779	13.10420150
-0.299883935134E-03	-0.441707647381E-03	-0.139475460195E-03
-1.36225178560	-2.01079752626	-0.668157326763
Si 437		
-1.630345400	-0.2684638429	2.422258565
-0.229194252542E-05	-0.796505860161E-05	-0.196338519723E-05
-0.157979968609	0.165564134404	0.158672054643
Si 438		
-3.642620531	-1.073131583	4.699545043
-0.375567662695E-03	0.428090966955E-03	0.180738634619E-03
-1.03545224507	1.11190496567	0.361832399249
Si 439		
-8.220405361	3.301824348	4.284980032
-0.119410691039E-04	-0.535394232840E-05	-0.109853220970E-04
-0.364774034882	-0.146349780925	-0.348003494370
Si 440		

	-5.769062196	2.298796459	2.534967694
-0.793424622407E-04	0.184998842248E-03	-0.212669797697E-03	
-0.436854966794	0.947289616976	-1.21990069532	
Si 441			
-5.559246683	3.428504005	13.07108124	
-0.283055907094E-04	-0.104078707297E-05	0.626865013958E-05	
-0.735426352709	-0.288877075582E-01	0.157296435311	
Si 442			
-2.463715472	3.631216592	13.31571731	
-0.979197639847E-03	-0.920835726842E-03	-0.125589598171E-02	
-1.02929809981	-0.742327653177	-1.23452770603	
Si 443			
-1.372677261	2.872387072	2.354052860	
-0.501311130079E-03	0.110603171716E-02	-0.763912647593E-03	
-0.424648324381	0.847903396909	-0.562089595290	
Si 444			
-3.465128780	3.399074813	4.364507433	
-0.348787998682E-03	-0.991726375121E-04	-0.509983834378E-03	
-0.355764038604	-0.933217075690E-01	-0.619003818501	
Si 445			
-1.160550947	8.383063901	10.52730769	
0.192875861734E-03	0.990074917128E-04	-0.129273887446E-02	
0.201857054518	0.108351101553	-1.38227004848	
Si 446			
-3.316757492	9.231045200	8.582854401	
0.542093354808E-03	-0.544732707712E-03	-0.124634140034E-02	
0.326017723061	-0.314997545610	-0.773167456177	
Si 447			
-4.360572092	8.924369826	5.630991835	
0.528058063340E-04	0.534898467524E-04	-0.255339776192E-03	
0.219575830175	0.249672184924	-1.20868140946	
Si 448			
-7.508818653	8.937435622	5.634249098	
0.294200596560E-03	-0.452460729266E-03	-0.197678960943E-03	
0.359622067126	-0.572205628640	-0.237637916836	
Si 449			
-8.569360941	9.263976753	8.530527883	
0.294457501619E-03	-0.666087893500E-04	-0.663334742076E-04	
0.985708659518	-0.202176261319	-0.256664186831	
Si 450			
-5.921136982	8.491574201	10.12965182	
0.633910315800E-03	-0.174164908530E-03	-0.450868037507E-03	
0.689870749091	-0.176138991577	-0.468112595621	
Si 451			
-1.334747253	-6.496630788	10.77317919	
0.305974247846E-04	-0.452932868370E-04	-0.537844668035E-04	
0.248148198945	-0.370242295085	-0.517094311980	
Si 452			
-3.410767160	-7.481929256	8.617995713	
0.300006872100E-03	-0.246833686914E-03	-0.803868401087E-03	
0.316280920873	-0.225969829287	-0.699047209855	
Si 453			
-4.137208369	-6.667931033	5.786321196	
-0.525906409504E-05	-0.214841903754E-05	-0.180456328236E-04	
-0.125577907963	-0.247009525992E-03	-0.429563379592	
Si 454			
-7.266119263	-6.730680205	5.876779544	
0.150787730219E-05	-0.221486908646E-05	-0.238536106178E-05	
0.457466028456E-01	-0.108296481445	-0.212898264896	
Si 455			
-8.499419897	-7.526015653	8.688456770	
0.131072004913E-04	0.199479836446E-05	-0.337909488785E-04	
0.222252281805	0.375056836128E-01	-0.628355992947	
Si 456			
-5.878377481	-6.620688712	10.27941461	
0.106392866139E-04	0.356755369607E-05	-0.276059182635E-04	
0.296460656966	0.875548355907E-01	-0.821818523687	
Si 457			
-8.445296974	-8.562053990	3.692805567	
0.240531453697E-04	-0.202197327163E-03	-0.135658337822E-03	
0.139688359692	-0.984689039653	-0.639239725118	

Si	458		
-6.354581748	-9.355705156	1.797279598	
0.285813956960E-03	-0.133271299890E-02	-0.644225092063E-03	
0.133652780743	-0.738875713119	-0.290532260778	
Si	459		
-5.186680581	-9.054559014	12.20061076	
-0.185418970444E-03	0.683000819453E-03	-0.580468406862E-03	
-0.141470910381	0.537058089645	-0.539903285804	
Si	460		
-2.014445791	-9.096419881	12.45289934	
-0.425256135076E-04	0.208064692255E-03	-0.564426767915E-03	
-0.335171390307E-01	0.156583463104	-0.588553222398	
Si	461		
-1.347015247	-9.749813603	1.966148863	
0.695119083876E-03	-0.319725606435E-03	0.196761450499E-03	
0.703812532603	-0.272966281923	0.162109862787	
Si	462		
-3.843374179	-8.587369450	3.531666415	
0.469026168206E-04	-0.989055336976E-05	-0.747934343117E-04	
0.507354504844	-0.748803518945E-01	-0.790577662447	
Si	463		
-8.448387868	6.362710804	4.049918005	
0.305578224334E-03	-0.281544244748E-03	-0.277160298285E-03	
-0.140296597092E-01	0.201622425066E-01	0.135449470836E-01	
Si	464		
-6.613572201	7.331998408	1.940432358	
-0.267298722462E-04	-0.428576811507E-03	-0.133469480314E-03	
-0.659735499939E-01	-1.00794950429	-0.308112518107	
Si	465		
-5.767148648	6.535361893	12.40294326	
0.172368019018E-03	0.208222804655E-03	-0.127170249835E-03	
0.435357062340	0.594235611457	-0.282720370116	
Si	466		
-2.677236202	6.776644773	12.66550127	
0.428099754012E-03	-0.791104746542E-03	-0.188146255176E-02	
0.760623625596	-1.40306892567	-3.36616680584	
Si	467		
-1.593320799	6.978253083	1.948855639	
-0.340726081298E-03	-0.577816254366E-04	-0.977038265852E-04	
-0.705090917218	-0.124209321079	-0.164822467988	
Si	468		
-4.176489595	6.357572387	3.714448847	
-0.355444129031E-03	-0.369749682677E-03	-0.419383624927E-03	
-0.608235675099	-0.666769524149	-0.752801903276	
Si	469		
-1.516680427	1.367314549	11.43938779	
0.241782571894E-04	-0.562498723348E-04	0.625941519351E-05	
0.430877966624	-0.937940471889	0.767081812737E-01	
Si	470		
-3.963941675	0.6511549929	9.547686653	
-0.213943635995E-05	0.788804235170E-05	-0.431283632994E-05	
-0.150593877326	0.488061309381	-0.110398508983	
Si	471		
-4.410615709	1.395521005	6.528525222	
-0.130925078245E-03	-0.450398350800E-04	0.414604852069E-04	
-1.09785987059	-0.272962435265	0.360393319883	
Si	472		
-7.614652489	1.276396183	6.393786477	
-0.114225955415E-02	0.738914699763E-04	-0.905538445447E-03	
-0.535094188941	0.236817086879E-01	-0.356800048980	
Si	473		
-8.776403991	0.4277258535	9.235497035	
-0.789898882159E-04	0.183883945398E-05	-0.835317111760E-04	
-0.382673744716	0.269320638017E-01	-0.376584454238	
Si	474		
-6.585682370	0.9493539544	11.38295283	
-0.247756394266E-03	0.155862861489E-03	0.210742953869E-03	
-1.47161927467	1.00342379564	1.22611464279	
Si	475		
-1.794988916	-3.449736808	11.20251361	
-0.159672370693E-04	-0.962465873253E-05	0.524636839399E-05	

	-0.395793612584	-0.236819682654	0.907271753431E-01
Si	476		
	-4.055065878	-2.494137708	9.316053713
	-0.605298510509E-04	0.912290274500E-03	-0.438016598422E-03
	-0.178725506383	1.83846922037	-0.969773393822
Si	477		
	-4.266453601	-3.516063715	6.397202815
	-0.504327373737E-03	0.752053400324E-03	-0.155715954423E-02
	-0.478157016369E-01	0.115032771300E-01	-0.121397257470
Si	478		
	-7.410544878	-3.543525017	6.346315550
	0.409344959995E-06	0.316537508664E-05	0.433660829502E-07
	-0.175197077006E-01	0.260996861452E-01	-0.175027731919
Si	479		
	-8.814097600	-2.806411496	9.142836059
	-0.683216633671E-04	-0.196035107017E-04	-0.190637815431E-03
	-0.555532476159	-0.158033751512	-1.88469885502
Si	480		
	-6.427461079	-3.528100470	10.83323244
	-0.433609219629E-04	-0.141906907400E-04	-0.127081813750E-03
	-0.529677145298	-0.141653022243	-1.64887959131
Si	481		
	8.398823963	0.9682535970	-5.051599880
	-0.578353885859E-03	-0.593812906353E-03	0.741691591875E-03
	-1.15606883846	-1.13578181614	1.71059704394
Si	482		
	5.922097838	0.6632247066	-3.039975532
	-0.148360179722E-02	0.197235245950E-03	0.762098628014E-04
	-0.942663451346	0.125197514750	-0.134518170566E-01
Si	483		
	5.494856289	1.366085595	13.29757029
	0.229414943645E-03	0.889235798689E-04	0.196371407553E-03
	0.463489148020	0.232174253222	0.345738762575
Si	484		
	2.379444014	1.095989361	13.25539731
	0.609082800853E-03	0.810043051262E-03	-0.209705832381E-03
	0.427322341136	0.505034394540	-0.140845932608
Si	485		
	1.375054949	0.4881848877	-3.124886773
	0.539657275807E-03	0.667263130162E-03	0.641535329511E-03
	0.805771206797E-02	-0.499972701691E-01	0.637405080488E-02
Si	486		
	3.514739244	0.9464113037	-5.108923477
	-0.254505617499E-03	-0.337535263252E-04	-0.105379543150E-03
	-1.27542781967	-0.237134916599	-0.536070199691
Si	487		
	8.194362712	-3.599353785	-4.768997323
	-0.115067416922E-03	-0.565037245979E-03	0.127826603493E-02
	-0.608777305135E-01	-0.382800298778	0.821909442720
Si	488		
	5.825751398	-2.449181820	-2.932068963
	0.605606286235E-03	0.301875849425E-03	0.758362593789E-03
	0.283461600099	0.191954859019	0.352751154718
Si	489		
	5.292254196	-3.436276145	13.09594692
	0.394377726061E-03	-0.572770524042E-04	0.100427829792E-04
	0.617515301959	-0.367736249209E-01	0.804084305200E-01
Si	490		
	2.190311332	-3.578222823	13.16146050
	0.563877038648E-06	-0.231476615845E-05	-0.231117909756E-05
	0.8517916524949E-01	0.351261748256E-01	-0.403678786970E-01
Si	491		
	1.230195545	-2.710784688	-2.995986595
	0.305967202095E-03	0.378893878035E-03	0.105398013085E-02
	0.557343773653	0.848150939624	2.01912195251
Si	492		
	3.568315408	-3.633521947	-4.715835879
	0.840494510051E-04	-0.141212036642E-03	0.362999819266E-03
	0.279535426747	-0.610079502305	1.47358059628
Si	493		
	1.515713199	-8.394254061	-10.72739015

	0.142752530688E-03	0.259105590804E-03	-0.876639171173E-04
	0.139028378246	0.332145953023	-0.288193288952E-01
Si 494			
	3.514279005	-9.575867618	-8.958476738
	-0.502565423477E-04	0.318413048879E-03	0.122172567058E-03
	-0.211876377783	1.37725265537	0.583850534596
Si 495			
	4.879682595	-9.077418352	-6.178708746
	-0.514725077223E-03	-0.476894862314E-03	0.870564371265E-03
	-0.145868968149	-0.149781265913	0.232264667175
Si 496			
	7.958251037	-9.185389956	-6.148837958
	-0.346082423786E-05	-0.850175622316E-06	0.231988333280E-05
	-0.166285662133	-0.622163589542E-01	0.451321189312E-01
Si 497			
	8.593593089	-9.186363196	-9.133002063
	0.197533095809E-03	-0.300987435735E-03	0.433124903206E-03
	0.470471051874	-0.805181857666	1.10635384145
Si 498			
	5.995869909	-8.477231546	-10.65579449
	0.782828081495E-05	-0.140635689757E-04	0.261255703688E-04
	0.175809501634	-0.258210964304	0.474912432943
Si 499			
	1.482110365	6.355936540	-11.20321272
	0.214176988166E-02	-0.711520253788E-03	0.518906184004E-03
	1.37031598308	-0.418237556756	0.373443792474
Si 500			
	3.376808254	7.123655221	-9.112453970
	0.658885165393E-05	0.131708387096E-04	0.242570776015E-04
	0.168874741808	0.341714316615	0.600814714155
Si 501			
	4.596780376	6.440382899	-6.245014920
	0.465062768275E-03	-0.475528458805E-03	0.278855098176E-03
	0.556936286815	-0.568803772810	0.255756769635
Si 502			
	7.777491178	6.519168980	-6.333801960
	0.292222823196E-03	-0.641561522685E-03	0.595279309096E-03
	0.334829304193	-0.744648996902	0.702093268466
Si 503			
	8.502584535	7.535830400	-9.139922658
	0.212336081646E-03	-0.360977273371E-03	0.232564513352E-03
	0.742648568645	-1.23053521720	0.820981324194
Si 504			
	5.992575731	6.530179067	-10.82207193
	-0.757840106500E-05	-0.496824235131E-05	0.842408671807E-05
	-0.162017557624	-0.112424462932	0.247368831768
Si 505			
	8.848273384	8.333421059	-4.125066500
	-0.189041842009E-03	-0.498461433104E-04	0.214317315375E-03
	-0.993394597290E-01	-0.544453253860E-02	0.153730240851
Si 506			
	6.697891089	9.100141335	-2.122288126
	0.959026039519E-04	-0.934766784606E-04	0.313715570717E-03
	0.481238333232	-0.482671160098	1.55370865565
Si 507			
	5.656558879	9.085206406	-12.71534792
	0.827335753215E-05	-0.144261340995E-04	0.145591363347E-04
	0.204682664502	-0.274260651538	0.276947760532
Si 508			
	2.457844823	9.045964651	-12.60960413
	0.504024912698E-03	0.522544168101E-05	0.161922239929E-03
	0.652171720892	0.114974911844	0.347434158224
Si 509			
	1.541567176	9.268526570	-2.459852344
	0.163388362931E-02	-0.359694770152E-02	0.114270644035E-02
	-0.990586398166E-01	0.227849178213	-0.481567038805E-01
Si 510			
	4.245912499	8.605959296	-3.991636812
	-0.115853794751E-05	0.203676789503E-05	-0.260062408947E-06
	0.450335951755E-01	-0.720364970330E-01	0.121996381695E-01
Si 511			

	8.518646076	-6.623499144	-4.345096314
-0.103552140377E-04	-0.154203453489E-04	0.564286772496E-05	
-0.388382958172	-0.534600401013	0.235223174546	
Si 512			
6.580890892	-7.546132196	-2.239512186	
-0.401172667742E-03	-0.354521794681E-03	0.297208462974E-02	
-0.717093684079E-01	-0.860372226107E-01	0.726946957086	
Si 513			
5.527287032	-6.561912598	-12.97125786	
-0.706378970992E-04	0.915509044382E-04	0.226166650957E-03	
-0.222925326478	0.305405816866	0.846177980507	
Si 514			
2.482593306	-6.746559725	-13.07773809	
-0.237729756474E-03	0.621788249532E-03	0.363129620767E-03	
-0.649470704309	1.67812199996	0.963640672264	
Si 515			
1.657618201	-7.463970111	-2.809888040	
-0.383838638577E-03	-0.140181603303E-03	0.109488195483E-03	
-1.92778746500	-0.745710585754	0.568506356609	
Si 516			
4.325430414	-6.705450907	-4.386075879	
-0.435510121419E-03	-0.661297089455E-03	0.187079023378E-02	
-0.214433180940	-0.410746954425	1.13328576498	
Si 517			
1.501845724	-1.264365465	-11.64944567	
-0.177684011388E-03	0.381614625631E-03	0.230421984544E-03	
-0.780403733870	1.63304113343	0.982069278427	
Si 518			
3.976758772	-0.5531895069	-9.693553728	
0.505670645044E-05	-0.643063874382E-05	0.938286759835E-05	
0.758054872786E-01	-0.279643705388	0.284576250018	
Si 519			
4.256400957	-1.627229994	-6.779068307	
-0.193901306280E-02	-0.184883627736E-02	0.143609227270E-02	
-0.401405121493	-0.445138041727	0.350050203921	
Si 520			
7.441409368	-1.513628322	-6.829427394	
-0.166287162238E-03	-0.123175762718E-03	0.202028034420E-03	
-1.49365520223	-1.07714379828	2.09975220633	
Si 521			
8.509306391	-0.7488656535	-9.683939943	
-0.135426981636E-02	-0.426113518582E-04	0.360352701207E-02	
-0.144438252772	-0.283137792619E-01	0.389899766424	
Si 522			
6.374331548	-1.095273139	-11.75778382	
0.148926679623E-03	0.692998929927E-05	0.104666308326E-03	
1.01940878648	0.547278517115E-01	0.728651926285	
Si 523			
1.746858797	3.372317698	-11.52684602	
0.490273324348E-03	-0.249024840585E-03	-0.152392963424E-03	
0.229621755780	-0.119154607028	-0.837570073611E-02	
Si 524			
4.165997068	2.566678323	-9.586293774	
-0.432085247126E-03	-0.230555419831E-02	0.724138547138E-04	
-0.338763999593	-1.60631133901	0.107898954157	
Si 525			
4.661721760	3.418538259	-6.769313443	
0.433777850683E-03	-0.132149400717E-02	-0.249699308892E-03	
0.136622898799	-0.268788172281	-0.763835527177E-01	
Si 526			
7.863452314	3.402945495	-6.958171569	
0.298726003590E-04	-0.189372436687E-04	0.529763890842E-04	
0.205467664773	-0.972896583407E-01	0.322926391721	
Si 527			
8.830061688	2.419229691	-9.824670370	
-0.100193991287E-02	-0.173870477374E-03	0.235466534264E-03	
-0.726272865410	-0.164681762617	0.278919548611	
Si 528			
6.508924264	3.464331798	-11.45202759	
-0.505836447616E-03	-0.118435113148E-03	-0.264664262437E-03	
-1.38772186440	-0.350308128858	-0.788698142433	

Si	529		
	-8.538655421	-1.305517187	-8.847821447
	0.171806065591E-03	0.477955081413E-03	0.349013679200E-04
	0.699832908278	1.95147196474	0.131949330358
Si	530		
	-6.020354180	-0.7026038855	-10.74666713
	-0.167923081290E-04	-0.340375524169E-04	-0.121482717885E-03
	-0.199329913088	-0.570127388649	-1.79228581514
Si	531		
	-5.625533020	-1.685131532	-0.3098274412
	0.112272402764E-04	0.965107475362E-05	-0.113538462197E-04
	0.311360029227	0.295037823475	-0.299767156437
Si	532		
	-2.482276912	-1.464042360	-0.3596798653
	0.478998815073E-03	0.178698969191E-03	0.946728196709E-03
	0.822703310118	0.355128621784	1.68651864314
Si	533		
	-1.418732287	-0.4240366236	-10.81011655
	-0.166136783925E-02	0.279736560683E-02	-0.270719129788E-02
	-0.283898094611	0.550690462842	-0.596014159128
Si	534		
	-3.570224856	-1.003033344	-8.663311758
	-0.601674882774E-03	0.170329021958E-02	-0.356747862415E-03
	-0.946285304097	2.46950274426	-0.562257791258
Si	535		
	-8.407964296	3.218360840	-9.034161628
	-0.189982542839E-04	-0.243216192493E-04	-0.549777334979E-04
	-0.334292534142	-0.355295491294	-0.952914014183
Si	536		
	-5.905557097	2.423632917	-10.81883421
	0.377550290571E-03	-0.836037438006E-03	-0.155777020449E-03
	0.994271140717	-2.32278303430	-0.509126829304
Si	537		
	-5.599420240	3.278879284	-0.3366308512
	0.316378296913E-03	0.789481210688E-03	-0.157232651990E-02
	0.691983203469E-01	0.167398529324	-0.361825556101
Si	538		
	-2.522074707	3.377819467	-0.3635679602
	-0.452133038929E-05	0.471515586518E-03	0.348461385813E-04
	-0.376056435962E-01	1.54696043109	0.153493925849
Si	539		
	-1.188084216	2.771587122	-10.68120394
	-0.358625184383E-04	0.584022573732E-04	-0.261604480164E-04
	-0.594535514224	1.06473353368	-0.553278201907
Si	540		
	-3.590258830	3.385875193	-9.037527661
	0.234710134445E-03	0.157312994444E-03	-0.171939994692E-03
	0.229684859667	0.207767917978	-0.175326483150
Si	541		
	-1.289547846	8.395114212	-3.087720034
	0.221023937933E-03	0.247030099092E-03	-0.340185592691E-04
	0.907603561173	1.18018385012	-0.109655303779
Si	542		
	-3.460433984	9.006065117	-4.966651165
	0.588403055401E-03	0.220257533300E-05	-0.100000051219E-02
	0.456873504590	0.687337334239E-02	-0.828014986535
Si	543		
	-4.710106628	8.845767901	-7.870953118
	0.716841638418E-05	-0.329767577979E-04	-0.220653501853E-04
	0.134979298098	-0.539496559683	-0.397138533393
Si	544		
	-7.879646436	8.806545922	-7.655294157
	0.441106527394E-04	-0.560384874400E-04	-0.239541810115E-04
	0.542097197060	-0.850391512033	-0.314603495704
Si	545		
	-8.459198236	9.330853281	-4.620973998
	-0.209581532702E-03	-0.121115297567E-03	-0.422872900706E-03
	-0.503158718126	-0.404006315877	-1.16974716500
Si	546		
	-5.809760639	8.435423240	-3.102469946
	0.589594409067E-05	0.590333727308E-04	-0.842172857533E-04

	0.802903635704E-01	0.681809555712	-1.03882022011
Si	547		
	-1.209119517	-6.654490022	-2.731780267
	-0.145631052726E-02	-0.252885611301E-03	0.642646031766E-03
	-0.504138817229	-0.128034605781	0.164244779405
Si	548		
	-3.418502114	-7.690802363	-4.811067553
	-0.278698735301E-04	0.127968388041E-05	0.114979759330E-05
	-0.599591881510	0.944322611031E-02	-0.217684921372E-01
Si	549		
	-4.235724651	-6.650312004	-7.512498037
	0.189613097744E-02	0.275030707584E-03	-0.116586948669E-02
	4.39143190726	0.670295978767	-2.62353414942
Si	550		
	-7.358758325	-6.878443533	-7.526988128
	0.302224528866E-02	0.199789801018E-02	0.166687880784E-04
	1.56381763516	1.17921280905	0.170283238986
Si	551		
	-8.562034289	-7.447093198	-4.671821287
	0.624485125528E-03	0.485814613737E-03	0.210959990040E-02
	0.679830125955E-01	-0.294837673782E-01	0.397830837619
Si	552		
	-5.862471989	-6.617887850	-3.174831890
	-0.342455458931E-03	0.739869097400E-04	0.520282752308E-03
	-0.877820378075	0.154186365071	1.64710906108
Si	553		
	-8.592655079	-8.788595805	-9.725447825
	0.189346901730E-03	-0.364038854521E-04	0.282677359974E-03
	1.00218935482	-0.279251871681	1.55484389962
Si	554		
	-6.340145875	-9.462547461	-11.60533643
	0.660302116201E-03	0.155079924006E-02	-0.288082709224E-03
	0.946688831296	2.09198576395	-0.341323103952
Si	555		
	-5.152328070	-8.979228167	-1.133079653
	0.142450286474E-02	-0.114638066315E-02	0.387712242096E-03
	0.610601765175	-0.497888377296	0.158967170988
Si	556		
	-1.957150344	-9.110564355	-1.034030610
	0.486175089054E-03	-0.122380890510E-03	0.385261267988E-03
	0.992782833509	-0.216346792365	0.888212568447
Si	557		
	-1.266548700	-9.347504777	-11.24014289
	0.148945042765E-03	-0.289178392697E-03	-0.113295042561E-03
	1.43954518806	-2.70062030996	-1.18197388346
Si	558		
	-3.981864063	-8.575398494	-9.772639285
	0.984070451152E-04	-0.454457189227E-04	-0.581641187083E-04
	1.42761948371	-0.613022359292	-0.817738500073
Si	559		
	-8.671606159	6.385998140	-9.348126700
	0.799833201543E-03	-0.674696436342E-04	-0.105786516329E-02
	1.46632896797	-0.436716037675E-01	-2.02422814204
Si	560		
	-6.446228700	7.255782183	-11.49368813
	0.100011948291E-03	0.224417968950E-03	-0.119402197155E-03
	0.818956100452	1.94965734510	-1.02228435760
Si	561		
	-5.643780706	6.401019685	-0.9170116448
	0.109484273596E-03	0.548762520198E-03	-0.400757243204E-03
	0.819842664514E-01	0.465564424651	-0.326664494729
Si	562		
	-2.516064783	6.407847462	-1.009267788
	0.266314470699E-04	0.795727132449E-03	-0.707605915376E-04
	0.343106013679E-02	0.833707874634	-0.469589345339E-01
Si	563		
	-1.423562130	7.471346950	-11.32828982
	0.139568957073E-02	-0.192254197718E-02	-0.130617927527E-02
	2.61290647983	-3.52206680614	-2.43024903267
Si	564		
	-4.047329211	6.413896768	-9.847357613

	0.116333093684E-02	0.255003980866E-03	-0.258486393027E-02
	0.376997711108	0.735039007050E-01	-0.939772764890
Si	565		
	-1.531408945	1.056414216	-2.061169886
	0.146980216844E-04	0.708941289477E-07	0.219395617630E-04
	0.527749695757	-0.245092784644E-02	0.816721648887
Si	566		
	-4.068596929	0.7136556586	-3.878654690
	0.275960106666E-03	-0.763782287686E-04	0.853326658237E-04
	1.89075194942	-0.596219843395	0.651973443481
Si	567		
	-4.567036737	1.400563825	-6.886310806
	0.126743990691E-04	0.210513733382E-04	0.148974319801E-04
	0.292740358129	0.553132129435	0.369169738900
Si	568		
	-7.736124664	1.145939308	-6.964137434
	-0.220121053446E-04	0.111955669681E-03	0.132441362069E-04
	-0.321719921558	1.86130313509	0.186039521616
Si	569		
	-8.736688147	0.1988340752	-4.149735196
	-0.100149322239E-02	0.709589511163E-04	0.331978832317E-03
	-2.50588114056	0.197387109507	0.832965319974
Si	570		
	-6.638130528	0.8163663206	-1.927919078
	0.353048623385E-03	0.195969600181E-03	-0.868966555143E-03
	0.365939331925	0.177544790153	-0.846764304960
Si	571		
	-1.698299558	-3.587941545	-2.245389120
	0.248237146575E-05	0.627456050538E-05	0.712689964268E-05
	0.116447010296	0.258548361442	0.307513264030
Si	572		
	-4.064510663	-2.427765267	-4.064656323
	0.136375183072E-02	-0.553718846079E-03	-0.688576944141E-03
	0.890227871372	-0.372438742320	-0.400192416768
Si	573		
	-4.452081504	-3.494200078	-6.992175674
	0.525855602186E-03	0.162497556609E-03	-0.666302734179E-04
	2.25407443074	0.628806608700	-0.246363273408
Si	574		
	-7.589824958	-3.731189769	-7.098336651
	0.206554119820E-02	0.107110755350E-02	-0.925374181615E-04
	2.26608656126	1.18802944823	0.182487811762E-01
Si	575		
	-8.801261434	-3.012608873	-4.258637323
	0.529227089814E-04	0.729012274855E-05	-0.562527002771E-05
	0.708692757027	0.139468199646	-0.113044535212
Si	576		
	-6.408820401	-3.607388890	-2.501509447
	0.739639045767E-04	0.307221864152E-04	-0.314612830144E-04
	0.973463287768	0.392023572611	-0.386297889676
OT	577		
	1.592833622	-9.854355632	-6.138645160
	-0.121660185974E-03	0.280113941759E-02	0.312369533561E-03
	-0.379729106233	0.525076799526	0.257761172742
HT	578		
	1.385165949	-8.924917397	-6.281903675
	-0.169568200977E-02	0.254618648222E-02	0.596226527750E-03
	0.202157344042E-01	0.998421255622E-01	-0.191389780393E-01
HT	579		
	2.465485213	-9.887105094	-6.530737825
	-0.144464033021E-02	0.886807756440E-03	0.703825084708E-03
	0.614509505435E-01	0.177872454723	-0.478880124908E-01
OT	580		
	1.713417010	-7.310078955	-7.165299044
	-0.228512512190E-03	0.647641436251E-03	-0.149158076431E-03
	-0.192808084076	0.152206411142	-0.790113599610E-01
HT	581		
	1.995686895	-6.414075630	-7.353101812
	-0.453886943660E-03	-0.271116085244E-03	-0.147652723689E-03
	-0.385892910444E-01	0.122238279534	-0.724092654727E-01
HT	582		

	1.852007941	-7.745114943	-8.017730327
-0.173779080921E-03	0.259900876615E-03	-0.138603925038E-03	
-0.569660876472E-01	0.103853196743	-0.149457061375E-01	
OT 583			
4.656511497	-6.845494157	-8.190374184	
0.804496457893E-03	-0.528108349907E-03	0.509113556070E-03	
0.118333125307	0.925233691464E-01	0.745472300599	
HT 584			
4.092124222	-6.076482572	-8.287065809	
-0.333008648875E-03	0.493173563370E-03	0.706902479432E-03	
0.536751601791E-01	-0.607350138143E-01	0.257377881106	
HT 585			
4.732886322	-6.888990455	-7.230129653	
-0.204278357868E-03	0.298498592010E-03	0.313729202900E-02	
-0.285903794044E-01	-0.609568093751E-02	-0.290770892638	
OT 586			
2.822572124	-4.784821883	-7.871800593	
-0.182949840344E-04	0.139880212102E-04	-0.119641130539E-03	
-0.306917945773E-01	-0.503550242502E-02	-0.238568458577	
HT 587			
2.339098499	-4.247915821	-8.488136463	
0.429312583745E-03	0.133089979377E-03	-0.399782203481E-03	
0.976904779673E-01	0.324562887531E-01	-0.784439320012E-01	
HT 588			
3.168124225	-4.109676254	-7.263494302	
-0.527998815449E-03	-0.401259858993E-03	0.594171119510E-03	
-0.542816001398E-01	-0.271337816957E-01	0.638558507944E-01	
OT 589			
-0.2769632248	8.048527115	-6.510206467	
0.161917460851E-04	0.968657862211E-05	0.183286743693E-05	
0.347152680952	0.285980804967	0.879722067165E-01	
HT 590			
-0.9072290507	8.216112415	-5.800945431	
0.722881942173E-03	0.809871635039E-03	0.436926293116E-03	
0.745389473593E-01	0.805666567588E-01	0.438560788302E-01	
HT 591			
0.3808913819	8.733595218	-6.340905255	
0.466729390031E-03	0.605318761267E-03	0.307765177207E-03	
0.800558384304E-02	0.162849940502E-01	0.167121167892E-01	
OT 592			
0.6116977757	5.700832207	-7.620272400	
0.179137126284E-03	0.589260275993E-03	0.688456651365E-03	
0.114536924992	-0.408255185943E-01	0.860990257829E-01	
HT 593			
0.2437815439	6.519589412	-7.261661728	
0.850505589174E-03	0.103637209272E-03	0.340179155875E-03	
-0.358057906521E-02	0.162747456350	0.884937149465E-01	
HT 594			
1.056267369	6.003513643	-8.420301944	
0.137610940667E-03	0.224209915723E-03	0.538087442904E-03	
0.188577259225E-01	0.386977205202E-01	0.723164098895E-01	
OT 595			
3.363462146	3.776741301	-3.888057661	
0.373018021602E-03	-0.160748096054E-03	0.540844388891E-04	
0.180529442246	-0.753741697167E-01	0.216892926601E-01	
HT 596			
3.877303269	4.346193182	-4.459019361	
0.210367280653E-03	-0.114202639641E-03	-0.882037307960E-04	
0.681324507032E-01	-0.324601753764E-01	-0.255773195859E-01	
HT 597			
2.567700265	3.701945077	-4.418085993	
0.640893509788E-03	-0.498110505358E-03	-0.207831585463E-03	
0.283779013391E-01	-0.328108866088E-01	-0.153410173189E-01	
OT 598			
1.644759126	3.779147318	-6.054594857	
0.270703646393E-03	-0.146510685835E-03	-0.105558780881E-03	
0.450020167609E-01	-0.232191186178E-01	-0.391563065441E-01	
HT 599			
0.9202690186	3.168539385	-6.027868347	
0.136838173908E-03	0.239474764393E-04	0.470136600764E-04	
0.110080272762	0.208675438421E-01	0.369041199485E-01	

HT	600		
	1.281169122	4.484788486	-6.611142067
	0.246781143573E-03	0.326483301355E-04	-0.517539576936E-04
	0.960100090788E-01	-0.292186408842E-02	-0.310913235717E-02
OT	601		
	3.256162601	-5.995858131	3.273754706
	0.590412282354E-03	-0.293252753791E-03	-0.376619922432E-03
	0.265292262547	-0.151251979119	-0.183116021853
HT	602		
	2.853974674	-6.835856650	3.500683089
	0.145318483304E-03	0.212073615777E-04	-0.108513391989E-03
	0.765333256769E-01	0.114843654296E-01	-0.659672404117E-01
HT	603		
	3.371604371	-5.601017030	4.140915189
	0.119150907843E-03	-0.106970311578E-03	-0.551408836107E-03
	0.349326556037E-01	-0.954257301373E-02	-0.118319087888
OT	604		
	3.646991815	-5.246825175	5.926030744
	0.979538911025E-04	-0.526936672025E-03	-0.446010360376E-03
	-0.653640505950E-01	0.139952372410E-02	-0.777097589162E-01
HT	605		
	3.578652922	-4.358739733	6.303584802
	-0.653183103435E-03	0.642297067244E-04	-0.447407619513E-03
	-0.106975162496E-01	-0.126227207339	-0.701297290034E-01
HT	606		
	4.594781082	-5.400105381	6.040558146
	-0.213935703880E-03	-0.305698025791E-04	-0.532078124272E-04
	-0.466836063275E-01	-0.251548441443E-01	-0.191451868077E-01
OT	607		
	6.353328734	-5.396715218	6.251015774
	-0.370092517131E-03	-0.407877753205E-03	0.352213761820E-04
	-0.119443768815	-0.159557324535	-0.911022426626E-01
HT	608		
	6.866760552	-5.420127452	5.453152769
	-0.651553983284E-05	-0.502127509337E-04	-0.818714659729E-04
	-0.418125425967E-01	-0.594536584154E-01	-0.742013504910E-01
HT	609		
	7.038863041	-5.372707688	6.932228287
	-0.229115231828E-03	-0.111868471336E-02	-0.602447231973E-03
	0.235016987881E-01	-0.522521420778E-01	0.314155226934E-01
OT	610		
	2.023298555	-6.680010376	7.675653386
	0.123939650709E-03	-0.917508345803E-03	-0.408430609562E-03
	-0.770628191515E-02	-0.269072803565	-0.854501424665E-01
HT	611		
	1.168921379	-6.697866911	7.268167339
	0.316606165132E-04	-0.125368306953E-02	-0.353839669937E-03
	0.179706016913E-01	-0.123062419779	-0.304505180104E-01
HT	612		
	2.569461685	-6.286616794	6.987143099
	-0.478952608677E-04	-0.128124281756E-02	-0.495894999461E-03
	0.198535005404E-01	-0.818205273272E-01	-0.647433792133E-01
OT	613		
	0.6899184965	4.392584801	4.371651011
	-0.506358681458E-03	-0.413377746378E-03	-0.199297662216E-03
	-0.291679763122E-01	-0.303593556496	-0.346957775419
HT	614		
	-0.2345339641	4.174361193	4.450695720
	0.291273581713E-03	-0.888944617300E-03	0.164672956730E-03
	-0.118378387026	-0.940807152265E-01	0.332756176958E-01
HT	615		
	0.8288077048	4.926599824	5.166296603
	0.697550181980E-03	-0.361055610399E-02	-0.141274425543E-03
	0.838612413290E-01	-0.914788467398E-01	0.250803699633
OT	616		
	1.486748505	6.285317324	9.169224671
	0.799953220864E-03	-0.339762096259E-03	0.871454981596E-03
	0.147751248651	-0.565811623346E-02	0.288331462581
HT	617		
	1.087668258	6.966631257	9.726497802
	0.767346511247E-03	-0.215412246954E-03	0.151021308819E-02

	0.113424647015	-0.934644284644E-01	0.873954428034E-01
HT	618		
	2.423178224	6.498908177	9.195879815
	0.846239952968E-03	-0.433958997372E-03	0.117794052385E-02
	0.103063172111	-0.564276208788E-01	0.132870974981
OT	619		
	6.332658844	3.876862230	9.159919035
	-0.855383197281E-03	-0.914687979786E-03	-0.223452933339E-04
	-0.345127140622	-0.424108880757	-0.140631910745E-01
HT	620		
	6.664415892	2.996369964	9.376752599
	0.627580297903E-04	-0.892600991150E-03	-0.866066815103E-04
	-0.675123384553E-02	-0.178552376614	-0.302520335163E-01
HT	621		
	6.653219462	4.403865318	9.878993199
	-0.144847961786E-02	-0.903964922020E-03	0.914588864160E-04
	-0.216246650498	-0.129266818223	0.286399032359E-01
OT	622		
	1.027234139	5.948006077	6.528043805
	0.695142556562E-03	-0.181585333001E-02	0.919499736217E-03
	0.316194198308	-0.635156181133	0.373704121273
HT	623		
	0.9923742079	5.942157104	7.491539462
	0.651012997830E-03	-0.184536877165E-02	0.109300546275E-02
	0.167333657820	-0.442642551899	0.235691454907
HT	624		
	1.821387642	6.467900871	6.377111595
	0.641203399742E-03	-0.123274365244E-02	0.643866204494E-03
	0.100632743633	-0.341004175616	0.166273994484
	#####	#####	#####

SPC water / silicalite

	577		
OSPC	0.8750078723	-8.200264884	-5.534747483
	0.580583513652E-01	0.581860303327E-01	0.133073248266
	1443.03011896	-15512.3150204	5226.67500481
HSPC	578		
	0.5938845209	-7.516382789	-4.861490019
	0.455281482019	0.493678765018	-0.143428678442
	-2001.47696283	7833.29589695	2955.71833304
HSPC	579		
	1.010365929	-7.759268922	-6.421991238
	1.11741669677	-0.238461806199	0.147243186192
	582.369958877	7690.35894582	-8162.00580385
OSPC	580		
	1.381779514	-6.855731486	-7.805429997
	0.767581808368E-01	0.600310196194E-01	-0.235752639255E-01
	-13190.7858458	3514.76003598	11200.7924512
HSPC	581		
	2.181520797	-6.266343522	-7.691253028
	0.209914233324	-0.142353277414	0.884655146239E-01
	7806.74543122	2663.97358164	-1963.36651313
HSPC	582		
	1.549454871	-7.506084444	-8.546325891
	-0.159394714126E-01	0.714623000424E-01	-0.545883646749E-01
	5419.95470786	-6156.27113473	-9246.09479488
OSPC	583		
	3.776170193	-5.601532284	-7.282731276
	0.200505869090E-01	-0.194382177654E-01	0.228179517400E-01
	1647.12271960	2233.06759648	-15376.7228315
HSPC	584		
	3.182951206	-4.996667585	-6.751477475
	-0.947466899113E-01	-0.103349369675	-0.983128420692E-02
	-4000.49026778	3114.93626409	6948.03874316
HSPC	585		
	4.179893769	-6.288319960	-6.678305365
	0.166440202426	0.102396582727	0.634742176316E-01
	2389.60489296	-5376.80143952	8467.34114616
OSPC	586		
	1.896792014	-4.709252415	-5.547893627
	0.259448390000E-01	-0.236032331462E-01	0.348328875849E-02
	2563.59671538	-2610.50415245	-9270.54476260
HSPC	587		
	1.923757349	-4.369114418	-4.607904433
	0.115086285675	-0.110741264897	0.324572671995E-01
	-340.843095163	3186.24821211	9189.50866009
HSPC	588		
	0.9738626838	-5.030274118	-5.760372422
	-0.726853121916	2.74750191717	-0.913340329277
	-2223.58581373	-566.198647062	77.5498720734
OSPC	589		
	1.273528705	8.975563337	-5.460580667
	-0.155008546751E-01	-0.681577005816E-01	-0.573872012845E-01
	7246.91096952	-10515.3447856	-9981.57900936
HSPC	590		
	0.8817879995	8.716728297	-4.577662599
	1.78968923244	-0.507083863067	0.614880123184
	-4452.55228519	968.564806070	8377.58437647
HSPC	591		
	1.140010461	-9.920527505	-5.610712268
	-1.38719278264	-0.221276400396	0.163415189313
	-2784.62018268	9432.32058143	1595.23294714
OSPC	592		

	0.8486537774	6.651622295	-6.860301403
	0.623132874202	-0.794800917332	0.579739532102
	-5909.95703170	-10312.5526652	5037.62755531
HSPC	593		
	1.219024568	6.623559712	-7.788761763
	-0.18669694619	-1.24462977960	0.270287594038
	3538.59378554	1095.75682829	-7525.19208844
HSPC	594		
	1.027076797	7.549002106	-6.456723131
	0.235769062319	-0.315765422642	-0.314169248908
	2378.66780493	9206.38607904	2494.29509228
OSPC	595		
	2.318865917	6.586305636	-2.792758009
	-0.264896047161E-01	0.485559986110	0.671920938398E-02
	1225.18339593	-299.784664319	13407.9729266
HSPC	596		
	1.446429860	6.357744080	-3.224748303
	2.21198303067	-9.21101891677	0.616318357858
	-5369.86352760	-1135.81458977	-5543.63994881
HSPC	597		
	2.991712675	6.810769406	-3.497665079
	-1.26730406092	1.83506066844	-0.747939092340
	4278.90509031	1535.21277765	-7870.56521996
OSPC	598		
	0.1174113096	5.919193428	-4.319160772
	1.34370061215	0.267706507700E-02	0.139307106780
	-669.67219259	926.552852684	12492.5308488
HSPC	599		
	0.1030960303	4.922977340	-4.233433002
	-27.7006269812	0.326524270602	-0.947340351425
	-689.821422892	-1302.67559414	-2317.56594360
HSPC	600		
	0.2497945707	6.169841722	-5.278145040
	5.99774944851	-2.80411382419	0.481698622950E-01
	1347.01491612	238.552197463	-10099.9324240
OSPC	601		
	0.8625195840	-7.112867078	5.148295281
	-0.158072611714E-01	-0.238599608309E-01	0.177291507137E-01
	1996.91395592	13306.4154173	9200.58497841
HSPC	602		
	1.418106398	-7.650656182	4.514176331
	-0.177677381141	-0.189565399348	0.164386594373E-01
	3947.30659413	-8106.34198834	-7660.07808270
HSPC	603		
	-0.4707757138E-01	-7.521366886	5.224200769
	-0.667210585107E-01	0.121296089079	0.188799434046
	-6007.01006273	-5256.87731969	-1478.78275762
OSPC	604		
	0.9547255076	-8.068719184	7.720761986
	0.629864029305E-01	-0.275425248725E-01	0.129006666026
	-8309.18824887	-9792.57349653	3709.98981109
HSPC	605		
	1.583531540	-7.675429163	8.391527672
	-0.234792015575	0.620150425416	0.283958129150E-01
	5557.88173868	4390.66255846	3436.48377962
HSPC	606		
	1.078297784	-7.612265555	6.839637308
	-0.187579016823	-0.252129594138	-0.224775967279E-01
	2798.98519376	5396.01377561	-6977.78318853
OSPC	607		
	9.391498251	-4.070276425	6.254286547
	-0.143253274617E-02	0.196580674389E-01	0.168787477315E-02
	-3886.62537020	76.9629212615	-9300.91606583

HSPC	608		
-9.817904410	-3.657134334	6.601935612	
0.596670689100E-02	-0.235612881315E-02	0.993490043657E-02	
6423.55401081	2906.32081887	3603.37734046	
HSPC	609		
8.919900517	-4.543554068	6.998332628	
0.334470058447E-02	-0.894012908097E-02	-0.134751035700E-01	
-2537.11059725	-2979.22735651	5697.85260172	
OSPC	610		
-1.278909181	-8.581108858	5.978499173	
0.217673889966E-01	0.291246506138E-01	-0.578820543611E-02	
5638.63342669	-4389.97301986	-8850.92337001	
HSPC	611		
-2.153412683	-8.177210361	6.247032787	
-0.156428817564	-0.292360121411	-0.102558177962	
-9006.86622751	4268.52955630	3542.28174835	
HSPC	612		
-0.6669371065	-8.608069123	6.768919343	
-0.208253939012	-0.145439567600	0.166348509824	
3360.07350474	135.050767883	5294.58205620	
OSPC	613		
-1.130768361	5.760106990	5.049702763	
0.122958136027	-0.131176264021	-0.408580941066E-01	
-10195.0199305	-8101.42218807	2692.87783271	
HSPC	614		
-0.5358448130	6.102581303	5.776873988	
-1.67741537086	2.82633655142	0.391951631146E-01	
5715.77188018	3785.31268201	3515.05713236	
HSPC	615		
-0.8190775540	6.115255723	4.168386169	
-0.109974843340	-0.477613348272	-0.262843883428	
4505.95036123	4353.77217816	-6339.20382616	
OSPC	616		
5.167256016	3.559840999	10.87183427	
-0.711051572043E-02	-0.820019957375E-01	-0.100771390374E-01	
-3655.57044493	-5036.51205503	9553.20305161	
HSPC	617		
4.754851060	3.335107870	9.988987829	
0.121520914955	-0.858345069627E-01	-0.691892842727E-01	
-925.029334742	234.616204775	-6265.30221730	
HSPC	618		
5.884177832	4.244558928	10.74074198	
-0.594814629780E-01	-0.512102844652E-02	0.105077625197	
4580.51688892	4799.64541277	-3288.10183672	
OSPC	619		
7.180525371	5.120537470	9.818945242	
-0.257084202093E-01	-0.538738123165E-02	0.237267147279E-01	
-8316.49600813	-1972.37339895	5449.61301685	
HSPC	620		
7.716027705	4.347169223	9.479623159	
-0.277117493068E-01	0.460190366792E-01	-0.965981350425E-01	
4143.20260002	-4523.97579457	-2637.09524342	
HSPC	621		
7.608659311	5.976196432	9.528170775	
-0.852684720248E-01	0.374926567176E-01	0.622136189177E-01	
4171.44619317	6496.33996600	-2811.30175402	
OSPC	622		
0.7346023158	6.983564838	6.725960005	
-0.669101739450	0.298387891274	0.148107057297	
-8551.26230148	-2506.45529385	-1207.98488018	
OSPC	623		
0.3780111158	7.674913847	7.354354734	
2.79527475950	-12.7201375088	16.4367713876	

53.7348038188	1519.05488625	1346.24635054
HSPC 624		
1.729436215	7.066750541	6.667767461
-0.503411479127	-1.67472844556	0.160122649349
8485.05719159	973.121143603	-110.124651650

#####

Benzene / silicalite

CA 577		
0.9613146859	6.286584159	-5.558104154
0.571352501817E-04	0.646028221817E-04	0.946750196568E-04
2.59800512008	2.87987888915	5.63510931130
HP 578		
0.9175497117	7.366372895	-5.545968131
0.639614415037E-02	0.109741648842E-01	0.145166527156E-01
1.76603419150	1.82071708943	3.87103250537
CA 579		
1.469344416	5.596249672	-4.451993688
0.486037665854E-02	-0.181037522857E-02	0.128046635175E-01
2.20668679015	-0.650759856982	6.30281898410
HP 580		
1.819997524	6.145878443	-3.590270122
0.104462812317E-02	-0.989375112068E-03	0.515829975914E-02
0.922958314090	-0.227845106198	3.78225381634
CA 581		
1.523976949	4.197528559	-4.464708041
0.533666446611E-03	-0.727428549121E-04	0.260075473403E-02
1.56026117014	-0.353850199729	6.79173698378
HP 582		
1.914868953	3.664250326	-3.610394587
-0.603700906909E-02	-0.443318853278E-02	0.232977448517E-02
-0.242292132723	-0.246374660239	0.141886471289
CA 583		
1.071710678	3.488599008	-5.584007310
0.192759195565E-02	0.264978469326E-02	0.638616505717E-02
3.38304602639	4.49473579357	11.0358880067
HP 584		
1.109782620	2.408871479	-5.589824972
-0.928401185291E-03	0.207347144831E-02	0.651374339207E-03
-0.118334644793	0.306321194817	0.113455937307
CA 585		
0.5669676307	4.178868404	-6.692435663
0.833822599367E-02	0.116527272607E-01	0.130885397045E-01
2.38844961117	3.48662251474	3.93146027473
HP 586		
0.2156942400	3.633592804	-7.556837913
0.824890468482E-02	0.153485964172E-01	0.161847445467E-01
1.37523667744	2.71772617335	2.53848501332
CA 587		
0.5106996856	5.577635161	-6.677935309
0.105232632454E-01	0.110280879003E-01	0.208707406483E-01
5.06672397640	4.78775275049	9.15627920311
HP 588		
0.1202309815	6.111107145	-7.532569035
0.128279643848E-01	0.839927938661E-02	0.193017861477E-01
1.44954180276	1.10948027030	2.22332423449

#####

Phenol / silicalite

```
#####
CA      577
       -0.8930224309      6.488278307      -6.425291503
      -0.149755682816E-02  -0.533209483602E-03  0.237137089181E-02
      -5.30888435135      -1.89024378258      8.40658169497
OH1     578
       -0.6314229795      7.803031207      -6.089713240
      0.689558770517E-02  -0.436263969278E-02  0.539776892799E-02
      2.30005348700      -1.45517758122      1.80044947228
H       579
       -1.143503345      8.066995160      -5.308343196
      0.190384265722E-02  -0.140440841367E-02  0.157658602090E-02
      0.625995915972      -0.461778670618      0.518391793840
CA      580
       -1.743149580      5.691261667      -5.643923114
      0.242255863020E-01  -0.775596815654E-02  0.255250504012E-01
      21.3249491733      -6.82731161450      22.4688226598
HP      581
       -2.219974583      6.080099103      -4.756111478
      0.149098366696E-01  -0.200817654449E-02  0.182752623081E-01
      2.23378652163      -0.300864308410      2.73799341520
CA      582
       -1.980304841      4.360750383      -6.006188790
      0.286774577047E-03  -0.144975690056E-03  0.934675348257E-03
      3.24616049206      -1.64106024396      10.5801086681
HP      583
       -2.629359280      3.745711288      -5.401296792
      0.455441953878E-01  -0.418244156461E-02  0.207221110912E-01
      6.27763405364      -0.576491413885      2.85625487818
CA      584
       -1.374805851      3.821168945      -7.146385841
      0.251408572104E-01  -0.111202272739E-01  0.277378208433E-01
      15.9289921311      -7.04566321103      17.5744019485
HP      585
       -1.554747892      2.791858652      -7.420273383
      0.504856870286E-02  -0.203732233657E-02  0.998241500476E-02
      1.10787275342      -0.447076001032      2.19057048601
CA      586
       -0.5301282689      4.617109726      -7.926132493
      -0.385188099381E-02  -0.332095013325E-02  0.452590571685E-02
      -7.36801645382      -6.35243281489      8.65731517765
HP      587
       -0.5753218806E-01  4.203758618      -8.802486446
      -0.121241786469E-01  0.105174635283E-02  -0.192531408914E-02
      -2.63601838038      0.228668910142  -0.418598527352
CA      588
       -0.2886467648      5.945863203      -7.564729089
      0.224920414357E-02  -0.521633706180E-02  0.601816558075E-02
      0.955040143422      -2.21492180239      2.55538819622
HP      589
       0.3695353357      6.553723052      -8.166502258
      -0.449597748119E-02  -0.207909674263E-02  0.618315950396E-03
      -1.45383878140      -0.672305741604      0.199941327910
#####
```

Toluene / silicalite

CT3	577		
	-0.4717634569	-2.536427487	6.565101643
	0.379153381511E-02	0.177901574808E-01	0.135568539815E-02
	-0.516792052097E-01	5.34110461541	1.03928086069
HA	578		
	-0.4025822660E-01	-1.898196214	5.793521635
	-0.160312929520E-02	0.844789075085E-02	0.543402292842E-02
	0.593663995824	1.09845820763	-0.926223654071
HA	579		
	-1.477469170	-2.178630509	6.784652504
	0.304134677713E-02	0.232420195181E-01	0.230290327099E-02
	0.643201089783	2.21630568936	0.165368199555
HA	580		
	0.1316150651	-2.448401389	7.468188914
	0.298210827669E-02	0.205328136341E-01	-0.231102331610E-02
	0.539267765309	1.68990235155	0.183497157434
CA	581		
	-0.5208555852	-3.970769806	6.092278039
	-0.443175756287E-02	0.163282118057E-01	0.356453976720E-02
	-1.03818017402	5.28730480206	2.74762182371
CA	582		
	-0.1780041219	-5.014640626	6.961524608
	-0.149805955175E-01	0.150338311459E-01	0.136231448420E-01
	-6.53108593960	6.44253663660	3.12859659224
HP	583		
	0.1273693914	-4.810385750	7.977507586
	-0.230720667279E-01	0.178738071540E-01	0.750984228214E-02
	-1.92544920269	1.89046851168	1.84469334134
CA	584		
	-0.2301708369	-6.340104158	6.515812891
	-0.228113490629E-01	0.161925130574E-01	0.122570316539E-01
	-8.43917904197	5.07704599492	7.21542202140
HP	585		
	0.3821397969E-01	-7.144494428	7.184418592
	-0.292102958597E-01	0.100900826539E-01	0.240622988601E-01
	-3.64356898091	2.27191544009	1.66199457400
CA	586		
	-0.6268040450	-6.625721279	5.204969780
	-0.154964487196E-01	0.102186084276E-01	0.161724073081E-01
	-5.96287751759	4.95929025692	4.26983693898
HP	587		
	-0.6646895352	-7.648636664	4.858853259
	-0.191520246606E-01	0.143256347184E-01	0.164828743565E-01
	-1.69331652168	0.688451456769	1.42956344885
CA	588		
	-0.9752713772	-5.584227726	4.338712851
	-0.474720454870E-02	0.122646545961E-01	0.692796783707E-02
	-1.53209388617	4.41344207480	4.08289484711
HP	589		
	-1.290007501	-5.808535598	3.329691909
	0.137363682473E-02	0.865455929627E-02	0.893167873798E-02
	0.120523447595E-02	0.846218707616	0.453417481836
CA	590		
	-0.9197504227	-4.257858701	4.780700284
	0.267563913240E-02	0.127525348229E-01	0.561948005508E-02
	0.766247085114	6.18218168895	1.27079355074
HP	591		
	-1.195599798	-3.458296423	4.108158981
	0.111590849823E-01	0.142742863120E-01	-0.258522480553E-02
	1.25621641526	0.981362159465	0.159306860055

Neopentane / silicalite

CT1	577		
-0.3757827310	5.641821643	6.760784050	
-0.900086477530E-04	0.247688655065E-03	-0.949700306125E-04	
-3.77166228416	10.3789800407	-3.97956075920	
CT3	578		
0.6661500635	5.942768576	7.859693188	
-0.115440050850E-01	0.143645157117E-01	-0.126014735603E-01	
-9.05257609362	11.2643636736	-9.88182155640	
HA	579		
1.465865760	5.202326016	7.878040092	
-0.205901887426E-01	0.392433287711E-02	-0.809358878990E-02	
-1.09752959508	0.209180766987	-0.431416794591	
HA	580		
1.138499268	6.915415987	7.720964535	
0.171290805939E-01	0.526816051727E-02	0.466737869325E-02	
1.58728169566	0.488178843752	0.432506854405	
HA	581		
0.2211886292	5.949360846	8.854717199	
-0.139471954313E-01	0.943472098432E-02	-0.135050257597E-01	
-1.59216787835	1.07703801574	-1.54169118206	
CT3	582		
-1.630620069	5.008418678	7.397628578	
-0.151476046391E-02	0.346712027913E-02	-0.122162083237E-02	
-10.9730201606	25.1160375706	-8.84949821538	
HA	583		
-2.043179371	4.210828307	6.779147279	
-0.459394223096E-02	0.505026271915E-02	-0.179886692983E-02	
-0.555961911918	0.611186117688	-0.217700059625	
HA	584		
-1.418429592	4.572035762	8.373977714	
-0.183616454048E-02	-0.426078464321E-02	-0.912184847550E-03	
-0.362024928139	-0.840071910912	-0.179849706605	
HA	585		
-2.425118464	5.740507571	7.544608434	
0.399548054170E-02	0.357243616906E-01	-0.148610961322E-01	
0.418331150707	3.74037945582	-1.55597290010	
CT3	586		
-0.7698998427	6.951692837	6.047067368	
0.270985503448E-01	0.657019110787E-01	-0.230903523885E-01	
15.3050146909	37.1078416181	-13.0412209519	
HA	587		
-1.836088026	6.987470176	5.824532358	
0.285882527992E-01	0.971516604949E-01	-0.361294926039E-01	
2.04958068535	6.96510445389	-2.59023560246	
HA	588		
-0.5451203211	7.829792299	6.652735307	
0.443727324638E-01	0.614288552868E-01	-0.225826228704E-01	
2.10881764802	2.91941124500	-1.07324095235	
HA	589		
-0.2422234206	7.074626225	5.101440509	
0.404826732164E-01	0.586947828821E-01	-0.173127448051E-01	
1.88299837071	2.73011073022	-0.805279584334	
CT3	590		
0.2264621537	4.662952475	5.732189365	
-0.309565549254E-01	0.372154123430E-01	-0.156354875622E-01	
-16.5686184390	19.9184944400	-8.36845146851	
HA	591		
-0.9427747443E-01	3.636099827	5.908428018	
-0.609776190023E-01	0.510665343119E-01	-0.741664222310E-02	

	-4.50271642933	3.77086096173	-0.547660557017
HA	592		
	-0.7017627898E-01	4.914985149	4.714160670
	-0.215371294676E-01	0.295129654741E-01	-0.150344419668E-01
	-1.00003466204	1.37037707360	-0.698095032294
HA	593		
	1.316558971	4.664475250	5.751909594
	-0.320255069540E-01	0.159115945177E-01	-0.153601498839E-01
	-0.807530570356	0.401214538604	-0.387309734528

#####

Nonylphenol / silicalite

#####

CA	577		
	-0.9403542414E-01	2.871507283	6.248936506
	0.114142697872E-01	-0.304550434892E-01	0.155431212470E-01
	5.54383660911	-14.7918165748	7.54919291336
CA	578		
	0.6534393171	3.961465379	6.712932642
	0.983362046676E-02	-0.233526435762E-01	0.238874880757E-01
	2.60478313818	-6.18577587216	6.32744840656
HP	579		
	1.680490727	3.831780412	7.012782076
	0.287601449914E-02	-0.256993063814E-01	0.501943331731E-01
	0.197639718754	-1.76605635573	3.44935461707
CA	580		
	0.8264770204E-01	5.238962441	6.773494441
	0.171148434015E-01	-0.149401442206E-01	0.888631450614E-02
	37.8233981895	-33.0173645536	19.6385443979
HP	581		
	0.6826555358	6.071640153	7.112578448
	0.279730581537E-02	-0.232533811362E-02	0.277412467244E-02
	1.56245169519	-1.29883134606	1.54950373081
CA	582		
	-1.250671219	5.435035317	6.389733022
	0.254725100036E-01	-0.180958244056E-01	0.420756687231E-02
	8.96028964529	-6.36544368899	1.48006685924
OH1	583		
	-1.800611488	6.685241373	6.424704641
	0.263258283890E-01	-0.180572349583E-01	0.209110002087E-01
	2.08096398857	-1.42736080803	1.65294089729
H	584		
	-2.638840506	6.788580203	5.960333336
	0.409372459501E-01	0.601323609151E-03	-0.340550111124E-02
	2.89752900317	0.425615489603E-01	-0.241040597899
CA	585		
	-2.009512987	4.341522613	5.962425547
	0.133980475488E-01	-0.396318791161E-02	-0.352402357641E-02
	7.86138899894	-2.32542553201	-2.06774308531
HP	586		
	-3.047626745	4.462151910	5.697781615
	0.114725693020E-01	-0.188212664990E-03	0.417923531005E-03
	5.68229677702	-0.932206371146E-01	0.206995091576
CA	587		
	-1.425432429	3.075712535	5.868984674
	0.581688226193E-03	-0.396778514764E-03	0.463890866978E-05
	12.0549636284	-8.22287670374	0.961371964765E-01
HP	588		
	-2.016063368	2.256053721	5.496095348

	0.228375822605E-01	0.192951941375E-02	-0.410230808348E-01
	1.19138408296	0.100658585094	-2.14007967145
CT2	589		
	0.5370359523	1.496530078	6.118206435
	0.938019613815E-03	-0.399374657081E-01	0.241634487980E-01
	0.347657154608	-14.8019780033	8.95567185475
HA	590		
	0.8763876016	1.402583404	5.086570283
	0.235763489739E-01	-0.358496655921E-01	0.311253857135E-01
	1.74023950882	-2.64616902772	2.29745606522
HA	591		
	1.427025828	1.450917797	6.744851639
	-0.136696528328E-01	-0.551277150381E-01	0.440696404625E-01
	-0.788101663454	-3.17829899965	2.54076364493
CT2	592		
	-0.4184798367	0.3334964177	6.425691716
	-0.147179513276E-01	-0.374423481714E-01	-0.122358860172E-01
	-1.16294648036	-2.95852636370	-0.966824815563
HA	593		
	-1.286792438	0.7231350595	6.947496032
	-0.464273970521E-01	-0.537418959656E-01	-0.545105493180E-01
	-1.58363179068	-1.83312828947	-1.85934694402
HA	594		
	-0.7930460740	-0.6298334767E-01	5.482998095
	0.117204619983E-01	-0.234549461348E-01	-0.252642782251E-01
	0.578426999416	-1.15754601791	-1.24683998363
CT2	595		
	0.1615547859	-0.7941294250	7.293374433
	-0.433182952286E-01	-0.536178451011E-01	-0.115682505703E-01
	-0.239497434684	-0.296441406275	-0.639583418680E-01
HA	596		
	1.183592263	-0.5646271650	7.589565913
	-0.477332182728E-01	-0.594744425329E-01	0.546151110360E-02
	-2.33915135735	-2.91452636156	0.267639634900
HA	597		
	-0.4137221085	-0.8350611486	8.218335114
	-0.476879468810E-02	-0.231967216970E-02	0.272323345789E-02
	-4.32544200288	-2.10401329728	2.47005567504
CT2	598		
	0.7938325722E-01	-2.170734979	6.613511090
	-0.297921061479E-01	-0.593843635784E-01	0.110538566044E-01
	-4.05295463579	-8.07872160713	1.50378020090
HA	599		
	-0.8347486976	-2.665745755	6.935883656
	-0.265177439905E-01	-0.772130958666E-01	0.645772369384E-02
	-1.01967565554	-2.96904269729	0.248316132893
HA	600		
	-0.1152284095E-01	-2.054420267	5.533540699
	-0.225906355517E-01	-0.651401525199E-01	0.920290211425E-02
	-0.368215403386	-1.06175001061	0.150002433821
CT2	601		
	1.290853231	-3.064098424	6.905700313
	-0.208668930992E-01	-0.463656763441E-01	0.312066756946E-01
	-4.38339301280	-9.73978161264	6.55541404953
HA	602		
	1.837932313	-3.196659324	5.973683648
	-0.224844735896E-02	-0.315735741894E-01	0.399813954223E-01
	-0.618145398764E-01	-0.868023862333	1.09917252534
HA	603		
	1.970250563	-2.556140926	7.585948414
	-0.408909078947E-01	-0.445319846335E-01	0.497546712174E-01
	-1.34684423863	-1.46677220014	1.63879443437
CT2	604		

	0.9386802136	-4.431910952	7.512479088
	-0.587457716299E-02	-0.486490158428E-01	0.164551224345E-01
	-1.45887493780	-12.0813512177	4.08641593295
HA	605		
	1.444450829	-4.541273553	8.471547742
	-0.190647223159E-02	-0.173568275138E-01	0.131343152995E-01
	-0.949872708760E-01	-0.864779276236	0.654398603058
HA	606		
	-0.1233744595	-4.489573118	7.745302379
	-0.16477958184E-02	-0.169785731033E-02	0.498831250403E-03
	-2.27653434902	-2.34569211528	0.689165410902
CT2	607		
	1.337183222	-5.610763845	6.612885714
	0.499234530033E-02	-0.307505284017E-01	0.559128894630E-02
	1.17092507920	-7.21235466261	1.31140377086
HA	608		
	1.972441266	-5.289603697	5.787845407
	0.240314183577E-01	-0.279328607639E-01	0.214797328863E-01
	0.762012560593	-0.885723449136	0.681101132440
HA	609		
	1.954238859	-6.294561476	7.193819992
	-0.114336118145E-01	-0.523229383208E-01	0.999316664858E-04
	-0.537951793489	-2.46179588454	0.470178803380E-02
CT2	610		
	0.1285598538	-6.353662914	6.030769248
	0.465333923784E-02	-0.111435393844E-01	-0.949333475694E-02
	1.95307855881	-4.67711609418	-3.98449965019
HA	611		
	-0.7537999581	-5.714549135	6.046439058
	0.118798544284E-01	-0.631962365090E-02	-0.586080343518E-02
	3.70649061213	-1.97170982822	-1.82855884666
HA	612		
	0.3199244818	-6.575451997	4.980214863
	0.336980935637E-02	-0.340496560094E-02	-0.115361559458E-01
	1.42445460410	-1.43931552622	-4.87645700773
CT3	613		
	-0.1916975367	-7.653898540	6.773761348
	-0.114061777920E-01	-0.460433946717E-02	-0.117327772108E-01
	-4.63539922205	-1.87117472421	-4.76812718051
HA	614		
	0.4649429100	-7.815914772	7.627538229
	-0.214063540236E-01	-0.365493143299E-02	-0.331639763339E-02
	-2.06478967604	-0.352543206619	-0.319889299576
HA	615		
	-1.214607411	-7.638328013	7.145887501
	-0.166079089656E-01	0.347940575351E-03	-0.270434931451E-01
	-0.714461816867	0.149681851064E-01	-1.16339409657
HA	616		
	-0.9485414572E-01	-8.512349407	6.108257090
	-0.804194103116E-04	-0.550896051226E-02	-0.439072843682E-02
	-0.513425031433E-01	-3.51710888355	-2.80319126558

#####
#####

Bisphenol-a / silicalite

CT1	577		
	0.6969125865	-4.384248794	-6.903109774
	0.253687823314	-0.186395408627	-0.172547413678
	122.866475479	-90.2753100416	-83.5684278996
CT3	578		
	2.222457749	-4.586906571	-6.985621473
	0.175868923627	-0.263829438313	0.461474354871E-01
	90.5324615787	-135.812103667	23.7554244606
HA	579		
	2.613339992	-5.232032470	-6.201683093
	0.963203574189E-01	-0.547888656284E-02	0.255845863500
	8.25685862433	-0.469665945812	21.9318447434
HA	580		
	2.478204552	-5.035588845	-7.945673521
	0.143337096134	-0.459106767189	-0.747782729617E-01
	15.8276162725	-50.6956394066	-8.25719120790
HA	581		
	2.723398327	-3.624988295	-6.919878365
	0.256607247458	-0.291256866733	-0.396857693676
	18.0336842984	-20.4687686589	-27.8901177969
CT3	582		
	0.1448303467	-5.094117705	-5.652069880
	0.225356867053	0.443523193698	0.208841380198
	163.217736194	321.227626969	151.256173132
HA	583		
	-0.5209811507	-5.903268412	-5.952294951
	0.368917878254	0.479700293473	0.368354017993
	120.422717748	156.584477060	120.238661651
HA	584		
	0.9238723971	-5.506401736	-5.015393403
	0.174961251501	0.711697513106	0.450825121475
	19.3977412949	78.9050382354	49.9824332563
HA	585		
	-0.4311969983	-4.380392578	-5.071093646
	0.237014445598	0.747015059306	-0.134694207294
	17.5836935994	55.4197609509	-9.99273130670
CA	586		
	0.3515049184	-2.795629250	-6.729992542
	0.585869268164	-0.595605876840E-01	-1.03880126808
	7845.24121663	-31390.5473313	-4101.15545428
CA	587		
	-0.7059088851	-2.193589452	-7.399525313
	2.45813467916	0.559325581925	-3.43922923253
	-8030.66666257	14375.9402495	-1310.73022956
HP	588		
	1.982209145	-2.395554312	-5.406085911
	-2.74051196907	-1.17460308556	3.39538190010
	-1029.84026234	1234.71674820	226.623905452
CA	589		
	-0.9564233391	-0.8411427937	-7.285312601
	2.48252971830	0.555550742059	-3.34102143005
	-175.180914792	141.698359207	-44.2870076864
HP	590		
	1.532792220	-0.3478050583E-02	-5.214303262
	-2.67094177153	-1.17414707775	3.55272261391
	366.309645926	-514.655262773	-983.307996965
CA	591		
	-0.1472287618	-0.4931250002E-01	-6.491182937
	0.617613464059	-0.73376685525E-01	-0.813620673287

	-77.2936642434	-1837.01863240	947.737894934
OH1	592		
	-0.4369695694	1.268201356	-6.307656177
	0.157059654873	-0.256275664942	-0.420667380860
	83.5724265513	-136.365887233	-223.839749413
H	593		
	-1.067888448	1.363164322	-5.583714671
	0.490516293723	-0.177437869630	-0.247033439502
	78.1587171369	-28.2728962100	-39.3622331581
CA	594		
	0.9101051373	-0.6258591523	-5.821344910
	-1.24941798517	-0.692412250841	1.60065366469
	304.207514590	-139.873415738	-424.749512413
HP	595		
	-1.780472933	-0.4067915356	-7.818714186
	3.96342374216	1.04426390278	-5.23088634434
	838.376266463	-436.861702113	-521.388393824
CA	596		
	1.153223875	-1.982496912	-5.941279339
	-1.26001858008	-0.683736141193	1.48102545363
	1450.24641782	17126.7445443	6397.08077416
HP	597		
	-1.333242882	-2.790907581	-8.033774561
	3.95588244146	1.05715615633	-5.38948982891
	-1282.93899770	1417.35967352	-503.470818578
CA	598		
	0.7931136817E-01	-5.071908779	-8.246130382
	0.225882352422	-0.555999855116	0.458379658061E-01
	10722.3610647	11926.8132854	26496.9463947
CA	599		
	0.2482117583	-4.476100498	-9.496085242
	5.13356409866	-3.79919004516	-0.836922079203
	-2789.66666860	-2322.51358860	-17145.3858181
HP	600		
	-0.8670122069	-6.705544469	-7.250367297
	-8.66363834013	5.51560997084	1.55868326991
	-757.159613407	-1090.45131063	-321.694452167
CA	601		
	-0.3314578621	-4.997792459	-10.62739715
	5.01681891192	-3.58702704252	-0.874939972009
	8.29521061524	-100.867340828	-66.8936056234
HP	602		
	-1.897125384	-7.626630941	-9.239142687
	-8.88599030072	5.93623135152	1.47904583084
	1783.01681556	854.877408137	2553.71407740
CA	603		
	-1.110363662	-6.142335649	-10.54539323
	-0.549889803285E-01	-0.751221144477E-01	-0.327084447976E-01
	-285.160701492	2172.23764751	612.843455503
OH1	604		
	-1.709146814	-6.647608428	-11.66015202
	0.184715359225	-0.942304482752E-01	-0.145550080386
	112.216921581	-57.2461914862	-88.4235183547
H	605		
	-2.237198969	-7.426056034	-11.44700834
	-0.152572443693	0.153254324499	-0.924803979319E-01
	-43.2971819652	43.4906868773	-26.2441927293
CA	606		
	-1.293570921	-6.743643679	-9.321783507
	-4.93682038928	3.17648035188	0.834257307900
	564.492024399	339.442572227	423.617501962
HP	607		
	-0.2022463204	-4.537039802	-11.58516923

8.79542792877	-6.07121442910	-1.56023457838
406.449132674	505.898849585	-14.3598727728
CA 608		
-0.7016121506	-6.209966905	-8.183591117
-4.78150261676	2.92537187519	0.871218585010
-9528.55281226	-12195.7885806	-11382.5471019
HP 609		
0.8316571916	-3.581269086	-9.575212799
9.12702649443	-6.46546216238	-1.54333395513
-93.0474503755	-187.807999790	-1156.18099066

#####

FIELD:

TIP3P water / silicalite

#####

```

UNITS kj
MOLECULES 2
Silicalite
NUMMOLS 1
ATOMS 576
OZ      15.99940   -1.02500   384    0
Si      28.08550    2.05000   192    0
FINISH
Molecule name Water
nummols 16
atoms 3
OT      15.99940   -0.83400    1    0    1TIP3
HT      1.00797     0.41700    1    0    1TIP3
HT      1.00797     0.41700    1    0    1TIP3
bonds 2
harm   1      2      4623.08     0.94500
harm   1      3      4623.08     0.94500
angles 1
harm   2      1      3      459.80000   104.52000
finish
VDW    10
OZ      OZ      buck   125997.200   0.35940   18920.32
Si      OZ      buck   1717021.83    0.20490   13063.80
Si      Si      lj     0.0000    0.0000
OT      OT      lj     0.6357    3.1506
HT      OT      lj     0.3496    1.1226
HT      HT      lj     0.1923    0.4000
OT      OZ      lj     0.6885    2.9733
OT      Si      lj     0.0000    0.0000
HT      OZ      lj     0.3785    1.0594
HT      Si      lj     0.0000    0.0000
TBP    1
OZ      Si      OZ      bvs1   70337.9600   109.470000   0.32770000   0.32770000
2.0000000
CLOSE

#####

```

SPC water / silicalite

```
#####
UNITS kj
MOLECULES 2
Silicalite
NUMMOLS      1
ATOMS      576
OZ          15.99940    -1.025000   384      0
Si          28.08550     2.050000   192      0
FINISH
Molecule name Water
nummols 16
atoms 3
OSPC       16.0000    -0.82      1      0      1
HSPEC      1.0008      0.41      2      0      1
RIGID 1
  3   1   2   3
finish
VDW       10
OZ         OZ      buck  125997.200    0.35940  18920.32
Si         OZ      buck  1717021.83   0.20490  13063.80
Si         Si      lj    0.2450      3.3900
OSPC      OSPC     lj    0.6318      3.1657
HSPEC      OSPC     lj    0.0000      0.0000
HSPEC      HSPC     lj    0.0000      0.0000
OSPC      OZ      lj    0.6861      2.9804
OSPC      Si      lj    0.3934      3.2759
HSPEC      OZ      lj    0.0000      0.0000
HSPEC      Si      lj    0.000000    0.000000
TBP        1
OZ         Si      OZ      bvs1  70337.9600  109.470000  0.32770000  0.32770000
2.0000000
CLOSE
```

```
#####
```

OPLS-AA benzene / silicalite

```
#####
UNITS kj
MOLECULES 2
Silicalite
NUMMOLS      1
ATOMS      576
OZ          15.99940    -1.025000   384      0
Si          28.08550     2.050000   192      0
FINISH
Molecule name Benzene
nummols 1
atoms 12
CA          12.01100   -0.11500    1      0
HP          1.00797    0.11500    1      0
CA          12.01100   -0.11500    1      0
HP          1.00797    0.11500    1      0
CA          12.01100   -0.11500    1      0
HP          1.00797    0.11500    1      0
CA          12.01100   -0.11500    1      0
HP          1.00797    0.11500    1      0
CA          12.01100   -0.11500    1      0
HP          1.00797    0.11500    1      0
CA          12.01100   -0.11500    1      0
```

HP		1.00797	0.11500	1	0			
bonds 12								
harm	1	3	3924.59	1.40000				
harm	1	11	3924.59	1.40000				
harm	1	2	3071.05	1.08000				
harm	3	5	3924.59	1.40000				
harm	3	4	3071.05	1.08000				
harm	5	7	3924.59	1.40000				
harm	5	6	3071.05	1.08000				
harm	7	9	3924.59	1.40000				
harm	7	8	3071.05	1.08000				
harm	9	11	3924.59	1.40000				
harm	9	10	3071.05	1.08000				
harm	11	12	3071.05	1.08000				
angles 18								
harm	3	1	11	527.1840	120.00000			
harm	3	1	2	292.8800	120.00000			
harm	11	1	2	292.8800	120.00000			
harm	1	3	5	527.1840	120.00000			
harm	1	3	4	292.8800	120.00000			
harm	5	3	4	292.8800	120.00000			
harm	3	5	7	527.1840	120.00000			
harm	3	5	6	292.8800	120.00000			
harm	7	5	6	292.8800	120.00000			
harm	5	7	9	527.1840	120.00000			
harm	5	7	8	292.8800	120.00000			
harm	9	7	8	292.8800	120.00000			
harm	7	9	11	527.1840	120.00000			
harm	7	9	10	292.8800	120.00000			
harm	11	9	10	292.8800	120.00000			
harm	1	11	9	527.1840	120.00000			
harm	1	11	12	292.8800	120.00000			
harm	9	11	12	292.8800	120.00000			
dihedral 24								
opls	11	1	3	5	0.00000	0.00000	30.30500	0.00000
180.00000								
opls	11	1	3	4	0.00000	0.00000	30.30500	0.00000
180.00000								
opls	2	1	3	5	0.00000	0.00000	30.30500	0.00000
180.00000								
opls	2	1	3	4	0.00000	0.00000	30.30500	0.00000
180.00000								
opls	3	1	11	9	0.00000	0.00000	30.30500	0.00000
180.00000								
opls	3	1	11	12	0.00000	0.00000	30.30500	0.00000
180.00000								
opls	2	1	11	9	0.00000	0.00000	30.30500	0.00000
180.00000								
opls	2	1	11	12	0.00000	0.00000	30.30500	0.00000
180.00000								
opls	1	3	5	7	0.00000	0.00000	30.30500	0.00000
180.00000								
opls	1	3	5	6	0.00000	0.00000	30.30500	0.00000
180.00000								
opls	4	3	5	7	0.00000	0.00000	30.30500	0.00000
180.00000								
opls	4	3	5	6	0.00000	0.00000	30.30500	0.00000
180.00000								
opls	3	5	7	9	0.00000	0.00000	30.30500	0.00000
180.00000								
opls	3	5	7	8	0.00000	0.00000	30.30500	0.00000
180.00000								

```

opls   6      5      7      9      0.00000    0.00000    30.30500    0.00000
180.00000
opls   6      5      7      8      0.00000    0.00000    30.30500    0.00000
180.00000
opls   5      7      9      11     0.00000    0.00000    30.30500    0.00000
180.00000
opls   5      7      9      10     0.00000    0.00000    30.30500    0.00000
180.00000
opls   8      7      9      11     0.00000    0.00000    30.30500    0.00000
180.00000
opls   8      7      9      10     0.00000    0.00000    30.30500    0.00000
180.00000
opls   7      9      11     1      0.00000    0.00000    30.30500    0.00000
180.00000
opls   7      9      11     12     0.00000    0.00000    30.30500    0.00000
180.00000
opls   10     9      11     1      0.00000    0.00000    30.30500    0.00000
180.00000
opls   10     9      11     12     0.00000    0.00000    30.30500    0.00000
180.00000
finish
VDW   10
OZ    OZ      buck   125997.200    0.35940    18920.32
Si    OZ      buck   1717021.83    0.20490    13063.80
Si    Si      lj     0.0000    0.0000
CA    CA      lj     0.2930    3.5501
HP    CA      lj     0.1921    2.9310
HP    HP      lj     0.1260    2.4200
CA    Si      lj     0.0000    0.0000
CA    OZ      lj     0.4672    3.1562
HP    Si      lj     0.0000    0.0000
HP    OZ      lj     0.3063    2.6058
TBP    1
OZ    Si      OZ      bvs1   70337.9600   109.470000  0.32770000  0.32770000
2.0000000
CLOSE
#####

```

OPLS-AA phenol / silicalite

```

#####
UNITS kj
MOLECULES 2
Silicalite
NUMMOLS    1
ATOMS      576
OZ        15.99940   -1.02500   384     0
Si        28.08550    2.05000   192     0
FINISH
Molecule name Phenol
nummols 1
atoms 13
CA        12.01100    0.15000    1     0    1PHEN
OH1       15.99940   -0.58500    1     0    1PHEN
H         1.00797    0.43500    1     0    1PHEN
CA        12.01100   -0.11500    1     0    1PHEN
HP        1.00797    0.11500    1     0    1PHEN
CA        12.01100   -0.11500    1     0    1PHEN
HP        1.00797    0.11500    1     0    1PHEN
CA        12.01100   -0.11500    1     0    1PHEN
HP        1.00797    0.11500    1     0    1PHEN
CA        12.01100   -0.11500    1     0    1PHEN
HP        1.00797    0.11500    1     0    1PHEN

```

CA	12.01100	-0.11500	1	0	1PHEN			
HP	1.00797	0.11500	1	0	1PHEN			
bonds 13								
harm	1	4	3924.59	1.40000				
harm	1	12	3924.59	1.40000				
harm	1	2	2677.76	1.38000				
harm	2	3	4627.50	0.94500				
harm	4	6	3924.59	1.40000				
harm	4	5	3071.05	1.08000				
harm	6	8	3924.59	1.40000				
harm	6	7	3071.05	1.08000				
harm	8	10	3924.59	1.40000				
harm	8	9	3071.05	1.08000				
harm	10	12	3924.59	1.40000				
harm	10	11	3071.05	1.08000				
harm	12	13	3071.05	1.08000				
angles 19								
harm	4	1	12	527.1840	120.00000			
harm	4	1	2	585.7600	120.00000			
harm	12	1	2	585.7600	120.00000			
harm	1	2	3	292.8800	108.50000			
harm	1	4	6	527.1840	120.00000			
harm	1	4	5	292.8800	120.00000			
harm	6	4	5	292.8800	120.00000			
harm	4	6	8	527.1840	120.00000			
harm	4	6	7	292.8800	120.00000			
harm	8	6	7	292.8800	120.00000			
harm	6	8	10	527.1840	120.00000			
harm	6	8	9	292.8800	120.00000			
harm	10	8	9	292.8800	120.00000			
harm	8	10	12	527.1840	120.00000			
harm	8	10	11	292.8800	120.00000			
harm	12	10	11	292.8800	120.00000			
harm	1	12	10	527.1840	120.00000			
harm	1	12	13	292.8800	120.00000			
harm	10	12	13	292.8800	120.00000			
dihedral 26								
opls	12	1	4	6	0.00000	0.00000	30.30500	0.00000
180.00000								
opls	12	1	4	5	0.00000	0.00000	30.30500	0.00000
180.00000								
opls	2	1	4	6	0.00000	0.00000	30.30500	0.00000
180.00000								
opls	2	1	4	5	0.00000	0.00000	30.30500	0.00000
180.00000								
opls	4	1	12	10	0.00000	0.00000	30.30500	0.00000
180.00000								
opls	4	1	12	13	0.00000	0.00000	30.30500	0.00000
180.00000								
opls	2	1	12	10	0.00000	0.00000	30.30500	0.00000
180.00000								
opls	2	1	12	13	0.00000	0.00000	30.30500	0.00000
180.00000								
opls	4	1	2	3	0.00000	0.00000	7.037600	0.00000
180.00000								
opls	12	1	2	3	0.00000	0.00000	7.037600	0.00000
180.00000								
opls	1	4	6	8	0.00000	0.00000	30.30500	0.00000
180.00000								
opls	1	4	6	7	0.00000	0.00000	30.30500	0.00000
180.00000								
opls	5	4	6	8	0.00000	0.00000	30.30500	0.00000
180.00000								

```

opls      5     4     6     7     0.00000   0.00000   30.30500   0.00000
180.00000
opls      4     6     8    10     0.00000   0.00000   30.30500   0.00000
180.00000
opls      4     6     8     9     0.00000   0.00000   30.30500   0.00000
180.00000
opls      7     6     8    10     0.00000   0.00000   30.30500   0.00000
180.00000
opls      7     6     8     9     0.00000   0.00000   30.30500   0.00000
180.00000
opls      6     8    10    12     0.00000   0.00000   30.30500   0.00000
180.00000
opls      6     8    10    11     0.00000   0.00000   30.30500   0.00000
180.00000
opls      9     8    10    12     0.00000   0.00000   30.30500   0.00000
180.00000
opls      9     8    10    11     0.00000   0.00000   30.30500   0.00000
180.00000
opls      8    10    12     1     0.00000   0.00000   30.30500   0.00000
180.00000
opls      8    10    12    13     0.00000   0.00000   30.30500   0.00000
180.00000
opls     11    10    12     1     0.00000   0.00000   30.30500   0.00000
180.00000
opls     11    10    12    13     0.00000   0.00000   30.30500   0.00000
180.00000
finish
VDW      21
OZ       OZ     buck  125997.200   0.35940   18920.32
Si       OZ     buck  1717021.83   0.20490   13063.80
Si       Si     1j    0.00000   0.00000
CA       CA     1j    0.2930    3.5500
OH1      CA     1j    0.4564    3.3101
H        CA     1j    0.00000   0.0000
HP       CA     1j    0.19214   2.9310
OH1      OH1    1j    0.711     3.0700
H        OH1    1j    0.00000   0.0000
HP       OH1    1j    0.2822    2.7257
H        H      1j    0.00000   0.0000
HP       H      1j    0.00000   0.0000
HP       HP     1j    0.1260    2.4200
CA       Si     1j    0.0000   0.0000
CA       OZ     1j    0.4672    3.1561
HP       Si     1j    0.0000   0.0000
HP       OZ     1j    0.3064    2.6059
OH1      Si     1j    0.0000   0.0000
OH1      OZ     1j    0.7278    2.9350
H        Si     1j    0.0000   0.0000
H        OZ     1j    0.0000   0.0000
TBP      1
OZ       Si     OZ     bvs1   70337.9600  109.470000  0.32770000  0.32770000
2.0000000
CLOSE
#####

```

OPLS-AA toluene / silicalite

```
#####
#####
```

UNITS kj
MOLECULES 2
Silicalite
NUMMOLS 1
ATOMS 576
OZ 15.99940 -1.02500 384 0
Si 28.08550 2.05000 192 0
FINISH
Molecule name Toluene
nummols 1
atoms 15
CT3 12.01100 -0.06500 1 0 1TOLU
HA 1.00797 0.06000 1 0 1TOLU
HA 1.00797 0.06000 1 0 1TOLU
HA 1.00797 0.06000 1 0 1TOLU
CA 12.01100 -0.11500 1 0 1TOLU
CA 12.01100 -0.11500 1 0 1TOLU
HP 1.00797 0.11500 1 0 1TOLU
CA 12.01100 -0.11500 1 0 1TOLU
HP 1.00797 0.11500 1 0 1TOLU
CA 12.01100 -0.11500 1 0 1TOLU
HP 1.00797 0.11500 1 0 1TOLU
CA 12.01100 -0.11500 1 0 1TOLU
HP 1.00797 0.11500 1 0 1TOLU
bonds 15
harm 1 5 2652.65 1.51000
harm 1 2 2845.12 1.09000
harm 1 3 2845.12 1.09000
harm 1 4 2845.12 1.09000
harm 5 6 3924.59 1.40000
harm 5 14 3924.59 1.40000
harm 6 8 3924.59 1.40000
harm 6 7 3071.05 1.08000
harm 8 10 3924.59 1.40000
harm 8 9 3071.05 1.08000
harm 10 12 3924.59 1.40000
harm 10 11 3071.05 1.08000
harm 12 14 3924.59 1.40000
harm 12 13 3071.05 1.08000
harm 14 15 3071.05 1.08000
angles 24
harm 5 1 2 292.8800 109.50000
harm 5 1 3 292.8800 109.50000
harm 5 1 4 292.8800 109.50000
harm 2 1 3 276.1440 107.80000
harm 2 1 4 276.1440 107.80000
harm 3 1 4 276.1440 107.80000
harm 1 5 6 585.7600 120.00000
harm 1 5 14 585.7600 120.00000
harm 6 5 14 527.18400 120.00000
harm 5 6 8 527.18400 120.00000
harm 5 6 7 292.8800 120.00000
harm 8 6 7 292.8800 120.00000
harm 6 8 10 527.18400 120.00000
harm 6 8 9 292.8800 120.00000
harm 10 8 9 292.8800 120.00000
harm 8 10 12 527.18400 120.00000
harm 8 10 11 292.8800 120.00000

harm	12	10	11	292.8800	120.00000			
harm	10	12	14	527.18400	120.00000			
harm	10	12	13	292.8800	120.00000			
harm	14	12	13	292.8800	120.00000			
harm	12	14	5	527.18400	120.00000			
harm	12	14	15	292.8800	120.00000			
harm	5	14	15	292.8800	120.00000			
dihedral	30							
opls	2	1	5	6	0.00000	0.00000	0.00000	0.00000
180.00000								
opls	2	1	5	14	0.00000	0.00000	0.00000	0.00000
180.00000								
opls	3	1	5	6	0.00000	0.00000	0.00000	0.00000
180.00000								
opls	3	1	5	14	0.00000	0.00000	0.00000	0.00000
180.00000								
opls	4	1	5	6	0.00000	0.00000	0.00000	0.00000
180.00000								
opls	4	1	5	14	0.00000	0.00000	0.00000	0.00000
180.00000								
opls	1	5	6	8	0.00000	0.00000	30.305000	0.00000
180.00000								
opls	1	5	6	7	0.00000	0.00000	30.305000	0.00000
180.00000								
opls	14	5	6	8	0.00000	0.00000	30.305000	0.00000
180.00000								
opls	14	5	6	7	0.00000	0.00000	30.305000	0.00000
180.00000								
opls	1	5	14	12	0.00000	0.00000	30.305000	0.00000
180.00000								
opls	1	5	14	15	0.00000	0.00000	30.305000	0.00000
180.00000								
opls	6	5	14	12	0.00000	0.00000	30.305000	0.00000
180.00000								
opls	6	5	14	15	0.00000	0.00000	30.305000	0.00000
180.00000								
opls	5	6	8	10	0.00000	0.00000	30.305000	0.00000
180.00000								
opls	5	6	8	9	0.00000	0.00000	30.305000	0.00000
180.00000								
opls	7	6	8	10	0.00000	0.00000	30.305000	0.00000
180.00000								
opls	7	6	8	9	0.00000	0.00000	30.305000	0.00000
180.00000								
opls	6	8	10	12	0.00000	0.00000	30.305000	0.00000
180.00000								
opls	6	8	10	11	0.00000	0.00000	30.305000	0.00000
180.00000								
opls	9	8	10	12	0.00000	0.00000	30.305000	0.00000
180.00000								
opls	9	8	10	11	0.00000	0.00000	30.305000	0.00000
180.00000								
opls	8	10	12	14	0.00000	0.00000	30.305000	0.00000
180.00000								
opls	8	10	12	13	0.00000	0.00000	30.305000	0.00000
180.00000								
opls	11	10	12	14	0.00000	0.00000	30.305000	0.00000
180.00000								
opls	11	10	12	13	0.00000	0.00000	30.305000	0.00000
180.00000								
opls	10	12	14	5	0.00000	0.00000	30.305000	0.00000
180.00000								

```

opls     10    12    14    15      0.00000    0.00000   30.305000   0.00000
180.00000
opls     13    12    14     5      0.00000    0.00000   30.305000   0.00000
180.00000
opls     13    12    14    15      0.00000    0.00000   30.305000   0.00000
180.00000
finish
VDW     21
OZ     OZ      buck   125997.200      0.35940   18920.32
Si     OZ      buck   1717021.83       0.20490   13063.80
Si     Si      lj      0.0000      0.0000
CT3    CT3     lj      0.2760      3.5000
HA     CT3     lj      0.1865      2.9580
CA     CT3     lj      0.2844      3.5249
HP     CT3     lj      0.1864      2.9103
HA     HA      lj      0.1260      2.5000
CA     HA      lj      0.1921      2.9791
HP     HA      lj      0.1260      2.4597
CA     CA      lj      0.2930      3.5500
HP     CA      lj      0.1921      2.9310
HP     HP      lj      0.1260      2.4200
CA     Si      lj      0.0000      0.0000
CA     OZ      lj      0.4672      3.1562
CT3    Si      lj      0.0000      0.0000
CT3    OZ      lj      0.4534      3.1338
HA     Si      lj      0.0000      0.0000
HA     OZ      lj      0.3064      2.6486
HP     Si      lj      0.0000      0.0000
HP     OZ      lj      0.3064      2.6059
TBP     1
OZ     Si      OZ      bvs1   70337.9600   109.470000   0.32770000   0.32770000
2.0000000
CLOSE
#####

```

OPLS-AA neopentane / silicalite

```
#####

```

```

UNITS kj
MOLECULES 2
Silicalite
NUMMOLS     1
ATOMS      576
OZ        15.99940   -1.02500   384    0
Si        28.08550    2.05000   192    0
FINISH
Molecule name not_define
nummols 1
atoms 17
CT1      12.01100    0.00000    1    0    1PDIM
CT3      12.01100   -0.18000    1    0    1PDIM
HA       1.00797    0.06000    1    0    1PDIM
HA       1.00797    0.06000    1    0    1PDIM
HA       1.00797    0.06000    1    0    1PDIM
CT3      12.01100   -0.18000    1    0    1PDIM
HA       1.00797    0.06000    1    0    1PDIM
HA       1.00797    0.06000    1    0    1PDIM
HA       1.00797    0.06000    1    0    1PDIM
CT3      12.01100   -0.18000    1    0    1PDIM
HA       1.00797    0.06000    1    0    1PDIM
HA       1.00797    0.06000    1    0    1PDIM
HA       1.00797    0.06000    1    0    1PDIM

```

CT3		12.01100	-0.18000	1	0	1PDIM		
HA		1.00797	0.06000	1	0	1PDIM		
HA		1.00797	0.06000	1	0	1PDIM		
HA		1.00797	0.06000	1	0	1PDIM		
bonds	16							
harm	1	2	2242.62	1.52900				
harm	1	6	2242.62	1.52900				
harm	1	10	2242.62	1.52900				
harm	1	14	2242.62	1.52900				
harm	2	3	2845.12	1.09000				
harm	2	4	2845.12	1.09000				
harm	2	5	2845.12	1.09000				
harm	6	7	2845.12	1.09000				
harm	6	8	2845.12	1.09000				
harm	6	9	2845.12	1.09000				
harm	10	11	2845.12	1.09000				
harm	10	12	2845.12	1.09000				
harm	10	13	2845.12	1.09000				
harm	14	15	2845.12	1.09000				
harm	14	16	2845.12	1.09000				
harm	14	17	2845.12	1.09000				
angles	30							
harm	2	1	6	488.27300	112.70000			
harm	2	1	10	488.27300	112.70000			
harm	2	1	14	488.27300	112.70000			
harm	6	1	10	488.27300	112.70000			
harm	6	1	14	488.27300	112.70000			
harm	10	1	14	488.27300	112.70000			
harm	1	2	3	313.80000	110.7			
harm	1	2	4	313.80000	110.7			
harm	1	2	5	313.80000	110.7			
harm	3	2	4	276.144000	107.8000			
harm	3	2	5	276.144000	107.8000			
harm	4	2	5	276.144000	107.8000			
harm	1	6	7	313.80000	110.7			
harm	1	6	8	313.80000	110.7			
harm	1	6	9	313.80000	110.7			
harm	7	6	8	276.144000	107.8000			
harm	7	6	9	276.144000	107.8000			
harm	8	6	9	276.144000	107.8000			
harm	1	10	11	313.80000	110.7			
harm	1	10	12	313.80000	110.7			
harm	1	10	13	313.80000	110.7			
harm	11	10	12	276.144000	107.8000			
harm	11	10	13	276.144000	107.8000			
harm	12	10	13	276.144000	107.8000			
harm	1	14	15	313.80000	110.7			
harm	1	14	16	313.80000	110.7			
harm	1	14	17	313.80000	110.7			
harm	15	14	16	276.144000	107.8000			
harm	15	14	17	276.144000	107.8000			
harm	16	14	17	276.144000	107.8000			
dihedral	36							
opls	6	1	2	3	0.00000	0.00000	0.00000	1.25400
180.00000								
opls	6	1	2	4	0.00000	0.00000	0.00000	1.25400
180.00000								
opls	6	1	2	5	0.00000	0.00000	0.00000	1.25400
180.00000								
opls	10	1	2	3	0.00000	0.00000	0.00000	1.25400
180.00000								
opls	10	1	2	4	0.00000	0.00000	0.00000	1.25400
180.00000								

opls	10	1	2	5	0.00000	0.00000	0.00000	1.25400
180.00000								
opls	14	1	2	3	0.00000	0.00000	0.00000	1.25400
180.00000								
opls	14	1	2	4	0.00000	0.00000	0.00000	1.25400
180.00000								
opls	14	1	2	5	0.00000	0.00000	0.00000	1.25400
180.00000								
opls	2	1	6	7	0.00000	0.00000	0.00000	1.25400
180.00000								
opls	2	1	6	8	0.00000	0.00000	0.00000	1.25400
180.00000								
opls	2	1	6	9	0.00000	0.00000	0.00000	1.25400
180.00000								
opls	10	1	6	7	0.00000	0.00000	0.00000	1.25400
180.00000								
opls	10	1	6	8	0.00000	0.00000	0.00000	1.25400
180.00000								
opls	10	1	6	9	0.00000	0.00000	0.00000	1.25400
180.00000								
opls	14	1	6	7	0.00000	0.00000	0.00000	1.25400
180.00000								
opls	14	1	6	8	0.00000	0.00000	0.00000	1.25400
180.00000								
opls	14	1	6	9	0.00000	0.00000	0.00000	1.25400
180.00000								
opls	2	1	10	11	0.00000	0.00000	0.00000	1.25400
180.00000								
opls	2	1	10	12	0.00000	0.00000	0.00000	1.25400
180.00000								
opls	2	1	10	13	0.00000	0.00000	0.00000	1.25400
180.00000								
opls	6	1	10	11	0.00000	0.00000	0.00000	1.25400
180.00000								
opls	6	1	10	12	0.00000	0.00000	0.00000	1.25400
180.00000								
opls	6	1	10	13	0.00000	0.00000	0.00000	1.25400
180.00000								
opls	14	1	10	11	0.00000	0.00000	0.00000	1.25400
180.00000								
opls	14	1	10	12	0.00000	0.00000	0.00000	1.25400
180.00000								
opls	14	1	10	13	0.00000	0.00000	0.00000	1.25400
180.00000								
opls	2	1	14	15	0.00000	0.00000	0.00000	1.25400
180.00000								
opls	2	1	14	16	0.00000	0.00000	0.00000	1.25400
180.00000								
opls	2	1	14	17	0.00000	0.00000	0.00000	1.25400
180.00000								
opls	6	1	14	15	0.00000	0.00000	0.00000	1.25400
180.00000								
opls	6	1	14	16	0.00000	0.00000	0.00000	1.25400
180.00000								
opls	6	1	14	17	0.00000	0.00000	0.00000	1.25400
180.00000								
opls	10	1	14	15	0.00000	0.00000	0.00000	1.25400
180.00000								
opls	10	1	14	16	0.00000	0.00000	0.00000	1.25400
180.00000								
opls	10	1	14	17	0.00000	0.00000	0.00000	1.25400
180.00000								
finish								

```

VDW      15
OZ      OZ      buck   125997.200    0.35940    18920.32
Si      OZ      buck   1717021.83     0.20490    13063.80
Si      Si      lj      0.0000    0.0000
CT1     CT1     lj      0.2760    3.5000
CT3     CT1     lj      0.2760    3.5000
HA      CT1     lj      0.1844    2.9580
CT3     CT3     lj      0.2760    3.5000
HA      CT3     lj      0.1844    2.9580
HA      HA      lj      0.1260    2.5000
CT1     Si      lj      0.0000    0.0000
CT1     OZ      lj      0.4534    3.1338
CT3     Si      lj      0.0000    0.0000
CT3     OZ      lj      0.4534    3.1338
HA      Si      lj      0.0000    0.0000
HA      OZ      lj      0.3064    2.6486
TBP      1
OZ      Si      OZ      bvs1    70337.9600   109.470000  0.32770000  0.32770000
2.0000000
CLOSE
#####

```

OPLS-AA nonylphenol / silicalite

```

#####
UNITS kj
MOLECULES 2
Silicalite
NUMMOLS    1
ATOMS      576
OZ        15.99940   -1.02500   384     0
Si        28.08550    2.05000   192     0
FINISH
Molecule name not_define
nummols 1
atoms 40
CA        12.01100    0.00000   1     0    1NONY
CA        12.01100   -0.11500   1     0    1NONY
HP        1.00797    0.11500   1     0    1NONY
CA        12.01100   -0.11500   1     0    1NONY
HP        1.00797    0.11500   1     0    1NONY
CA        12.01100   -0.11000   1     0    1NONY
OH1       15.99940   -0.54000   1     0    1NONY
H         1.00797    0.43000   1     0    1NONY
CA        12.01100   -0.11500   1     0    1NONY
HP        1.00797    0.11500   1     0    1NONY
CA        12.01100   -0.11500   1     0    1NONY
HP        1.00797    0.11500   1     0    1NONY
CT2       12.01100   -0.12000   1     0    1NONY
HA        1.00797    0.06000   1     0    1NONY
HA        1.00797    0.06000   1     0    1NONY
CT2       12.01100   -0.12000   1     0    1NONY
HA        1.00797    0.06000   1     0    1NONY
HA        1.00797    0.06000   1     0    1NONY
CT2       12.01100   -0.12000   1     0    1NONY
HA        1.00797    0.06000   1     0    1NONY
HA        1.00797    0.06000   1     0    1NONY
CT2       12.01100   -0.12000   1     0    1NONY
HA        1.00797    0.06000   1     0    1NONY
HA        1.00797    0.06000   1     0    1NONY
CT2       12.01100   -0.12000   1     0    1NONY
HA        1.00797    0.06000   1     0    1NONY
HA        1.00797    0.06000   1     0    1NONY

```

HA		1.00797	0.06000	1	0	1NONY
CT2		12.01100	-0.12000	1	0	1NONY
HA		1.00797	0.06000	1	0	1NONY
HA		1.00797	0.06000	1	0	1NONY
CT2		12.01100	-0.12000	1	0	1NONY
HA		1.00797	0.06000	1	0	1NONY
HA		1.00797	0.06000	1	0	1NONY
CT2		12.01100	-0.12000	1	0	1NONY
HA		1.00797	0.06000	1	0	1NONY
HA		1.00797	0.06000	1	0	1NONY
CT3		12.01100	-0.18000	1	0	1NONY
HA		1.00797	0.06000	1	0	1NONY
HA		1.00797	0.06000	1	0	1NONY
HA		1.00797	0.06000	1	0	1NONY
bonds	40					
harm	1	13	2652.65	1.51000		
harm	1	2	3924.59	1.40000		
harm	1	11	3924.59	1.40000		
harm	2	4	3924.59	1.40000		
harm	2	3	3071.06	1.08000		
harm	4	6	3924.59	1.40000		
harm	4	5	3071.06	1.08000		
harm	6	9	3924.59	1.40000		
harm	6	7	3765.60	1.36400		
harm	7	8	4627.50	0.94500		
harm	9	11	3924.59	1.40000		
harm	9	10	3071.06	1.08000		
harm	11	12	3071.06	1.08000		
harm	13	16	2242.62	1.52900		
harm	13	14	2845.12	1.0900		
harm	13	15	2845.12	1.0900		
harm	16	19	2242.62	1.52900		
harm	16	17	2845.12	1.0900		
harm	16	18	2845.12	1.0900		
harm	19	22	2242.62	1.52900		
harm	19	20	2845.12	1.0900		
harm	19	21	2845.12	1.0900		
harm	22	25	2242.62	1.52900		
harm	22	23	2845.12	1.0900		
harm	22	24	2845.12	1.0900		
harm	25	28	2242.62	1.52900		
harm	25	26	2845.12	1.0900		
harm	25	27	2845.12	1.0900		
harm	28	31	2242.62	1.52900		
harm	28	29	2845.12	1.0900		
harm	28	30	2845.12	1.0900		
harm	31	34	2242.62	1.52900		
harm	31	32	2845.12	1.0900		
harm	31	33	2845.12	1.0900		
harm	34	37	2242.62	1.52900		
harm	34	35	2845.12	1.0900		
harm	34	36	2845.12	1.0900		
harm	37	38	2845.12	1.0900		
harm	37	39	2845.12	1.0900		
harm	37	40	2845.12	1.0900		
angles	73					
harm	13	1	2	585.76000	120.00000	
harm	13	1	11	585.76000	120.00000	
harm	2	1	11	527.18400	120.00000	
harm	1	2	4	527.18400	120.00000	
harm	1	2	3	292.88000	120.00000	
harm	4	2	3	292.88000	120.00000	
harm	2	4	6	527.18400	120.00000	

harm	2	4	5	292.88000	120.00000
harm	6	4	5	292.88000	120.00000
harm	4	6	9	527.18400	120.00000
harm	4	6	7	585.76000	120.00000
harm	9	6	7	585.76000	120.00000
harm	6	7	8	292.80000	113.00000
harm	6	9	11	527.18400	120.00000
harm	6	9	10	292.88000	120.00000
harm	11	9	10	292.88000	120.00000
harm	9	11	1	527.18400	120.00000
harm	9	11	12	292.88000	120.00000
harm	1	11	12	292.88000	120.00000
harm	1	13	16	527.18400	114.00000
harm	1	13	14	292.88000	109.50000
harm	1	13	15	292.88000	109.50000
harm	16	13	14	313.80000	110.70000
harm	16	13	15	313.80000	110.70000
harm	14	13	15	276.14400	107.80000
harm	13	16	19	488.27300	112.70000
harm	13	16	17	313.80000	110.70000
harm	13	16	18	313.80000	110.70000
harm	19	16	17	313.80000	110.70000
harm	19	16	18	313.80000	110.70000
harm	17	16	18	276.14400	107.80000
harm	16	19	22	488.27300	112.70000
harm	16	19	20	313.80000	110.70000
harm	16	19	21	313.80000	110.70000
harm	22	19	20	313.80000	110.70000
harm	22	19	21	313.80000	110.70000
harm	20	19	21	276.14400	107.80000
harm	19	22	25	488.27300	112.70000
harm	19	22	23	313.80000	110.70000
harm	19	22	24	313.80000	110.70000
harm	25	22	23	313.80000	110.70000
harm	25	22	24	313.80000	110.70000
harm	23	22	24	276.14400	107.80000
harm	22	25	28	488.27300	112.70000
harm	22	25	26	313.80000	110.70000
harm	22	25	27	313.80000	110.70000
harm	28	25	26	313.80000	110.70000
harm	28	25	27	313.80000	110.70000
harm	26	25	27	276.14400	107.80000
harm	25	28	31	488.27300	112.70000
harm	25	28	29	313.80000	110.70000
harm	25	28	30	313.80000	110.70000
harm	31	28	29	313.80000	110.70000
harm	31	28	30	313.80000	110.70000
harm	29	28	30	276.14400	107.80000
harm	28	31	34	488.27300	112.70000
harm	28	31	32	313.80000	110.70000
harm	28	31	33	313.80000	110.70000
harm	34	31	32	313.80000	110.70000
harm	34	31	33	313.80000	110.70000
harm	32	31	33	276.14400	107.80000
harm	31	34	37	488.27300	112.70000
harm	31	34	35	313.80000	110.70000
harm	31	34	36	313.80000	110.70000
harm	37	34	35	313.80000	110.70000
harm	37	34	36	313.80000	110.70000
harm	35	34	36	276.14400	107.80000
harm	34	37	38	313.80000	110.70000
harm	34	37	39	313.80000	110.70000
harm	34	37	40	313.80000	110.70000

harm	38	37	39	276.14400	107.80000		
harm	38	37	40	276.14400	107.80000		
harm	39	37	40	276.14400	107.80000		
dihedral	104						
opls	2	1	13	16	0.00000	0.00000	0.00000
180.00000							
opls	2	1	13	14	0.00000	0.00000	0.00000
180.00000							
opls	2	1	13	15	0.00000	0.00000	0.00000
180.00000							
opls	11	1	13	16	0.00000	0.00000	0.00000
180.00000							
opls	11	1	13	14	0.00000	0.00000	0.00000
180.00000							
opls	11	1	13	15	0.00000	0.00000	0.00000
180.00000							
opls	13	1	2	4	0.00000	0.00000	30.305000
180.00000							
opls	13	1	2	3	0.00000	0.00000	30.305000
180.00000							
opls	11	1	2	4	0.00000	0.00000	30.305000
180.00000							
opls	11	1	2	3	0.00000	0.00000	30.305000
180.00000							
opls	13	1	11	9	0.00000	0.00000	30.305000
180.00000							
opls	13	1	11	12	0.00000	0.00000	30.305000
180.00000							
opls	2	1	11	9	0.00000	0.00000	30.305000
180.00000							
opls	2	1	11	12	0.00000	0.00000	30.305000
180.00000							
opls	1	2	4	6	0.00000	0.00000	30.305000
180.00000							
opls	1	2	4	5	0.00000	0.00000	30.305000
180.00000							
opls	3	2	4	6	0.00000	0.00000	30.305000
180.00000							
opls	3	2	4	5	0.00000	0.00000	30.305000
180.00000							
opls	2	4	6	9	0.00000	0.00000	30.305000
180.00000							
opls	2	4	6	7	0.00000	0.00000	30.305000
180.00000							
opls	5	4	6	9	0.00000	0.00000	30.305000
180.00000							
opls	5	4	6	7	0.00000	0.00000	30.305000
180.00000							
opls	4	6	9	11	0.00000	0.00000	30.305000
180.00000							
opls	4	6	9	10	0.00000	0.00000	30.305000
180.00000							
opls	7	6	9	11	0.00000	0.00000	30.305000
180.00000							
opls	7	6	9	10	0.00000	0.00000	30.305000
180.00000							
opls	4	6	7	8	0.00000	0.00000	7.0307600
180.00000							
opls	9	6	7	8	0.00000	0.00000	7.0307600
180.00000							
opls	6	9	11	1	0.00000	0.00000	30.305000
180.00000							

opls	6	9	11	12	0.00000	0.00000	30.305000	0.00000
180.00000								
opls	10	9	11	1	0.00000	0.00000	30.305000	0.00000
180.00000								
opls	10	9	11	12	0.00000	0.00000	30.305000	0.00000
180.00000								
opls	1	13	16	19	0.00000	5.43400	-0.209000	0.83600
180.00000								
opls	1	13	16	17	0.00000	5.43400	-0.209000	0.83600
180.00000								
opls	1	13	16	18	0.00000	5.43400	-0.209000	0.83600
180.00000								
opls	14	13	16	19	0.00000	0.00000	0.0000000	1.25400
180.00000								
opls	14	13	16	17	0.00000	0.00000	0.0000000	1.25400
180.00000								
opls	14	13	16	18	0.00000	0.00000	0.0000000	1.25400
180.00000								
opls	15	13	16	19	0.00000	0.00000	0.0000000	1.25400
180.00000								
opls	15	13	16	17	0.00000	0.00000	0.0000000	1.25400
180.00000								
opls	15	13	16	18	0.00000	0.00000	0.0000000	1.25400
180.00000								
opls	13	16	19	22	0.00000	5.43400	-0.209000	0.83600
180.00000								
opls	13	16	19	20	0.00000	0.00000	0.0000000	1.25400
180.00000								
opls	13	16	19	21	0.00000	0.00000	0.0000000	1.25400
180.00000								
opls	17	16	19	22	0.00000	0.00000	0.0000000	1.25400
180.00000								
opls	17	16	19	20	0.00000	0.00000	0.0000000	1.25400
180.00000								
opls	17	16	19	21	0.00000	0.00000	0.0000000	1.25400
180.00000								
opls	18	16	19	22	0.00000	0.00000	0.0000000	1.25400
180.00000								
opls	18	16	19	20	0.00000	0.00000	0.0000000	1.25400
180.00000								
opls	18	16	19	21	0.00000	0.00000	0.0000000	1.25400
180.00000								
opls	16	19	22	25	0.00000	5.43400	-0.209000	0.83600
180.00000								
opls	16	19	22	23	0.00000	0.00000	0.0000000	1.25400
180.00000								
opls	16	19	22	24	0.00000	0.00000	0.0000000	1.25400
180.00000								
opls	20	19	22	25	0.00000	0.00000	0.0000000	1.25400
180.00000								
opls	20	19	22	23	0.00000	0.00000	0.0000000	1.25400
180.00000								
opls	20	19	22	24	0.00000	0.00000	0.0000000	1.25400
180.00000								
opls	21	19	22	25	0.00000	0.00000	0.0000000	1.25400
180.00000								
opls	21	19	22	23	0.00000	0.00000	0.0000000	1.25400
180.00000								
opls	21	19	22	24	0.00000	0.00000	0.0000000	1.25400
180.00000								
opls	19	22	25	28	0.00000	5.43400	-0.209000	0.83600
180.00000								

opls	19	22	25	26	0.00000	0.00000	0.000000	1.25400
180.00000								
opls	19	22	25	27	0.00000	0.00000	0.000000	1.25400
180.00000								
opls	23	22	25	28	0.00000	0.00000	0.000000	1.25400
180.00000								
opls	23	22	25	26	0.00000	0.00000	0.000000	1.25400
180.00000								
opls	23	22	25	27	0.00000	0.00000	0.000000	1.25400
180.00000								
opls	24	22	25	28	0.00000	0.00000	0.000000	1.25400
180.00000								
opls	24	22	25	26	0.00000	0.00000	0.000000	1.25400
180.00000								
opls	24	22	25	27	0.00000	0.00000	0.000000	1.25400
180.00000								
opls	22	25	28	31	0.00000	5.43400	-0.209000	0.83600
180.00000								
opls	22	25	28	29	0.00000	0.00000	0.000000	1.25400
180.00000								
opls	22	25	28	30	0.00000	0.00000	0.000000	1.25400
180.00000								
opls	26	25	28	31	0.00000	0.00000	0.000000	1.25400
180.00000								
opls	26	25	28	29	0.00000	0.00000	0.000000	1.25400
180.00000								
opls	26	25	28	30	0.00000	0.00000	0.000000	1.25400
180.00000								
opls	27	25	28	31	0.00000	0.00000	0.000000	1.25400
180.00000								
opls	27	25	28	29	0.00000	0.00000	0.000000	1.25400
180.00000								
opls	27	25	28	30	0.00000	0.00000	0.000000	1.25400
180.00000								
opls	25	28	31	34	0.00000	5.43400	-0.209000	0.83600
180.00000								
opls	25	28	31	32	0.00000	0.00000	0.000000	1.25400
180.00000								
opls	25	28	31	33	0.00000	0.00000	0.000000	1.25400
180.00000								
opls	29	28	31	34	0.00000	0.00000	0.000000	1.25400
180.00000								
opls	29	28	31	32	0.00000	0.00000	0.000000	1.25400
180.00000								
opls	29	28	31	33	0.00000	0.00000	0.000000	1.25400
180.00000								
opls	30	28	31	34	0.00000	0.00000	0.000000	1.25400
180.00000								
opls	30	28	31	32	0.00000	0.00000	0.000000	1.25400
180.00000								
opls	30	28	31	33	0.00000	0.00000	0.000000	1.25400
180.00000								
opls	28	31	34	37	0.00000	5.43400	-0.209000	0.83600
180.00000								
opls	28	31	34	35	0.00000	0.00000	0.000000	1.25400
180.00000								
opls	28	31	34	36	0.00000	0.00000	0.000000	1.25400
180.00000								
opls	32	31	34	37	0.00000	0.00000	0.000000	1.25400
180.00000								
opls	32	31	34	35	0.00000	0.00000	0.000000	1.25400
180.00000								

opls	32	31	34	36	0.00000	0.00000	0.000000	1.25400
180.00000								
opls	33	31	34	37	0.00000	0.00000	0.000000	1.25400
180.00000								
opls	33	31	34	35	0.00000	0.00000	0.000000	1.25400
180.00000								
opls	33	31	34	36	0.00000	0.00000	0.000000	1.25400
180.00000								
opls	31	34	37	38	0.00000	0.00000	0.000000	1.25400
180.00000								
opls	31	34	37	39	0.00000	0.00000	0.000000	1.25400
180.00000								
opls	31	34	37	40	0.00000	0.00000	0.000000	1.25400
180.00000								
opls	35	34	37	38	0.00000	0.00000	0.000000	1.25400
180.00000								
opls	35	34	37	39	0.00000	0.00000	0.000000	1.25400
180.00000								
opls	35	34	37	40	0.00000	0.00000	0.000000	1.25400
180.00000								
opls	36	34	37	38	0.00000	0.00000	0.000000	1.25400
180.00000								
opls	36	34	37	39	0.00000	0.00000	0.000000	1.25400
180.00000								
opls	36	34	37	40	0.00000	0.00000	0.000000	1.25400
180.00000								
finish								
VDW	45							
OZ	OZ	buck	125997.200	0.35940	18920.32			
Si	OZ	buck	1717021.83	0.20490	13063.80			
Si	Si	lj	0.0000	0.0000				
CA	CA	lj	0.2930	3.5500				
HP	CA	lj	0.1921	2.9310				
OH1	CA	lj	0.4564	3.3013				
H	CA	lj	0.0000	0.0000				
CT2	CA	lj	0.2844	3.5249				
HA	CA	lj	0.1921	2.9310				
CT3	CA	lj	0.2844	3.5249				
HP	HP	lj	0.1260	2.4200				
OH1	HP	lj	0.2993	2.7257				
H	HP	lj	0.0000	0.0000				
CT2	HP	lj	0.1865	2.9103				
HA	HP	lj	0.1260	2.4200				
CT3	HP	lj	0.1865	2.9103				
OH1	OH1	lj	0.7110	3.0700				
H	OH1	lj	0.0000	0.0000				
CT2	OH1	lj	0.4429	3.2779				
HA	OH1	lj	0.2993	2.7257				
CT3	OH1	lj	0.4429	3.2779				
H	H	lj	0.0000	0.0000				
CT2	H	lj	0.0000	0.0000				
HA	H	lj	0.0000	0.0000				
CT3	H	lj	0.0000	0.0000				
CT2	CT2	lj	0.2760	3.5000				
HA	CT2	lj	0.1865	2.9103				
CT3	CT2	lj	0.2760	3.5000				
HA	HA	lj	0.1260	2.4200				
CT3	HA	lj	0.1865	2.9103				
CT3	CT3	lj	0.2760	3.5000				
CA	Si	lj	0.0000	0.0000				
CA	OZ	lj	0.4672	3.1562				
HP	Si	lj	0.0000	0.0000				
HP	OZ	lj	0.3064	2.6058				

```

OH1      Si      lj      0.0000      0.0000
OH1      OZ      lj      0.7278      2.9350
H       Si      lj      0.0000      0.0000
H       OZ      lj      0.0000      0.0000
CT2      Si      lj      0.0000      0.0000
CT2      OZ      lj      0.4534      3.1338
CT3      Si      lj      0.0000      0.0000
CT3      OZ      lj      0.4534      3.1338
HA      Si      lj      0.0000      0.0000
HA      OZ      lj      0.3064      2.6059
TBP      1
OZ      Si      OZ      bvs1    70337.9600   109.470000   0.32770000   0.32770000
2.0000000
CLOSE
#####

```

OPLS-AA bisphenol-A / silicalite

```

#####
UNITS kj
MOLECULES 2
Silicalite
NUMMOLS 1
ATOMS 576
OZ      15.99940   -1.02500   384     0
Si      28.08550    2.05000   192     0
FINISH
Molecule name not_define
nummols 1
atoms 33
CT1      12.01100    0.23000    1     0    1BPA
CT3      12.01100   -0.18000    1     0    1BPA
HA      1.00797     0.06000    1     0    1BPA
HA      1.00797     0.06000    1     0    1BPA
HA      1.00797     0.06000    1     0    1BPA
CT3      12.01100   -0.18000    1     0    1BPA
HA      1.00797     0.06000    1     0    1BPA
HA      1.00797     0.06000    1     0    1BPA
HA      1.00797     0.06000    1     0    1BPA
CA      12.01100   -0.11500    1     0    1BPA
CA      12.01100   -0.11500    1     0    1BPA
HP      1.00797     0.11500    1     0    1BPA
CA      12.01100   -0.11500    1     0    1BPA
HP      1.00797     0.11500    1     0    1BPA
CA      12.01100    0.11000    1     0    1BPA
OH1     15.99940   -0.54000    1     0    1BPA
H       1.00797     0.43000    1     0    1BPA
CA      12.01100   -0.11500    1     0    1BPA
HP      1.00797     0.11500    1     0    1BPA
CA      12.01100   -0.11500    1     0    1BPA
HP      1.00797     0.11500    1     0    1BPA
CA      12.01100   -0.11500    1     0    1BPA
HP      1.00797     0.11500    1     0    1BPA
CA      12.01100   -0.11500    1     0    1BPA
CA      12.01100    0.11000    1     0    1BPA
OH1     15.99940   -0.54000    1     0    1BPA
H       1.00797     0.43000    1     0    1BPA
CA      12.01100   -0.11500    1     0    1BPA
HP      1.00797     0.11500    1     0    1BPA
CA      12.01100    0.11000    1     0    1BPA

```

HP		1.00797	0.11500	1	0	1BPA		
bonds	14							
harm	1	2	2242.62	1.52900				
harm	1	6	2242.62	1.52900				
harm	1	10	2652.65	1.51000				
harm	1	22	2652.65	1.51000				
harm	2	3	2845.12	1.09000				
harm	2	4	2845.12	1.09000				
harm	2	5	2845.12	1.09000				
harm	6	7	2845.12	1.09000				
harm	6	8	2845.12	1.09000				
harm	6	9	2845.12	1.09000				
harm	15	16	3765.60	1.36400				
harm	16	17	4627.50	0.94500				
harm	27	28	3765.60	1.36400				
harm	28	29	4627.50	0.94500				
angles	28							
harm	2	1	6	585.20000	116.00000			
harm	2	1	10	527.18400	114.00000			
harm	2	1	22	527.18400	114.00000			
harm	6	1	10	527.18400	114.00000			
harm	6	1	22	527.18400	114.00000			
harm	10	1	22	710.60000	120.00000			
harm	1	2	3	279.47480	110.10000			
harm	1	2	4	279.47480	110.10000			
harm	1	2	5	279.47480	110.10000			
harm	3	2	4	296.78000	108.40000			
harm	3	2	5	296.78000	108.40000			
harm	4	2	5	296.78000	108.40000			
harm	1	6	7	279.47480	110.10000			
harm	1	6	8	279.47480	110.10000			
harm	1	6	9	279.47480	110.10000			
harm	7	6	8	296.78000	108.40000			
harm	7	6	9	296.78000	108.40000			
harm	8	6	9	296.78000	108.40000			
harm	13	15	16	585.2	120.00000			
harm	18	15	16	585.2	120.00000			
harm	15	16	17	292.6000	113.00000			
harm	25	27	28	585.2	120.00000			
harm	30	27	28	585.2	120.00000			
harm	27	28	29	292.6000	113.00000			
harm	11	10	1	585.7600	120.00000			
harm	20	10	1	585.7600	120.00000			
harm	23	22	1	585.7600	120.00000			
harm	32	22	1	585.7600	120.00000			
dihedral	30							
opls	6	1	2	3	0.00000	0.000000	0.00000	1.25400
180.00000								
opls	6	1	2	4	0.00000	0.000000	0.00000	1.25400
180.00000								
opls	6	1	2	5	0.00000	0.000000	0.00000	1.25400
180.00000								
opls	10	1	2	3	0.00000	0.00000	0.00000	1.93116
180.00000								
opls	10	1	2	4	0.00000	0.00000	0.00000	1.93116
180.00000								
opls	10	1	2	5	0.00000	0.00000	0.00000	1.93116
180.00000								
opls	22	1	2	3	0.00000	0.00000	0.00000	1.93116
180.00000								
opls	22	1	2	4	0.00000	0.00000	0.00000	1.93116
180.00000								

```

opls    22      1      2      5      0.00000      0.00000      0.00000      1.93116
180.00000
opls    2      1      6      7      0.00000      0.000000      0.00000      1.25400
180.00000
opls    2      1      6      8      0.00000      0.000000      0.00000      1.25400
180.00000
opls    2      1      6      9      0.00000      0.000000      0.00000      1.25400
180.00000
opls   10      1      6      7      0.00000      0.00000      0.00000      1.93116
180.00000
opls   10      1      6      8      0.00000      0.00000      0.00000      1.93116
180.00000
opls   10      1      6      9      0.00000      0.00000      0.00000      1.93116
180.00000
opls   22      1      6      7      0.00000      0.00000      0.00000      1.93116
180.00000
opls   22      1      6      8      0.00000      0.00000      0.00000      1.93116
180.00000
opls   22      1      6      9      0.00000      0.00000      0.00000      1.93116
180.00000
opls   16     15     18     19      0.00000      0.000000      30.30500      0.00000
180.00000
opls   14     13     15     16      0.00000      0.000000      30.30500      0.00000
180.00000
opls   11     13     15     16      0.00000      0.000000      30.30500      0.00000
180.00000
opls   16     15     18     20      0.00000      0.000000      30.30500      0.00000
180.00000
opls   13     15     16     17      0.00000      0.00000      7.03076      0.00000
180.00000
opls   18     15     16     17      0.00000      0.00000      7.03076      0.00000
180.00000
opls   25     27     28     29      0.00000      0.00000      7.03076      0.00000
180.00000
opls   30     27     28     29      0.00000      0.00000      7.03076      0.00000
180.00000
opls   26     25     27     28      0.00000      0.000000      30.30500      0.00000
180.00000
opls   28     27     30     31      0.00000      0.000000      30.30500      0.00000
180.00000
opls   23     25     27     28      0.00000      0.000000      30.30500      0.00000
180.00000
opls   28     27     30     32      0.00000      0.000000      30.30500      0.00000
180.00000
rigid 2
10 12 11 13 14 15 18 19 20 21 10
10 22 23 24 25 26 27 30 31 32 33
finish
VDW      43
OZ      OZ      buck    125997.200      0.35940      18920.32
Si      OZ      buck    1717021.83      0.20490      13063.80
Si      Si      lj      0.0000      0.0000
CT1     CT1     lj      0.2760      3.5000
CT3     CT1     lj      0.2760      3.5000
HA      CT1     lj      0.1865      3.1916
CA      CT1     lj      0.2844      3.5124
HP      CT1     lj      0.1865      3.1915
OH1     CT1     lj      0.4429      3.2779
H       CT1     lj      0.0000      0.0000
CT3     CT3     lj      0.2760      3.5000
HA      CT3     lj      0.1865      2.9103
CA      CT3     lj      0.2844      3.5249
HP      CT3     lj      0.0000      0.0000

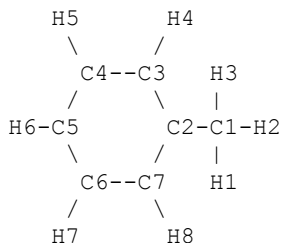
```

OH1	CT3	lj	0.4429	3.2779			
H	CT3	lj	0.0000	0.0000			
HA	HA	lj	0.1260	2.4200			
CA	HA	lj	0.0000	0.0000			
HP	HA	lj	0.0000	0.0000			
OH1	HA	lj	0.2993	2.7257			
H	HA	lj	0.0000	0.0000			
CA	CA	lj	0.2930	3.5500			
HP	CA	lj	0.1921	2.9310			
OH1	CA	lj	0.4564	3.3013			
H	CA	lj	0.0000	0.0000			
HP	HP	lj	0.1260	2.4200			
OH1	HP	lj	0.2993	2.7257			
H	HP	lj	0.0000	0.0000			
OH1	OH1	lj	0.7110	3.0700			
H	OH1	lj	0.0000	0.0000			
H	H	lj	0.0000	0.0000			
CA	Si	lj	0.0000	0.0000			
CA	OZ	lj	0.4672	3.1562			
CT3	Si	lj	0.0000	0.0000			
CT3	OZ	lj	0.4534	3.1338			
HA	Si	lj	0.0000	0.0000			
HA	OZ	lj	0.3064	2.6486			
HP	Si	lj	0.0000	0.0000			
HP	OZ	lj	0.3064	2.6059			
OH1	Si	lj	0.0000	0.0000			
OH1	OZ	lj	0.7278	2.9350			
H	Si	lj	0.0000	0.0000			
H	OZ	lj	0.0000	0.0000			
TBP	1						
OZ	Si	OZ	bvs1	70337.9600	109.470000	0.32770000	0.32770000
2.0000000							
CLOSE							
#####	#####	#####	#####	#####	#####	#####	#####

Appendix 2: DL_FIELD CHARMM.sf examples

Toluene

```
#####
MOLECULE tolu 15 0.0
C1  C_aliphatic3 -0.27
H1  H_aliphatic   0.09
H2  H_aliphatic   0.09
H3  H_aliphatic   0.09
C2  C_aromatic    0.000
C3  C_aromatic    -0.115
H4  H_aromatic    0.115
C4  C_aromatic    -0.115
H5  H_aromatic    0.115
C5  C_aromatic    -0.115
H6  H_aromatic    0.115
C6  C_aromatic    -0.115
H7  H_aromatic    0.115
C7  C_aromatic    -0.115
H8  H_aromatic    0.115
CONNECT C1 > C2 H1 H2 H3
CONNECT H1 > C1
CONNECT H2 > C1
CONNECT H3 > C1
CONNECT C2 > C1 C3 C7
CONNECT C3 > C2 C4 H4
CONNECT H4 > C3
CONNECT C4 > C3 C5 H5
CONNECT H5 > C4
CONNECT C5 > C4 C6 H6
CONNECT H6 > C5
CONNECT C6 > C5 C7 H7
CONNECT H7 > C6
CONNECT C7 > C6 C2 H8
CONNECT H8 > C7
END MOLECULE tolu
```



```
#####
```

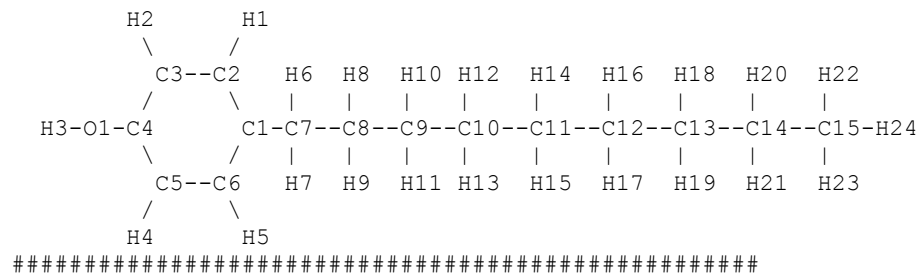
Nonylphenol:

```
#####
MOLECULE nonylphenol 40 0.0
C1  C_aromatic    0.000
C2  C_aromatic   -0.115
H1  H_aromatic    0.115
C3  C_aromatic   -0.115
H2  H_aromatic    0.115
C4  C_aromatic   -0.110
O1  O_hydroxyl   -0.540
H3  H_hydroxyl    0.430
C5  C_aromatic   -0.115
H4  H_aromatic    0.115
C6  C_aromatic   -0.115
H5  H_aromatic    0.115
C7  C_aliphatic2 -0.18
H6  H_aliphatic    0.09
H7  H_aliphatic    0.09
C8  C_aliphatic2 -0.18
H8  H_aliphatic    0.09
H9  H_aliphatic    0.09
C9  C_aliphatic2 -0.18
H10 H_aliphatic    0.09
H11 H_aliphatic    0.09
C10 C_aliphatic2 -0.18
H12 H_aliphatic    0.09
H13 H_aliphatic    0.09
C11 C_aliphatic2 -0.18
H14 H_aliphatic    0.09
H15 H_aliphatic    0.09
C12 C_aliphatic2 -0.18
H16 H_aliphatic    0.09
H17 H_aliphatic    0.09
C13 C_aliphatic2 -0.18
H18 H_aliphatic    0.09
H19 H_aliphatic    0.09
C14 C_aliphatic2 -0.18
H20 H_aliphatic    0.09
H21 H_aliphatic    0.09
C15 C_aliphatic3 -0.27
H22 H_aliphatic    0.09
H23 H_aliphatic    0.09
H24 H_aliphatic    0.09
CONNECT C1 > C7 C2 C6
CONNECT C2 > C1 C3 H1
CONNECT H1 > C2
CONNECT C3 > C2 C4 H2
CONNECT H2 > C3
CONNECT C4 > C3 C5 O1
CONNECT O1 > C4 H3
CONNECT H3 > O1
CONNECT C5 > C4 C6 H4
CONNECT H4 > C5
CONNECT C6 > C5 C1 H5
CONNECT H5 > C6
CONNECT C7 > C1 C8 H6 H7
CONNECT H6 > C7
CONNECT H7 > C7
CONNECT C8 > C7 C9 H8 H9
CONNECT H8 > C8
CONNECT H9 > C8
CONNECT C9 > C8 C10 H10 H11
```

```

CONNECT H10 > C9
CONNECT H11 > C9
CONNECT C10 > C9 C11 H12 H13
CONNECT H12 > C10
CONNECT H13 > C10
CONNECT C11 > C10 C12 H14 H15
CONNECT H14 > C11
CONNECT H15 > C11
CONNECT C12 > C11 C13 H16 H17
CONNECT H16 > C12
CONNECT H17 > C12
CONNECT C13 > C12 C14 H18 H19
CONNECT H18 > C13
CONNECT H19 > C13
CONNECT C14 > C13 C15 H20 H21
CONNECT H20 > C14
CONNECT H21 > C14
CONNECT C15 > C14 H22 H23 H24
CONNECT H22 > C15
CONNECT H23 > C15
CONNECT H24 > C15
END MOLECULE nonylphenol

```



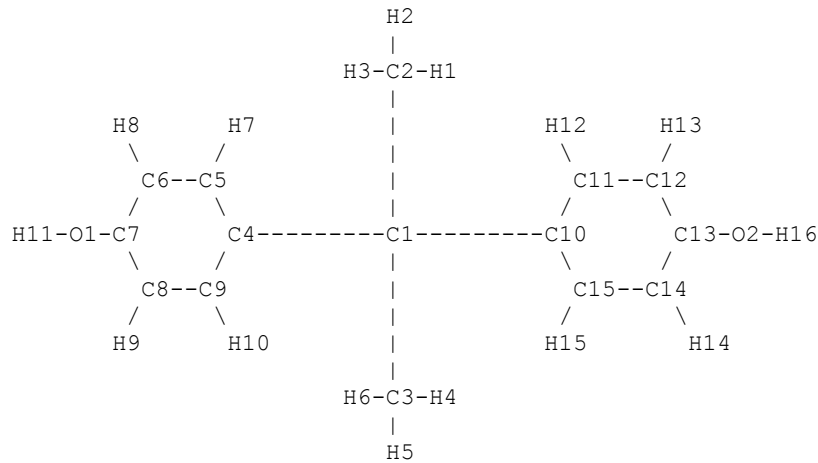
Bisphenol-A:

```
#####
MOLECULE bpa 33 0.0
C1  C_aliphatic1    0.00
C2  C_aliphatic3   -0.27
H1  H_aliphatic     0.09
H2  H_aliphatic     0.09
H3  H_aliphatic     0.09
C3  C_aliphatic3   -0.27
H4  H_aliphatic     0.09
H5  H_aliphatic     0.09
H6  H_aliphatic     0.09
C4  C_aromatic      0.000
C5  C_aromatic      -0.115
H7  H_aromatic      0.115
C6  C_aromatic      -0.115
H8  H_aromatic      0.115
C7  C_aromatic      0.110
O1  O_hydroxyl     -0.540
H11 H_hydroxyl      0.430
C8  C_aromatic      -0.115
H9  H_aromatic      0.115
C9  C_aromatic      -0.115
H10 H_aromatic      0.115
C10 C_aromatic      0.000
C11 C_aromatic      -0.115
H12 H_aromatic      0.115
C12 C_aromatic      -0.115
H13 H_aromatic      0.115
C13 C_aromatic      0.110
O2  O_hydroxyl     -0.540
H16 H_hydroxyl      0.430
C14 C_aromatic      -0.115
H14 H_aromatic      0.115
C15 C_aromatic      -0.115
H15 H_aromatic      0.115
CONNECT C1 > C2 C3 C4 C10
CONNECT C2 > C1 H1 H2 H3
CONNECT H1 > C2
CONNECT H2 > C2
CONNECT H3 > C2
CONNECT C3 > C1 H4 H5 H6
CONNECT H4 > C3
CONNECT H5 > C3
CONNECT H6 > C3
CONNECT C4 > C1 C5 C9
CONNECT C5 > C4 C6 H7
CONNECT H7 > C5
CONNECT C6 > C5 C7 H8
CONNECT H8 > C6
CONNECT C7 > C6 C8 O1
CONNECT O1 > C7 H11
CONNECT H11 > O1
CONNECT C8 > C7 C9 H9
CONNECT H9 > C8
CONNECT C9 > C8 C4 H10
CONNECT H10 > C9
CONNECT C10 > C1 C11 C15
CONNECT C11 > C10 C12 H12
CONNECT H12 > C11
CONNECT C12 > C11 C13 H13
CONNECT H13 > C12
```

```

CONNECT C13 > C12 C14 O2
CONNECT O2 > C13 H16
CONNECT H16 > O2
CONNECT C14 > C13 C15 H14
CONNECT H14 > C14
CONNECT C15 > C14 C10 H15
CONNECT H15 > C15
IMPROPER C4 C1 C5 H7
IMPROPER C4 C1 C9 H10
IMPROPER C10 C1 C15 H15
IMPROPER C10 C1 C11 H12
END MOLECULE bpa

```



```
#####
#
```

Appendix 3: Programs used to calculated averaged mean square displacement in the x, y and z direction.

Coordinates from HISTORY file:

```
#####
#!/usr/bin/env python
import string
import sys
import math

argc = len(sys.argv)
if argc < 2:
    print "Takes a HISTORY file from DL_POLY and"
    print "print coordinates of certain atom"
    print "Syntax: ./HIST-get-atom.py [atom_number] "
    sys.exit(0)

atom_num=int(sys.argv[1])

#####
it = 0
nsec = 0
go = 0
x = []
y = []
z = []
atom_count = 0
nocross = 0
zf=open('HISTORY','r')
first_time = 0
second_time = 0
while 1:
    line2 = zf.readline()
    it+=1
#   print it
    line = line2.strip()
    if not line:
        break

    if go ==4 :
        atom_count = atom_count + 1
        go = 5

    elif go == 5:
        if atom_count == atom_num:
            ls = line.split()
            x.append(str(ls[0]))
            y.append(str(ls[1]))
            z.append(str(ls[2]))
        go = 4

    if go == 3:
        go = go+1
        ls = line.split()
        lenz = float(ls[2])

    if go == 2:
        go = go+1
```

```

ls = line.split()
leny = float(ls[1])

if go == 1:
    go = go+1
    ls = line.split()
    lenx = float(ls[0])

if line.startswith("timestep"):
    nsec = nsec + 1
    go = 1
    atom_count = 0
    ls = line.split()
    if nsec == 1:
        time_scale = ls[5]
        first_time = ls[1]
        #print "time", time_scale, first_time
    if nsec == 2:
        second_time = ls[1]
        time_scale = float(time_scale)*(float(second_time)-float(first_time))
        #print "time", time_scale, first_time, second_time

zf.close()

### NEED TO REFOLD
scalex = []
scaley = []
scalez = []
for i in range(len(x)):
    scalex.append(int("0"))
    scaley.append(int("0"))
    scalez.append(int("0"))
for i in range(len(x)-1):
    if (float(x[i]) > lenx/4) and (float(x[i+1]) < -lenx/4):
        nocross = nocross + 1
        #print "*****", x[i], x[i+1]
        for j in range(i+1,len(x)):
            scalex[j] = scalex[j]+1
    if (float(x[i]) < -lenx/4) and (float(x[i+1]) > lenx/4):
        nocross = nocross + 1
        #print x[i], x[i+1]
        for j in range(i+1,len(x)):
            scalex[j] = scalex[j]-1
    #print i

    if (float(y[i]) > leny/4) and (float(y[i+1]) < -leny/4):
        nocross = nocross + 1
        for j in range(i+1,len(x)):
            scaley[j] = scaley[j]+1
    if (float(y[i]) < -leny/4) and (float(y[i+1]) > leny/4):
        nocross = nocross + 1
        for j in range(i+1,len(x)):
            scaley[j] = scaley[j]-1

    if (float(z[i]) > lenz/4) and (float(z[i+1]) < -lenz/4):
        nocross = nocross + 1
        for j in range(i+1,len(x)):
            scalez[j] = scalez[j]+1
    if (float(z[i]) < -lenz/4) and (float(z[i+1]) > lenz/4):

```

```

nocross = nocross + 1
for j in range(i+1,len(x)):
    scalez[j] = scalez[j]-1

##### GET RESCALED VALUES
for i in range(len(x)):
    scalex[i] = float(scalex[i])*float(lenx)+float(x[i])
    scaley[i] = float(scaley[i])*float(leny)+float(y[i])
    scalez[i] = float(scalez[i])*float(lenz)+float(z[i])
    #print "O",scalex[i], scaley[i], scalez[i], x[i], y[i], z[i]
    #print i, time_scale, float(i)*float(time_scale)
    print float(i)*float(time_scale),scalex[i], scaley[i], scalez[i]
    #print i, x[i], scalex[i], scaley[i], scalez[i]
# print "1"
# print "1"
#print "O", float(x[i])+float(scalex[i])*float(lenx),
float(y[i])+float(scaley[i])*float(leny), float(z[i])+float(scalez[i])*float(lenz)

#print lenx,leny, lenz, atom_count, nocross
#####

```

Calculate MSDx,y,z for each atom of one type:

```

#####
#!/usr/bin/env python
import string
import sys
import math

argc = len(sys.argv)
if argc < 2:
    print "Takes a data file and"
    print "finds MSD of atom"
    print "Syntax: ./MSD-2.py [file_name] "
    sys.exit(0)

file_name=str(sys.argv[1])
#print atom_num

#####
##### First determine number sections,number atoms, get preliminary data
#####
nocross = 0
it=0
nsec = 0
go = 0
x = []
y = []
z = []
zf=open(file_name,'r')
while 1:
    line2 = zf.readline()
    it+=1
    line = line2.strip()
    if not line:
        break
    ls = line.split()
    nsec = nsec + 1
    if it == 1:
        t0 = float(ls[0])

```

```

if it == 2:
    t1 = float(ls[0])
x.append(float(ls[1]))
y.append(float(ls[2]))
z.append(float(ls[3]))


zf.close()

time_step = t1-t0
#print "Number data points: ", nsec
#print "Timestep: ", time_step
#print x, len(x)
#for i in range(len(x)):
#    print x[i], y[i], z[i]

#####
## NOW CALCULATE MSDS
#### reset counter every stepres
numt = int(math.floor(len(x)/4))
#print "Size of loop ", numt
count = []
SDx = []
SDy = []
SDz = []
for i in range(numt):
    SDx.append(float("0.0"))
    SDy.append(float("0.0"))
    SDz.append(float("0.0"))
    count.append(int("0"))
#print ncyc

#for i in range(len(x)):
for i in range(5000):
    #if float(i % 100) == 0:
    #    print i,
    for j in range(i,i+numt):
        if j < len(x):
            #print "test",j, i, j-i
            dx = (x[i]-x[j])**2
            dy = (y[i]-y[j])**2
            dz = (z[i]-z[j])**2
            SDx[int(j-i)] = SDx[int(j-i)] + dx
            SDy[int(j-i)] = SDy[int(j-i)] + dy
            SDz[int(j-i)] = SDz[int(j-i)] + dz
            count[int(j-i)] = count[int(j-i)] + 1
#            print i,j,j-i,x[i],x[j],dx

#print "\n"
for i in range(len(SDx)):
    SDx[i] = SDx[i]/count[i]
    SDy[i] = SDy[i]/count[i]
    SDz[i] = SDz[i]/count[i]
    #print i*time_step,SDx[i], SDy[i],SDz[i], count[i]
    print i*time_step,SDx[i], SDy[i],SDz[i]
#####

```

Calculate averaged MSDx,y,z for one atom type

```
#####
#!/usr/bin/env python
import string
import sys
import math

argc = len(sys.argv)
if argc < 3:
    print "Takes an MSD data file and"
    print "combines with other data files"
    print "Syntax: ./MSD-combine.py [file_name] [file_name] etc"
    sys.exit(0)

#print atom_num

data = []
t = []
zf=open(str(sys.argv[1]),'r')
time = []
while 1:
    line2 = zf.readline()
    line = line2.strip()
    if not line:
        break
    t.append(line)
    ls = line.split()
    time.append(ls[0])

zf.close()

for i in range(2,argc):
    it = 0
    zf=open(str(sys.argv[i]),'r')
    while 1:
        line2 = zf.readline()
        line = line2.strip()
        if not line:
            break
        ls = line.split()
#     print it, t[it-5], ls[1], ls[2], ls[3]
        t[int(it)] = t[int(it)]+" "+ls[1]+" "+ls[2]+" "+ls[3]
        it+=1
#zf.close()

tavg = []
for i in range(len(t)):
    tt = t[i].split()
    avgx = 0.0
    avgy = 0.0
    avgz = 0.0
    #print tt
    for j in range(argc-1):
        #print j, tt[j*3+1]
        avgx = avgx + float(tt[j*3+1])
        avgy = avgy + float(tt[j*3+2])
        avgz = avgz + float(tt[j*3+3])
    avgx = float(avgx)/float(argc-1)
    avgy = float(avgy)/float(argc-1)
    avgz = float(avgz)/float(argc-1)
```

```
ttt = time[i]+ " " + str(avgx)+ " " + str(avgy) + " " + str(avgz)
print ttt
#for i in range(len(t)):
# print t[i]
#####
```